Integration of photocatalytic and biological processes for treatment of biorecalcitrant pharmaceuticals

A thesis submitted in fulfilment of the requirement for the award of the degree of

DOCTOR OF PHILOSOPHY

By

VIBHU BHATIA

(Regd. No. 901200007)

School of Energy and Environment

Thapar University,

Patiala-147004 (INDIA)

October, 2016

Candidate's Declaration

I, hereby declare that the work presented in the thesis entitled "Integration of photocatalytic and biological processes for treatment of biorecalcitrant pharmaceuticals" in fulfilment of the requirement for the award of the Degree of Doctor of Philosophy, School of Energy and Environment, Thapar University, Patiala, is an authentic record of my own work carried out under the supervision of Dr. Amit Dhir, Associate Professor, School of Energy and Environment, Thapar University, Patiala. The matter embodied in this thesis has not been submitted in part or full to any other university or institute for the award of any degree in India or Abroad.

Place: Patiala

Date: 24/10/2016

Vibhu

Vibhu Bhatia

Certificate

Certified that the thesis "Integration of photocatalytic and biological processes for treatment of biorecalcitrant pharmaceuticals" which is submitted by Ms. Vibhu Bhatia, in fulfilment of the requirement for award of the degree of Doctor of Philosophy in the School of Energy and Environment, Thapar University, Patiala, is a record of candidate's own independent and original research work carried out by herself under my supervision and guidance. The material embodied in this thesis has not been submitted in part or full to any other university or Institute for the award of any degree.

24/10/2016

Supervisor

(Dr.Amit Dhir)

Associate Professor

School of Energy & Environment

Thapar University

Patiala-147007 (INDIA)

EXECUTIVE SUMMARY

The present study facilitated exploring avenues for examining effective solutions to treat pharmaceutical model compounds and simulated effluent. The research primarily focussed on the degradation of pharmaceutical model compounds such as Aspirin, Ibuprofen, Ofloxacin and Atenolol by heterogeneous photocatalysis using various metal doped photocatalyst and its efficacy was compared with P25 TiO_2 under optimized conditions. Fe-TiO_2 (0.5wt %) photocatalyst was synthesized by solgel method and its efficiency was evaluated in the degradation of the Aspirin (25 ppm).The Brunauer–Emmett–Teller (BET) surface area of Fe–TiO_2 was found to be 72 m^2/g and it has been observed that Fe-TiO_2 resulted in higher degradation (96%) when compared to P25 TiO_2 (72%) after 6 h of solar irradiations.Higher activity of Fe doped catalyst was attributed to its higher surface areabecause TiO_2 crystallite grain sizes decreased with the increase of Fe contents and the diffuse reflectance spectra of Fe-doped TiO_2 nanoparticles displayed a red shift in the band gap transition and the absorbing band edge moved to visible range. Similarly, photocatalytic degradation of Ibuprofen (IBP) was carried out under solar irradiation (30-35W/m^2) using two different catalyst viz. Bi-TiO_2 and Ni-TiO_2synthesized by solgel method with dopant concentration varying from 0.25wt% to 1.0wt% and were characterized using XRD, SEM and UV-reflectance spectroscopy. The rate of solar induced photocatalytic degradation of IBP was observed to be in the order of Bi–TiO_2> P25 TiO_2> Ni–TiO_2 with rate constants as 0.0064, 0.0046 and 0.0043 min^{-1}, respectively. Degradation of 89% was achieved with 2g/L of (0.25wt %) Bi–TiO_2 photocatalyst at pH 6 after 6 h of solar illuminations, whereas, 78% degradation was attained under similar experimental condition with (0.50wt %) Ni doped TiO_2. Bi–TiO_2 nanoparticles exhibited higher photocatalytic activity, due to reduction in band gap(2.99 ev) when compared to band gap of P25 TiO_2 (3.2 ev). Further Bi–Ni co-doped TiO_2 was synthesized using sol gel method and its efficacy was observed to be higher under solar light when compared to P25 TiO_2 for the degradation of 25 ppm Ofloxacin (OFL). The BET surface area was found to be 74, 55 and 18.66 m^2/g for 0.25, 0.5 and 1.0 wt% of Bi - Ni co-doped TiO_2,respectively and the corresponding band-gap energies were found to be 2.89, 3.09 and 3.11 eV, respectively. Degradation efficiency of 86% was attained at pH 3 with 1.5 g/L of Bi-Ni co-doped catalyst after 6 h of solar irradiations which may be attributed to decrease in band gap of Bi–Ni co-doped TiO_2.

Possibility of employing Graphene oxide based composites was explored with TiO_2 as well as ZnO, so TiO_2-G & ZnO-G composites were synthesized by hydrothermal method and their important characteristics were determined. XRD data showed the highly crystalline nature of TiO_2-G. By adding graphene to TiO_2, the band gap noticeably decreased from 3.2 to 2.2 eV and surface area increased to 76m^2/g. Photocatalytic degradation of Atenolol (ATL) was examined using graphene TiO_2 (TiO_2-G) compositesunder solar simulator(75mW/cm^2). Results indicated that 72% degradation of ATL (25ppm) with 1.5 g/L TiO_2-Gat pH 6 under solar irradiations in 1h, whereas 56%degradation was attained with P25 TiO_2. Kinetic regime was also studied by varying the catalyst dose from 0.01- 2.0g/L and the degradation rate was found to be almost constant for catalyst loading between 0.01 and 0.08 g/L and thereafter, rate drops gradually as the catalyst loading was increased from 0.08 to 2.0 g/L. Complete TOC removal (94.5%) of Atenolol solution was obtained after 7h.

Further, a four factor three level Box-Benkhen design (BBD) was employed to define the photocatalytic degradation of ATL in an aqueous media under slurry mode using TiO_2-G and ZnO-G as photocatalyst. The four process variables considered were catalyst dose (0.5-2.0g/L), pH (4-9), ATL concentration (5-25ppm) and light intensity (25-100mW/cm^2).The surface area of ZnO-G was found to be 84m^2/g. The data obtained from run of 29 experiments suggested that maximum reaction rate of 0.783min^{-1} was achieved with 25ppm atenolol concentration within 1h of solar irradiation (100mW/cm^2)at pH 6.5 when catalyst (ZnO-G) concentration was 1.25g/L, however reaction rate obtained with TiO_2-G was 0.514min^{-1} under similar experimental conditions. So ZnO-G was found to be better photocatalyst when compared to TiO_2-G in the degradation of ATL under solar irradiations.

Further, immobilization of photocatalyst (TiO_2-G)was carried out on Pyrex glass plate by dip coating method and optimization of process parameters such as catalyst concentration, pH, UV intensity and substrate concentration was done using BBD technique. Moreover, efficiency of TiO_2-G was compared with P25 TiO_2at optimized conditions for degradation of ATLunder immobilized mode which resulted in reaction rate of 0.0722 and 0.0497 min^{-1},respectively.Comparing the efficacy of TiO_2-G in slurry/immobilized mode indicate that degradation efficacy was 35% more in case of slurry mode under similar experimental conditions,but, photocatalytic treatment under immobilized mode increase the industrial viability of process.

Simulated effluent was subjected to independent photocatalytic, biological and thereafter, integrated photocatalytic-biological sequential treatment scheme to access its degradation efficacy in terms of BOD/COD. Biodegradability (BOD_5/COD ratio) increased

from 0.23 to 0.42 after 4 h of photocatalytic treatment (1.5g/L TiO_2) with COD removal of 69.7% under solar simulator. In the independent biological treatment, the amount of sludge was varied as 2, 5, 10 and 15%, in order to optimize sludge concentration at three different temperatures of 20, 27 and 37°C. The maximum BOD and COD reduction of 46.3 and 46.2%, respectively was achieved with 5% activated sludge at 37°C for a time period of 48h at natural pH of 6.9 under continues aeration. By employing 4h of photocatalytic treatment using TiO_2 (1.5g/L) followed by 48h of biological treatment (37°C, 5% Sludge concentration) resulted in 90.5 and 80.8% removal of COD and BOD, respectively. Thus, it is concluded from the present study that the sequential photocatalytic-biologicaltreatment was more effective in the degradation of simulated effluent when compared to independent photocatalytic and biological processes.

ACKNOWLEDGEMENT

*First and Foremost, I would like to express my special appreciation and thanks to my advisor **Dr. Amit Dhir**, Associate Professor, School of Energy and Environment, Thapar University, Patiala, who have been a tremendous mentor for me. It has been an honour to be his first Ph.D. student. I appreciate all his contributions of time, ideas, and funding to make my Ph.D. experience productive and stimulating. The joy and enthusiasm he has for his research was contagious and motivational for me, even during tough times in the Ph.D. pursuit. I would like to thank him for encouraging my research and for allowing me to grow as a research scientist. His advice on both research as well as on my career have been invaluable.*

*I would also like to express my heartfelt gratitude to my mentor **Dr Ajay K Ray**, Chair and Professor, Department of chemical and Biochemical engineering, University of Western Ontario, London, Canada, who has been a truly dedicated mentor. I thank him wholeheartedly, not only for his tremendous academic support, but also for giving me so many wonderful opportunities. I am also hugely appreciative him for sharing his expertise so willingly, and for being so dedicated to his role. Thanks to him I had opportunity to gather experience of visiting graduate student at University of Western Ontario.*

*I express my gratitude to **Dr. Prakash Gopalan**, Director, Thapar University, Patiala, for all the facilities which have been immensely helpful for the completion of my work.*

*I am highly thankful to **Dr. O.P Pandey**, Dean, (Research and Sponsored projects) for his encouragement and motivation during my PhD work.*

*I feel a special gratitude towards **Dr. N.Tejo Prakash,** Head of School of Energy & Environment, for providing lab facilities.*

*I would also like to thank my committee members, **Dr N.Tejo Prakash, Dr V.K Sangal and Dr Anita Rajor** for serving as my committee members even at hardship. I also want to thank you for your brilliant comments and suggestions.*

*I am indebted to **Dr. Sushil Kansal**, Associate Professor, University institute of Chemical Engg. And Technology, Panjab University, Chandigarh, for his support, encouragement and guidance.*

*I would also like to acknowledge **Dr. Madhumita Ray**, Professor, Department of Chemical and Biochemical Engineering, University of Western Ontario, London, Canada, who has been an inspiration on how to make things 'perfect'. She always guided me to come up in life even at most difficult time of life.*

*No amount of words can adequately express the debt I owe to **Mrs. Rupali Dhir**, for her kind support that cultivated endurance in me to do the work throughout the course of project.*

I extend my thanks to all the faculty members of School of Energy and Environment, Thapar University, Patiala for providing necessary guidance during my research work..

*I am highly thankful to **Mr. Pradeep** for his help, constant encouragement, support and timely assistance.*

*I take this opportunity to thank **Mr. Sumit** for their assistance in laboratory and timely suggestions. I owe a word of thanks to all research scholars, at the School of Energy and Environment, for providing constant support, encouragement and a good working atmosphere that has given me necessary time to relax from my work.*

*I am highly thankful to **Mr. Mohammad Sohail** and **Mr. Gurpreet**, for timely assistance.*

*I feel a deep sense of gratitude for **Dr. Parteek Bhatia** (Bhaiya) and **Dr. Sanmeet Bhatia** (Bhabi) who have always showered unconditional love on me, encouraged and supported me in every aspect.*

*A special thanks to my family. Words cannot express how grateful I am to my mother, father, Brother, sister in-law for all of the sacrifices that they've made on my behalf. Their prayer for me was what sustained me thus far. Thank you for supporting me for everything, and especially I can't thank you enough for encouraging me throughout this experience. I am indebted of my brother **Mr. Vikas Bhatia,** as during the most difficult times when writing this thesis, he gave me the moral support and the freedom I needed to move on. A special thanks to my fiance **Mr. Ankur Chhabra** Words cannot describe how lucky I am to have him in my life. He has selflessly given more to me than I ever could have asked for. I love you, and look forward to our lifelong journey.*

Finally I thank my God, my Father, for letting me through all the difficulties. I have experienced your guidance day by day. You are the one who let me finish my degree. I will keep on trusting you for my future. Thank you, Lord.

Dedicated to my Papa

List of Symbols/Abbreviations

UV	Ultraviolet
ATL	Atenolol
IBF	Ibuprofen
OFL	Ofloxacin
HPLC	High performance liquid chromatography
h	Hours
min	minute
%	Percentage
XRD	X-Ray diffraction
SEM	Scanning electron microscope
EDS	Energy Dispersive spectroscopy
rpm	Revolution per minute
OD	Optical Density
nm	Nanometre
ASP	Activated sludge process
AOP's	Advanced Oxidation Processes
Bi-TiO_2	Bismuth doped TiO_2
Ni-TiO_2	Nickel doped TiO_2
N	Normality
Sec	Second
Hcl	Hydrochloric acid
NaOH	Sodium Hydroxide
Ppm	Parts per million
mg/L	Milli gram per litre
g	Gram
L	Litre
NSAID	Non-Steroidal Anti-inflammatory drug
t	Time

BOD	Biological oxygen demand
WWTP	Waste water treatment plant
UV-Vis	Ultraviolet and Visible (Light)
COD	Chemical Oxygen Demand
TDS	Total Dissolved salts
MEE	Multiple effect evaporators
TiO_2-G	Graphene oxide TiO_2 composite
ZnO-G	Graphene oxide ZnO composite
BBD	Box Behnken design
TOC	Total organic content
SRT	Sludge retention time
Fe-TiO_2	Ferrous doped TiO_2
m^3/s	metre cube per sec
w.r.t	with respect to time
TIP	Titanium isopropoxide
RSM	Response surface methodology
Bi-Ni Co-doped TiO_2	Bismuth Nickel codoped TiO_2
ANOVA	Analysis of variance
TC	Total carbon
TIC	Total inorganic carbon
W	Watt
ml	millilitre
mg	milligram
photo + Bio	Photocatalytic followed by biological treatment
LED	Light Emitting Diode

INDEX

List of Tables

List of Figures

1.0 INTRODUCTION

Pharmaceutical industry is the world's third largest industry in terms of volume in the world and is estimated to worth $ 4-5 billion. Indian production of pharmaceuticals constitutes about 13 % of world market in value terms and about 8% in volume terms. There are more than 20,000 registered units of this industry in India [James, 2014]. Producing effective medicines and vaccines to improve health of patients is the prime function of the pharmaceutical corporations. It is usually anticipated that in industrialised countries, due to the local legal restrictions, usually the manufacturing of pharmaceuticals is precise and are not harmful to the environment. However, a significant portion of the worldwide manufacturing of pharmaceuticals occurs in developing countries like India and China, where production cost is low [Mudgal et al., 2013].

Pharmaceutical medications are consumed by human as well as livestock which comprise antibiotics, hormones, anti-inflammatory, pain killers and chemotherapy drugs. Many drugs have been aimed to be firm, so that they may maintain their chemical structure till their therapeutic work is complete.

More than one hundred pharmaceuticals consumed by humans have been spotted in effluents and surface waters at concentrations ranging from parts per trillion to parts per billion and include various analgesics, anti-inflammatories, anti-depressants, lipid regulators, antibiotics, β-blockers, hormones etc., [Monteiro and Boxall, 2010]. Though the detected amounts of pharmaceuticals are very less, but are highly toxic for human, animal and aquatic lives because these drugs effect the hormonal system of body. Various sources from which the contaminants entered the environment include various waste stream such as domestic wastewater, domestic solid wastes (via landfill leachate), industrial discharges (such as from hospitals, other healthcare facilities, and manufacturing facilities), and from animal feeding operations and aquaculture. It is need of an hour to regulate and monitor the release of pharmaceutical compounds in effluents and drinking water sources so as to protect environment and living beings from health hazards. The detected occurrence of pharmaceutical compounds in enormous water bodies created awareness that chemicals that are man-made and used in relatively lesser volumes when compared to industrial chemicals could still be inflowing the environment at noticeable levels.

Sewage treatment plants have not been able to remove these elements completely and the remains sometime pass through treatment amenities and go in natural streams such as rivers, streams, lakes, etc. The conventional procedures to treat such effluents involve

physical, chemical, electro-chemical and biological techniques however; the presence of hazardous compounds has been magnified as the complete degradation of the recalcitrant organic matter is not possible [Kummererr, 2001]. Conventionally, treatment of pharmaceutical industry wastewater has been carried out by biological treatment [Raj et al., 2005], which include aerobic and anaerobic processes. Aerobic processes include activated sludge, membrane batch reactors and sequence batch reactors [Raj et al., 2005; Noble, 2006; Chen et al., 2008]. Antibiotics generally have low biodegradability as they are primarily biocidal materials and the mineralization of these compounds cannot be productive in the biological treatment systems [Ternes et al., 1998].

With increased environmental awareness and stringent international standards, research on developing new and efficient clean technologies such as membrane separation, chemical removal, adsorption, and Advanced Oxidation Processes (AOPs) for the degradation of such pollutants has drawn more attention.

1.1 PHARMACEUTICAL WASTE

Pharmaceutical manufacturing industries usually have batch operations for the production of most basic drugs and their derivatives in pharmaceutical manufacturing industries. The composition and the magnitude of waste produced by pharmaceutical industries usually fluctuates with type of raw material, the process involved in manufacturing of different pharmaceuticals and with season. Primarily, physical operations are employed in formulation units for manufacturing of tablets, capsules, syrups, injections, ointments etc. Several steps which are involved in manufacturing of pharmaceuticals are oxidation, reduction, nitration, sulphonation, halogenation, amination, aminolysis, alkylation, esterification, crystallisation, hydrogenation, precipitation, etc. On the basis of drug to be manufactured, the ingredients of these pharmaceutical by-products varies and moreover, the materials involved in the production and the operations involved may vary. The ingredients involved during manufacturing can comprises of biological components such as fermentation wastes, pharmacologically-active ingredients like anti-coagulants, chemotherapeutic agents, disinfectants and excess extraction solvents left after the isolation and purification of active ingredients from natural sources. Therefore, it is very hard to specify a particular treatment system for such a diversified pharmaceutical industry.

It has been originated that huge volume and range of wastes formed during the pharmaceuticals production is higher than the amount of the water used in real final product and it has been reported that 200 to 30,000 kg of wasteis generated for every kg of ingredient produced [Wu et al., 2009]. Effluent generated from pharmaceutical and bulk drug industries

comprises of high organic contents with high COD and TOC. The most vigorous subject matter of research nowadays is the presence of pharmaceutical compounds in the environment, its damaging effects on humans and also the level to which they can be eradicated during wastewater treatment [Joss et al., 2005]. The norms for discharge of pharmaceutical wastewater in India are given in Table 1.1.

Table 1.1 Discharge norms for large scale pharmaceutical manufacturing industries

Parameters	**Standards**
pH	5.5-9.0
Suspended solids	100-150mg/L
BOD	30-100mg/L
COD	250-350mg/L

Source: CPCB, 2010

1.2 TREATMENT TECHNOLOGIES

The treatment of pharmaceutical wastewater is of great challenge due to the presence of large variety of organic compounds; some of them are biorecalcitrant in nature. Biological treatment (aerobic or anaerobic tailed by aerobic) is one of the most viable technology in the treatment of industrial effluents. Conventional wastewater treatment methods for pharmaceutical effluents was either incineration or some appropriate technologies like carbon adsorption, ion exchange, chemical precipitation, reverse osmosis etc. Generally, for handling pharmaceutical effluents with high total dissolved solids (TDS), multiple effect evaporation (MEE) followed by incineration is used but problem with MEE is the scaling of the tubes through evaporation which consequently results in reduced efficiency and increased cost of operation [CPCB, 2007]. Sludge produced after incineration is disposed off by landfilling technique. The most widely employed biological treatment for effluents with low TDS is activated sludge process because of rational operating and maintenance costs. Moreover, it treat effluents to meet mandatory discharge standards.These biological treatment technologies rely on several parameters such as composition of wastewater, ecotoxicants and extent of xenobiotics involved [Jelic et al., 2012]. This type of treatment is found to have limited competence as far as removal of biorecalcitrant is concerned.

The concern of accumulation of such substances and their consequent human contact has stimulated the development of advanced methods for their removal to avoid the contamination of aquatic environment.

Advanced oxidation processes (AOPs) are centred on the production of hydroxyl radicals (·OH) which can oxidize organic compounds present in aqueous streams [Han et al., 2004; Qamar et al., 2006]. AOP's have been classified as homogeneous and heterogeneous. The homogeneous AOPs involve an oxidant to generate radicals in the presence of ultraviolet light, which trigger the oxidation and attack the organic pollutants. The efficiency of the system depends on the strong oxidant species which can oxidize almost all organic pollutants. The major processes used for the homogeneous degradation are: Hydrogen peroxide (UV/H_2O_2), Ozone (UV/O_3), Hydrogen peroxide and Ozone ($UV/ H_2O_2/O_3$) and Photo-Fenton system (Fe^{2+}/ H_2O_2). Heterogeneous AOP includes photocatalysis which is a versatile technology that involves the semiconductors as photocatalyst for treating organic pollutants in an environmental friendly manner. Basically the acceleration of photoreaction has been carried out using catalyst in heterogeneous photocatalysis. Splitting of water using solar light and the purification of water containing pollutants is the most noteworthy applications of photocatalysis. The foremost drawback of AOPs is its high operating cost because of the requirement of catalyst/ oxidant and high energy utilization. Also, commercialization of this technology is hampered due to the fast recombination rate of photo generated electron and hole. Therefore, integration of AOP process as coupling treatment with economical biological methods, seem very auspicious from economical point of view. AOP can be applied at pre or post treatment options to enhance the efficacy of treatment with minimal increase in operational cost.

1.3 MECHANISM OF PHOTOCATALYSIS

When Ultraviolet (UV) radiation from sunlight or illuminated light source, with energy equal to or greater than band gap, is allowed to fall on photocatalyst, it absorb the light and it will produce electrons and holes as shown in Fig 1.1. The electrons get excited to conduction band from valence band resulting in generation of the electron (e^-) and hole (h^+) pair. This phase is denoted as the photoexcitation state of semiconductor. For excitation of electron, energy greater than the width of band gap is required i.e. the energy difference between the valence band and the conduction band. The h^+ of photocatalyst break down the water and leads to formation of hydroxyl radical whereas e^- reacts with oxygen molecule to form super oxide anion. This process persists till the light is obtainable and energy greater than the band gap is available to photocatalyst.

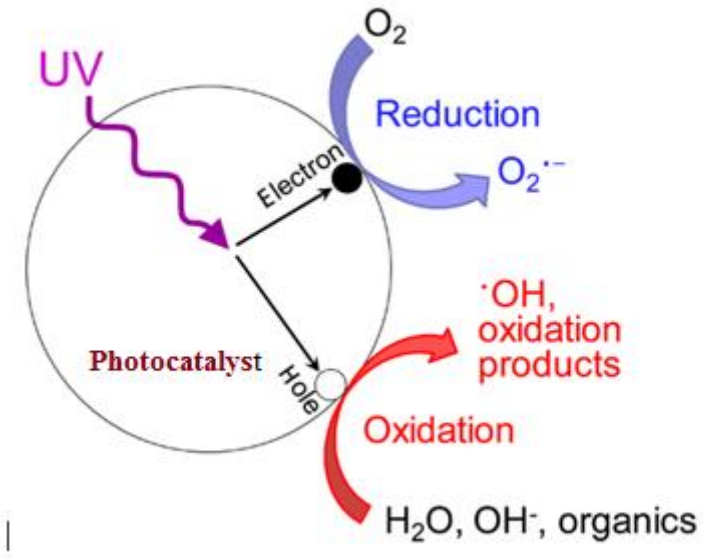

Fig 1.1. Mechanism of photocatalytic Degradation

Semiconductors like TiO_2, ZnO, SnO_2 and CeO_2, which are abundant in nature, are employed as photocatalysts for the mineralization of organic pollutants present in aqueous streams [Hoffman et al., 1995]. Among these, TiO_2 is extensively used photocatalyst because it is exceptionally stable (with respect to photocorrosion/chemical corrosion), non-toxic, chemically inert and highly reactive. It has Band gap of 3.2ev and surface area of $50m^2/g$ with particle size of approximately 21nm. [Chen et al., 2012; Palaez et al., 2012]. Yang et al. 2012 studied photocatalytic degradation of Paracetamol using TiO_2 in aqueous solution and obtained 95% degradation with 0.8g/L catalyst dose. Usually, semiconductors with wide band gap work as better photocatalyst when compared to lower band gap semiconductor materials because of large free energy of photogenerated electrons and holes of the former and the intrinsically less photochemical and chemical stability of the latter. On the other hand, more adapted semiconductors to the solar spectrum are those which are having lower band gap, thereby offering the compelling benefit and potential utilization of affordable treatment. ZnO is a semiconductor having wide band gap of 3.3 eV, large exciton binding energy (60 MeV), ample in nature, environment friendly and natural n-type conductivity [Li et al., 2007]. High band gap, recombination of electron hole pair and UV light absorption are some of the drawbacks of these semiconductors.

1.4 DOPING OF PHOTOCATALYST

In principle, doping is the insertion of extrinsic components into the parent semiconductor without altering the actual crystalline structure or phases. The objectives are

to improve the separation of electron and holes and effectively use the visible-light constituent which is about 43% in the solar spectrum when compared to the narrow ultraviolet section (only 5%). Anionic impurities such as N, C, S, B and P have been utilized as dopants for extending the optical absorption of TiO_2 to the visible region of the spectrum [Hoffmann et al., 1995]. Investigations have also been carried out into the development of visible light-responsive photocatalysts by adding slight amounts of constituents such as cations and metal oxides. Basically impurities are inserted such as metal ions in the pure photocatalyst, mostly d block metal ions which results in the initiation of impurity energy levels between the conduction and valence bands. In this instance, actually the fermi levels are introduced in the semiconductor which provide sub-bandgap for irradiation and electrons can be excited from dopant d-band to conduction band or from valance band to dopant d-band by lower energy photons. Typically the insertion of metal ions as dopant results in enhancement of charge separation as well as interfacial charge transfer [Lam et al., 2007]. However, there are various concerns of doping, linked to their efficacyand cost effectiveness.

Sometimes co-doping may also be carried out to enhance photocatalytic activity. However, this may not surely avoid structural defects rising from the modifications in cationic radii between dopants and the parent photocatalyst. Doping was actually results in oxygen vacancies that prolonged photo-response instead of rising from d-band supplement [Serpone et al., 2006]. Further, doping using the non-metals has also been explored (such as N, C and S) [Murase et al., 2004; Asahi et al., 2001]. The advantage of using the non-metal dopant are the higher photocatalytic activity, stability [Cherepy et al., 1998] and nontoxicity of dopant ions. In general, TiO_2 and numerous other materials have been extensively studied comprising the consequence of impurity intensities in the dopant on photocatalytic efficiency [Yu et al., 2002; Carp et al., 2004; Li et al., 2006].

Various methods employed for doping include sol-gel, hydrothermal method, Liquid phase deposition, ion-assisted sputtering, wet impregnation, coprecipitation, chemical vapour deposition (CVD), etc. Sol-gel method results in the homogeneous distribution of the dopant ion in the crystal of semiconductor and is the most widely used method. Similarly, the hydrothermal synthesis has emerged as another doping method, in which dopant ions allocates consistently in system during the whole hydrothermal process. The advantage this method is that the prepared materials have well crystalline phase, which leads to thermal stability of materials. The hydrothermal process consist of solvents as reaction medium that is eco-friendly because it is carried out in a closed reactor and the ingredients can be recovered and reused after bringing down to room temperature. In the impregnation method, insertion

of metal ions in the TiO_2 crystallites do not takes place effectively and therefore, only substitution may take place on the surfaces [Paola et al., 2002; Grzybows et al., 2002]. Further, in the co-precipitation method, mixed metal hydroxides are allowed to undergo post-heat p

rocessing for the production of metal doped catalyst. So the high temperature and heating for long time may separate out the dopant metal ions into respective metal oxides and therefore, get segregated on the surfaces.

1.5 GRAPHENE BASED COMPOSITES

As a novel material, graphene has lately exhibited to have many amazing physical properties, such as high specific surface area ($2600 m^2/g$), exceptional mobility of charge carriers (20,000 $cm^2 V^{-1} s^{-1}$), high chemical stability and good optical transparency [Geim et al., 2007; Park et al., 2008].Therefore, it is highly desirable to explore its potential to form a hybrid structure with different nanomaterials for photocatalytic uses.

The improvement in the photocatalytic activity is attained due to a clear red shift of the absorption spectrum and greater absorbance in the visible region. Thus, the fusion of graphene enhanced the fascination of visible light. Further, the conduction band of TiO_2 is more negative than the work function of graphene, such that the transmission of photogenerated electrons from photocatalyst to graphene is easily possible. A graphene is acceptor of electrons, it repressed the charge recombination, and also, graphene has exceptional conductivity and speedy movement of charge carriers that enabled the charge transfer. Generally, both the electron accepting and transporting possessions of graphene in graphene based composites successfully curbed the electron–hole recombination and boosted the photocatalytic activity [Zhang et al., 2011].

1.6 IRRADIATION SOURCE

Heterogeneous photocatalytic processes under irradiation of traditional ultraviolet (UV) sources are extensively explored in the field of removal of pollutants from wastewater, but the industrial scale development desires an energy efficient source to conquer the rigorous energy crisis going ahead. In a photocatalytic reactor, UV-A (315-400nm) radiation is emitted by low-pressure mercury lamps that generate low-intensity UV-A radiation. Medium pressure mercury lamps discharge high intensity UV light in the short, medium and long UV spectrums. Whereas, short (UV-C; 200-280 nm) and medium (UV-B; 280-320 nm) UV radiation emitted by the lamp is usually barricaded by thephotoreactor material made of quartz.

Recent novelties includes the use of energy efficient UV/visible light emitting diodes (LEDs) as source of light in lab-scale reactors [Natarajan et al., 2011; Nickels et al., 2012]. Solar simulators have also been employed now a days for process of photocatalysis. A solar simulator is a device that work as artificial sun and delivers illumination resembling natural sunlight. The advantage of solar simulator is that it mimics with the solar spectrum, so it provide facility to use either full solar spectrum intensity or by using filters so as to employ only UV light. Apart from UV/Solar light, other irradiation sources include gamma and electron beam. Gamma irradiation, is an electromagnetic radiation of high frequency which is generated by interaction of sub atomic particles. Gamma rays have the smallest wavelengths and the highest energy when compared to other radiations in the whole electromagnetic spectrum [Fang and Wu, 1999]. Ionizing radiation have enough energy to release the electrons from atoms and molecules to transform them to electrically charged particles called ions. Further reactions of these generated ions, will result in the generation of free radicals which are reactive and ultimately lead to chemical oxidation [Dahlan, 2001].The process of irradiation by electron beam in water can result in oxidation and reduction reaction, simultaneously. The treatment of water by e-beam results in the generation of numerous radicals and ions [Leitner et al., 2011].

1.7 PHOTOREACTOR

Photocatalytic reaction can be carried out in slurry/ immobilized mode. In slurry type reactor, the photocatalyst particles are present in the aqueous solution with the aid of mechanical stirring [Wei et al., 2011] or air sparging [Chong et al., 2011]. Slurry reactors can be executed in batch or continuous mode. Slurry reactors offer some advantages, such as high surface area, high degradation rate, no mass transfer limitation and simple reactor structure [Mohammadiet al., 2014]. However, they also have some drawbacks, which include light penetration limitation due to the opacity of the slurry, fouling of catalysts due to the decomposition of the catalyst particles, problem of catalyst separation from the treated liquid in view of catalyst recycling and low light utilization efficiency [Shah, 2014]. At industrial level, the catalyst must be filtered before treated water being discharged, hence, a liquid–solid separator is required in the slurry reactor. The cost of the overall process increases due to installation of these separator, as the removal of the ultrafine particles is a sluggish and costly process.

In order to reduce downstream processing cost, the photocatalyst can be used in immobilized form onto some inert support. Fixed bed photocatalysis do not require separation of catalyst in a separate unit operation and the operation can be continuous.

Adsorption characteristics are also influenced by the type of support material and subsequently, the decomposition rate of pollutants also get altered [Sakthivel et al., 2002]. Furthermore, flow rate also play a significant role in tailoring rate of reaction in case of immobilized catalyst [Bideau et al., 1995; Kobayakawa et al., 1998]. The characteristics of support that should be taken into consideration include transparency to irradiation, strong bonding to the surface of photocatalyst without hampering any reactivity, high specific surface area, and separability and chemical inert [Pozzo et al., 1997]. Support materials that have been employed in the photocatalytic oxidation of water pollutants include glass, carbon fibres and woven fibre cloths. Generally loss of pressure and pore diffusion resistance is low, when fibrous supports are employed when compared with pellet shaped catalysts. Glass support have advantage to be used as a catalyst support because of its transparency to UV light in photocatalytic reactions [Kleiman-Shwarsctein et al., 2008].

In order to attain an efficacious commercial application, a number of reactor design parameters need to be optimized, such as the geometry of photo reactor, the sort of photo-catalyst and the radiation energy to be applied [Albini et al., 2010]. The essential point which need to be taken into consideration is the transmission of irradiation which should be extremely scattering and the absorbing medium having water and fine photocatalyst particles concerning the successful execution of photocatalytic reactors [Ramesh et al., 2008]. The successful scaling-up of photo-catalytic reactors comprises increasing the number of photons absorbed per unit time and per unit volume.

1.8 KINETICSTUDIES

Chemical kinetics plays a vital role in heterogeneous photocatalysis. Generally, it includes the analysis of the amount of a substrate in terms of concentration as a function of time as depicted in equation 1. The reaction rate is expressed as decreasing rate of any of the reactants with respect to time. Power law is commonly used to express the reaction rate

$$r = \frac{dc}{dt} = -kC^n \qquad (1)$$

Where, rate constant is k and n is the order of reaction.

Usually kinetic models are employed to describe photocatalytic processes, such as, pseudo first order and second order models. The term ‘pseudo’ has been placed as prefix to the order of a reaction because one of the reactants in catalytic reaction is a catalyst and its concentration remains unaltered in such a way that instead of having second order reaction, a pseudo-first order reaction is observed. Secondly, the surface of catalyst gets fully covered when the substrate is in surplus amount and the degradation of the substrate doesn’t depend

on its concentration. At such saturation level, a pseudo zero order photocatalytic reaction is observed [Theurich et al., 1996].

Langmuir–Hinshelwood (L–H) rate expression (Equation 2) has been effectually used for heterogeneous photocatalytic degradation to analyse the relation between the initial degradation rate and the initial concentration of the organic compound [Vasanth et al., 2007; Krishnakumar et al., 2011].

$$1 \div k_{obs} = 1 \div k_c K_{LH} + [MY]_0 \div k_c \quad (2)$$

Where $[MY]_0$ is the initial concentration of organic compound (mgL^{-1}), K_{LH} the Langmuir–Hinshelwood adsorption equilibrium constant ($L\ mg^{-1}$) and k_c the rate constant of surface reaction ($mg\ L^{-1}\ min^{-1}$). Dark adsorption measurement is always prerequisite for L-H type kinetic models. If the kinetically obtained Langmuir–Hinshelwood adsorption equilibrium constant is different from that obtained in dark adsorption measurement, the L–H mechanism cannot be considered [Ohtani, 2008].

1.9 OPTIMIZATION OF PROCESS PARAMETERS

The effectiveness of a photocatalytic reaction rely on various factors, which direct the performance of photocatalysis. Initial concentration of pollutant, photocatalyst loading, pH of the reaction mixture, volume of solution, agitation, irradiation time, light intensity, irradiation wavelength, and geometrical factors of the experimental setup are the important considerations. Due to the various detrimental factors, it is difficult to analyse the relative inference of several factors that affect reaction, mainly in the existence of tedious interactions. Generally, effect of one factor at a time have been tested in experiments for analysing the effect of functional factors on the efficiency of photocatalytic process which is time consuming, work demanding and also lack illustration of the effect of relations between different factors.. There are various steps involved in RSM optimization process: execution of statistically designed experiments; assessing figures of a mathematical model by using method of regression analysis for calculating the response and then evaluating the fitness of the model [Myer et al., 2002; Ray, 2006]. Box Behnken design (BBD), one of the RSM technique is used to design the experiments. The BBD is an effective technique generally used for studying three level design [Sharma et al., 2009; Patel et al., 2010]. It is applied to non-sequential experiments and allow and efficient estimation for the first order and second order coefficients with fewer design points than the central composite design (CCD). Amongst the existing statistical design approaches, a full factorial design (FFD) is reflected

as unfeasible because of its condition of a huge number of experiments for precisely guessing the response [Myer et al., 2002; Ray, 2006].

1.10 INTEGRATION OF PHOTOCATALYTIC AND BIOLOGICAL PROCESSES

AOPs are effective when compared to biological treatment but are relatively expensive. However, the use of AOPs is necessary when the solution to be treated is non-biodegradable or hardly biodegradable and there is presence of some toxic pollutants in wastewater. One economically feasible possibility to treat wastewater containing non-biodegradable pollutants consist of combining AOP and a biological treatment. AOP can be used as pre-treatment or post treatment depending on the organic content and toxicity/ biodegradability of wastewater. In order to measure the biodegradability, BOD_5/COD Ratio, Zahn-wellen's test, EC_{50} value, etc have been employed. For such type of toxic wastewater, AOPs could be employed at pre-treatment on the basis of concentrations of the compounds. Further in AOP, biorecalcitrant residuals are attenuated to smaller and biodegradable molecules which can be treated aerobically in the final stage. So photocatalysis as pretreatment may be employed to enhance the biodegradability of such pollutants and to lower the toxicity [Auzay et al., 2007]. Therefore, integration of chemical treatment and biological processes can provide alternative treatment options in purifying wastewater that are not readily biodegradable.

2.0 REVIEW OF LITERATURE

Pharmaceutical remnant may enter the living world by a various different pathways. Excretion from patients undergoing pharma treatment is the most probably utmost pathway for pharmaceutical excesses to enter in the aquatic environment. Since many pharmaceutical substances are expelled in biologically active form, generally by urine as they remain un-metabolized in the body. Drugs are emitted and released into the environment through domestic sewage as well as industrial effluents.

The pharmaceutical excesses have been identified in groundwater, surface water and municipal wastewater [Jones et al, 2005]. These compounds remain in the environment and move in the food chain, accumulate, magnify and cause damaging effects to wildlife, aquatic life and human beings. Because of contamination of water bodies by these pharmaceutical agents, the microbial community in the aquatic environs become more resistant to these chemicals. This results in the growth of more virulent pathogens and antibiotic defiant in the environment.

Various kind of pharmaceutical compounds have been identified in sewage waste water and surface waters in the past several years [Kolpin et al., 2002; Stumpf et al., 1999]. It has been reported that up to 95% of antibiotic compounds can escape unvaried into the sewage system [Patneedi et al., 2015]. Several broad spectrum antibiotics were found in high concentration in effluents that are toxic to bacteria and plants. In the sewage treatment plant, there were enterococci microorganisms that are resistant to antibiotics, that's why these antibiotics are not mineralized by sewage treatment plants. As a result, quality of drinking may get influenced when river water is used as water source [Heberer et al., 1997].

Generally, the maximum concentrations are usually reported for Non-steroidal anti-inflammatory drugs, which could be accredited to their extensive usage because they can be easily obtained without medical prescription. Most commonly consumed drug, Ibuprofen, is usually identified at an elevated concentrations of 5-10$\mu g\, l^{-1}$ [Nakada et al. 2006; Radjenovic et al., 2007; Santos et al., 2007]. Although these drugs are removed in high quantity, it is still spotted in rivers downstream due to enough consumption in human medicine. Acetaminophen (Paracetamol) and Aspirin are also other prevalent pain killer. Besides these drugs, some prescribed drugs such as β-blockers are also identified in raw sewage [Gros et al., 2007; Radjenovic et al., 2007]. The most commonly detected β-blocker in influents appears to be Atenolol [Castiglioni et al., 2006; Nikolai et al., 2006]. Furthermore, many studies have provided evidence that ATL could inhibit the growth of human embryonic cells

and was ecotoxic to freshwater species [Della-Greca et al., 2009]. Also, chlorination of ATL after the process of wastewater disinfection had phytotoxic activity [Hapeshi et al., 2010].

There are certain classes of antibiotics that may cause irreversible change in the genome of microorganism and making them resistant even at low concentration. The release of antibiotic drugs into the environment has direct lethal effect on vultures which get exposed to a nonsteroidal anti-inflammatory drug, and leads to reduction of soil microbial community. Endocrine disruption is perhaps the uppermost research urgency as a potential adverse ecological health consequences.

Similar to pharmaceuticals compounds, the Drug attritions are measured to be pseudo persistent in the environment, and thus, they are identified to be an emergent ecological pollutants of concern. They enter the aquatic stream mostly by sewage wastewater. After drug is consumed, altered form of the parent compound and metabolites are expelled by urine and enter into sewage.

2.1 BIOLOGICAL TREATMENT

Conventional activated sludge process (ASP) has been employed for the eradication of contaminant present in pharmaceutical wastewater [Gohary et al., 1995]. Kummerer and Al-Ahmad (1997) considered that due to chemical structures, there is ample variances in biodegradability of parent pharmaceutical compounds and they become more or less biodegradable due to the occurrence of sugar component or due to fluorination, respectively. As biodegradation occurs by the enzymatic reactions of chemical structures, therefore, the biodegradability of pharmaceutical compounds with different chemical structures band in the similar therapeutic class is even anticipated to diverge. Many different systems such as aerobic treatment, membrane bioreactors (MBRs), sequencing batch reactors (SBRs), sand columns, and constructed wetlands, have been studied for the biodegradation of pharmaceutical pollutants. Some of the studies highlighted biodegradation as a removal process, whereas, some inspect the complete removal by combination of processes with biodegradation. These experiments have been done both at lab scale and pilot scale.

A biodegradation study of anticancer drug 5-fluorouracil (>800 mg/l) yielded a removal of 2% [Kummerer and Al-Ahmad, 1997], whereas 50% removal has been reported with initial concentration of 50 mg/l or less of 5-fluorouracil. Pharmaceutical and personal care products (PPCPs) such as Galaxolide and tris (2- chloroethyl) phosphate are categorised as having poor removal, had specific sludge retention time (SRTs) of more than 15 d [Oppenheimer et al., 2007]. Gobel et al.(2007) reported that using activated sludge, upto 50% removal of trimethoprim and several macrolide antimicrobials was achieved with SRTs of 16

± 2 and 33 ± 3 d, but when the SRT was raised to 60–80 d, up to 90% removal was observed. Schroder et al.(2012) studied biological degradation of Non-steroidal anti-inflammatory drug (NSAIDs) and antibiotics with membrane bioreactor for SRT of 15/30 days and it was reported that NSAIDs were removed with higher efficiencies than the antibiotics, with SRT of 30 days. Biodegradation of organonitriles using activated sludge consortium was carried out and the results show that an average removal rate of 0.083 g acetonitrile g/L was achieved in the batch bioreactor at 25°C [Li et al., 2007c]. Kimura et al.(2007) considered six pharmaceuticals (Clofibric acid, Diclofenac, Ibuprofen, Ketoprofen, Mefenamic acid, and Naproxen) in a real wastewater treatment plant (WWTP) and analyse their elimination employing an ASP and membrane bioreactors (MBRs) with SRTs varied from 7-65 days and it was reported that the MBR with a longer SRT of 65 days showed enhanced performance when compared to smaller SRT of 15 days. Theoretically, it is assumed that by enhancing the SRT a positive impact on the biodegradation of pollutants is expected. But in a study of Joss et al. (2005) observed no enhancement in degradation of Roxythromycin with increased SRT. Radjenovic et al. (2007) analyzed biological removal of various analgesics, anti-inflammatory and antibiotics in a Bench scale reactor using MBR technology.

For Diclofenac, less removal efficacy has been reported (21.8 ± 28.5%) in a field scale membrane bioreactor, but for Ibuprofen, 97% of removal rate has been reported [Radjenovic et al., 2009]. In general, it has been reported that Ibuprofen has the highest removal rate among all pharmaceutical drugs, as it is easily biodegradable, and degradation over 95% has been documented in bench scale experiments and wastewater treatment plants [Monteiro et al., 2010]. For most of the compounds, 80% degradation has been achieved almost in 60 days. One of the study reported that anaerobic bench scale experiment that showed removal of Ibuprofen (30–60%) under anoxic conditions and degradation of Diclofenac upto 80% has been reported [Carballa et al., 2007]. In few WWTPs 50–70% reduction of Diclofenac (DCF) was stated [Ternes, 1998; Thomas and Foster, 2005; Castiglioni et al., 2006; Radjenovic et al., 2007].

Casas et al.(2015) studied biological degradation of hospital wastewater using moving bed biofilm reactor in both batch and continuous mode and found removal rate to be maximum in batch mode when compared to continuous mode. Blanch et al.(2014) assessed biological degradation of 28 different pharmaceutical compounds by employing MBR sludge and observed 66% degradation of 12 out of 28 compounds.

In general, biological methods are inadequate for exclusion of all possibly harmful components present in the wastewater even with an extended Hydraulic retention time (HRT)

[Joss et al., 2005; Raj et al., 2005]. The biological and physiochemical treatment methods are less efficient for purification of pharmaceutical wastewater [Hahn et al., 1999; Kornaros et al., 2006; Ginnivan et al., 1981].

A combined anaerobic-aerobic treatment for pharmaceutical wastewater proved to be effective in reducing COD but not in removal of antibiotics [Kummerer, 2001]. Alexy et al. (2004) demonstrated that antibiotics are not readily biodegradable and their genotoxicity is not eliminated by biological treatment. Conventional biological processes do not show adequate performance, specifically for industrial wastewater treatment, because various organic components generated by the industry are non-biodegradable and are toxic [Lapertot et al., 2006]. Therefore, the use of advanced technologies is the possible option which is based on chemical oxidation and is recognized as highly proficient treatment for biorecalcitrant compounds.

2.2 ADVANCED OXIDATION PROCESSES (AOPs)

AOPs have been known in the initial 1970s as the auspicious arena of research for degradation of pollutants and therefore, research and development work started on this technology. AOPs have been lately getting the attention, as showed by the enormous kind of research studies [Herrmann et al., 1999; Tarr, 2003; Gogate and Pandit, 2004; Parsons, 2004]. AOPs comprise oxidation in two phases i.e. the production of strong oxidants and then followed by the reaction of the oxidants with contaminants in water sample. The utmost commonly used AOP is the Fenton process to attenuate persistent organic pollutants (POPs) [Andreozzi et al., 1999]. However, the effectiveness and application of this method can be improved by exposing the treated water by UV light or visible light [Tarr, 2003]. Other photochemical methods, such as heterogeneous photocatalysis, using catalyst in suspensions or immobilized mode [Herrmann et al., 1999; Konstantinou and Albanis, 2003] as well as ozonolysis [Rosenfeldt et al., 2006], have also been cited in literature for degradation of pollutant. Degradation of Amoxicillin by photofenton showed that under optimum operating conditions, complete degradation of Amoxicillin was achieved in a minute [Trovo et al., 2011]. The degradation of Paracetamol was assessed using laterite soil and $FeSO_4$ as iron source in Fenton process and it has been observed that degradation of Paracetamol with iron from soil was less when compared to iron from $FeSO_4$ [Manu et al., 2011]. Oxidation of theophylline in water has been carried out using oxidation process by H2O2/UV photolysis and observed $k_2 = (8.22 \pm 0.03) \times 109\ dm^3\ mol^{-1}\ s^{-1}$ at pH 6 [Paul et al., 2014]. The oxidative degradation of drugs such as Ibuprofen and Diclofenac have been studied with combined application of ozone and hydrogen peroxide resulting in almost 98% of degradation

efficiency [Zwiener et al., 2000]. The treatment of concentrated Sulfamethoxazole (SMX) solutions was evaluated by AOPs using photolysis, UV/ H_2O_2 and photo-Fenton under UV/ sunlight and results indicated that SMX showed the maximum photolytic degradation efficiency with UV light [Gonzalez et al., 2009]. The photodegradation of pharmaceutical antibiotic (Cephalosporin, Penicillin) and veterinary antibiotics in aqueous suspension using H_2O_2 and ozone has been reported [Balcioglu et al., 2003]. The efficacy of UV/ H_2O_2 treatment for the removal of six pharmaceuticals compounds has been investigated (Meprobamate, Carbamazepine, Dilantin, Primidone and Trimethoprim) and it was found that degradation efficiency is directly associated to amount of hydroxyl radicals produced [Ortiz et al., 2010]. Photocatalytic degradation has been asses for removal of dyes using green approach and assessed the various parameters affecting degradation of dyes [Chowdhury et al., 2015].Degradation of ECF bleaching wastewater has ben carried out by employing TiO2 (0.5g/L) at pH 7 and observed 66% removal of COD in 4h of irradiation under UV irradiation [Kumar et al., 2012].

Heterogeneous photocatalysis in the aqueous medium using TiO_2 has been employed widely, primarily for the oxidation of organic contaminants [Mills and Le Hunte, 1997]. This treatment is effective for removing a various inorganic and organic pollutants. Number of applications of heterogeneous TiO_2 photocatalysis, primarily in the area of water purification, have been recently analyzed [Mills and Le Hunte, 1997; Fujishima et al., 2000; Pelaez et al., 2012]. For example, various toxic compounds, such as cyanide, bromate etc. have been attenuated into nontoxic or least toxic compounds such as CO_2, bromide, sulphate [Mills and Le Hunte, 1997]. Heterogeneous TiO_2 photocatalytic degradation has also been explored for pesticides [Herrmann et al., 1999; Konstantinou and Albanis, 2003] and pharmaceuticals [Sakkas et al., 2007].

There are numerous published papers about degradation of Pharmaceutical and personal care products (PPCPs) in waters by TiO_2 photocatalyst. TiO_2 has been reported to be one the most popular and efficient photocatalysts in the degradation of some antibiotics such as Lincomycin, Tetracycline, Oxolinic acid, and Fluoroquinolone. [Paola et al., 2006, Palominos et al., 2008]. Ghajar et al. (2012) studied photocatalytic degradation of Aspirin in aqueous solution using TiO_2 as photocatalyst under UV irradiation and obtained 73% degradation of the model compound. Chatzitakis et al. (2008) studied photocatalytic degradation of Chloramphenicol using TiO_2 and ZnO and observed that both photocatalyst showed equal mineralization in 90 mins. Pouretedal et al. (2013) analyzed photocatalytic degradation of β-lactam antibiotics such as Amoxicillin and Ampicillin. Photocatalytic

degradation of Paracetamol showed that degradation efficiency increased with combined effect of TiO_2 / H_2O_2 and reaction followed second order rate kinetics [Yang et al., 2009]. Degradation of Bezofibrate in the presence of TiO_2/solar light showed that photocatalysis is more efficient than photolysis [Lambropoulou et al., 2008]. Xekoukoulotakis et al. (2010) reported the use of UV/TiO_2 to achieve 90% TOC reduction of Erythromycin after 90 minutes of reaction. Similarly, 82% of Sulfamethoxazole degradation and 23% TOC removal by UV/TiO_2 has been reported in 6h [Abellan et al., 2007]. Photocatalytic degradation performed in an annular slurry photoreactor for two organic solvents in water was studied in the presence of carbonate and bicarbonate, which are hydroxyl radical scavengers and observed that bicarbonate and carbonate ions acted as hydroxyl radical scavengers and slowed down the DIOX degradation rate but did not significantly affect the THF degradation rate [Mehrvar et al., 2001].

Hapeshi et al. (2010) investigated the effect of type of catalyst, catalyst dose, initial substrate concentration, pH and H_2O_2 as an additional oxidant on substrate conversion and mineralization in photocatalytically degradation of drugs like Ofloxacin and Atenolol using P25 TiO_2. Zhang et al. (2008) analyzed the photocatalytic activity for Acetaminophen in TiO_2 solution in slurry mode under 250 W of halide lamp. The effect of various factors such as initial concentration of drug, initial pH value, TiO_2 dosage, etc were analyzed in the degradation of Acetaminophen. Hu et al. (2007) assessed the degradation of Sulfamethoxazole by TiO_2 under UV light and found the rates of degradation are reliant upon numerous factors, such as the initial concentration of SMX, concentration of catalyst and the occurrence of non-target water ingredients like bicarbonate ions may act as $HO^{\cdot}$ scavengers. Hu et al. (2007) also analyzed that the occurrence of natural organic matter hinders photocatalytic degradation of SMX to a greater extent at pH 5 when compared to pH 9. Further, the occurrence of bicarbonate result in enhancing photocatalytic degradation of SMX at pH 9. Direct photolysis and solar TiO_2 photocatalysis of Trimethoprim (TMP) in various water matrices have also been reported [Sirtori et al., 2010]. It was found that, TMP was totally eradicated in both water matrices (demineralise and simulated seawater) at a similar rate, however, the degradation rate was significantly reduced in seawater, which can be due to presence of inorganic species that act as $HO^{\cdot}$ Scavengers [Sirtori et al. 2010].

Photocatalytic degradation of Amoxicillin was studied using TiO_2 under solar radiation with the degradation efficiency of 71% [Pereira et al., 2013].Braz et al.(2014) assessed photocatalytic degradation of Ibuprofen under TiO_2/UV irradiations and observed complete IBF removal in less than 60 mins of irradiation time. Jallouli et al.(2016)

investigated photocatalytic degradation of Naproxen using TiO_2 as photocatalyst and observed 98% removal at pH 6.5.

2.3 ADVANCEMENTS IN PHOTOCATALYSTS

One of the main drawbacks of using commercially available TiO_2 photocatalyst is that its band gap (3.2 eV) is high and lies in the UV range of the electromagnetic spectrum [Wang et al., 2008]. As a result, only UV light can generate the electron–hole pairs and start the photocatalytic process. However, it is well known that solar light consist of only 3–5% of the UV light. To study photoactivity under various environmental conditions, P25 TiO_2 is considered as standard reference catalyst [Serpone et al., 1996]. Further, it is important to mention that the recent progress of various methodologies to alter TiO_2 for enhanced use of visible light, include non-metal and metal doping, dye sensitization, and coupling of semiconductors [Pelaez et al., 2012]. Sud et al. (2012) studied photocatalytic degradation by employing TiO_2 and ZnO as photocatalyst in different ratios for degradation of malachite green and observed maximum degradation using 9:1 (TiO_2: ZnO) at 1g/L concentration.

So scientists are working extensively to shift TiO_2 optical response to the range of solar light. In order to achieve this, various attempts have been made to enhance the photocatalytic activity of photocatalyst by inculcating an adequate percentage of a metals and Non-metals [Penner et al., 2006; Choi et al., 2007; Yoong et al., 2009] known as dopants. In the early 1980s, it was discovered as a modification technique and since then, doping has been frequently used method in the treatment of waste water for degrading organic compounds [Kamat et al., 2010]. In order to increase efficacy in solar light, it is of great interest to employ doped catalyst so that its cost of operation can be reduced[Sivalingam et al., 2003].

The insertion of different types of dopants in the synthesis of nano doped TiO_2 photocatalysts has been studied so as to improve the morphology and photocatalytic activity of catalyst. Various metal dopants, including Cobalt [Hsieh et al., 2009, Suriye et al., 2005], Barium [Atashfaraz et al., 2007], Manganese [Zhang et al., 2006], Nickel [Wang et al., 2008] and Iron [Janes et al., 2004, Deng et al., 2009], have been examined for their potential to boost the photocatalytic performance.

Doping of Non-metals anion has been inspected thoroughly because the electronic states of non-metals are above the valence band edge of TiO_2. So, different non-metal dopants (C, N, S) has been verified to check their ability to enhance the morphology and photocatalytic activity [Chen et al., 2007, Livraghi et al., 2009]. Anionic impurities such as

N, C, S, B and P were employed as dopants for extending the optical absorption of TiO_2 to the visible region of the spectrum [Hoffmann et al., 1995]. Basically the percentage of the anatase phase increases on addition of non-metal anions in TiO_2, and it also limit the growth of crystallite size of TiO_2, and leads to increases of specific surface area [Yu et al., 2009]. Degradation of 2-chlorophenol has been studied using S doped TiO_2 synthesized by ultrasonic radiations and profound improvement in photocatalytic activity was observed at pH 6 due to reduction in band gap to 2.47ev from 3.2ev [Sud et al., 2015].

Similarly, doping with non-metals such as N/F-TiO_2 and C/N-$ZnWO_4$ [Yamakata et al., 2003; Kudo et al., 2009] has been used to lower charge faults, but in few cases, the quantum efficiencies remain incomparable with the excited photocatalysts. The presence of metals as dopant, such as Pt, Pd, Au and Ag has been reported to boost the photocatalytic activity of catalyst. Wang et al. (2012) synthesized Ag–AgBr/TiO_2 photocatalyst to analyze degradation of IBP and result showed that after 6h of LED irradiations, 81% of organic carbon was mineralized with decrease in toxicity, however, same experiment conducted in solar light using Ag doped TiO_2 showed less degradation efficiency, Moreover, the use of Ag metal ions as dopants seems to be expensive when compared to other metal ions or transition metals.

Various studies have shown that class of Bismuth Oxide such as Bi_2WO_6, $BiVO_4$, Bi_2O_3, Bi_3O_4Cl, Bi_2MoO_6 and Bismuth-doped TiO_2 have shown noteworthy results in visible light for degradation of organic pollutants [Tang et al., 2004; Wang et al., 2008]. Among various transition metal ion dopants, Ni^{2+} ions also appears to be a proficient doping agent for TiO_2 as it enhances the photocatalytic activity of semiconductor photocatalysts by trapping the electrons and helps in charge separation [Begum et al., 2008]. Photocatalytic degradation of phenol as been carried out using surface modification of TIO_2 with Ag metal ions and significant enhancement in degradation has been reported as compare to bare TIO_2 [Grabowska et al., 2013].

Studies have been carried out to enhance the photocatalytic efficiency of TiO_2 or ZnO doped with metal oxide like SnO_2 [Zheng et al., 2008; Shi et al., 2000], WO_3 and some rare earth oxides like LaO_2, TbO_2, ErO_2 [Lin et al., 1998]. Doping of these metals fundamentally reduces the band gap of TiO_2 for the photo-excitation (red shift) and also reduces the recombination of electron–hole pairs generated by photons. Currently, a foremost demanding objective is to have stable doped nanomaterials with suitable possessions that can successfully absorb visible light and is affordable. Kouame et al. (2015) synthesize the Bi

zero-valent clusters on TiO2-P25 by radiolysis and analyzed its efficiency for photocatalytic degradation of Rhodamine B and observed highest efficiency with 0.5wt% Bi ions.

Different doping methods such as sol gel, coprecipitation, hydrothermal and impregnation have been applied to impregnate the small amount of dopant into the crystal lattice. Research findings have revealed that sol gel method is the most commonly used method for preparation of TiO_2 or doped TiO_2 since nanocrystals synthesized are of high purity at even low temperatures [Mogal et al., 2013; Kim et al., 2008]. Yu et al. (2007) analyzed degradation efficiency of nitrogen doped TiO_2 prepared by sol gel method at the calcinations temperature ranging from 300–700^oC and found that maximum dye degradation of 98% was attained with catalyst calcined at 500^oC.

Gurkan et al. (2012) studied photocatalytic degradation of Cefazolin using N-doped TiO_2 synthesized by wet impregnation method and reported 76% degradation in 90 mins of irradiation. Hayder et al. (2012) analyzed degradation of Ofloxacin using Ag-TiO_2 prepared by Liquid Impregnation Method and observed 90% degradation in 120 mins of irradiations. Shokri et al. (2013) studied photocatalytic degradation of Chloramphenicol by synthesizing Ag-TiO_2 using photo deposition method and reported 88% reduction in TOC after 120 mins of irradiations. Hossaini et al.(2014) reported 96.3% degradation of Dizinon by modification of TiO_2 by mix-doping with metal (Fe) and non-metal (F,N,S) elements (FeFNS-doped TiO_2) in presence of UV LED in 100 minutes of irradiation exposure. It was indicated that synthesized Fe^{3+} doped TiO_2 elongate its absorption wavelength to 500 nm and exist in trivalent ionic state replacing Ti^{4+} in TiO_2 lattice. Asiltürk et al. (2009) stated that the crystallite size and the particle size of the Fe^{3+} doped TiO_2 were lesser than that of undoped-TiO_2, which could indicate that the occurrence of Fe^{3+} in the reaction might be used to regulate the particle and crystallite sizes of the oxides. Cu doped ZnO prepared by precipitation method and Ni doped TiO_2 prepared by liquid phase deposition for degradation of organic compounds showed that degradation efficiency increased with increase in amount of dopant [Begum et al., 2008; Milenova et al., 2013]

2.4 GRAPHENE BASED COMPOSITES

In order to enhance the photocatalytic effectiveness, composites consisting of carbonaceous materials have been studied. Composite of graphene and TiO_2 / ZnO have shown valuable increase of photocatalytic activity because of the property of the graphene that it can result in charge separation and performed effectively when employed as an electron carrier in hybrid materials. [Zhang et al., 2010; Kim et al., 2012; Ng et al., 2011]

Ashkarran et al. (2015) studied photocatalytic degradation of methyl orange and phenol red using graphene ZnO composite prepared by combination of improved hummer and arc discharge methods in liquidand found a major enhancement in degradation of parent compounds. Zhang et al. (2010) synthesized a graphene-TiO_2 composite and stated enhancement in the photocatalytic activity for the removal of methylene blue. Most lately, it has been revealed that TiO_2-graphene express an improvement of photocatalytic activity for removing methylene blue in an aqueous solution. Numerous graphene−semiconductor combinations have been reported [Zhang et al., 2010, Liang et al., 2010, Fan et al., 2011, Zhang et al., 2011] by means of either surfactant aided growth or simple physical mixing of pre synthesized nanoparticles and graphene.

Photocatalytic degradation of Tetracycline was carried out using CdS/ ZnS-RGO heterostructure nanoparticles under visible light and 88% degradation has been observed in 60 min [Tang et al., 2015]. Zhou et al. (2015) studied photocatalytic degradation of Tetracycline employing Alkaline earth ions- doped CdSe/rGO photocatalyst, resulting in 85% reduction of model compound under visible light. Tao et al. (2015) analyzed the photocatalytic degradation of acetaminophen using graphene/TiO_2 nanotubes and observed 95% degradation of parent compound. Yu et al. (2015) studied photocatalytic degradation of Metoprolol by employing Ag- Bi_2WO_6- GO nanocomposite under solar irradiation and observed 100% elimination within 2h.

2.5 PARAMETRIC OPTIMIZATION

In a process which involve multiple responses, need optimization of the experimental conditions so as to produce desirable values for all variables to be considered simultaneously. Degradation of various dyes has been studied using BBD technique by employing either TiO_2 or ZnO and obtain upto 97% degradation with R^2 value of more than 0.915 [Annadurai et al., 2000; Ay et al., 2009; Vaez et al., 2012; Chaibakhsh et al., 2015].Kansal et al. (2007a, 2007b) carried out photocatalytic degradation of 2,4,6-trichlorophenol and catechol with P25 TiO_2 and found significant COD reduction at optimum process parameters (catalyst dose-1.1g/L, pH 4) and complete degradation of catechol at pH 6 with 2g/L TiO_2 obtained by employing Response surface methodology. Kansal et al. (2009) attempted for photocatalytic degradation of 2,4 DCP under UV light using P25 TiO_2 and sodium hypochlorite as oxidant by inculcating Box Behnken design for optimization of process parameters and found total abatement of model compound at optimum conditions. Ray et al. (2009) applied Box Behnken design to analyse photocatalytic degradation of phenol and study effect of four

different variables and attain maximum degradation rate of 0.083min^{-1} with 1g/L TiO_2 for 40ppm phenol concentration.

Zhang et al. (2010) applied experimental design methodology for degradation of chloramphenicol using TiO_2 as photocatalyst and approached 85% degradation under optimum conditions with significant effect of pH on reaction. Tantriratna et al. (2011) investigated photocatalytic degradation of Paraquat by employing Box Behnken Design experimental method for optimization of process parameters using immobilized TiO_2 and obtained 90% removal with 2g/L catalyst dose for 10ppm initial concentration. Sahoo et al. (2013) elaborated the application of response surface methodology for photocatalytic degradation of Thiazine Dye using Ag doped TiO_2 and observed 96% degradation at optimum dose of 1.97g/L of photocatalyst by employing BBD method. Singh et al. (2014) assessed the photocatalytic degradation of aqueous solution of Acrylonitrile using ZnO as photocatalyst and H_2O_2 as oxidant under UV light and attained 89% of degradation efficiency under optimum conditions of pH, catalyst dose and oxidant concentration as suggested by BBD Technique.

2.6 IMMOBILIZATION OF PHOTOCATALYST

In order to eliminate the step of separation of catalyst from the effluent after treatment, catalyst needs to be immobilized on some inert surface. Different techniques for immobilization such as chemical vapour deposition, slip coating [Djafer et al., 2012], dip coating [Djafer et al., 2012], film casting [Damodar et al., 2009], electrospinning [Liu et al., 2012; Bedford et al., 2012] and dip-evaporation has been employed to attain the immobilization of TiO_2 on substrates.

Amongst numerous approaches, the solgel method has been extensively employed because of advantage of low cost and an easiness to apply to a different sizes and forms of the substrates. Sol gel method comprises the distribution of suspended particles in Brownian motion in substrate solution. The suspensions of particles of catalyst get transformed to viscous gels and finally to solid materials by the sol–gel treatment [Hench, 1990].

Laoufi et al. (2013) reported photocatalytic degradation of Tylosin onto P25 TiO_2 catalyst immobilised on glass substrate by dip coating technique and found 98% degradation after 7h under UV irradiations. Koutantoua et al. (2013) investigated the photocatalytic degradation of synthetic Estrogen 17-ethynylestradiol (EE2), using ZnO catalyst immobilized on glass plate with dip coating method and reported 80% conversion in 90 mins.

Similar to slurry mode experiments, there also prevails an optimal catalyst concentration for immobilized system [Mehrotra et al., 2003]. Ray and Beenackers. (1997)

reported the effect of thickness of layer of catalyst for immobilized system for the photocatalytic degradation of dye. Similarly, Chen et al. (2000b) analyse of the effect of mass transfer and catalyst layer thickness on photocatalytic degradation rate. Immobilization of TiO_2 on different adsorbents was carried out to analyse degradation of orange II dye with catalyst loading varying from 10-80% and it was observed that overall removal efficiency was better by immobilized TiO2 adsorbed on adsorbent than that of bare TiO_2 produced by the sol–gel method and commercial catalyst, Degussa-P25 [Bhattacharyya et al., 2004]

For degradation of organic pollutants different type of support materials can be employed such as glass, carbon, and woven cloths fibres [Pozzo et al., 1997]. Glass is mostly used as rigid support for the immobilization of TiO_2 [Zhuang et al., 2010; Pelentridou et al., 2009]. The prime benefit of using glass substrate is the transparency in the whole treatment process even after the immobilization which results in improved photocatalytic rate. Chen et al. (2000b) reported an immobilization of TiO_2 on glass using non-ionic surfactant templated by the dip coating technique. Surfactant has been used so as to get uniform and crack free TiO_2 surface with mesoporosity to the calcined glass TiO_2 films. The catalyst can be recovered by [Ibanez et al., 2003] cross-flow filtration [Doll and Frimmel, 2005] or other membrane filtrations [Zhao et al., 2002; Zhang et al., 2008a]. Coupling of coagulation with the microfiltration (MF) reported the recovery of the residual 3% of the catalyst particles for reprocess [Malato et al., 2009]. Even with membrane integration process, various functional issues with slurry TiO_2 still persist. These include the types of membrane, pore size, blockage, back washing and fouling [Lee et al., 2001; Molinari et al., 2002]. Large surface area to volume ratio can be achieved with nanosize TiO_2 catalyst and it also enhance the effective charge separation and trapping of charges at the surface [Nagaveni et al., 2004a, b]. No doubt that the physical and chemical properties of nanoscale TiO_2 catalysts get enhanced significantly, but size of the particle and its morphology are the major matter of concern in a pilot scale water treatment process [Byrne et al., 1998b; Yu et al., 2002].

Problem of mass transfer can be fixed using nanofibers, nanowires or nanorods, due to their thin longitudinal structure. However, an advantage of using nano fibres is that they can be designed into MF, ultrafiltration (UF) and photocatalytic membranes (PMs). Zhang and co-workers explained the commercial accomplishment of synthesized MF and UF membranes [Zhang et al., 2008a, b].

Due to cost effectiveness and the high adsorption capacity, natural clays have been used widely in immobilization as support. No doubt that clays are catalytically inactive, but their increased adsorption capacity has been enhancing the surface contact during

photocatalysis reaction. It was anticipated that to immobilise TiO_2,natural clays should not be employed because of the presence of different impurities bounded to lattice that interact and alter the catalyst efficiency of the immobilised layer [Chong et al., 2009]. Photocatalytic degradation of drugs such as Ibuprofen, Atenolol and Carbamazepine has been conducted using immobilized TiO_2 with alginate beads by impregnation technique [Sarkar et al., 2015].

2.7 INTEGRATION OF PHOTOCATALYTIC AND BIOLOGICAL PROCESSES

Pharmaceuticals are considered as harmful pollutant among various emerging contaminants because they have endocrine disrupting properties. Biological treatment has lower operating cost compared to other alternatives because microorganisms that are already present in wastewater treatment feed on the complex substances in the wastewater, and converting them into simpler substances. On the basis of type of wastewater, compound involved and its concentrations, the integration of AOPs and biological processes could be considered in various alignments. In order to enhance the biodegradability and to detoxify effluents containing such compounds, coupling of AOPs with various other treatments such as with AOPs have been considered [Coleman et al., 2005; Belgiorno et al., 2007; Naddeo et al., 2010]. In general, the removal efficiency of pharmaceutical compounds could be improved by coupling the biological treatment with advanced oxidation technologies (AOTs) such as ozonation, Fenton process and photocatalyst treatments [Klavarioti et al., 2009]. Bandara et al. (1997) employed photo Fenton as pretreatment method followed by biological method for the removal of paranitrotoluene-ortho-sulfonic acid. The intermediary formed in the photocatalytic treatments were identified as biodegradable. Horsch et al. (2003) studied degradation of stilbene-based fluorescent whitening agents by combination of advanced oxidation and biodegradation processes. AOPs boost the biodegradability of low biodegradable of such wastewater generally by reducing the COD load [Aye et al., 2004; Tabrizi et al., 2004]. Reddy et al. (2004) assessed degradation of Pyrazinamide drug by employing photocatalysis using TiO_2 as photocatalyst followed by biological treatment and found 91% removal of COD in 44h of treatment. Similarly, Pretreatment by photocatalysis can be employed to enhance the biodegradability of pollutants and also to reduce its toxicity [Auzay et al., 2007].Similar concern arises from the study of Oller et al. (2007), showing the degradation of α-methylphenylglycine at pilot scale, by combining Fenton process with a biological reactor. In this study, the degradation attained by the combined process was assessed in terms of DOC and was perceived to reach values up to 95%. Degradation of α-methylphenylglycine, Alachlor, Atrazine, Chlorfenvinphos, Diuron, Isoproturon using photo fenton along with biological treatment showed 90% degradation of compound [Oller et al.,

2007; Lapertot et al., 2007]. Sangave et al. (2007) assessed the efficacy of a combination of US/ozone treatment in refining the aerobic degradation of distillery wastewater and reported a COD reduction up to 45%. Integrated method having ozonation as pre-treatment before biological processing of distillery wastewater resulted in around 79% removal of pollutants, compared to 35% COD removal without ozonated treatment. Varatharajan et al. (2007) investigated the treatability of wastewater from a pharmaceutical industry by combined solar photofenton oxidation and activated sludge process and obtain BOD and COD removal of 93 and 95 %, respectively.

Sirtori et al. (2009) assessed the efficiency of photofenton process biological treatment for degradation of Nalidixic acid and attain 95% degradation of which 33% correspond to the solar photochemical process (190 min) and 62% to the biological treatment. Fenton reaction sequential with membrane bioreactor (MBR) was employed for the treatment of the waste water from an integrated dyeing wastewater treatment plant and biodegradability was assessed, both after coupling Fenton with MBR system and the Fenton treatment alone [Feng et al., 2010]. The sequential photocatalytic/biological treatment of a contaminated groundwater from a local industrial site was studied using a corrugated plate photoreactor and observed that optimal pretreatment time of Photocatalysis significantly enhance the extent of biological nitrification [Zhang et al., 2002]. Yahiat et al. (2011) studied degradation of Tetracycline and Tylosin by employing photocatalysis as pretreatment followed by activated sludge process resulting in significant decrease in COD. Integrated biological and advanced oxidation process employing TiO_2 has been evaluated forthe degradation of Carbamazepine (CBZ) drug which showed 95% removal of CBZ [Laera et al., 2011].

The effect of coupling of AOP and biological treatment has been studied on degradation of wastewater from chemical process industries by applying Fenton treatment along with varied concentration of H_2O_2. Similarly effect of integration of biological and photocatalytic processes for degradation of bio-recalcitrant compounds from pulp and paper mill effluent has been investigated and sequential treatment was found to possess higher degradation efficiency than the independent treatments [Dhir et al., 2011]. Kumar et al. (2012) treated the pharmaceutical waste water by coupling photo-Fenton process with an aerobic sequential batch reactor (SBR) and obtain 90% COD removal after 60min of photocatalytic treatment at optimum conditions followed by biological treatment.Degradation of Atenolol by coupling of AOP and biological treatment showed 66% reduction in COD in 4 h [Hussain et al., 2013].

2.8. RATIONALE FOR STUDY

Although the homogeneous and heterogeneous photocatalytic processes have been widely recognized for the degradation of model compounds and wastewater from pharmaceutical industry but the applicability of this technology is still lacking. The literature on this aspect reveals the following technological gaps.

a) The treatment of pharmaceutical industry effluents remains a challenge for the environmentalist because of its high COD loading and the presence of bio-recalcitrant compounds.
b) Biological processes which include activated sludge process have been employed in the degradation of pharmaceuticals from sewage/ industrial effluents and reported to be inefficient even with longer retention time.
c) AOP's are expensive due to high electrical energy demand for production of photons and the consumption of chemical reagents. In order to make the process cost and energy effective.
d) In case of photocatalytic processes, the recover and reusability of photocatalyst from the aqueous suspension is another associated problem and further research on immobilization of catalyst needs to be explored further.
e) Electron hole recombination is the major problem associated with photocatalysis which needs to be addressed.
f) Use of doped photocatalysts for the treatment of pharmaceutical compounds under solar irradiation need to be investigated.
g) Further, composites consisting of carbonaceous materials have not been extensively studied for the photocatalytic degradation of pharmaceuticals.
h) There are limited reports that exist on the integrated photocatalytic-biological treatment of pharmaceutical compounds present in wastewater so further study is required in this direction.
i) To the best of our knowledge, no report manifests the integration of solar assistive photocatalytic processes in the existing biological treatment for the degradation of pharmaceuticals simulated effluents.

Keeping these observations in mind, the present study is focused on the photocatalytic degradation of commonly used pharmaceuticals with commercial (P25 TiO_2) and doped (such as Fe, Bi, Ni, Bi-Ni co-doped) TiO_2under UV/solar irradiations at optimized conditions. Additionally, Graphene based TiO_2/ZnO composites were also synthesized and their efficacy

was assessed in comparison to P25 TiO_2/ZnO for the degradation of Atenolol under solar irradiations. To overcome the problem of separation of catalyst after photocatalysis, activity of the synthesized composite(TiO_2-G) was also analyzed under immobilized mode. Moreover, parametric optimization of composite in slurry and immobilized mode was carried out using BBD. Finally, integrated treatment involving sequential photocatalytic-biological processwas employed for the degradation of simulated pharmaceutical effluents and optimal time required in each process of the integrated treatment was assessed.

3.0 MATERIALS AND METHODS

This chapter includes all the chemicals and reagents required for photocatalytic degradation of model compounds and simulated effluent. The experimental methodologies applied for synthesis and immobilization of catalyst has been discussed. Further the various reactor systems employed in the study has been elaborated.

3.1 MATERIALS

In order to carry out degradation of model compounds and synthesis of doped photocatalyst/ composites, various chemical and reagents have been procured and used as given below:

3.1.1 Chemicals

Model compounds such as Aspirin, Ibuprofen, Ofloxacin and Atenolol were procured from Sigma Aldrich, USA and used as such without further purification. Sodium acetate, methanol, potassium dihydrogen phosphate and sodium chloride employed in making simulated effluent were also procured from Sigma Aldrich. Ferrous Nitrate (Fe (NO_3) $5H_2O$), Bismuth Nitrate (Bi (NO_3) $5H_2O$) and Nickel Nitrate (Ni (NO_3) $5H_2O$) used as dopants were procured from Merck. Titanium Isopropoxide, Acetylacetone, Ethanol, acetonitrile (HPLC grade), methanol (HPLC grade), ortho-phosphoric acid, acetone and phosphate buffer were also purchased from Merck. Hydrochloric acid (HCI) and Sodium hydroxide (NaOH) were obtained from HD Fine chemicals, India. Double distilled water was used for preparation of solutions.

3.1.2 Photocatalyst

Titania P-25 (surface area 50 m^2/g and average particle size 30 nm) was obtained from P25, Germany and was used as received. ZnO (5 m^2/g) was purchased from Merck, Germany and were used as such. Graphene oxide was procured from University of Waterloo, Canada.

3.1.3 Sludge sample

Fresh Activated sludge was procured from waste water treatment plant, Kipps lane, London, Ontario, Canada and was used as such in experiments. Sludge sample was added in different percentage of 2% (20ml), 5% (50ml), 10% (100ml) &15% (150ml) in 1000ml of simulated effluent.

3.2PHOTOCATALYTIC REACTORS

Various reactors employed in the photocatalytic degradation of pharmaceutical compounds & effluents have been listed below:

3.2.1 UV reactor

The UV reactor (rectangular) was made up of cast iron sheets with wooden roof equipped with seven UV tubes of 36W (Philips) each having wavelength of 365 nm (Fig 3.1). Maximum UV intensity was found to be 5-10 W/m^2 at the middle of the UV reactor and all experiments were performed at this UV intensity. The photon flux was approximately 0.625 W. The intensity of light was measured with help of radiometer (EPPLEY, USA).

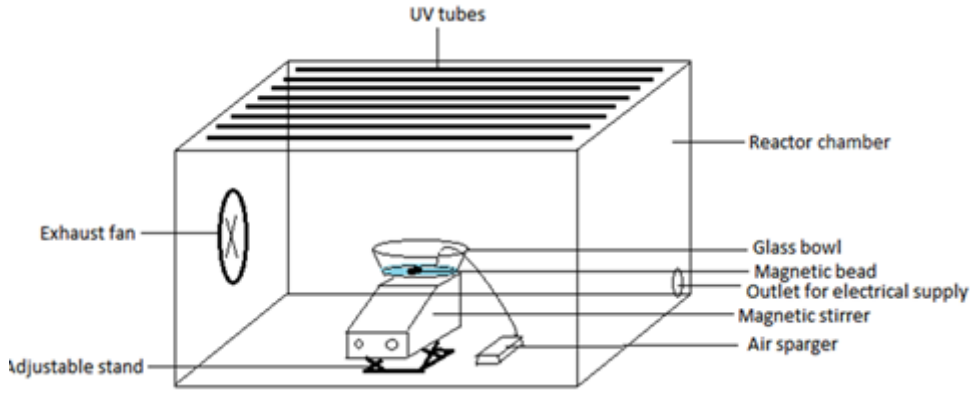

Fig 3.1 Schematic representation of UV reactor

3.2.2 UV LED reactor

The reactor having UV-LED as an irradiation source was made up of wood with dimensions of 45"×28"×28" and inner lining of cast iron which absorbs excessive heat. The reactor was divided into three chambers using sliding cast iron sheets (Fig 3.2). The whole chamber was painted black from inner side. The chamber used in this study consists of 10 watts UV LED (wavelength of 365nm).

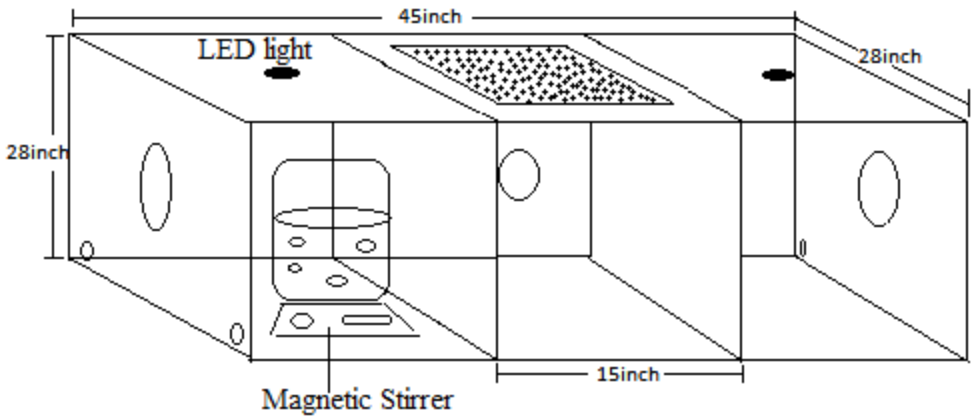

Fig 3.2 Diagrammatic representation of LED Reactor chamber

3.2.3 Swirl flow reactor

The swirl flow reactor having two spherical glass plates (each of diameter 0.09 m) were sited between soft padding held within stainless steel and aluminium casing parted by 0.01 m distance (Fig. 3.3). The catalyst was immobilized on the top side of the bottom glass plate. The solution of model compound was allowed to flow tangentially within the reactor. This reactor was placed inside wooden box having lamp and fan to guard the lamp from overheating. The lamp (Sylvania-Mercury vapour lamp: 175W) was placed at a distance of 0.1 m from the bottom glass plate on a holder. Facility was made for employing metal screens of diverse mesh size among the lamp and bottom glass plate to attain different light intensities. Complete experimental set-up consists of swirl flow reactor illuminated with UV light, pump, air sparger and storage tank of 1 L capacity with provisions for stirring as shown in Fig. 3.4. Reactor was operated in recycle mode at a flowrate of $1.15 \times 10{-}5\ m^3/s$. Same set-up with similar conditions was used for slurry mode experiments without coating photocatalyst on the glass plates of swirl flow reactor.

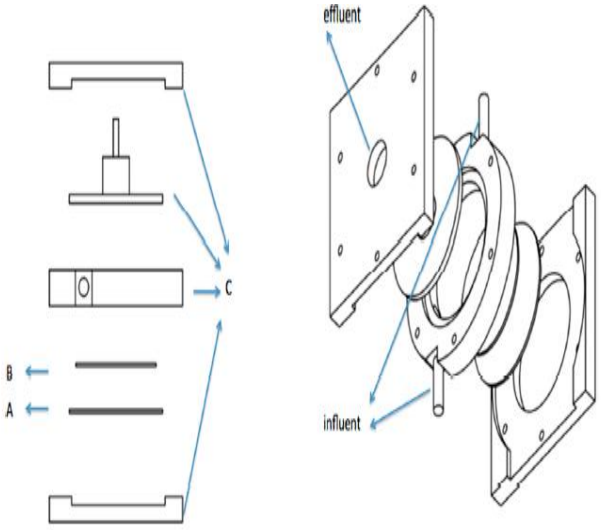

Fig 3.3 Swirl Flow Reactor

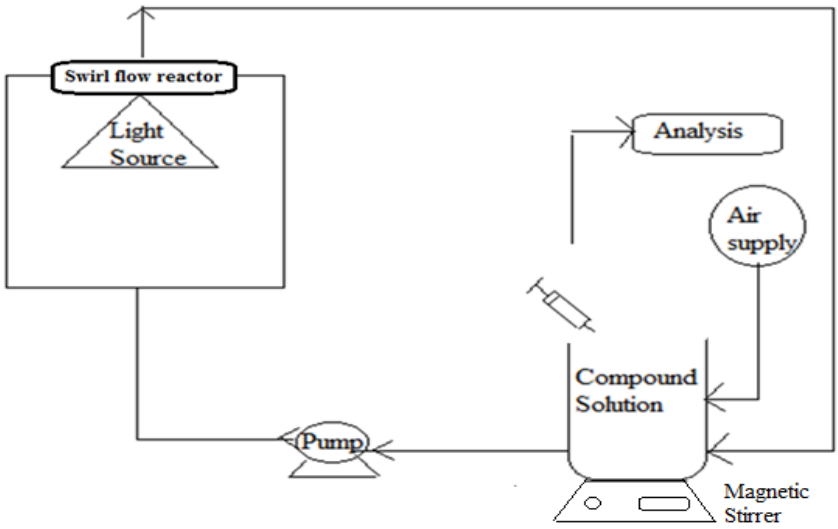

Fig 3.4 Schematic diagram of the experimental setup consisting of swirl flow reactor

3.2.4 Solar simulator

Simulated air mass (AM) 1.5 solar light was generated using a solar simulator (model SS1KW, Science tech, Ontario, Canada, with a 1000 W Xe arc lamp and an AM 1.5G filter) as shown in Fig 3.5.

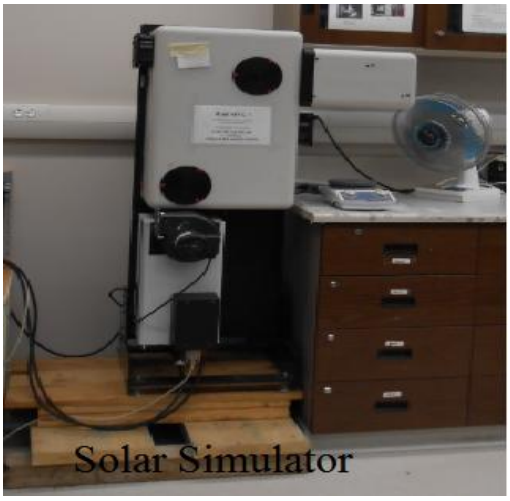

Fig 3.5 Solar simulator

3.2.5 Biological reactor

Reactor system to carry out aerobic biological reaction (Fig 3.6) was a fully mixed bench scale reactor with a constant temperature water circulator and monitoring device for temperature. The working volume of the reactor was 1000mg/L.

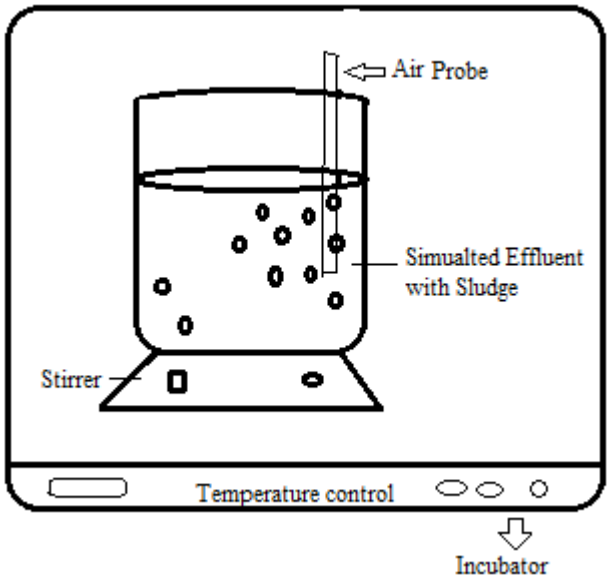

Fig 3.6 Schematic Diagram of Biological Reactor

3.3 METHODS

In order to study photocatalytic degradation, aqueous solution of various pharmaceutical compound were prepared. Aspirin (25ppm) was prepared by adding 25mg of Aspirin in 1000ml distilled water and was allowed to undergo mixing for 24h at 500rpm. Similarly Ibuprofen and Ofloxacin solution (25ppm) were prepared by pouring 25mg of compound in 1000ml distilled water taken in volumetric flask and were stirred overnight for uniform mixing. Atenolol (5-30ppm) was prepared by adding 5-30mg in 1000ml of distilled water under continuous stirring for 24h, so as to obtain homogeneous solution of model compound. The pH of prepared solution was measured using Thermo Orion 920A pH meter. Various doped photocatalysts and Graphene based composites were synthesized using sol gel and hydrothermal methods, respectively.

3.3.1 Preparation of doped TiO_2

Doped TiO_2 photocatalyst were prepared using sol gel method as shown in Fig. 3.7 with Titanium isopropoxide (TIP) as precursor. 2.5 mL of TIP was added drop by drop to a solution of 10 mL ethanol and 2.5 mL acetylacetone at room temperature and stirred for 30 minutes. Then 2 mL distilled water was added to above solution and pH was adjusted to 1.8 with 1 N HCl. Predetermined amount of dopant ions (such as Fe (NO_3) $5H_2O$, Bi (NO_3) $5H_2O$ or Ni (NO_3) $5H_2O$) were added in proportion of 0.25, 0.50 and 1.0wt% into prepared solution so as to synthesizedoped catalyst of different concentration and a stable sol was finally obtained after stirring for 2 h. Then concentrated solution was placed at 90°C for drying and

dried powder was calcined at 400°C for 2 h. In case of Bi-Ni co-doped TiO_2, equal proportion of Bi and Ni were added to make catalyst of different dopant concentrations (0.25, 0.50 and 1.0wt %).

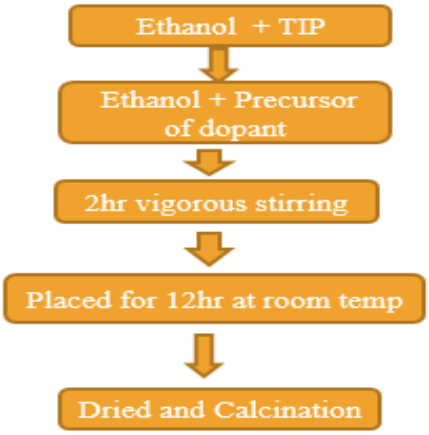

Fig 3.7 Synthesis of doped TiO_2 catalyst

3.3.2Preparation of graphene-TiO_2

To obtain graphene TiO_2/ZnO composite, 2 mg of GO was added to a solution of water and ethanol (2:1) followed by 1 h ultrasonic treatment as shown in Fig 3.8. Thereafter, 200mg of TiO_2/ ZnOwas added and furthersolution was allowed to stir for 2 h. The mixture was then transferred to a Teflon-lined autoclave, and then the hydrothermal process was performed for 3h at 120 °C. During this process, GO was reduced to graphene and concurrently the deposition of TiO_2/ZnOoccurred. The obtained composites were centrifuged using Thermo scientific (D-37520) 8×2000ml swinging bucket rotor, further rinsed with deionized water, and vacuum-dried at 60°C. The prepared samples are denoted as TiO_2-G/ ZnO-G.

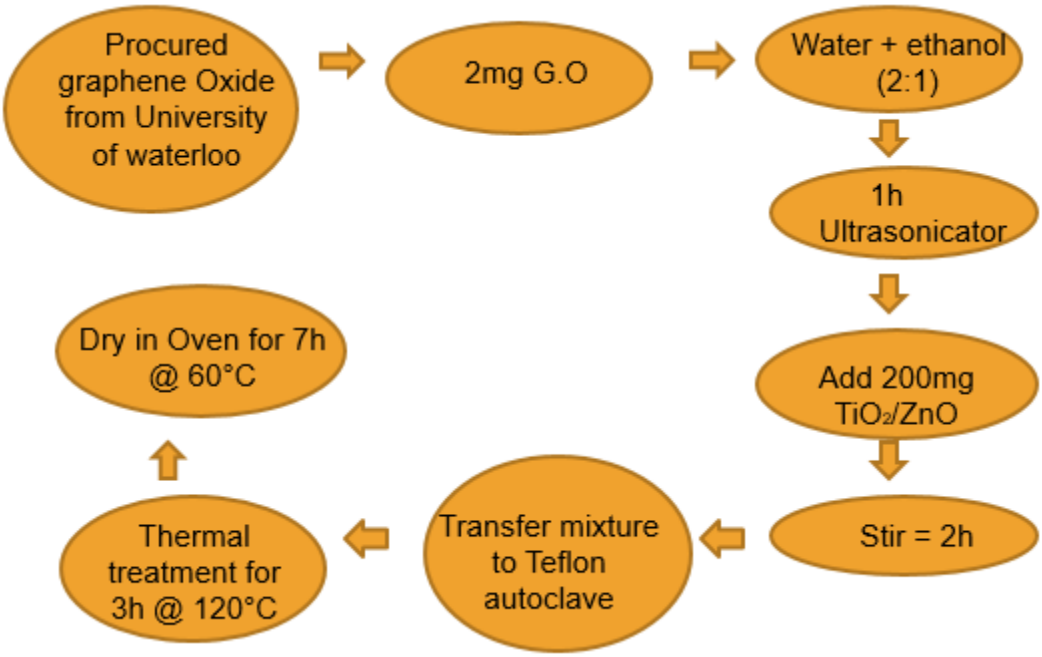

Fig 3.8 Synthesis of Graphene- TiO_2/ZnOcomposite

3.4 CHARACTERIZATION OF SYNTHESIZED CATALYST

The synthesized photocatalytic materials were analyzed for band gap, structure, morphology, crystallinity and surface area so as to compare its properties with commercially available photocatalytic materials.

3.4.1 Band gap

The band gap generally refers to the energy difference (in electron volts) between the top of the valence band and the bottom of the conduction band in insulators and semiconductors. For the evaluation of band gap energy of photocatalyst, UV-VIS spectrophotometry (Hitachi, U3900H) equipped with diffuse reflectance accessory was used in powder form for analysis.

3.4.2 Structure and morphology of synthesized catalyst

To study structure and morphology of the photocatalysts, the Scanning electron microscope (SEM, Hitachi-S-3400N)) unit was operated at 15 kV of accelerating voltage and SEM photographs were taken at resolution of 20000X.

3.4.3 Crystalline size

The average crystallite size of photocatalysts was calculated using the following Scherrer Equation (Eq. 3.1) [Tian et al., 2009].

$$t = K\lambda \div B\ cos\theta \quad \text{(Eq. 3.1)}$$

Where K is a coefficient = 0.9, λ = 0.1541 nm, B (in radian, r=θ/57.27) is the full width half maximum (FWHM) of the catalyst and θ is the diffraction angle.

3.4.4 Crystallinity

The nature of the nano photocatalyst in terms of its crystallinity and determination of lattice points was determined using XRD (Phillips diffractometer) over the 2θ collection range of 20-100°. The accelerating voltage of 40 kV, emission current of 30 mA and the scanning speed of 4.4 counts per second were used.

3.4.5 Surface area

The BET surface area of samples was analyzed by N_2 adsorption analyser (NOVA2000e) USA in which combustion of sample was done at 450°C employing pressure of gas carrier (N_2) at 0.016mmHg.

3.5 MODE OF EXPERIMENTS

Photocatalytic degradation of various model compounds was analyzed under different mode of experiments, which are listed below:

3.5.1 Adsorption experiments

Adsorption study was done so as to assess the reduction in concentration of model compound solely by adsorption phenomenon on the surface of photocatalyst. Experiments were conducted in the presence of catalyst without light under immobilized mode. The initial concentration of Atenolol was varied as 10, 20 and 30mg/L and reaction was allowed to take place for 1 h.The concentration of model compound adsorbed on the surface was calculated from the difference between the initial and final concentrations measured through spectrophotometric technique.

3.5.2 Slurry mode experiments

Photocatalytic degradation experiments were carried out in UV chamber using Pyrex glass reactor units as shown in Fig 3.1. In each set of experiments, 150 mL aqueous compound solution was kept in the glass reactor and mixed with pre-determined quantity of photocatalyst (0.5-2.0g/L). This slurry was agitated with a magnetic stirrer and aerated with sparger. 5 mL of aliquot was pipetted out after regular interval from the reactor and was filtered to take apart the catalyst. The UV absorbance spectrum of the sample was taken to determine the degradation of model compound. Further TOC analysis were done to evaluate the reduction in organic content.

3.5.3 Immobilized mode experiments

In order to obtain immobilization of catalyst on surface of glass plates *Dip coating technique*(as shown in Fig 3.9) was employed.In this method,Pyrex glass was used which was

roughened by sand blasting,so that catalyst binding can be strong. The glass surface was further degreased, and washed with 5% HNO_3 solution followed by washing with water and then finally dried at 393 K. catalyst suspension of 10% was prepared with Milli-Q water in an Ultrasonicator (Fisher Scientific; model F560) for 30 min so as to obtain a milky suspension. Then catalyst was coated on glass surface by inserting into the suspension and taking it out slowly by Dip-Coating technique (Ray and Beenackers, 1998a). The glass plate coated with catalyst was allowed to dry at 393 K for 30 min and thereafter calcined in a furnace for 3 h (Thermo scientific: model no. F30430CM) in a vertical position by raising the temperature gradually to 573K (to avoid cracking of the film). Then, the glass plate was allowed to cool down to room temperature.

Immobilized mode experiments were conducted in an experiment set up shown in Fig 3.4 and its efficiency was compared with slurry mode using same setup. The solution of model compound was allowed to flow tangentially within the swirl flow reactor with help of peristaltic pump and allowed to exit from the centre of the top plate. Flow rate during recycle was1.15×10^{-5} m^3/s, for both immobilized and slurry mode.

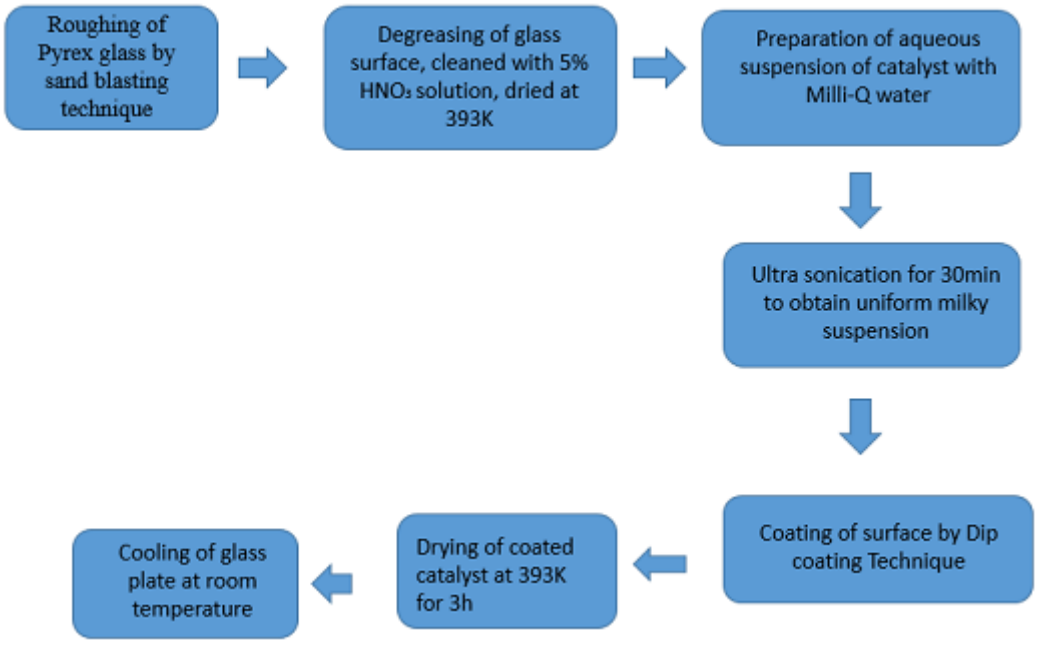

Fig 3.9 Immobilization of photocatalyst by Dip coating method

3.5.4 Degradation assessment

The degradation of the models compounds was assessed by monitoring absorbance as a function of irradiation time using spectrophotometer (Hitachi V-500UV/Vis) Japan, in the

wavelength associated with the concerned compound. The degradation efficiency was calculated as follows:

$$\text{Degradation Efficiency (\%)} = 100 \times \left[Co - \frac{C}{Co}\right] \qquad \text{(Eq. 3.2)}$$

Where C_0 is initial concentration of solution and C is concentration of solution after photo irradiation as shown in Eq 3.2. The experimental matrix was developed by varying the dose of photocatalysts, pH of the solution, concentration of oxidant and initial concentration of substrate. TOC reduction was evaluated in order to track its degradation.

HPLC was performed using Shimadzu UV/VIS Diode array detector (SPD-M20A) and Shimadzu LC-20AD pumps with 20µL sample loop. The flow rate was set to 1 mL/min using C18 column with solvent system water/Acetonitrile (85/15) taking absorbance at 254 nm.

3.5.5 Parametric optimization

The photocatalytic degradation of Atenolol was optimized at each design point of the four factors (pH, catalyst concentration, substrate concentration, Intensity) using three level Box Benkhen design (BBD).Design expert 9.0.0 was employed to use BBD. The factors and the experimental levels for each factor were selected based on literature values, available resources and results from preliminary experiments. The maximum and minimum levels of TiO_2-G concentrations were determined by preliminary experimental study. Considering this design, 29 set of experiments were performed. The remaining Atenolol concentration was determined at regular interval and data were used to calculate the degradation rate constant (min^{-1}). The quadratic model described by Eq (3.3) was assessed for the experimental response.

$$K = a_o + a_1(pH) + a_2(\text{catalyst \%}) + a_3(\text{substrate concentration}) + a_4(\text{Light Intensity}) + a_5(pH)(\text{catalyst \%}) + a_6(pH)(\text{substrate concentration}) + a_7(pH)(\text{Light Intensity}) + a_8(\text{catalyst \%})(\text{Substrate concentration}) + a_9(\text{catalyst \%})(\text{Light Intensity}) + a_{10}(\text{substrate concentration})(\text{Light Intensity}) + a_{11}(pH)^2 + a_{12}(\text{catalyst dose})^2 + a_{13}(\text{substrate concentration})^2 a_{13}(\text{Light Intensity})^2 \qquad \ldots\text{(Eq.3.3)}$$

Analysis of variance (ANOVA) was used to statistically analyse the experimental data for estimation of rate of reaction. Adequate precision measures the signal to noise ratio and ratio greater than 4 is desirable.

3.6 INTEGRATIION OF PHOTOCATALYSIS AND BIOLOGICAL TREATMENT

Simulated pharmaceutical effluent was prepared by dissolving Sodium acetate (16.3g), methanol (11.8g), potassium dihydrogen phosphate (11.7g) and Ammonium chloride (9.48g) in 1000ml distilled water and Atenolol (10ppm) was added as model pharmaceutical compound. Simulated effluents was subjected to independent solar induced photocatalytic, biological as well as sequential photocatalytic-biological (Photo+Bio) treatments. Photocatalytic experiments were carried out in slurry mode in specially designed glass reaction vessels placed in solar simulator (Fig. 3.4). In order to optimize the time of photocatalytic process, the experiment was carried under solar simulator for different time duration ranging from 0.5-5.0h in which the dose of TiO_2 was kept at 1.5g/l (optimum) determined through pre-conducted experiments. Aeration was facilitated through the aqueous suspension. At each time interval of 1h, aliquots were collected using syringe filter and degradation efficacy was assessed. All the tests were carried out in triplicate for reproducibility of results.

For Biological experiments, 1000mL of effluent was taken and activated sludge was added in varying proportions (2-15%) at natural pH of 6.9. The flasks were incubated at different temperatures (20^{o}C 27^{o}C, 37^{o}C) at 120 rpm for 48h to study the degradation of effluent. Samples (10 ml each) were drawn after every 3h and centrifuged at 10,000 rpm for 5 min. at 27^{o}C.

Photocatalytic–biological (Photo+Bio) treatment was applied in order to evaluate the efficiency of the sequential treatment in comparison to independent treatments. In integrated approach, individual simulated effluent samples (1000ml) treated by photocatalysis under optimized conditions with time duration of 0.5 to 5.0 h was subjected to biological treatment upto 48h at 37 ^{o}C. For instance, 0.5 h of photocatalytic followed by 48 h of biological treatment; 1 h of photocatalytic and 48 h of biological treatment and so on. Sample was withdrawn after the application of photocatalytic as well as biological treatment for assessing the degradation of simulated effluent in terms of Biochemical Oxygen Demand (BOD) & Chemical Oxygen Demand (COD). Mineralization was also assessed in terms of Total Organic Carbon (TOC) for the optimized set of experiments.

COD was measured by closed reflux method (spectrophotometric) using standard protocols [APHA, method 5220 C]. COD reactor (DRB 200) was used for digestion of samples. The intensity of the resultant coloured solution was measured by COD analyser (HACH, DR2800) against blank sample. BOD of the sample were analyzed by standard protocol [APHA, method 5201B] using HACH BOD meter (HQ40d multi). TOC of the

samples were analyzed using TOC Analyser (TOC-V control), Shimadzu SI-V, (UWO), which measures TOC intensity by measuring total carbon (TC) and the total inorganic carbon (TIC).

4.0 RESULTS & DISCUSSION

This chapter presents the results of photocatalytic degradation of various pharmaceuticals as model compounds using lab synthesized and commercial photocatalysts. Pharmaceutical compounds such as Aspirin, Ibuprofen, Ofloxacin and Atenolol were taken as model compounds. Various photocatalyst such as Iron doped TiO_2, Bismuth doped TiO_2, Nickel doped TiO_2, Bismuth and Nicked co-doped TiO_2 and TiO_2/ZnO graphene composites were synthesized and their photocatalytic activity was assessed for the degradation of model compounds. Degradation of model compounds was assessed in terms of TOC, chromatographic studies (HPLC) and UV-Vis spectrophotometry. Simulated effluent was subjected to independent photocatalytic, biological and integrated treatment scheme (photocatalysis followed by biological treatment) and its degradation efficacy was assessed under various treatments.

In order to make the process economical, the efficiency of solar light was evaluated in the heterogeneous photocatalysis. The application of photocatalyst in slurry mode is not suitable from industrial point of view because of the inconvenient and expensive separation of photocatalyst after treatment, so efficacy of the photocatalyst was also adjudged in immobilized mode.

4.1 PHOTOCATALYTIC DEGRADATION OF ASPIRIN

Aspirin, also known as acetylsalicylic acid (ASA), used to treat pain, fever, and inflammation. It is class of non-steroidal anti-inflammatory (NSAID's) drugs. It has been reported that rate of hydrolysis of Aspirin to its metabolites is 4µg per minute in human urine at normal body temperature (Cham et al., 1982). Aspirin is produced and consumed in large amount, thereby increasing its concentration in waste water and surface/groundwater which affects the aquatic ecosystem (Liu et al., 2006). Aspirin is a white, crystalline, weakly acidic substance with dissociation constant (pKa) of 3.5. Chemical structure and physical properties of Aspirin are given in Table 4.1.

Fe doped TiO_2 (0.5 wt %) was prepared using sol gel method with Titanium isopropoxide (TIP) as precursor and Ferrous Nitrate as dopant as explained in Section 3.3.1 and its characterization was done. Further, the photocatalytic degradation of Aspirin (25mg/L) was compared using Fe doped TiO_2 and P25 TiO_2 as photocatalyst in slurry mode under UV/solar irradiations.

Table 4.1 Physical properties and Chemical structure of Aspirin

Name of compound	**Aspirin**
Synonym	Acetylsalicylic acid
IUPAC	2(acetoxy) benzoic acid
Molecular Formulae	$C_9H_8O_4$
Molecular weight	180.157 g/mol
Density	1.40 g/cm^3
Melting point	135°C
Boiling point	140°C
Lambda max	254nm
Solubility in water	3 mg/ml
Structure	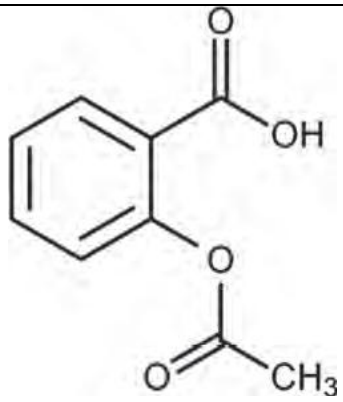

4.1.1 Characterization of Fe doped TiO_2

Fe doped TiO_2 prepared using solgel method was characterized further to analyse various parameters such as particle size, surface morphology and surface area using XRD, SEM and BET, respectively.

4.1.1.1 *X-raydiffraction pattern*

It can be seen that the XRD of Fe doped TiO_2 sample (Fig 4.1) almost coincides with that of P25 TiO_2 and there is no diffraction peak due to metal ions species, thus depicting that the metal particles are well dispersed on TiO_2 surface. It can also be observed that doping with metal ions does not disturb the crystal structure of anatase TiO_2 indicating the metal dopants are placed on surface of crystal. Diffractions that are attributable to anatase TiO_2 are clearly present in the calcined materials.

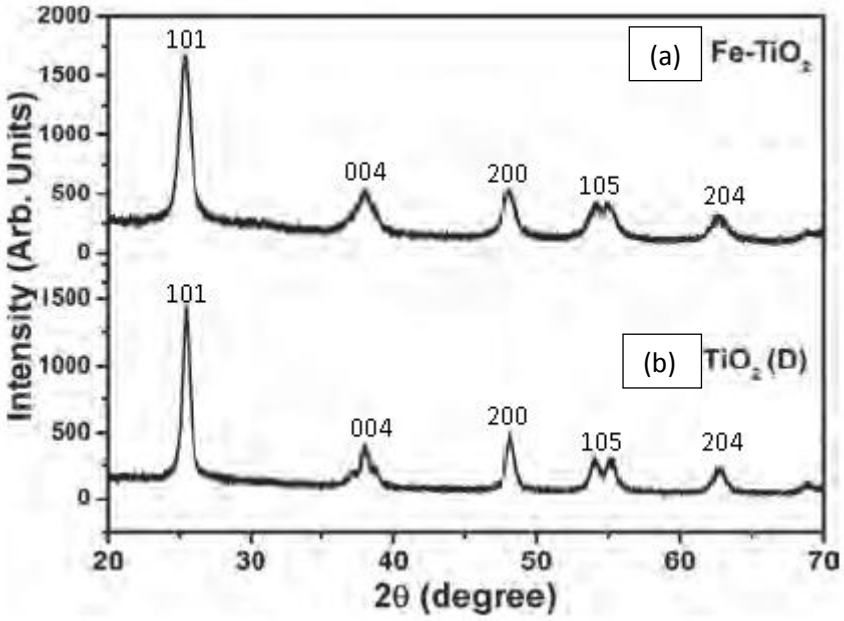

Figure 4.1. Typical XRD pattern of (a) Fe-doped TiO_2 and (b) P25 TiO_2 nanoparticles.

4.1.1.2 SEM Analysis

SEM image of Fe–TiO_2 (Fig. 4.2(a)) indicates that the particles have spherical morphology and the presence of ferric ions on the surface of TiO_2 is not uniform. The image also shows that Fe–TiO_2 catalyst contains irregular particles which are the aggregation of tiny crystals. However, it cannot be ignored that some Fe particles are too small to be identified at the resolution of used microscope. EDS analysis presented in Figure 4.2(b) shows that 0.5% (by wt.) Fe–TiO_2 contains 0.41% of Fe content. The SEM image of pure TiO_2 shows that size of Titanium dioxide particles is even.

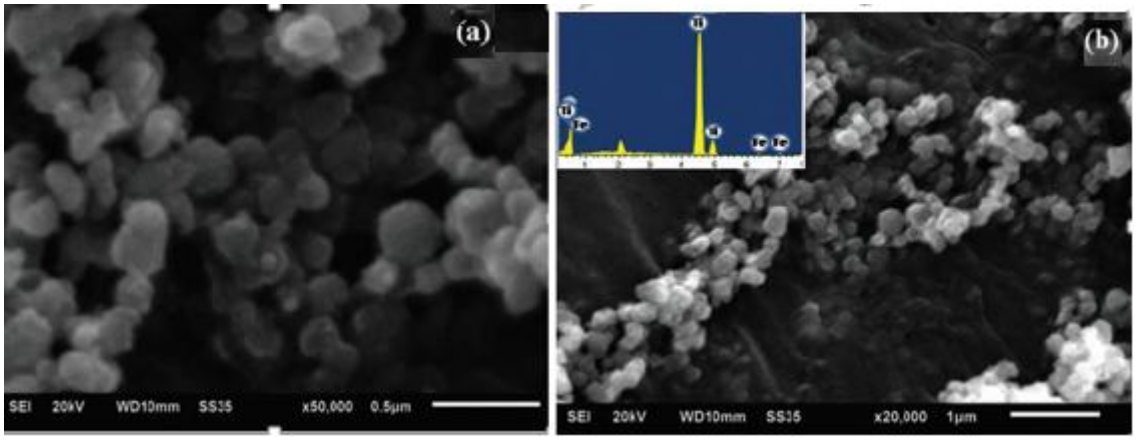

Figure 4.2 (a) Typical SEM images of synthesized Fe-doped TiO_2 nanoparticles (b) EDS spectrum of a synthesized Fe-doped TiO_2 nanoparticles

4.1.1.3 BET surface area

The surface area of Fe–TiO_2 was determined using nitrogen gas adsorption method and was found to be 72 m^2/g, which is higher than that of P25 TiO_2. Fe doping prevent particle agglomeration and has an effect on the crystallization of TiO_2, thus, forming well-defined nanocrystalline particles with high surface area. With the integration of Fe dopants during the sol–gel preparation technique, there was crystal growth suppression, favouring the formation of smaller TiO_2 crystallite. This effect may be due to the enhanced lattice strain in the doped TiO_2 network. Furthermore, this higher surface area values may also be because of the removal of nitrate from the crystal during calcinations at temperature of 400°C. It increases the porosity of surface which ultimately increases the surface area of the doped TiO_2 than undoped one.

4.1.2 Effect of operating parameters

The effect of process parameters viz. catalyst dose, pH, varying light source were assessed on the degradation efficiency of Aspirin using both catalyst (Fe-TiO_2& P25 TiO_2) as a function of time.

4.1.2.1 Effect of pH

The pH of the aqueous medium significantly influence the surface-charge properties of the photocatalysts and in turn governed the rate of photocatalytic reaction taking place on surface of semiconductor particle. The initial pH of the simulated Aspirin solution (25mg/L) was 4.6 and it was varied from 3 to 10 (Fig. 4.3) in order to assess its impact on the degradation efficiency. The maximum degradation of 48.0% and 72.0% was obtained at pH 6 after 6 h of UV exposure (11.2W/m^2) with Fe–TiO_2 and P25 TiO_2, respectively with 1.0g/L dose of either catalyst. pH of the treated solution was also analyzed every hour and it was observed that there was decrease in pH of treated solution every time. Decrease in solution pH was considered as an indication for the degradation of model compound. This behaviour may be attributed to the fact that variation in pH leads to alteration in properties of catalyst and aqueous solution, due to acid base equilibrium of hydroxyl radical. Tang et al.(1995) and Wang et al. (2000) also documented that there is a considerable dependence of the photocatalytic degradation efficiency on pH value, as the overall surface charge and hence the adsorptive properties of TiO_2 particles depend robustly on solution pH.

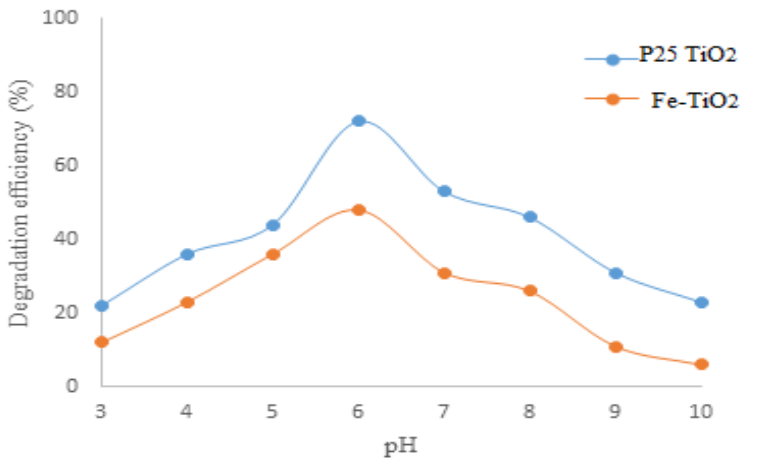

Fig 4.3 Effect of pH on the degradation of Aspirin under UV irradiation (Initial concentration=25ppm, catalyst dose=1.0g/L)

4.1.2.2 Effect of catalyst loading

The effect of catalyst dose on the degradation was assessed by varying catalyst concentration from 0.5–2.0 g/L at pH 6 under UV irradiation. Figures 4.4 (a) and (b) shows the Aspirin degradation curves with different doses of catalyst for both Fe–TiO_2 and P25 TiO_2 photocatalysts. Degradation increased with increasing catalyst loading up to 1 g/L with both photocatalysts, which may be attributed to the fact that the number of photons increase with increase in the number of catalyst molecules. Beyond 1g/L of catalyst dose, the degradation efficacy decreased which may be due to increase in the turbidity of the solution that hinder with penetration of light transmission.

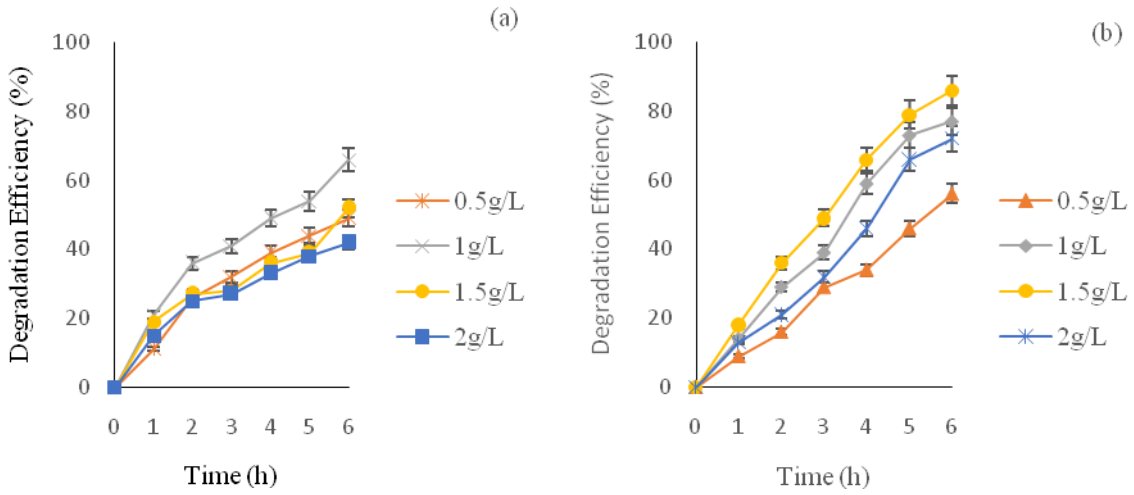

Fig 4.4 Effect of catalyst loading on degradation of Aspirin (a) P25 TiO_2 and (b) Fe-doped TiO_2 nanoparticles (Initial concentration=25ppm, pH=6.0)

4.1.2.3 Variation of light sources

The degradation efficiency of Aspirin solution (25 mg/L) was analyzed with Fe–TiO_2 and P25 TiO_2 under optimized conditions (pH 6 and catalyst dose of 1.0g/L) using different light sources viz UV Tube, UV LED and solar light. P25 TiO_2 mediated degradation efficiency was found to be 81.0 and 70.0 % (with UV LED (10W/m^2)) and UV tubes (11.2 W/m^2), respectively. However, Fe–TiO_2 photocatalyst resulted in58 and 48% degradation efficiency with UV LED and UV tube, respectively. Thus, higher degradation efficiency was observed with UV LED as light source at much lower power consumption, which would subsequently reduce the operational cost of photocatalytic processes. Under solar irradiations (30-35W/m^2), Fe–TiO_2 and P25 TiO_2 showed 96.0 and 72.0% degradation, respectively under optimized conditions (Fig. 4.5). The better photocatalytic activity of by Fe– TiO_2 under solar irradiations can be explained on the basis of higher absorption of light in visible region and secondly, iron being an acceptor impurity in doping of TiO_2, acts as an electron trap and prevents the electron hole recombination. Zhu et al. (2004) also reported that Fe^{3+} doped TiO_2 extends its absorption to visible region, which leads to an enhanced photocatalytic activity under solar irradiations.

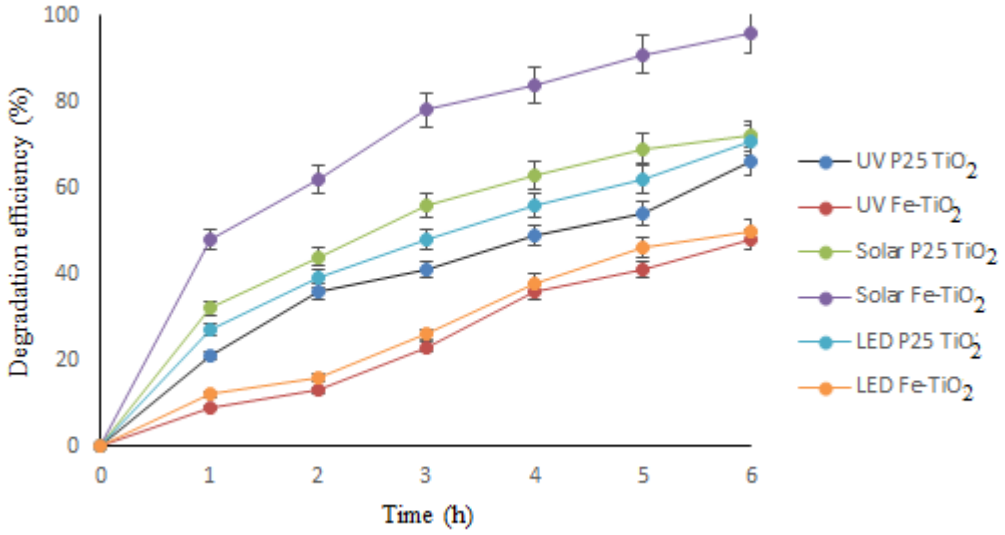

Fig 4.5 Effect of light source on degradation efficiency of Aspirin (Initial concentration=25ppm, catalyst dose=1.0g/L, pH 6.0)

4.1.3 Kinetic studies

Kinetic studies for degradation of Aspirin (25 mg/L) with catalyst dose of 1 g/L at pH 6 were carried out to find the reaction rate constant and order of reaction with Fe–TiO_2 and P25 TiO_2 under solar irradiations. The plot of ln C/C_0 v/s time gave straight line as shown in Fig. 4.6 and the correlation constant was found to be 0.9618 and 0.9936 for P25 TiO_2 and Fe–

TiO_2, respectively. Rate constant was calculated to be 0.275 and 1.0094min^{-1} for P25 TiO_2 and Fe–TiO_2, respectively. The results revealed that photocatalytic degradation of model compound followed first order kinetics and significantly higher degradation was observed with Fe-TiO_2 catalyst under optimized conditions.

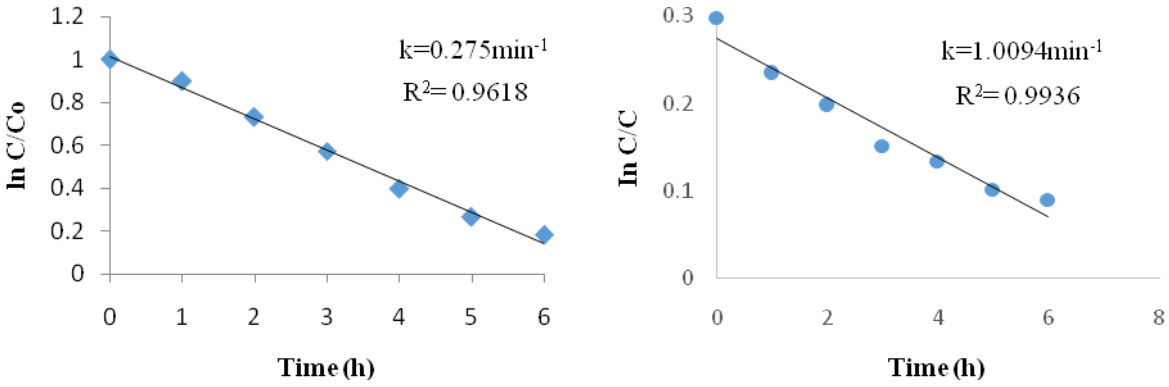

Fig 4.6 Kinetic analysis (a) P25 TiO_2, and (b) Fe-doped TiO_2 nanoparticles. (Initial concentration=25ppm, catalyst dose=1.0g/L, pH 6.0)

4.1.4 HPLC studies

HPLC technique was employed to assess the degradation of model compound as a function of time. Figure 4.7 shows the HPLC profiles recorded at 254 nm corresponding to the original Aspirin solution (25 mg/L) and after treatment upto 6 h with a gap of 1 h. Initially, strong peak was observed at retention time (t_R) of 4.8 minutes which corresponds to that of Aspirin and it was observed that as the time of photocatalytic treatment increased, the peak diminished which confirms its degradation.

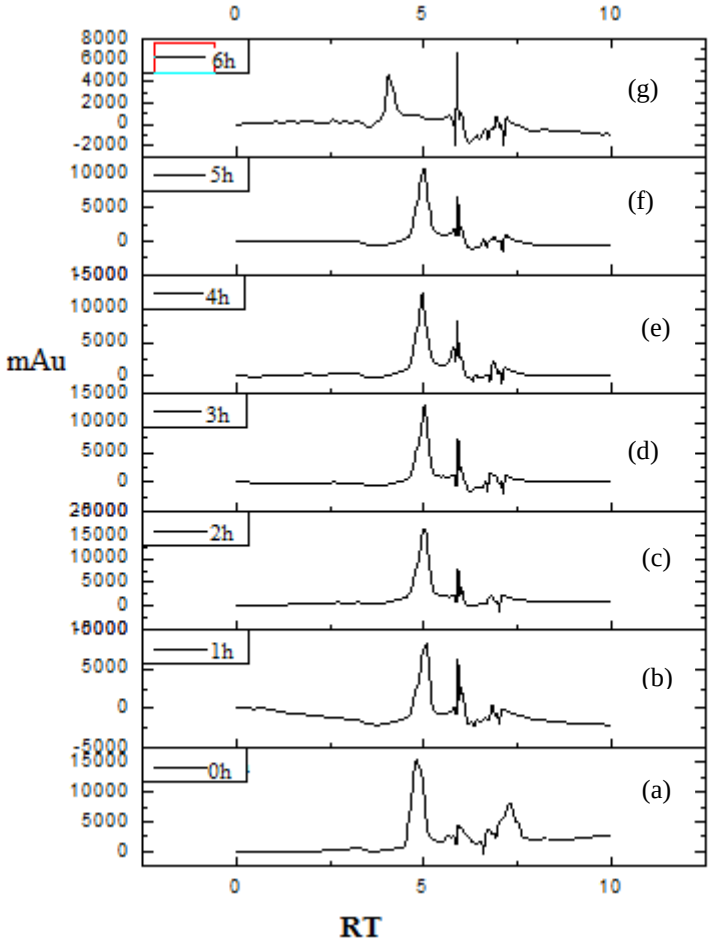

Fig 4.7 Time dependent HPLC studies of photocatalytically treated samples (Initial concentration=25ppm, catalyst dose=1.0g/L, pH 6.0)

4.2 PHOTOCATALYTIC DEGRADATION OF IBUPROFEN

Ibuprofen is a nonsteroidal anti-inflammatory drug (NSAID) used for treating fever, pain and inflammation.Ibuprofen [IBP] is one of the most commonly consumed medicines worldwide, mainly due to its use as a pain reliever. Concentration of IBP in the environment has been stated between 10 ng/L to 169 mg/L [Santos et al., 2007]. Sources of these contaminants are primarily the domestic wastewater due to excretion of non-metabolized drugs by animal or human urine and faeces. Properties & chemical structure of Ibuprofen is given in Table 4.2.

Bi and Ni doped TiO_2 (0.25-1.0 wt %) was prepared using sol gel method with Titanium isopropoxide (TIP) as precursor and Bismuth Nitrate and Nickel Nitrate as dopant as explained in Section 3.3.1 and its characterization was done. Further, the photocatalytic degradation of Ibuprofen (25mg/L) was assessed using Bi doped TiO_2, Ni doped TiO_2 and P25 TiO_2 as photocatalyst in the presence of UV/solar irradiations.

Table 4.2 Physical properties and Chemical structure of Ibuprofen

Name of compound	**Ibuprofen**
Synonym	isobutylphenyl propionic acid
IUPAC	2-(4-isobutylphenyl) propanoic acid
CAS No.	15687-27-1
Molecular Formulae	$C_{13}H_{18}O_2$
Molecular weight	206.28082 g/mol
Density	1.03 g/ml g/cm^3
Melting point	75 to 78 °C
Boiling point	157 °C (315 °F)
Lambda max	263.8nm
Solubility in water	21 mg/L
Structure	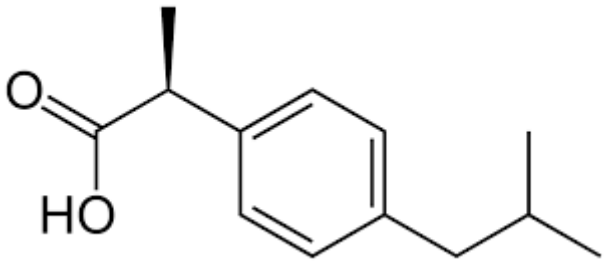

4.2.1 Characterization of Bi and Ni doped TiO_2

Bi doped TiO_2 and Ni doped TiO_2 were characterized in order to determine particle size, morphology and surface area using XRD, SEM and BET, respectively.

4.2.1.1 X-ray diffraction (XRD)

XRD patterns were collected in monochromatic high-intensity in a 2θ range of 20–70° as shown in Fig. 4.8. No noteworthy shift in XRD peaks of Bi–TiO_2 and Ni–TiO_2 was observed when compared to P25 TiO_2 indicating that Bi^{3+} did not move in the lattice to substitute Ti^{4+} particles. It may be due to higher radius of Bi^{3+} (1.03 Å) than that of Ti^{4+} (0.68 Å). The bismuth in the TiO_2 surface may increase the charge separation. Similar observation has been reported by Rengraj et al., 2006 and Xu et al., 2002 where doping of TiO_2 with Bi did not show any substantial variation in peaks of XRD. The reason for stabilizing Ni doped TiO_2 at lower levels has been credited to the almost similar ionic radius of Ni^{+2} (0.72 Å) to that of Ti+4 (0.68 Å), which was found to replace some portion of Ti^{+4} ions in TiO_2 lattice [Wang et al., 2012; Braz et al., 2014].

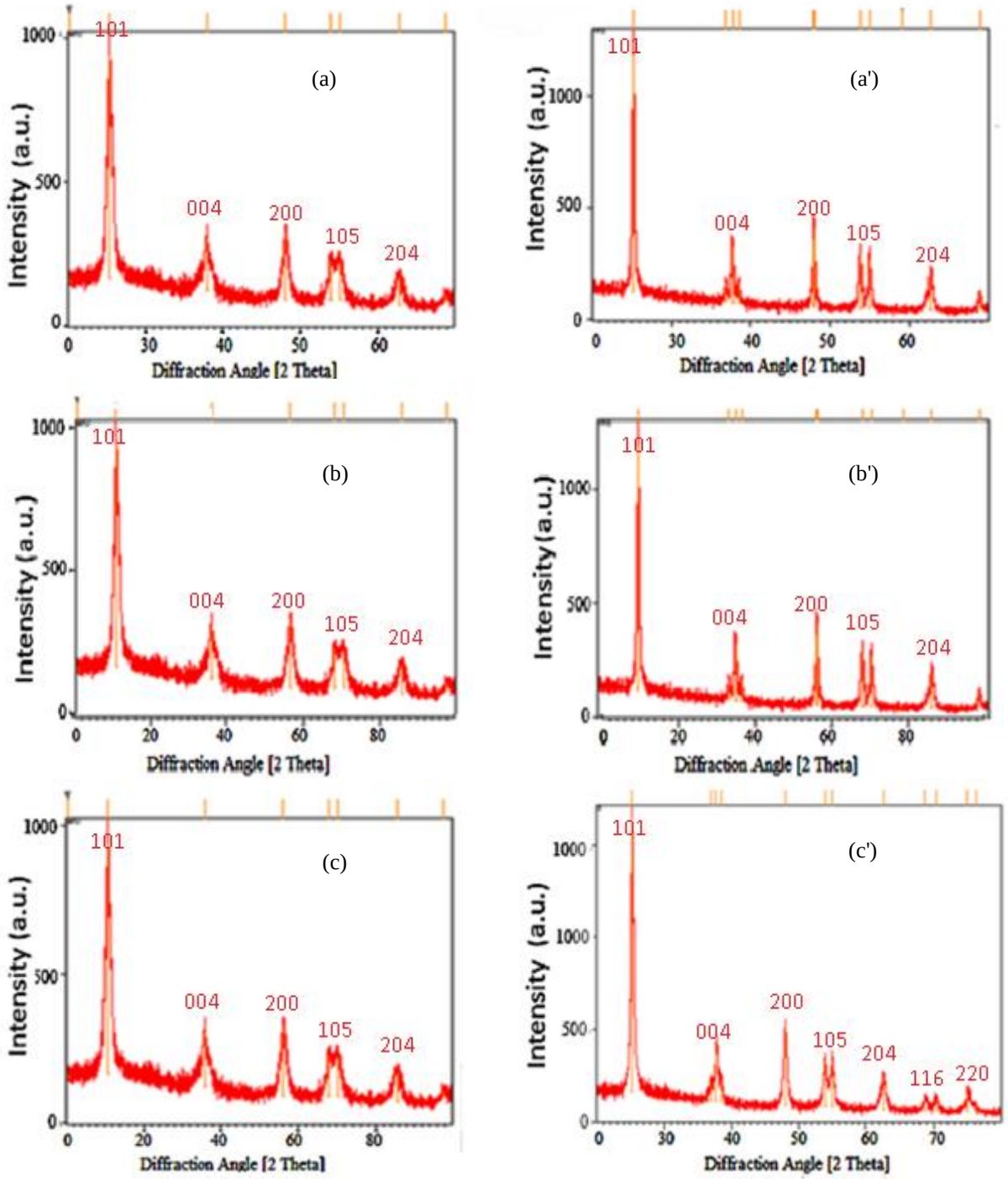

Fig 4.8 XRD pattern of synthesized (a) 0.25wt% Ni-TiO_2 (b) 0.5wt% Ni-TiO_2 (c) 1.0wt% Ni-TiO_2 (a') 0.25wt% Bi-TiO_2 (b') 0.5wt% Bi-TiO_2 (c') 1.0wt% Bi-TiO_2

4.2.1.2 SEM analysis

The morphology of doped photocatalysts has been depicted in Fig 4.9 which shows that particles have spherical shape and agglomeration had taken place. The EDS analysis of doped TiO_2 showed significant presence of Ni and Bi in synthesized samples. The analytical

results from EDS are in realistic arrangement with 0.25– 1.0 wt% of Bi^{3+} and Ni ions doped into TiO_2. The elemental records of samples for Ti, O and Bi showed homogeneous distribution of elements and no gathering of Bi ions was detected in the 0.25–1.0 wt% range of doped Bi–TiO_2 and Ni–TiO_2. From EDS analysis (Table 4.3), it has been observed that in 0.25 wt% of Bi–TiO_2 and Ni–TiO_2, 0.21 and 0.19% of Bi and Ni ions were present, respectively. Similarly, variations were observed in 0.25–1.0 wt% of Bi–TiO_2 and Ni–TiO_2.

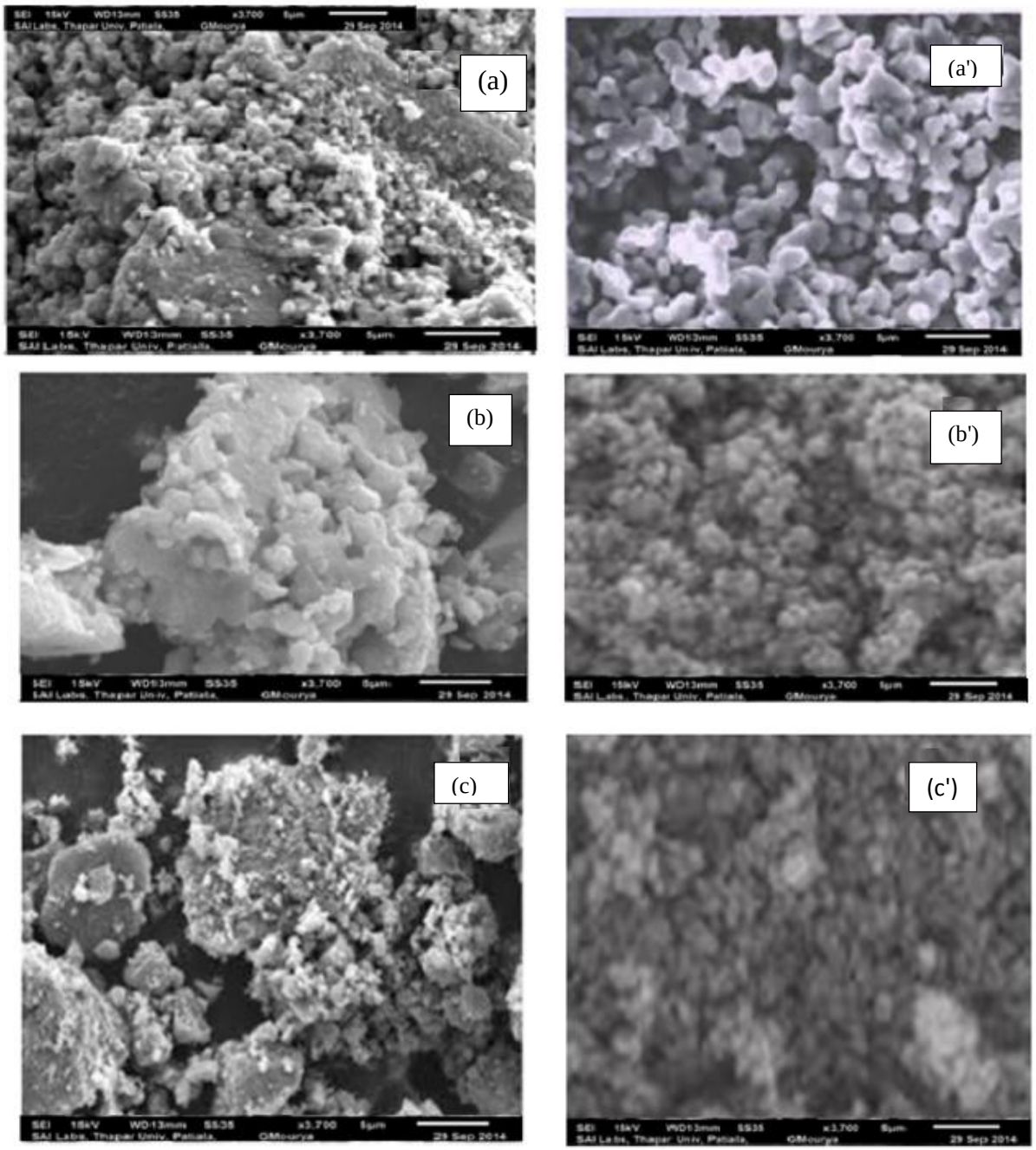

Fig 4.9 SEM images of synthesized (a) 0.25wt% Ni-TiO_2 (b) 0.5wt% Ni-TiO_2 (c) 1.0wt% Ni-TiO_2 (a') 0.25wt% Bi-TiO_2 (b') 0.5wt% Bi-TiO_2 (c') 1.0wt% Bi-TiO_2

Table 4.3 EDS of various dopant concentration of Bi and Ni

Bi-TiO_2	**Element**			**Ni-TiO_2**	**Element**		
Dopant concentration (wt %)	**Bi**	**O**	**Ti**	**Dopant concentration (wt %)**	**Ni**	**O**	**Ti**
0.25	0.21	0.02	0.02	0.25	0.18	0.02	0.05
0.50	0.43	0.03	0.04	0.50	0.36	0.5	0.9
1.0	0.88	0.20	0.10	1.0	0.74	0.08	0.18

4.2.1.3 BET surface area

The number of active sites increasesdue to increase in surface area, which further promotes the separation efficiency of the electron–hole pair and subsequently, results in enhanced photocatalytic activity. Upon doping with 0.25 wt% Ni, the crystallite size was observed to be 13.84 nm and the surface area was 41.71 m^2/g as shown in Table 4.4. As the dopant concentration was increased to 0.5 wt%, the crystallite size value decreased to 10.3 nm and the surface area increased to 45.70 m^2/g. These results suggest that TiO_2 doped with Ni (<0.5 wt %) dopant concentration effectively inhibits TiO_2 grain growth possibly by remaining at boundaries of the grain thereby, increasing the crystallite size and decreasing the surface area [Wang et al., 1999; Lin et al., 2006]. The decrease in growth of grain can also be due to the formation of Ni-O-Ti bonds in the doped powders, which inhibits the growth of the crystals. However, decrease in the dopant concentration to 0.25 wt%, leads to increase in crystalline size and decrease in surface area of synthesized catalyst. However in case of Bi–TiO_2, it was observed that the surface area and crystal size was found to be as 47.8 m^2/g and 12.4 nm, respectively for dopant concentration of 0.25 wt%. Further, by increasing the dopant concentration from 0.25 wt% to 1.0 wt%, the decrease in surface area and increase in crystalline size was observed which may likely decrease the photocatalytic activity as shown in Table 4.5

Table 4.4 Crystalline size and surface area of Ni doped TiO_2

Ni (wt %)	**Crystalline size**	**Surface area**
0.25	13.84nm	41.71 m^2/g
0.50	10.3nm	45.7 m^2/g
1.0	16.92nm	40.8m^2/g

Table 4.5 Crystalline size and surface area of Bi doped TiO_2

Bi (wt %)	Crystalline size	Surface area
0.25	12.4nm	47.8 m^2/g
0.50	13.67nm	43.4 m^2/g
1.0	15.6nm	42.1m^2/g

4.2.1.4 Band gap energy

The UV–vis diffuse reflectance spectrum of Bi and Ni doped TiO_2 are shown in Fig. 4.10. It is evident from the results that the UV–vis diffuse reflectance spectrum gave distinct band gap absorption edges at 422 nm, 415 nm, 405 nm for 0.25, 0.50 and 1.0 wt% Bi doped TiO_2, and 413 nm, 418 nm, 412 nm for 0.25, 0.50 and 1.0 wt% Ni doped TiO_2, respectively. The corresponding band gap energies were found to be 2.99, 3.05 and 3.08 eV for 0.25, 0.50, and 1.0 wt % Bi–TiO_2, respectively and 3.02, 2.99 and 3.03 eV for 0.25, 0.50 and 1.0 wt% Ni doped TiO_2, respectively. At lowest concentration of Bi dopant (0.25wt %), there is maximum shift in absorption edge and hence, band gap energy is minimum. This may be attributed to the fact that when the dopant is in less amount, the metals ions get inserted into the lattice. Whereas, when the dopant is in excess quantity, Bi ions cannot enter the lattice ofTiO_2 but covers the surface of TiO_2 and leads to the creation of heterogeneity junction. So, Bi (0.25 wt %) photocatalysts has lower band gap energy (2.9 eV) when compared to other dopant concentrations. For Ni–TiO_2 the minimum band gap energy of 2.9 eV was obtained with dopant concentration of 0.5 wt%. As the concentration of dopant is either increased or decreased from 0.5 wt%, increase in the value of band gap energy was noticed, which may be due to formation of layer of dopant over TiO_2, hence, ions might not get inserted into lattice of TiO_2.

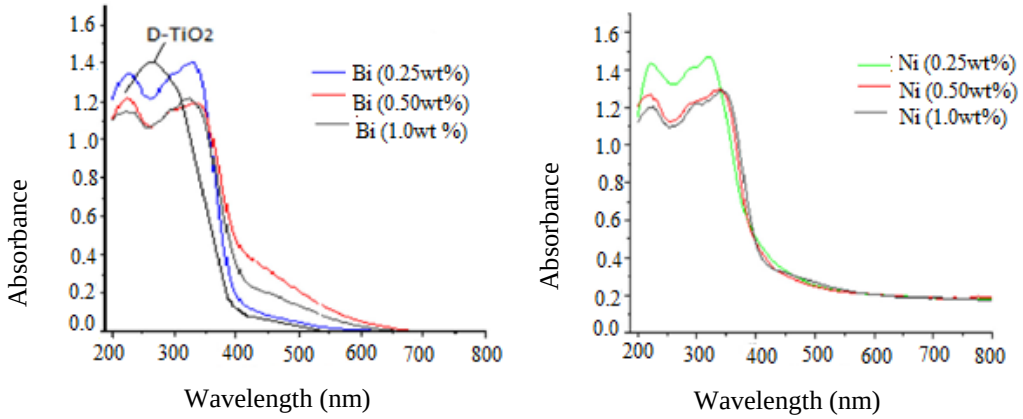

Fig 4.10 UV Diffuse reflectance spectrum of (a) Bi-TiO_2 (b) Ni-TiO_2

4.2.2 Photocatalytic degradation

Photocatalytic degradation of Ibuprofen has been studied by employing Bi/Ni doped TiO_2 and P25 TiO_2.Effect of different process parameters viz. catalyst dose, pH, dopant concentration, type of catalyst were assessed for degradation of IBP in slurry mode under UV/ solar irradiations.

4.2.2.1 Effect of pH

In order to obtain baseline data with standard P25 TiO_2, photocatalytic degradation of IBP (25ppm) was carried out in slurry mode under UV irradiation. pH of the IBP aqueous solution was varied from 3-10 using P25 TiO_2 (2g/L) as photocatalyst. It was observed (Fig.4.11) that the degradation efficiency increased with increase in value of pH up to 6.0 and thereafter, decrease in the degradation was observed. The maximum degradation of IBP was found to be 76.0% using 2g/L P25 TiO_2 at pH 6.0. The pKa value of IBP is 4.4 and it is reported as weak acid. Therefore, at lower pH range, the surface of TiO_2 will be positively charged as well as the carboxyl group of IBP and charge repulsion will be observed. At greater pH value, IBP and TiO_2 both will be negatively charged. Enhanced conditions are expected at pH 6-7 for degradation of IBF using P25 TiO_2 [Choina et al., 2013].

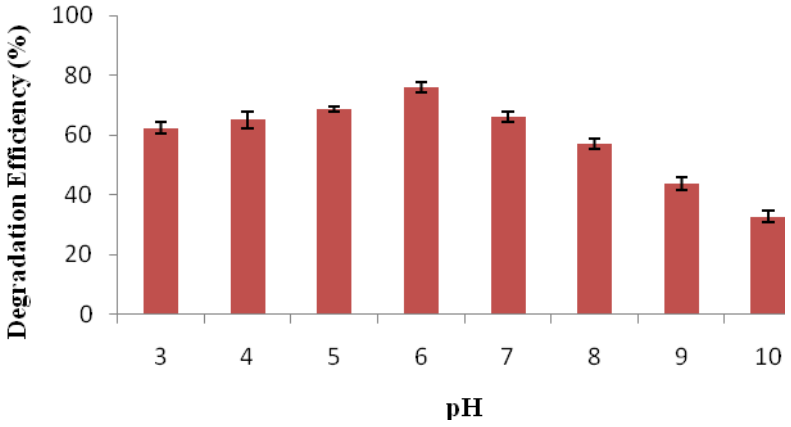

Fig 4.11 Effect of variation of pH
(Initial concentration=25ppm, catalyst dose=2.0g/L)

4.2.2.2 Effect of catalyst dose

Catalyst dose of P25 TiO_2 was varied from 0.5-2.5g/L as shown in Fig 4.12. It was observed that increasing the concentration of catalyst from 0.5 to 2.5g/L, the degradation efficiency kept on increasing upto 2 g/L (76.0%), indicating the significance of available catalyst surface for degradation under UV irradiation. Further, increasing the catalyst concentration beyond 2g/L, the efficacy decreased directing that the optimal photons have

been adsorbed. The amount of catalyst more than the certain limit may not be useful because of chances of aggregation, as well as reduction in irradiation field onto the surface due to increase in the turbidity of the solution. Moreover, at high concentration, there is a decrease in surface area availability for light-harvesting for the generation of h+ /e− pairs, induced by accumulation as also explained in previous findings (Neppolian et al., 2002; Martinez et al., 2011).

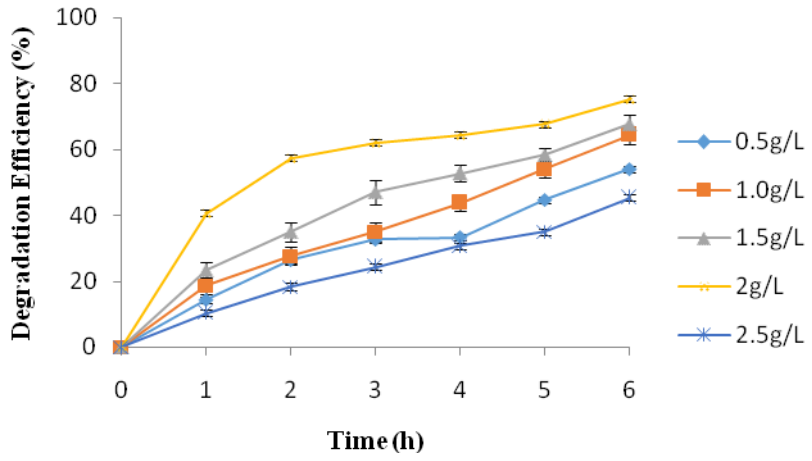

Fig 4.12 Effect of catalyst dose
(Initial concentration=25ppm, pH 6.0)

4.2.2.3Variation in dopant concentration

Insertion of transition metal can serve as electron/hole separator and can eradicate the hasty recombination of excited e^-/hole pair all through photoreaction, resulting in enhancing the efficiency of the TiO_2 photocatalyst, but this effect is subtle to dopant concentration also. The photocatalytic degradation of IBP (25ppm) was assessed using lab synthesized Bi / Ni doped TiO_2(2g/L) at pH 6.0 under solar irradiations with varying concentrations of dopant. Dopant concentration was varied from 0.25 to 1.0wt% for both Bi-TiO_2 and Ni-TiO_2. With (0.25wt %) Bi-TiO_2 concentration, 89.0% of IBP degradation was observed in 6 h of solar irradiation, as shown in Fig 4.13 and as concentration of dopant was raised from 0.25 to 1.0wt%, there was decrease in the degradation efficiency. The deferral effect of increase in Bi content on degradation rate may be credited to destruction of hydroxyl radicals due to entrapment of conduction band e^- by the adsorbed metal ions. However, with Ni- TiO_2, the maximum degradation of 78.0% was observed with 0.50wt% dopant concentration and it was observed that on either increasing or decreasing the concentration of dopant from 0.50wt%, there was decrease in degradation efficiency of IBP, which may be because of the increased

impact of ions with increased dopant concentration up to certain limit (up to 0.50wt%) and thereafter, the photocatalytic activity reduced due to surface charge separation.

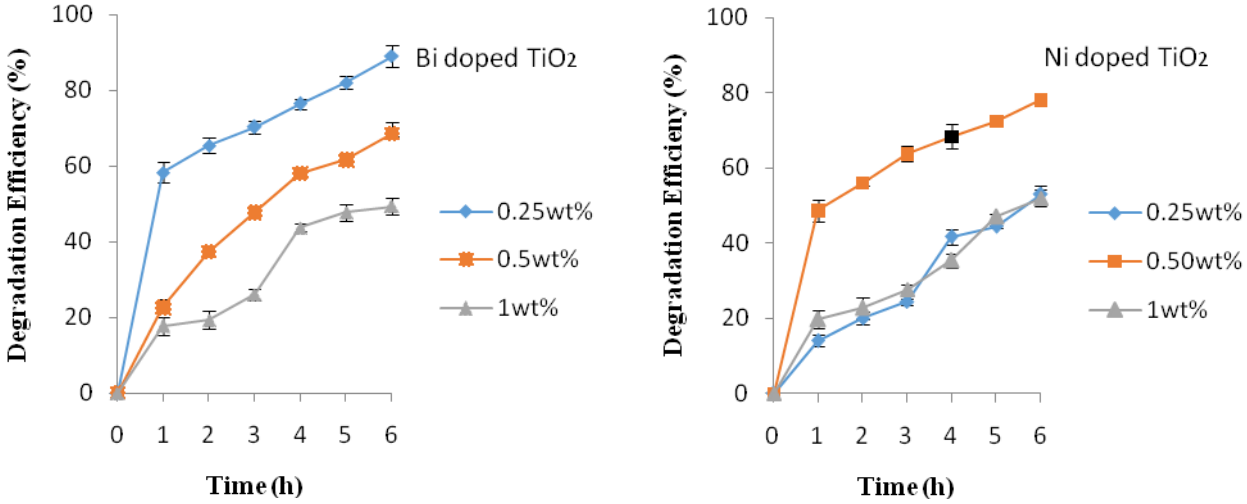

Fig 4.13 Variation of dopant concentration (a) Bi (TiO_2) (b) Ni (TiO_2) (Initial concentration=25ppm, catalyst dose=2.0g/L, pH 6.0)

4.2.2.4 Variation of type of catalyst

The effect of dopants might not be similar on trapping e^-/holes on the surface or during interface charge transfer because of the different locations of the dopant in the lattice. So, the photocatalytic competence would be different for various types of dopants [Barakat et al., 2004; Pouretedal et al. 2009]. In order to compare the efficiency of lab synthesized Bi and Ni doped TiO_2 with standard P25 TiO_2, IBP was subjected to photocatalytic degradation at pH 6 with catalyst dose of 2g/L under UV and solar irradiations. Maximum degradation of 89.0% has been achieved with Bi-TiO_2 (0.25wt %) under solar irradiation as shown in Fig 4.14, while 50 and 74.0% degradation has been achieved with Ni-TiO_2 and P25 TiO_2, respectively, under similar conditions. The Bismuth in the TiO_2 surface may enhance the charge separation and improves its photocatalytic activity. Thus, the orders of photocatalytic degradation of IBP followed by different catalyst has been observed as Bi-TiO_2> P25 TiO_2>Ni-TiO_2. The cause for this enhancement has been timidly credited to the overpowering of recombination of electron-hole pairs on the surface of the TiO_2 catalyst by low valence Bi ions. Literature also revealed that among numerous transition metal ion dopants, Bi appears to be efficient dopant as it enhanced the photocatalytic activity of some semiconductor photocatalyst [Begum et al., 2008; Sreethawong et al., 2005].

Kinetic studies of degradation of IBP (25ppm) with catalyst dose of 2 g/L at pH 6 under solar irradiations indicate rate constant of 0.0064, 0.0046 and 0.0043min^{-1} for Bi–TiO_2, P25 TiO_2 and Ni–TiO_2, respectively with first order kinetics.

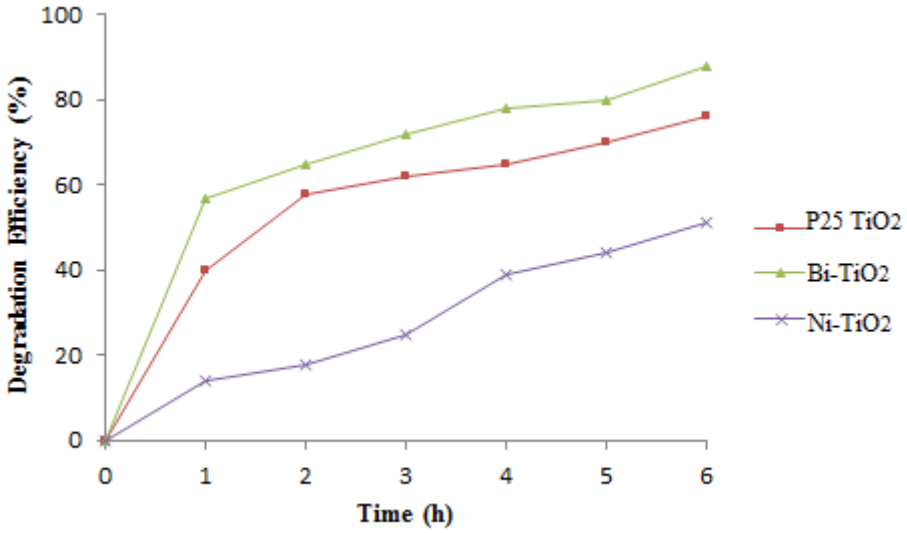

Fig 4.14 Variation of type of catalyst
(Initial concentration=25ppm, catalyst dose=2.0g/L, pH 6.0)

4.2.3Comparison of Solar/UV as Light source

Fig 4.15 shows the comparison of degradation of IBP in aqueous solution under UV/Solar irradiations. It was observed that under UV light the degradation was found to be 76.0% with P25 TiO_2 (2g/L) at pH 6 after 6 h of irradiations.The maximum degradation of 89.0% was achieved with Bi-TiO_2 as photocatalyst in 6h with dose of 2g/L at pH 6 under solar irradiations. With the same catalyst under UV light, only 48.0% degradation was observed. Therefore, the photogenerated electrons in the excited IBP molecules have sufficient energy to produce the superoxide ion and hydroxyl radicals under solar irradiation. Hence, it can be said that doping of catalyst with metal ions can reduce the power consumption as the absorbance spectra get shifted in visible region, therefore sunlight can be used as a cost effective source of irradiation.

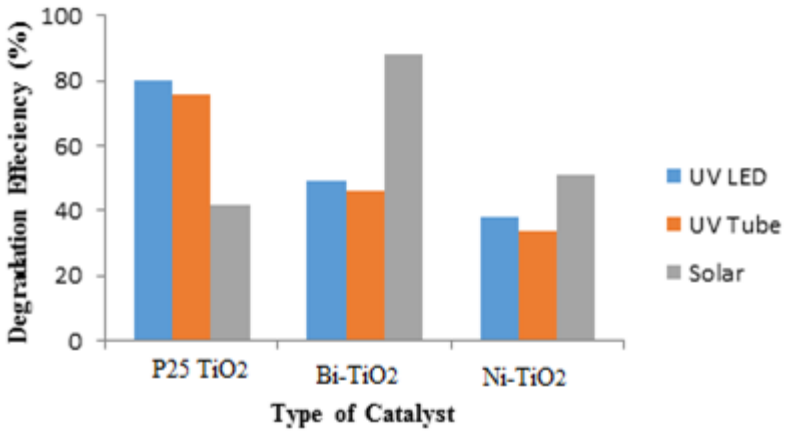

Fig 4.15 Variation of type of light source
(Initial concentration=25ppm, catalyst dose=2.0g/L, pH 6.0)

4.3 PHOTOCATALYTIC DEGRADATION OF OFLOXACIN (OFL)

Ofloxacin is a synthetic antibiotic of the fluoroquinolone drug class. It is on the WHO Model List of Essential Medicines, the most important medications needed in a basic health system [WHO, 2015]. Upto 80% ofdirected oral dose of OFL is excreatedas such within 48 hours of dosing. In particular, OFL is known to continue in sludge-treated soils in concentrations of few milligrams to kilogram [Beausse et al., 2004] and has recently been characterized as a high hazard to the aquatic ecosystem [Langdon et al., 2010]. Chemical and physical properties of OFL are given in Table 4.6.

Bi-Ni co-doped TiO_2 (0.25-1.0wt %) was prepared using sol gel method with Titanium isopropoxide (TIP) as precursor and Bismuth Nitrate and Nickel Nitrate as dopant in equal composition as explained in Section 3.3.1 and its characterization was done. Further, the photocatalytic degradation of Ofloxacin (25mg/L) was compared using Bi-Ni co-doped TiO_2 and P25 TiO_2 as photocatalyst under slurry mode in the presence of UV/solar irradiations.

Table 4.6 Physical properties and Chemical structure of Ofloxacin

Name of compound	**Ofloxacin**
IUPAC	(RS)-7-fluoro-2-methyl-6-(4-methylpiperazin-1-yl)-10-oxo-4-oxa-1-azatricyclo[7.3.1.05,13]trideca-5(13),6,8,11-tetraene-11-carboxylic acid
CAS No.	82419-36-1
Molecular Formulae	$C_{18}H_{20}FN_3O_4$
Molecular weight	361.36 g/mol

Density	1.48g/cm^3
Melting point	254°C
Boiling point	571.5°C
Lambda max	286.2nm
Solubility in water	28.3mg/L
Structure	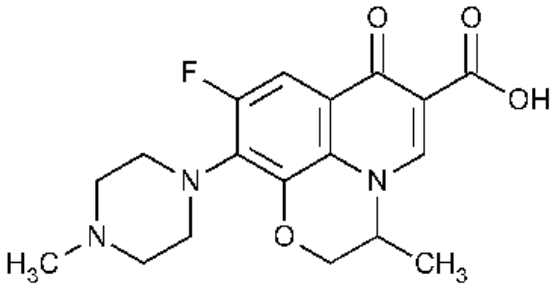

4.3.1 Characterization of Bi-Ni Co-doped TiO_2

Characterization of Bi-Ni Co-doped TiO_2 was carried out to analyse various parameters such as particle size, surface morphology and surface area using XRD, SEM and BET, respectively.

4.3.2 XRD Patterns

All XRD spectra presented in Fig. 4.16 shows the peaks confirming anatase structure and it was observed that the prepared Bi–Ni co-doped photocatalyst consisted only of anatase and the doping would enhance the photocatalytic activity. Since Bismuth might get fused into the crystal structure of TiO_2, which reduces the band gap of TiO_2, and it enhances its usability in the visible region. Nickel is dispersed on the surface of TiO_2, reduces the recombination of photogenerated electron–hole pairs, thus increases photo quantum efficiency.

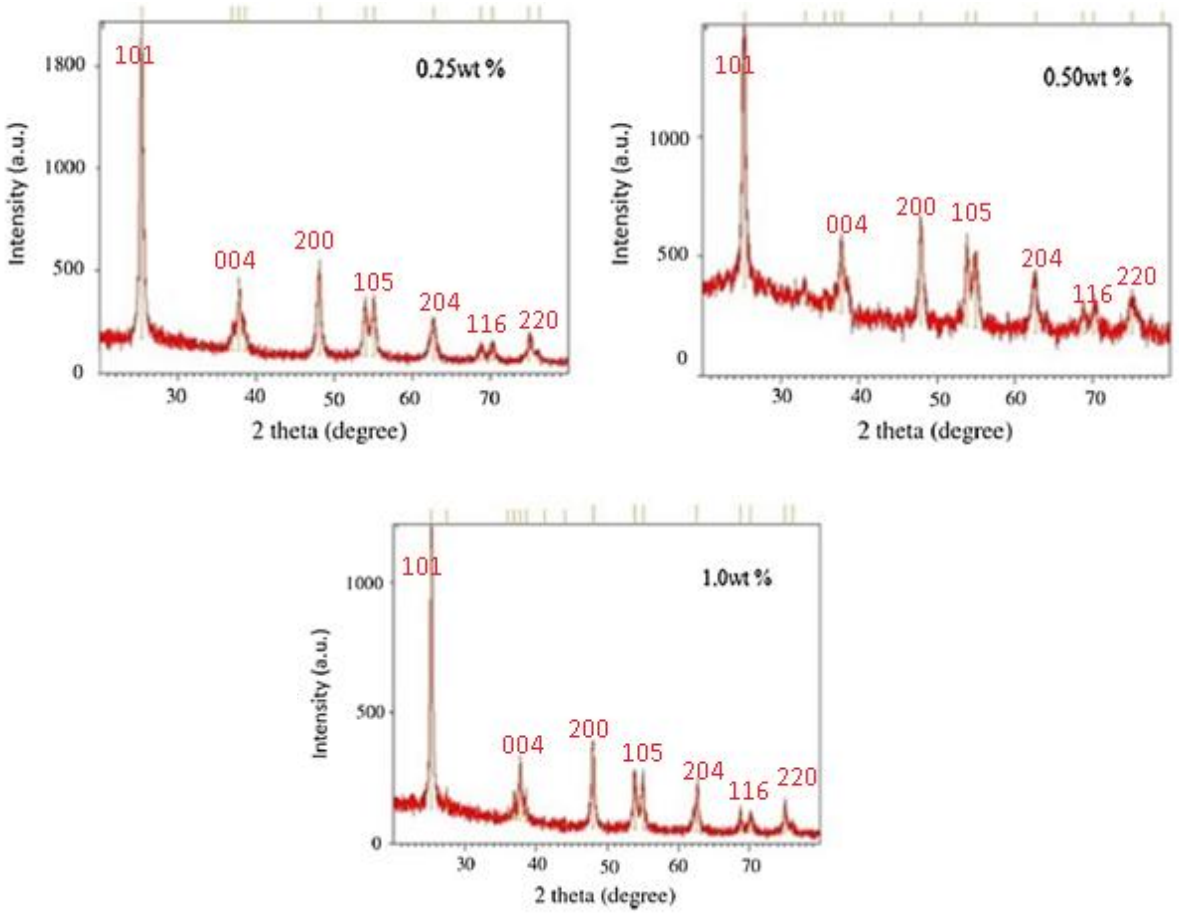

Fig 4.16 XRD pattern of Bi-Ni co-doped TiO_2 with different concentrations.

4.3.1.2 SEM Analysis

The SEM images were used to evaluate primary structure of doped TiO_2. The morphology of the samples has been presented in Fig. 4.17. The photocatalysts are in the form of small agglomerates of crystals. The nanometer size of the particles resulted in an increase in surface area and a subsequent increase in the amount of photocatalytic reaction sites, that may enhances its photocatalytic activity. The EDS analysis of codoped TiO_2 showed significant presence of Ni and Bi ions in synthesized samples. The analytical results from EDS are in realistic arrangement with 0.25–1.0 wt% of Bi and Ni ions doped into TiO_2. The elemental records of samples for Ti, O, Ni and Bi showed homogeneous distribution of elements in the 0.25–1.0 wt% range of Bi-Ni co-doped TiO_2. From EDS analysis (Table 4.7), it has been observed that 0.25 wt% of Bi-Ni co-doped TiO_2 contains 0.26, 3.04, 16.36 and 80.33% of Bi, Ni, O and Ti ions, respectively and similarly for other dopant concentration.

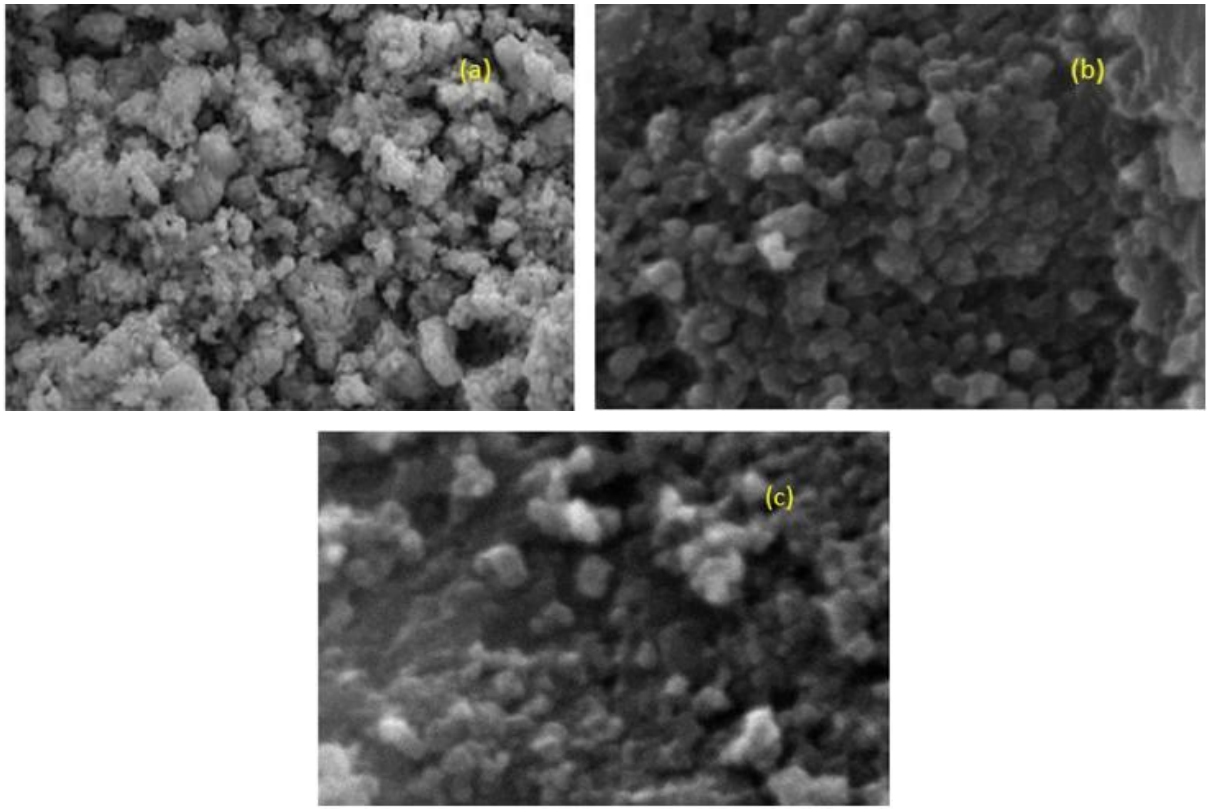

Fig 4.17 SEM images of Bi-Ni co-doped TiO_2 (a) 0.25wt% (b) 0.50wt% (c) 1.0wt%

Table 4.7 EDS of various dopant concentration in Bi-Ni co-doped TiO_2

Bi-Ni codoped TiO_2	**Elements**			
Dopant concentration (wt %)	**Bi (%)**	**Ni (%)**	**O (%)**	**Ti (%)**
0.25	0.26	3.04	16.36	80.33
0.50	1.37	1.88	43.52	53.4
1.0	2.48	0.72	70.70	26.10

4.3.1.3 BET surface area analysis

The BET surface area of Bi-Ni co-doped TiO_2 was found to be 74, 55 and 18.66 m^2/g for 0.25, 0.5 and 1.0 wt% of dopant concentration, respectively. It was observed that increase in dopant concentration resulted in reduction of surface area of catalyst, which may be due to increase in grain size, that is consistent with results of SEM.

4.3.1.4 Band gap energy

The UV–vis diffuse reflectance spectrum of all the compositions are shown in Fig. 4.18 It is evident from the results that the UV–vis diffuse reflectance spectrum of Bi-Ni codoped TiO_2, gave distinct band-gap absorption edges at 422 nm, 415 nm, 405 nm for 0.5 & 1.0wt%, Bi-Ni codoped TiO_2, respectively. The corresponding band-gap energies were found

to be 2.89, 3.09 and 3.11 eV for 0.25 wt%, 0.50 wt%, and 1.0 wt% Bi-Ni co-doped TiO_2, respectively. Band gap is minimum when dopant concentration is less as the absorption shift is maximum because when the amount of dopants is less, the metals ions get incorporated into the lattice but when the dopants are in excess, ions cannot enter the TiO_2 lattice, and therefore cover the surface of TiO_2 and leads to the formation of heterogeneity junction. So, Bi-Ni (0.25 wt %) photocatalysts has lower band gap energy (2.9 eV) when compared to other dopant concentrations.

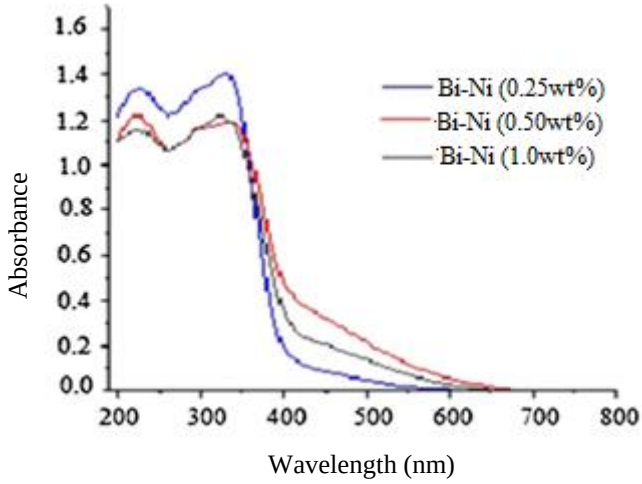

Fig 4.18 UV diffuse reflectance spectrum Bi-Ni co-doped TiO_2

4.3.2 TiO_2mediated degradation

Photocatalytic activity of OFL was assessed with P25 TiO_2 and its concentration was varied from 0.5-2.0 g/L at natural pH of 6.0. Fig. 4.19 depicts that maximum photocatalytic degradation of OFL to be 72.0% after 6 h of irradiation at catalyst dose of 1.5 g/L. It has been observed that as catalyst concentration was allowed to rise from 0.5 to 1.5 g/L; there was increase in extent of degradation, whereas further increase in concentration, results in reduction of degradation efficiency, which might be due to decline in penetration of light (shielding effect). The correlation between degradation rate and the catalyst concentration is due to large number of active TiO_2 sites accessible for the Photocatalytic reaction.

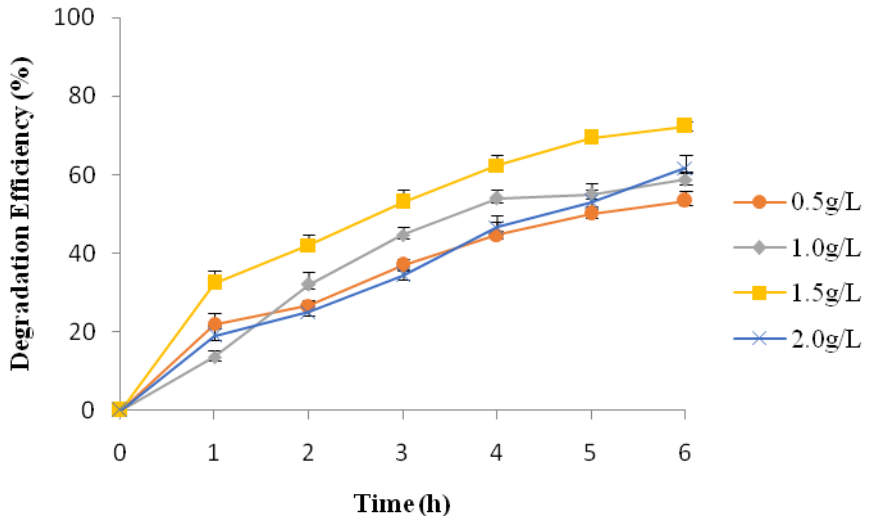

Fig 4.19 Effect of variation of catalyst concentration (Initial concentration=25ppm, pH 6.0)

The effect of pH of the solution is the major issue associated with the ionization states of surface of catalyst & substrate and also the rate of formation of radicals in the reaction mixture. Thereafter, the degradation of Ofloxacin OFL (25mg/L) also was investigated by varying pH of the initial OFL solution from 3-10 using P25 TiO_2 as catalyst with a dose of 1.5 g/L. It has been observed that photocatalytic activity is related to surface ionization state of catalyst. Change in the pH can change the adsorption of Ofloxacin on catalyst surface, which is determinant factor for the existence of photocatalytic oxidation reactions. At pH 3, 72.0% degradation of OFL was achieved within 6 h (Fig. 4.20).

Ofloxacin is cationic below pK_{a1} anionic above pK_{a2}, and neutral between pK_{a1} and pK_{a2}. Due to this, the effect of the pH of the OFL solution cannot be explained in terms of the ionization state of the catalyst and the substrate as both carry either negative or positive charges at alkaline or acidic conditions, respectively; i.e. neither environment should particularly favour substrate adsorption on the surface. At low pH values, positive holes are the main oxidation species, while at neutral or high pH, hydroxyl radicals are reflected as the major species. It appears that Ofloxacin oxidative transformation is primarily by valence band holes rather than radicals [Konstantinou et al., 2003; Sohrabi et al., 2008; Jaiswal et al., 2012].

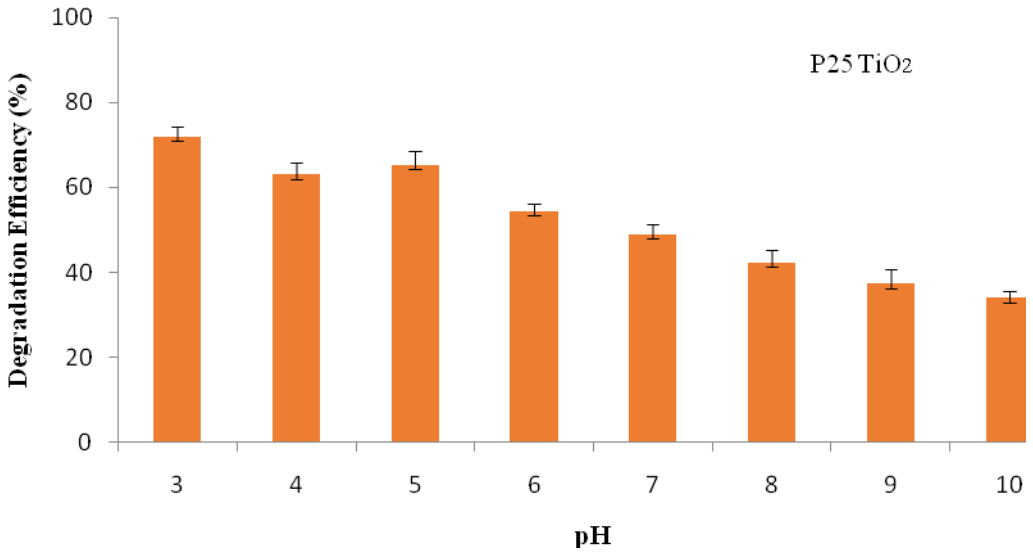

Fig 4.20 Effect of variation of pH
(Initial concentration=25ppm, catalyst dose=1.5g/L)

4.3.3 Co-doped TiO_2 mediated degradation

The concentration of dopant-metal ions (Bi-Ni co-doped TiO_2) plays a very significant role in photocatalytic activity. The concentration of dopant (Bi- Ni) was varied from 0.25 to 1.0 wt% at pH 3 with catalyst dose of 1.5g/L under 6h of solar irradiations (30-35W/m^2) as shown in Fig. 4.21. The maximum degradation efficiency of doped catalyst was obtained with dopant concentration of 0.25 wt%, further increasing the concentration of dopant lead to decrease in degradation efficiency. It may be attributed to the fact that, metal ions, at low concentration, act as trapping centres for photo-generated electron (e^-) and/or hole (h^+) within the titania band-gap thus increasing the recombination time of e^-/h^+ pairs. These primarily trapped charges may then migrate, towards the surface of the semiconductor where further redox reaction occurs, thus enhances the photocatalytic activity. However, a high concentration of metal ions results in the recombination of the photo-generated e^- and h^+. There persists a finest concentration amount of dopant-metal ions at which the concentrated amount of e^- and/or h^+ are confined without recombination; on increasing the amount above this optimum value the photocatalytic activity decreases because of the increase in recombination rate [Jaiswal et al., 2012].

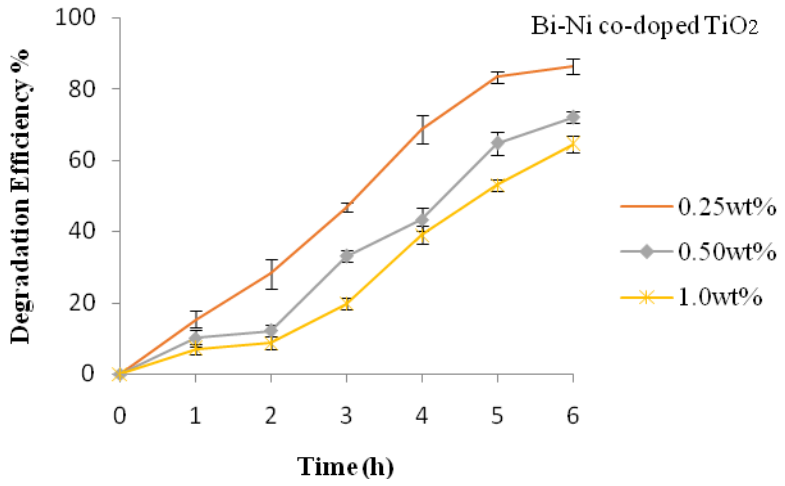

Fig 4.21 Effect of variation in dopant concentration (Initial concentration=25ppm, catalyst dose=1.5g/L, pH 3.0)

Degradation of OFL with Bi-Ni co-doped TiO_2 was compared with P25 TiO_2. The OFL (25 mg/L) was allowed to undergo photocatalytic treatment for 6 h using optimum catalyst concentration of 1.5 g/L at pH 3. It was observed (Fig. 4.22) that 86.0% of OFL was degraded using Bi-Ni co-doped TiO_2 under solar irradiations, whereas, 42.0% degradation occurred using P25 TiO_2,which shows that introduction of metal ions leads to increase in the efficiency of TiO_2 catalyst, and it may be attributed to decrease in band-gap of Bi-Ni co-doped TiO_2.

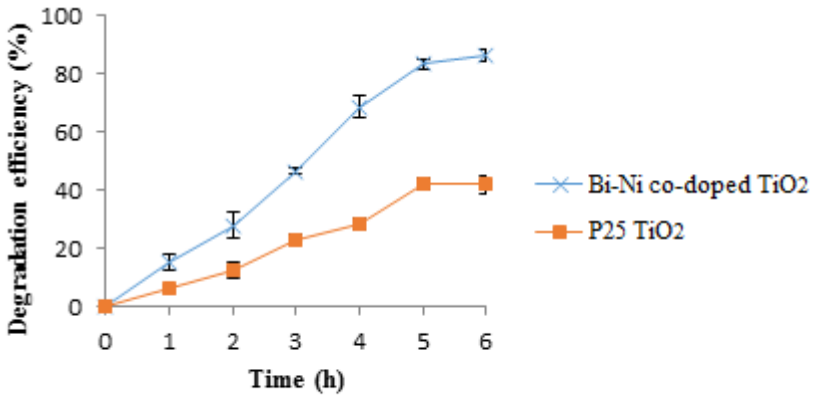

Fig 4.22 Effect of variation of type of catalyst (Initial concentration=25ppm, catalyst dose=1.5g/L, pH 3.0)

4.3.4 Comparison of solar/UV light

Plot of photocatalytic degradation of OFL under UV/solar irradiation as a function of time with 1.5 g/L (Bi-Ni co-doped TiO_2), at pH 3 has been presented in Fig. 4.23. The

photocatalytic degradation efficiency of OFL was higher under solar light (30-35W/m^2) when compared to UV light (11.2W/m^2) Maximum degradation of OFL were found to be 86.0 and 42.2 % under solar and UV irradiations, respectively. However, P25 TiO_2 resulted in 76.0 and 40.0% degradation under UV and solar light, respectively, under optimal condition.

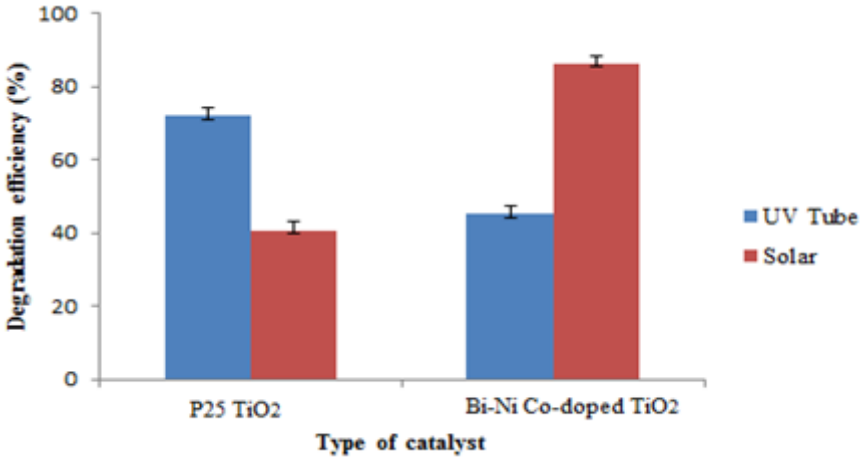

Fig 4.23 Effect of variation of light source
(Initial concentration=25ppm, catalyst dose=1.5g/L, pH 3.0)

4.3.5 Kinetic study

Kinetic studies for degradation of OFL under catalyst condition (catalyst dose of 1.5 g/L at pH 3) were carried out to find the reaction rate constant and order of reaction with Bi-Ni co-doped TiO_2 as photocatalysts under solar irradiations. The plot of ln C/C_0 v/s time gave straight line as shown in Fig. 4.24 and the correlation constant was found to be 0.963. Rate constant was calculated as 0.0062min^{-1} for Bi-Ni co-doped TiO_2 while, P25 TiO_2 gave rate constant of 0.0036min^{-1}, which shows higher activity of co-doped catalyst. Straight line of the graph shows that photocatalytic degradation of model compound followed first order kinetics.

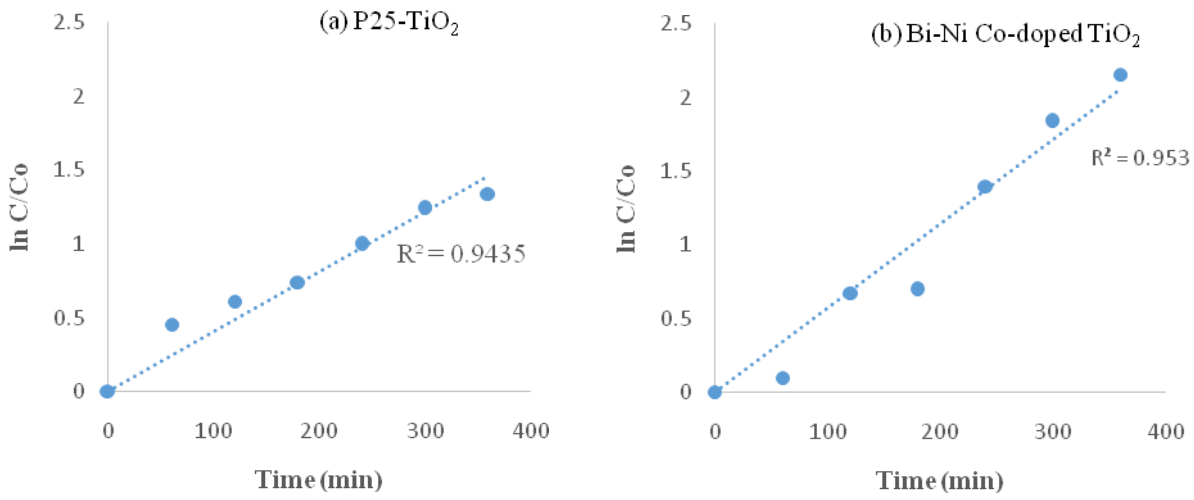

Fig 4.24 Kinetic study of degradation of OFL using P25 TiO_2 and Bi-Ni co-doped TiO_2 (Initial concentration=25ppm, catalyst dose=1.5g/L, pH 3.0)

4.4 PHOTOCATALYTIC DEGRADATION OF ATENOLOL

Atenolol is a selective β_1 receptor antagonist, used primarily in treatment of cardiovascular diseasessuch as a hypertension, coronary artery disease and arrhythmias [Maurer et al., 2007].Due to its wide consumption and less human metabolism, ATL was extensivelynoticed in sewage effluents [Alder et al., 2010, Huggett et al., 2003]. The studies also determined the daily aqueous mass output loads for the compounds though the treated wastewater is 2.2–50.8 g/d for Atenolol. Physical and chemical properties of Aspirin are explained in Table 4.8.

Table 4.8 Physical properties and Chemical structure of Atenolol

Name of compound	Atenolol
Synonym	4-[2-Hydroxy-3-[(1-methylethyl)amino]propoxyl]benzeneacetamide
IUPAC	{4-[2-Hydroxy-3-(propan-2-ylamino)propoxy]phenyl}acetamide
CAS No.	29122-68-7
Molecular Formulae	$C_{14}H_{22}N_2O_3$
Molecular weight	266.3g/mol
Density	1.13g/cm^3
Melting point	146°C-148°C
Boiling point	508.05°C
Lambda max	244nm
Solubility in water	26.5mg/ml

Structure	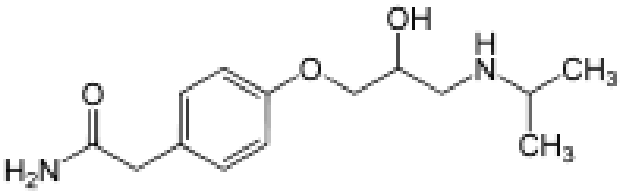

Graphene TiO_2 and Graphene ZnO composites were prepared using hydrothermal method as explained in Section 3.3.2 and its characterization was done. Further, the photocatalytic degradation of Atenolol (25mg/L) was compared using graphene composites and P25 TiO_2 as photocatalyst.

4.4.1 Characterization of graphene TiO_2

Graphene TiO_2/ZnO composites prepared using hydrothermal method was characterized for various parameters such as particle size, morphology, band gap and surface area.

4.4.1.1 XRD pattern

XRD pattern (Fig 4.25) of GO exhibits a diffraction peak at 2θ = 11.3°, which is in close agreement with the previous reports [Fan et al., 2011]. Figure 4.25 shows the highly crystalline nature of TiO_2-G, and both anatase and rutile crystalline phases are observed. However, peaks associated only with TiO_2 are observed, and no peak is assigned to GO, indicating that it was reduced to graphene during the hydrothermal process. Likewise, the XRD pattern of ZnO-G displays an excellent crystalline characteristic of the composite as shown in Fig

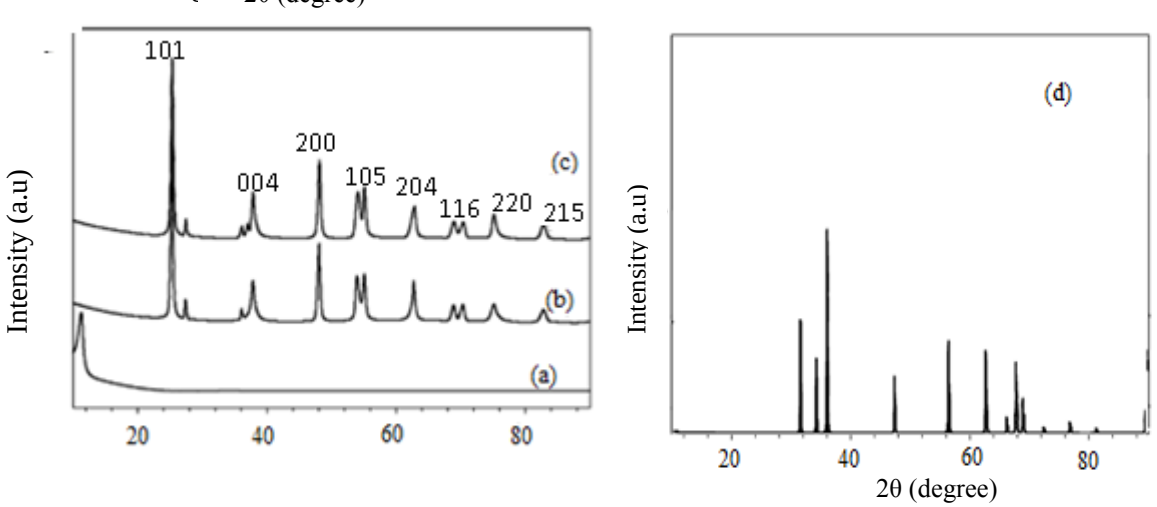

Fig 4.25 XRD pattern of (a) Graphene oxide (b) P25 TiO_2 (c) TiO_2-G(d) ZnO-G

4.4.1.2 UVdiffuse reflectance spectroscopy-

The optical properties of the samples were investigated by UV−vis spectroscopy. The absorption spectra of TiO_2, TiO_2-G and ZnO-G are compared in Figure 4.26. It has been observed that after introduction of graphene into the bare TiO_2, the absorption edge is noticeably shifted into the visible region, whereas the small shift is observed for ZnO-G. By adding graphene to TiO_2, the band gap is noticeably decreased from 3.1 to 2.2 eV, which can be associated with the enhanced chemical bonding between TiO_2 and graphene [Zhang et al., 2011]. However, the band gap corresponding to ZnO-G is 2.9 eV, which is slightly decreased compared to that of pure ZnO. Therefore, the degree of band gap narrowing is higher for TiO_2-G when compared to ZnO-G, implying that the interaction of TiO_2 and graphene was stronger. This may also suggest that the graphene mainly acts as a substrate for immobilization of ZnO particles [Sun et al., 2014]. As a result of this extension in photoresponse range, the solar spectrum could be utilized more efficiently and the solar degradation rate of ATL was improved by applying graphene into TiO_2 and ZnO.

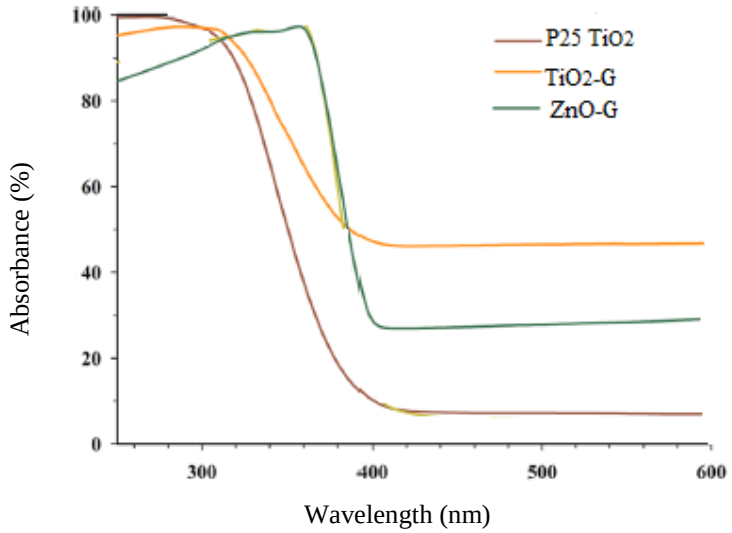

Fig 4.26 UV-DRS reflectance spectrum

4.4.1.3 SEM analysis

Typical SEM images of ZnO-G and TiO_2-G are shown in Figure 4.27. These images verify TiO_2 or ZnO loading on the graphene sheet. The interaction of the -OH and -COOH functional groups of GO with the surface of the semiconductors facilitates this loading.

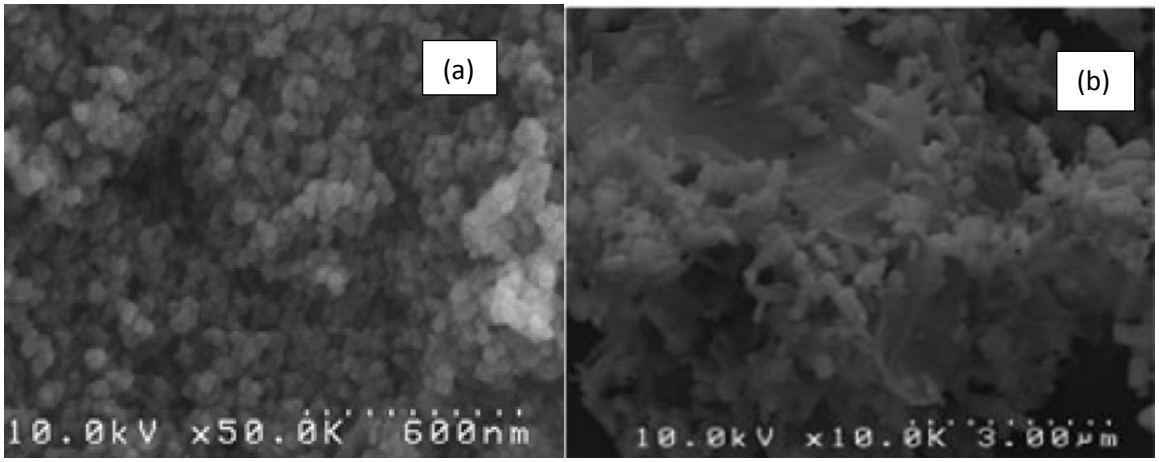

Fig 4.27 SEM images (a) TiO_2-G (b) ZnO-G

4.4.2 Effect of photocatalytic parameters

The photocatalytic degradation of Atenolol was carried out using P25 TiO_2& synthesized TiO_2-Gin slurry mode under solar simulator and the effect of various process variables viz. pH, light intensity, effect of light source has been studied.

4.4.2.1 Effect of catalyst loading

The effect of catalyst loading (P25 TiO_2& Graphene TiO_2) for the degradation of Atenolol (25mg/L) was studied in the range 0.5–2.0 g/L and the results are shown in Fig. 4.28 As indicated, the initial rate of reaction increases with increase in catalyst loading up to a certain value, whereas further increase beyond that value lead to reduction in rate of reaction. Basically increase in the catalyst loading leads to increase in number of active sites that are accessible for photocatalytic reactions and this take place up to a point where all catalyst particles are fully illuminated [Yang et al., 2008]. At higher concentrations, the screening effect of excess particles takes place, which leads to covering of the photosensitive surface and consequently hindering the penetration of light and these loss of photons lead to decrease in reaction rate. It was observed that 72.0 and 55.0% degradation was achieved using TiO_2-G and$P25\ TiO_2$as catalyst with dose of 1.5g/L in 1h under solar simulator at pH 6.

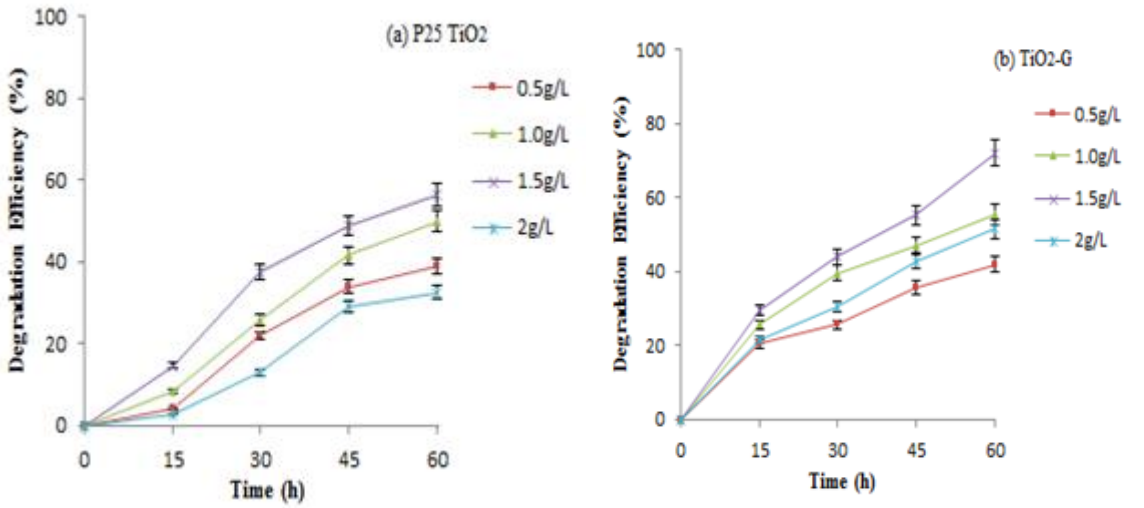

Figure 4.28 Effect of catalyst loading (a) P25 TiO_2 (b) TiO_2-G (Atenolol Concentration=25ppm, pH=6, Light Intensity= 75mW/cm^2)

4.4.2.2 Effect of initial substrate concentration

Experiments were carried out by varying the initial concentration of substrate in the range 5–25 mg/L with 1.5 g/L catalyst loading and the results are shown in Fig. 4.29(a) & (b). The rate of degradation decreased with increase in concentration of ATL. Atenolol conversion reduced from 85.0 to 57.0% and 92.0 to 72.0% after 60 min as concentration of substrate was increased from 5 to 25 mg/L using P25 TiO_2 and TiO_2-G, respectively.

When the concentrations of Atenolol is high, more and more Atenolol molecules are adsorbed on the surface of catalyst. In contrast, the relative number of ·OH and $\cdot O_2^-$ radicals attacking the Atenolol molecules decreases due to constant reaction conditions. As a result the photocatalytic degradation decreases. The limited number of surface sites on catalyst particles may control the photodegradation. Therefore, the requirement of reactive species (·OH and $\cdot O_2^-$) needed for the degradation of pollutant also increases. However, the formation of ·OH and $\cdot O_2^-$ on the catalyst surface remains constant for a given light intensity, catalyst amount and duration of irradiation. Hence, the available ·OH radicals are inadequate for the pollutant degradation at higher concentrations. Therefore the degradation decreased as the concentration of ATL was increased [Bahnemann et al., 2007].

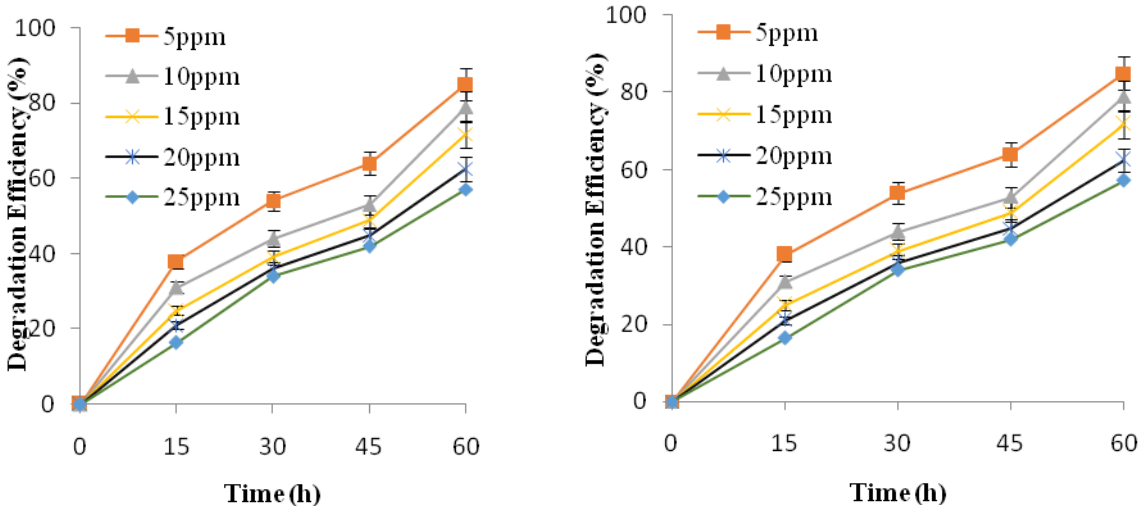

Figure 4.29 Effect of Initial Substrate concentration (a) P25 TiO_2 (b) TiO_2-G (Catalyst dose=1.5g/L, pH=6, Light Intensity= 75mW/cm^2)

4.4.2.3 Effect of pH

The natural pH of 25 mg/L Atenolol solutions was 9 and it was attuned at pH ranging from 4 to 9.0 by addition of appropriate amount of HCl or NaOH solutions. Fig. 4.30 (a) & (b) shows the effect of pH on the photocatalytic degradation of Atenolol. Experiments were conducted at acidic, alkaline and neutral conditions, and results showed that the degradation was maximum at neutral conditions, whereas, degradation declined at acidic or alkaline conditions. For instance, the conversion of Atenolol with TiO_2-G after 60 min of reaction was 60.0%, 72.0%, 63.0% and 57.0% at pH 4, 6, 8 and 9 respectively. While, for P25 TiO_2, 39.0%, 56.0%, 45.0% and 42.0% degradation was achieved at pH 4, 6, 8 and 9, respectively. As Atenolol have two reactive sites: an aromatic ring and a secondary amine-moiety. The reaction of the amine-moiety rest on pH of the solution, while the reaction of the aromatic ring does not. So, the reaction of Atenolol is influenced by the pK_a of the amines (i.e. 9.6) and the solution pH. At 9.6 > pH > 6, the amino group can get protonated while the catalyst surface is negatively charged. Thus, the electrostatic attraction between the surface of TiO_2 and Atenolol is enhanced, resulting in higher conversions at neutral conditions.

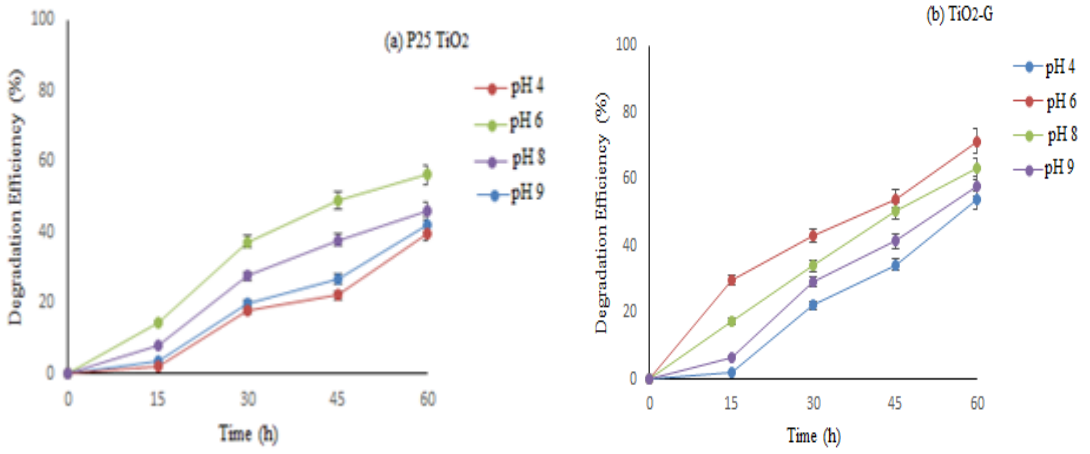

Figure 4.30 Effect of Variation of pH (a) P25 TiO_2 (b) TiO_2-G (Catalyst dose=1.5g/L, Atenolol concentration=25ppm, Light Intensity= 75mW/cm^2)

4.4.2.4 Variation of light intensity

The effect of variation of light intensity on the photocatalytic degradation of Atenolol was observed by keeping all other variables constant. The light intensity was varied from 25-100mW/cm^2. The results obtained are reported graphically in Figure 4.31(a) & (b). The observation shows that an increase in light intensity increases the rate of photocatalytic degradation, which is due to enhanced number of photons striking per unit area of the semiconductor. The increase in number of photons increases number of exited catalyst molecules and resultant increase in the number of hydroxyl radicals and super oxide ions (O_2^-). Thus, the degradation of ATL molecules increased with increase in light intensity.

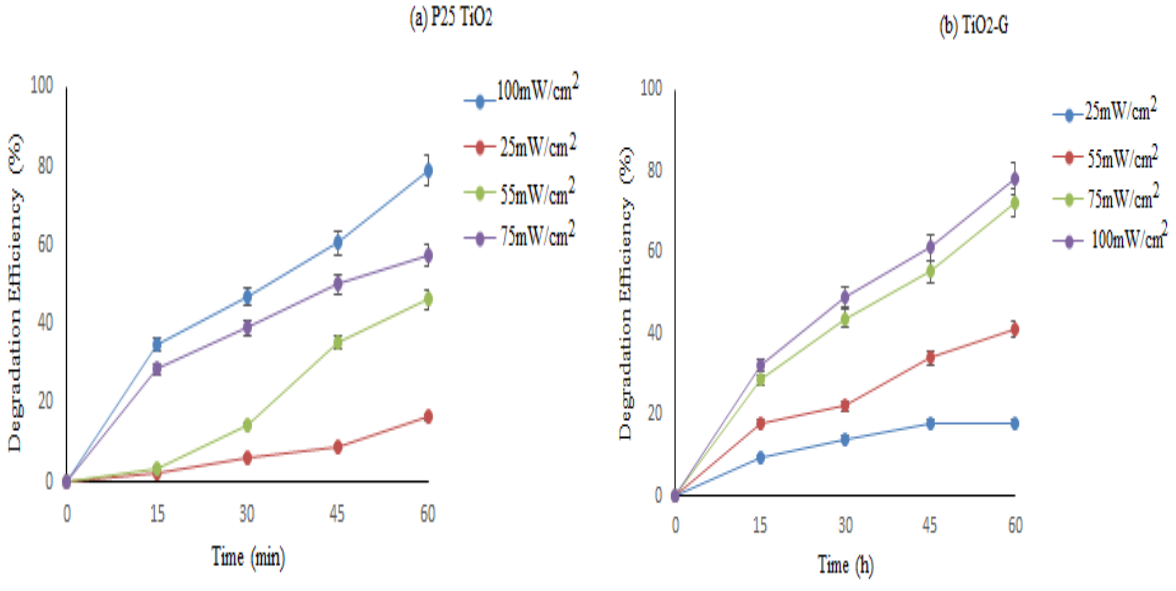

Figure 4.31 Effect of Variation of Light Intensity (a) P25 TiO_2 (b) TiO_2-G

(Catalyst dose=1.5g/L, Atenolol concentration=25ppm, pH=6)

4.4.2.5 Variation of light source

The light source has been varied using solar simulator with UV filter and without UV filter. Fig 4.32 depicted that using UV filter, higher degradation was obtained for Atenolol within 1h (pH 6 as 1.5g/L of catalyst dose). However, incorporation of UV filter resulted in the significant reduction of degradation both in case of TiO_2-G andP25 TiO_2.

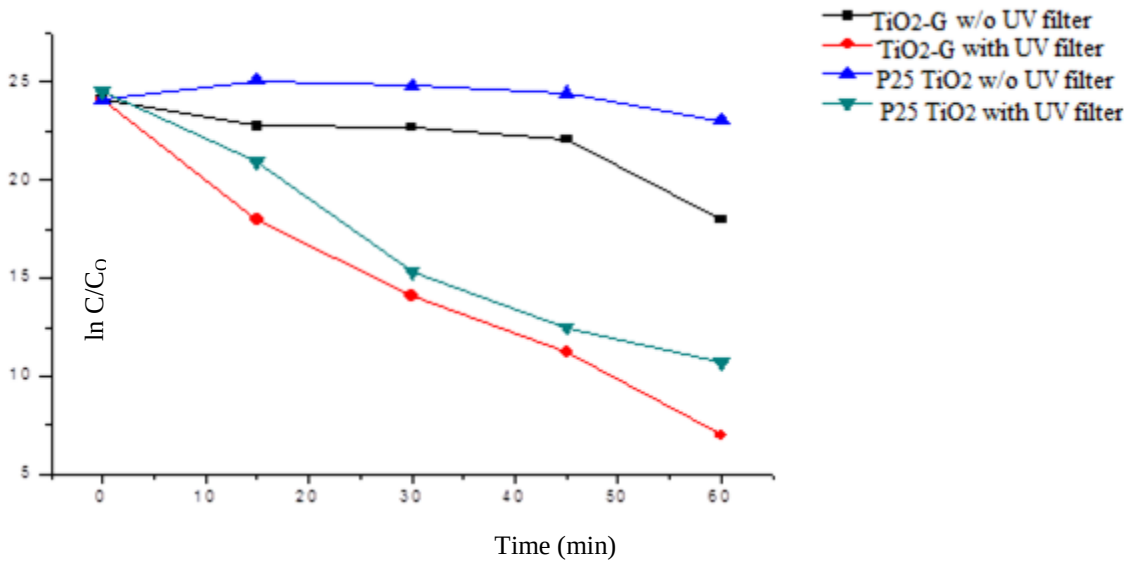

Figure 4.32 Effect of Variation of Light source (Atenolol concentration=25ppm, catalyst concentration =1.5g/L, pH=6, light intensity= 75mW/cm^2)

4.4.3 Kinetic regime for different catalyst loading

Fig 4.33 represents data for the photocatalytic degradation rate of Atenolol at different catalyst loadings. The catalyst load was varied from 0.01- 2.0 g/L. it is evident from the results that the rate of degradation is nearly constant and is independent of catalyst loading between 0.01 to 0.08 g/L and thereafter, rate reduces progressively as the catalyst loading was allowed to increase from 0.08 to 2.0 g/L. In the 0.01-0.08 g/L range, the overall rate is exclusively affected by kinetics because as the amount of catalyst is allowed to double (in g of catalyst), the conversion (in mg/L/min) also doubles; so resultant rate remains constant. When the catalyst was increased beyond 0.08 g/L, the rate of reaction decreased gradually. Therefore, in this range, the overall rate is not guided completely by kinetics and is also affected by the transport of pollutant molecules or light on the surface of catalyst. In this transport-limited area, the degradation process increases at a slower rate than the increase of

the amount of catalyst and, therefore, generally rate decreases instead of remaining constant. In other words, in this region conversion is affected by different factors: (i) Because of external mass-transfer resistance, all of the additional catalyst surface area does not come in contact with a pollutant, (ii) Because of agglomeration of the catalyst particles or internal mass-transfer resistance, the pollutant might not reach to some of the catalyst surface area, (c) light cannot extent upto some of the catalyst surface area due to absorption and scattering of light, (d) light cannot enter the agglomerates and trigger the inner surfaces, or (e) combination of all of the above. Thus, Figure 4.33 reveals two regimes: (1) the kinetic regime at the low catalyst range (<0.08g/L) and (2) the transport (mass or light) limitation regime at the high catalyst loading (0.08-2.0 g/L).

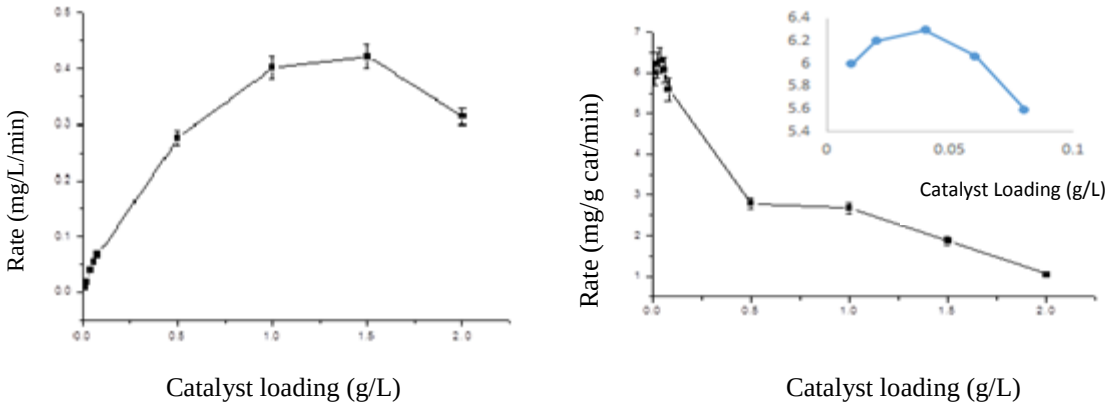

Figure 4.33 Kinetic regime for degradation of Atenolol at different catalyst dose (Atenolol concentration=25ppm, pH=6, light intensity=750mW/cm^2)

4.4.4 Kinetics of TOC disappearance

TOC analysis seems to be accurate and appropriate for evaluating the decontamination of polluted waters containing organics since it takes into account all the residual carbon-containing metabolites. The complete mineralisation of ATL was confirmed from total organic carbon (TOC) experiment. The kinetics isotherm of TOC disappearance [TOC] = f (t) is given in Fig. 4.34. For Atenolol compound of 25ppm, it was observed that TOC has totally disappeared in 7 h. TOC value decreased with increase in irradiation time. The initial TOC of Atenolol solution was found to be 16.9mg/L and diminished after 7h of irradiation time.

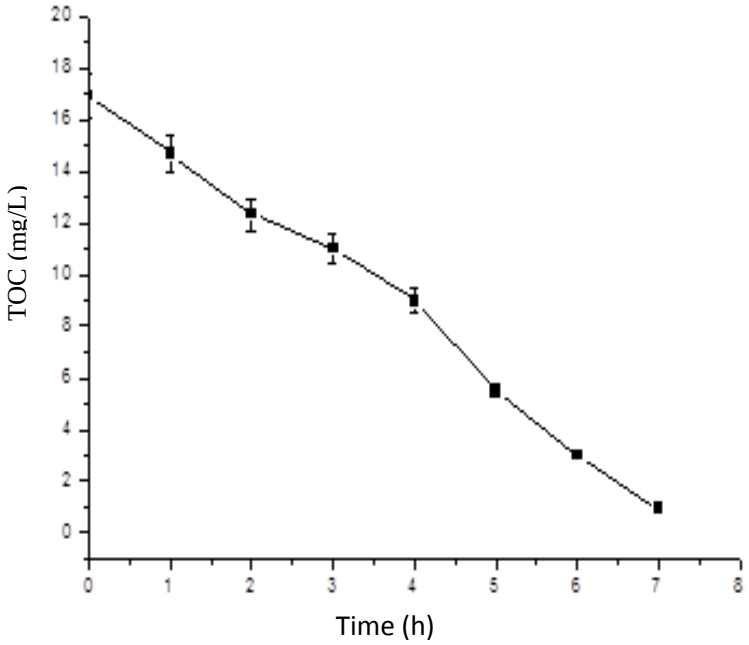

Figure 4.34TOC for Atenolol degradation (Atenolol concentration=25ppm, pH=6, catalyst dose TiO_2-G=1.5g/L, Light intensity=75mW/cm^2)

4.5 PHOTOCATALYTIC DEGRADATION OF ATENOLOL WITH GO–ZnO/TiO_2 COMPOSITE

The photocatalytic degradation of Atenolol was also evaluated and optimized with TiO_2-G and ZnO-Gin slurry mode under solar simulator for assessing the effect of various process parameters viz. pH (A), Catalyst dose (B), Substrate concentration (C), light intensity(D).Optimization of process parameters through Box-Benkhen design was done to maximize the photocatalytic degradation of Atenolol by optimizing four independent parameters simultaneously.

4.5.1 Experimental design and statistical analysis

A three level Box-Benkhen design with four factors was employed to know the optimum conditions so as to maximize the degradation rate of Atenolol. The method consisted of essential a low level (indicated as -1), a central (indicated as 0) and maximum level (indicated as +1) for each experimental factor (Table 4.9). The experiments were carried as suggested by BBD and are shown in Table 4.10. Twenty Nine set of experiments were done to analyse the extent of error in the experimental analysis. The experiment order No. 31-33 were conducted randomly just to validate the model.

Table 4.9 Four selected factors and three levels

Factors	**Factor level**		
	Low (-1)	**Middle (0)**	**High (+1)**
pH	4	6.5	9
Catalyst Dose (g/L)	0.5	1.25	2
Substrate Concentration (mg/L)	5	15	25
Intensity (W/m^2)	250	625	1000

The coefficients of the quadratic model, which represent the rate of reaction, were calculated by multiple regression analysis. The coefficients were analyzed using the analysis of variance (ANOVA) to assess if a given term has a significant effect ($p<0.05$).

The factors and the experimental levels for each factor were considered on basis of the results from preliminary experiments, literature values, and some other available resources. The maximum and minimum levels of ZnO-G concentrations were determined by preliminary experimental study. Below the lowest ZnO-G concentration, the photocatalytic effect was overwhelmed due to photolysis and further increase in concentration above the highest level was disadvantageous due to the turbidity of the solution which was causing photo-hindrance. The Atenolol concentration was selected by the applicability of the first-order kinetics over the range reported for an industrial effluent.

4.5.2 Experimental design and modeling analysis

For the response surface optimization study, the photocatalytic degradation of Atenolol was analyzed at each projected point of the four factors (pH, catalyst concentration, substrate concentration, Intensity) three level Box Benkhen design. The Atenolol concentration was determined at regular time intervals of each set of experiments and degradation reaction rate (min^{-1}) was considered as the response variables.

Table 4.10 Design conditions for experiment tal factors and response at different factor levels,

Expt. Order	Factors				Response
	pH	Catalyst dose (g/L)	Substrate Concentration (mg/L)	Intensity (W)	Reaction Rate (min^{-1})
1	6.5	1.25	15	625	0.458
2	9	1.25	15	250	0.0915
3	6.5	0.5	5	625	0.204
4	9	1.25	5	625	0.166
5	6.5	1.25	25	1000	0.783
6	6.5	2	25	625	0.670
7	4	1.25	15	250	0.215
8	6.5	0.5	15	1000	0.484
9	6.5	1.25	5	250	0.067
10	9	1.25	25	625	0.413
11	4	1.25	5	625	0.144
12	4	1.25	25	625	0.693
13	6.5	1.25	25	250	0.288
14	6.5	2	15	250	0.309
15	4	1.25	15	1000	0.374
16	9	1.25	15	1000	0.341
17	6.5	0.5	25	625	0.604
18	6.5	1.25	15	625	0.458
19	6.5	2	15	1000	0.596
20	6.5	1.25	15	625	0.451
21	6.5	1.25	5	1000	0.146
22	6.5	2	5	625	0.124
23	6.5	1.25	15	625	0.463
24	9	2	15	625	0.385
25	6.5	0.5	15	250	0.475
26	4	2	15	625	0.363
27	9	0.5	15	625	0.302
28	6.5	1.25	15	625	0.458
29	4	0.5	15	625	0.434
30	4	1.8	25	940	0.845
31	7	1	25	850	0.635
32	5	1	20	750	0.581
33	8	1.5	25	750	0.521

The F-value of 20.32 and corresponding p-values of < 0.0001 obtained from ANOVA for the responses, show the high significance of the models, indicating that there is only a 0.01% chance that the model F-Value could be this much large because of noise. The

ANOVA results for the coefficients of the regression models for rate of reaction are shown in Table 4.11 and 4.12.

Table 4.11 ANOVA results of the response surface quadratic model for Atenolol degradation

Source	Sum of squares	Degree of freedom	Mean square	F-Value	P-Value
Model	0.11	4	0.028	8.44	<0.0001
Residual	0.0306		4.91E-003		
Pure error	7.320E-005	4	1.830E-005		
	$R^{2=}$ 0.953	Adj $R^{2=}$ 0.906	Pred R^2=0.7302		

Table 4.12 ANOVA results for the coefficients of quadratic model for ATLdegradation

Factor	Coefficient Estimate	df	Standard Error	95% CI low	95% CI High
Intercept	0.46	1	0.026	0.40	0.51
A-pH	-0.044	1	0.017	-0.079	-8.27E-003
B-Catalyst Dose	-4.667E-003	1	0.017	-0.040	0.031
C- Substrate Concn.	0.22	1	0.017	0.18	0.25
D-Light Intensity	0.11	1	0.017	0.071	0.14
AB	0.038	1	0.029	-0.023	0.100
AC	-0.075	1	0.029	-0.14	-0.014
AD	0.023	1	0.029	-0.039	0.084
BC	0.037	1	0.029	-0.025	0.098
BD	0.070	1	0.029	8.124E-003	0.13
CD	0.10	1	0.029	0.043	0.17
A^2	-0.100	1	0.022	-0.15	-0.052
B^2	0.029	1	0.022	-0.020	0.077
C^2	-0.052	1	0.022	-0.10	-4.65E-003
D^2	-0.069	1	0.022	-0.12	-0.021

The predicted R^2 value (0.730) for removal of Atenolol, is in agreement with the corresponding adjusted R^2 value (0.906). Close R^2 and adjusted R^2 values indicate the adequacy of the model.

The adequate precision value of 17.168 indicate acceptable signal. Small prediction error sum of square (PRESS) values of 0.26 shows the fitness of the predicted values. The high values of R^2 and adequate precision and low PRESS values indicate that the quadratic polynomial equations can be employed to assess the removal of Atenolol in the experimental

range. From ANOVA analysis it is clear that pH, substrate concentration and light intensity are the significant terms playing a vital role in the removal of ATL at optimized conditions.

4.5.3 Verification of response surface model

A scatter plot of the experimental data as shown in Fig 4.35 against values predicted by model showed a rational correlation for all levels. A normal distribution of residual confirms a satisfactory results of model with the experimental data. A p value confirms a normal distribution of residuals and commends the model prediction correlated rationally well with the experimental results. Further experiments were done to confirm the rationality and correctness of the response surface model using the variables under consideration.

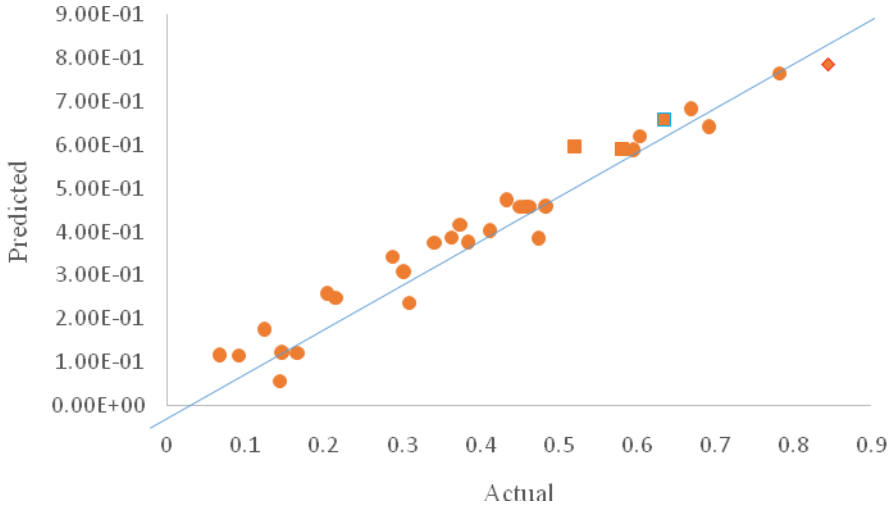

Fig 4.35 Predicted v/s actual Reaction rate (min^{-1})

4.5.4 Effect of factors on response variable

The effect of interaction of substrate concentration, pH, and light intensity were investigated and are shown in Fig 4. 36(a), (b) & (c). As it could be clearly seen from fig 4.25 a) that by increase in pH and substrate concentration, rate of reaction keep on increasing. It shows that both factors have direct effect on reaction and degradation of model compound. Similarly from Fig 4.35(b) it has been observed that by varying the pH and light intensity, maximum reaction rate is observed at pH 6.5, which is considered as an optimum pH and by increasing the light intensity, degradation keep on increasing and observed to be as maximum at $100W/m^2$. Further Fig 4.35(c) reveals the effect of light intensity and substrate concentration on rate of reaction. Similar trend has been observed, that with increase in light intensity, degradation increased and obtained maximum at $100W/m^2$ for 25ppm of substrate concentration.

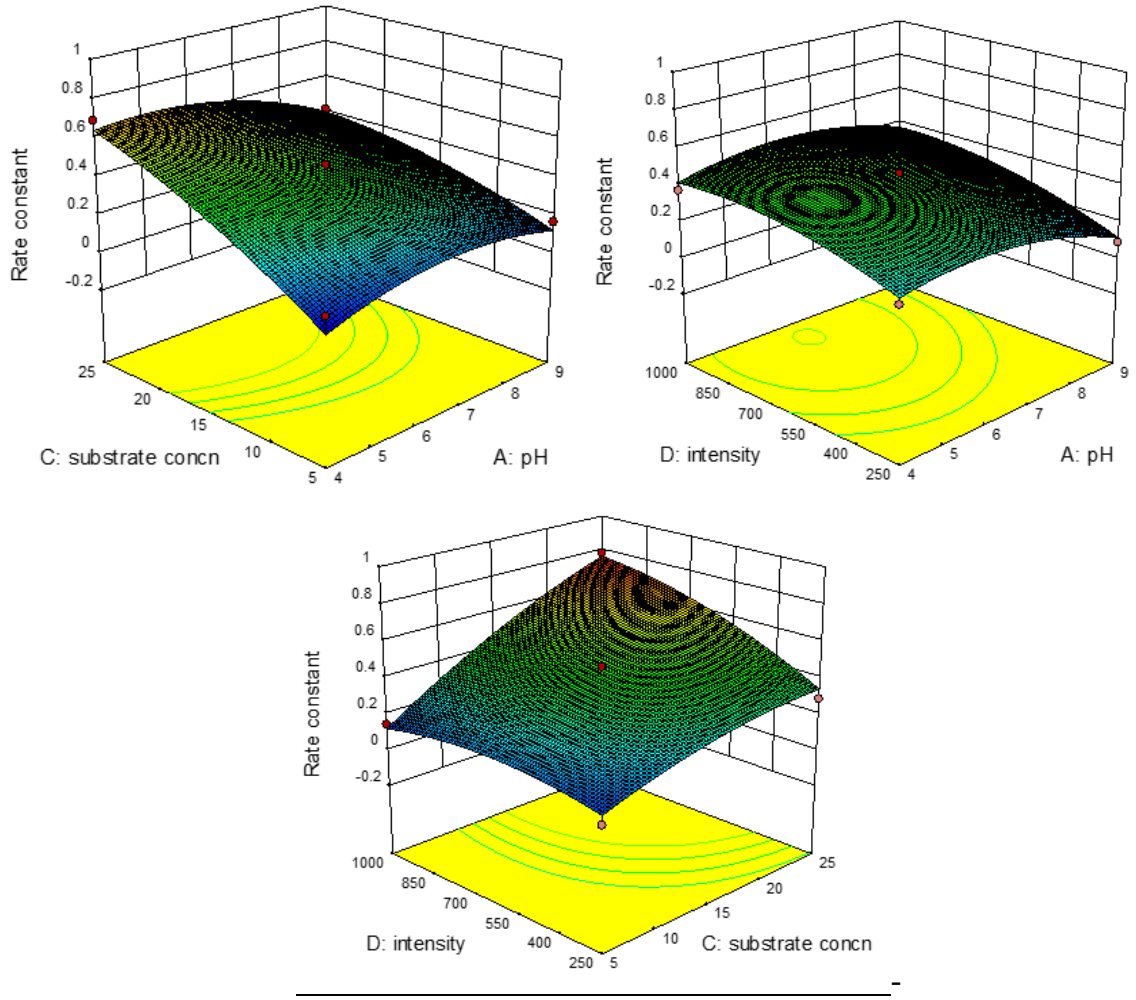

Fig 4.36 3D Response surface showing interaction between (a) substrate concentration and pH (b) Intensity of light and pH (c) Intensity of light and substrate concentration

4.5.5 Optimization of the degradation process

In the present study, the process was optimized under four constraints. The imposed constraints are pH of reaction mixture, minimization of the use of photocatalyst, maximization of the concentration of Atenolol and maximization of intensity of light. The optimum conditions for maximum rate of reaction for Atenolol degradation under imposed constraints were found to be dose of ZnO-G 1.2g/L, Concentration 25mg/L, Light intensity 940W and pH of the reaction mixture 4. The degradation of Atenolol was 85% under the optimum conditions. The result obtained proved the efficient use of RSM in the process optimization of photocatalytic degradation of Atenolol using ZnO-G composite.

4.5.6 Validation of the process optimization

In order to confirm the results, aqueous solution of Atenolol was irradiated under UV for 60 minutes in the batch reactor under the obtained optimum condition and the subsequent

degradation percentage attained was 85.0%. The experimental values were in worthy agreement with the predicted results. This showed the validity of the optimization result determined using RSM and it was confirmed that RSM can be competently employedfor the photocatalytic degradation process of Atenolol using ZnO-G Composite.

4.5.7 Comparative study ofTiO_2-Gand ZnO-G

Two composite of graphene i.e. ZnO-G&TiO_2-G were compared under optimum experimental conditions for each, at which ZnO-G has attained the higher rate of reaction. It can be analyzed that ZnO-G performed better catalyst when compared to TiO_2-G. The rate of reaction obtained with ZnO-G is $0.845min^{-1}$ whereas, the rate of reaction with TiO_2-Gobtained was $0.541min^{-1}$. Comparison of photocatalytic activity of two different photocatalyst has indicated that the ZnO-G is better for degradation of Atenolol. Besides higher efficiency, the other advantage of ZnO is its low cost.

4.6 PHOTOCATALYSIS IN IMMOBILIZED MODE

A novel semi-batch swirl-flow monolithic-type reactor (Fig. 3.3) with immobilized photocatalyst was used in continuous mode (Fig. 3.4) to study the kinetics of photocatalytic reactions, in order to eliminate the need of separation of catalyst after photocatalytic treatment. Monoliths are unique catalyst supports that provide a high surface-to-volume ratio and allow high flow rates with low-pressure drop. Both the catalysts (TiO_2-G and P25 TiO_2) wereassessed under immobilized/ suspended modes separately, to compare their efficacy in the degradation of Atenolol under UV irradiations. The simultaneous effect of parameters such aspH (A), Catalyst concentration (B), Substrate concentration (C) and light intensity (D)on degradation efficacy was optimized using BBD technique.

4.6.1 Adsorption study

Degradation of Atenolol was assessed with immobilized catalyst in dark (without UV lamp) in experimental set-up (Fig. 3.4) to study the adsorption of substrate on the surface of the catalyst as explained in Section 3.5.1.Fig. 4.37 depicts small decrease in Atenolol concentration in the absence of UV light when a fresh catalyst plate was used in swirl flow reactor for 1 h, which can be attributed to the adsorption of Atenolol onto the catalyst. The concentration of Atenolol adsorbed on the surface was calculated w.r.t. the difference between the initial and final concentrations.

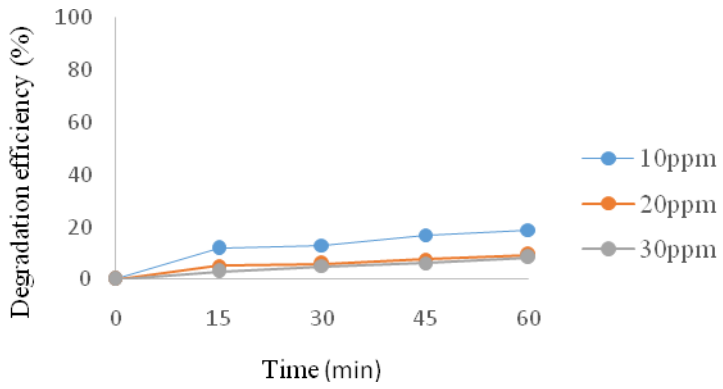

Fig 4.37 Adsorption of Atenolol at different initial concentrations (pH 6, catalyst percentage =10%)

4.6.2 Experimental design and statistical analysis

A four factor three level Box-Benkhen design having five central points with three replicates was used to determine the operating conditions for maximizing the Atenolol degradation rate. The method consisted of defining a minimum or low level (denoted as -1), a central or level (denoted as 0) and a high or maximum level (denoted as +1) for each experimental factor (Table 4.13).

The experiments were conducted under the conditions shown in Table 4.14. Twenty Nine experiments were conducted to estimate the extent of error in the experimental analysis. The experiment with Order No. 31-33 were conducted randomly just to validate the model.

The coefficients of the quadratic model, which describes the degradation rate as a function of the reaction condition (independent variables), were calculated by multiple regression analysis on the experimental data. The coefficients were analyzed using the analysis of variance (ANOVA) to evaluate if a given term has a significant effect ($p<0.05$).

Table 4.13 Four selected factors and three levels

Factors	**Factor level**		
	Low (-1)	**Middle (0)**	**High (+1)**
pH	4	6.5	9
Catalyst Concentration (%)	10	15	20
Substrate Concentration (mg/L)	10	20	30
Intensity (W/m^2)	60	160	260

4.6.3 Experimental design and modeling analysis

The photocatalytic degradation of Atenolol was analyzed by response surface optimization study, at each projected point of the four factors (pH, catalyst concentration, substrate concentration, Intensity) three level Box Benkhen design. Considering this design, 29 experiments were performed. The Atenolol concentration was determined at regular time intervals of each set of experiments and degradation reaction rate (min^{-1}) was calculated using data. Analysis of variance (ANOVA) was used to statistically analyse the experimental data for rate of reaction. The F-value of 15.85 and corresponding p-values of < 0.0001 obtained from ANOVA for the rate of reaction, show the high significance of the models. The ANOVA results for the coefficients of the regression models for rate of reaction are shown in Table 4.15 and 4.16. The predicted R^2 value (0.684) for Atenolol removal, is in accordance with the adjusted R^2 value (0.795). Adjusted R^2 value corrects the R^2 value for sample size and number of terms in the model. Close R^2 and adjusted R^2 values indicate the adequacy of the model.

The adequate precision value of 11.01 indicate acceptable signal. Small prediction error sum of square (PRESS) values of 0.19 shows the suitability of the predicted values. The low PRESS value, adequate precision and high values of R^2 depicted that the quadratic polynomial equations can be efficiently considered to analyse the degradation of Atenolol. From ANOVA analysis it is clear that catalyst concentration, substrate concentration and light intensity are the significant terms playing a vital role in the removal of ATL at optimized conditions in immobilized mode.

Table 4.14 Design matrix for experimental factors and response at different factor levels

Expt. Order	Factors				
	pH	Subs. Concentration (mg/L)	Catalyst Concentration (mg/L)	Intensity (W/m^2)	Reaction Rate (min^{-1})
1	6.5	20	10	260	0.659
2	6.5	30	20	160	0.46
3	6.5	10	10	160	0.551
4	6.5	30	15	260	0.523
5	6.5	20	20	260	0.49
6	9	20	15	260	0.342
7	9	20	20	160	0.201
8	6.5	10	15	60	0.231
9	6.5	20	15	160	0.451
10	4	30	15	160	0.41
11	4	20	15	260	0.509
12	9	30	15	160	0.3
13	6.5	30	10	160	0.667
14	6.5	20	20	60	0.42
15	6.5	20	15	160	0.648
16	6.5	20	15	160	0.65
17	6.5	30	15	60	0.45
18	9	10	15	160	0.25
19	4	20	20	160	0.289
20	6.5	20	15	160	0.567
21	4	20	10	160	0.369
22	6.5	10	15	260	0.65
23	9	20	15	60	0.24
24	6.5	20	10	60	0.279
25	9	20	10	160	0.323
26	6.5	20	15	160	0.45
27	6.5	10	20	160	0.485
28	4	10	15	160	0.331
29	4	20	15	60	0.215
30	8	10	15	60	0.227
31	7	20	15	160	0.41
32	5	15	10	260	0.57
33	6	30	20	160	0.456

Table 4.15 ANOVA results of the response surface quadratic model for Atenolol degradation

Source	Sum of squares	Degree of freedom	Mean square	F-Value	P-Value
Model	0.28	4	0.070	15.85	<0.0001
Residual	0.052	6	8.739E-003		
Lack of fit	0.023	10	2.26E-003	0.23	0.973
Pure error	0.040	4	9.911E-003		
	$R^{2=}$ 0.897	Adj $R^{2=}$ 0.795	Pred R^2= 0.684		

Table 4.16 ANOVA results for the coefficients of quadratic model for Atenolol degradation

Factor	Coefficient Estimate	Df	Standard Error	95% CI low	95% CI High
Intercept	**0.55**	1	0.030	0.49	0.62
A-pH	-0.039	1	0.019	-0.080	2.368E-003
B-Catalyst Dose	0.026	1	0.019	-0.015	0.067
C- Substrate Concn.	-0.042	1	0.019	-0.083	-6.316E-004
D-Light Intensity	0.11	1	0.019	0.070	0.15
AB	-7.250E-003	1	0.033	-0.079	0.064
AC	-0.010	1	0.033	-0.082	0.061
AD	-0.048	1	0.033	-0.12	0.024
BC	-0.035	1	0.033	-0.11	0.036
BD	-0.086	1	0.033	-0.16	-0.015
CD	-0.078	1	0.033	-0.15	-5.992E-003
A^2	-0.21	1	0.026	-0.26	-0.15
B^2	-0.015	1	0.026	-0.071	0.041
C^2	-0.029	1	0.026	-0.085	0.027
D^2	-0.052	1	0.026	-0.11	3.720E-003

4.6.4 Verification of response surface model

Additional set of tests were done to check the validity and correctness of the response surface model within the considered variables. For each set of experiments adiscreteconfirmation study was carried out for four factors and the model prediction (Fig 4.38) was in agreement with the observed results for Atenolol ranging from 10 to 30mg/L.

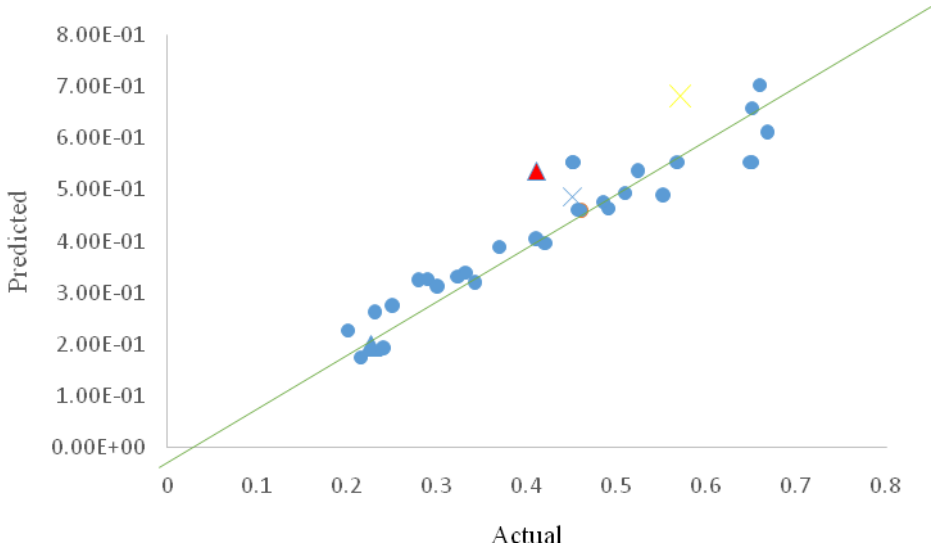

Fig 4.38 Predicted v/s actual Reaction rate (min^{-1})

4.6.5 Effect of factors on response variable

In the present study, the process was optimized under four factors. The factors that were taken into consideration are pH, amount of photocatalyst, concentration of Atenolol and intensity of light. Numerical optimization was carried out using Design expert version 9.0.0 considering one response. The optimum conditions for maximum rate of reaction for Atenolol degradation were found to be dose of GO- TiO_2 10%, Atenolol Concentration 30mg/L, Light intensity 160W/m^2 and pH of the reaction mixture 6.5. The degradation of Atenolol was 85% under the optimum conditions. The result obtained proved the efficient use of RSM in the process optimization of photocatalytic degradation of Atenolol using TiO_2-G composite.

The effect of interaction of substrate concentration, catalyst concentration and light intensity were investigated and are shown in Fig 4. 39(a) & (b). As it could be clearly seen from Fig 4.38 (a) that by increase in intensity of light and substrate concentration, rate of reaction keep on increasing. It shows that both factors have direct effect on reaction and degradation of model compound. Similarly Fig 4.38(b) depicts that by varying the catalyst concentration and light intensity, maximum rate of reaction is observed at catalyst concentration of 10%, was considered to be as optimum and rate of reaction further reduces by increasing the catalyst concentration beyond 10% and for the light intensity, it has been depicted that maximum constant is around 160W/m^2 and reduces on increasing or decreasing the light intensity on either side.

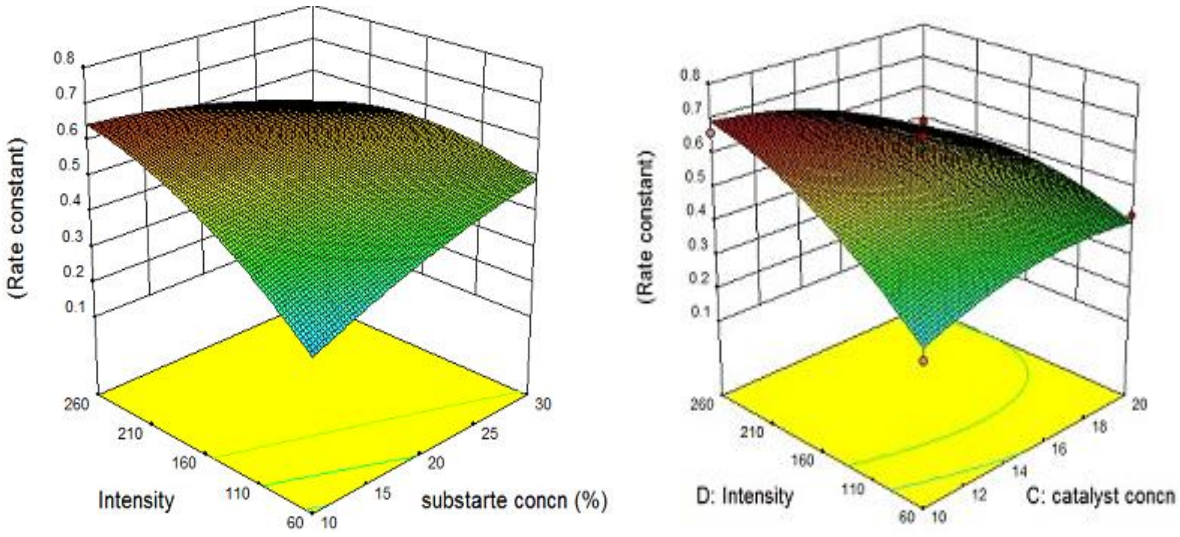

Fig 4.39 3D Response surface showing interaction between (a) substrate concentration and Intensity for photocatalytic degradation of Atenolol (b) Intensity of light and catalyst concentration

4.6.6 Validation of the process optimization

In order to validate the results of optimization, aqueous solution of Atenolol was irradiated under UV light for 60 minutes in the batch reactor under the different selected conditions from the range provided in model. The experimental values were in good agreement with the predicted results. This proved the validity of the optimization result determined using RSM under the imposed constraints and it was confirmed that RSM can be efficiently used to optimize the photocatalytic degradation process of Atenolol using TiO_2-G Composite.

4.6.7 Comparison of slurry and immobilized mode

In order to compare the efficacy of catalyst in slurry/ immobilized mode, P25 TiO_2 and TiO_2-G mediated photocatalytic degradation was carried out under optimum experimental conditions in UV irradiations and results indicate that both catalyst performed better in suspended mode when compared to immobilized mode. Moreover, TiO_2-Gattained higher reaction rate in comparison to P25 TiO_2 under immobilized mode with values of 0.0722 & 0.0497min^{-1}, respectively.

Table 4.17 shows the rate of reaction of Atenolol for suspended system (at optimum catalyst loading of 1.5 kg m^{-3}) and immobilized system (at optimum catalyst loading of 0.045 kg m^{-2}). Comparing the efficacy of TiO_2-G in slurry/immobilized mode indicate that degradation efficacy was more (35%) in case of slurry modewhen compared to immobilized mode under similar experimental conditions (10% catalyst concentration, 160W/m^2, pH 6.5)

with reaction rate of 0.0976and 0.0722min^{-1}, respectively. Low efficacy in case of immobilized catalyst may be because of the effect of external mass transfer particularly at low fluid flow rate, and due to the increasing diffusional length of reactant from bulk solution to the catalyst surface. However, it should be noted that it is always convenient to scale-up fixed catalyst system for photocatalytic degradation at industrial scale as it eliminates the problem of separation of ultrafine catalyst particles after treatment.

Table 4.17Reaction Rate for P25 TiO_2 and TiO_2-G catalyst in slurry/immobilized mode

S.No	Catalyst	System	Reaction Rate (min^{-1})
1.	P25 TiO_2	Immobilized	0.0497
2.	P25 TiO_2	Slurry	0.0672
3.	Graphene-TiO_2 composite	Immobilized	0.0722
4.	Graphene-TiO_2 composite	Slurry	0.0976

4.6.8 TOC analysis

The oxidation of an organic compound is a complex reaction; in many cases, it goes through complicated routes, leading to the formation of different intermediate compounds before being reduced to CO_2. So TOC was measured for TiO_2-G photocatalyst used in immobilized mode under optimal conditions (pH 6.5, catalyst concentration= 10%, light intensity = 160W/m^2) for the degradation of Atenolol (30 ppm).TOC value decreased from 16.9 to 4.8 mg/L within 90 minutes under UV irradiations (Fig. 4.40). So, results of TOC indicate that mineralization was significant with immobilized experiment.

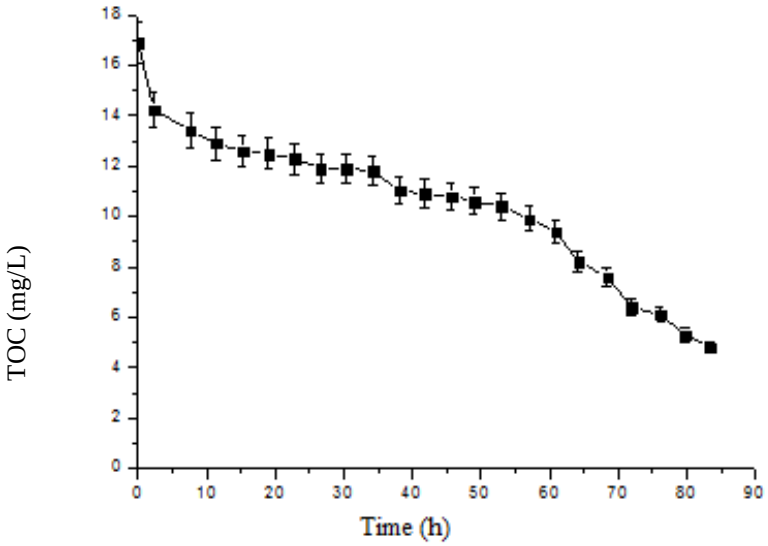

Fig 4.40 Photocatalytic degradation of Atenolol, TOC profile (Initial concentration=30ppm, catalyst loading=10%, pH=6.5, light intensity=160W/m^2)

4.7 INTEGRATED TREATMENT OF SIMULATED EFFLUENT

The present study evaluated the response of integrating photocatalytic and biological treatment for degradation of simulated effluent containing Atenolol (10ppm) as pharmaceutical compound and its efficacy was compared with independent photocatalytic and biological treatment. Degradation efficacy was evaluated in terms of BOD and COD removal.

4.7.1 Independent Photocatalytic treatment

Photocatalytic treatment of simulated effluent was employed with P25 TiO_2 as photocatalyst in slurry mode, illuminated under solar simulator at natural pH of 6.9. In order to optimize catalyst dose, the photocatalytic experiments were performed by varying P25 TiO_2 dose (0.5- 2.0g/L) in the presence of solar simulator (1000W/m^2) for a period of 1h. Fig 4.41 shows the extent of reduction in BOD & COD to be 10.0& 11.4%, respectively at dosage of 1.5g/L of TiO_2after 1h of treatment. Initially reaction rate increased with increasing catalyst loading up to a certain value, due to increase in the number of active sites, whereas further increase in dose lead to reduced rates. At higher concentrations, a screening effect of excess particles occurs, thus masking part of the photosensitive surface and consequently hindering or even reflecting the penetrating light [Yang et al., 2008].

Extending the time period of the photocatalytic decomposition of simulated effluent with 1.5g/L of P25 TiO_2 under solar simulator results in COD reduction of 45.3, 66.7 and 78.5% after 3, 4 and 5 h of treatment time, respectively (Fig 4.42). Keeping in view of

sluggish increase in degradation efficiency with increased duration, 4h of photocatalytic treatment was selected as suitable time period for the application of post biological treatment.

Moreover, Biodegradability assessment in terms of BOD_5/COD ratio was found to increase from 0.23 to 0.42 after 4h of irradiation. Several other studies from literature also documented increase in biodegradability as a result of photocatalytic treatment of real/simulated industrial effluents [Adameka et al., 2016; Lutterbeck et al., 2015; Varatharajan et al., 2007].

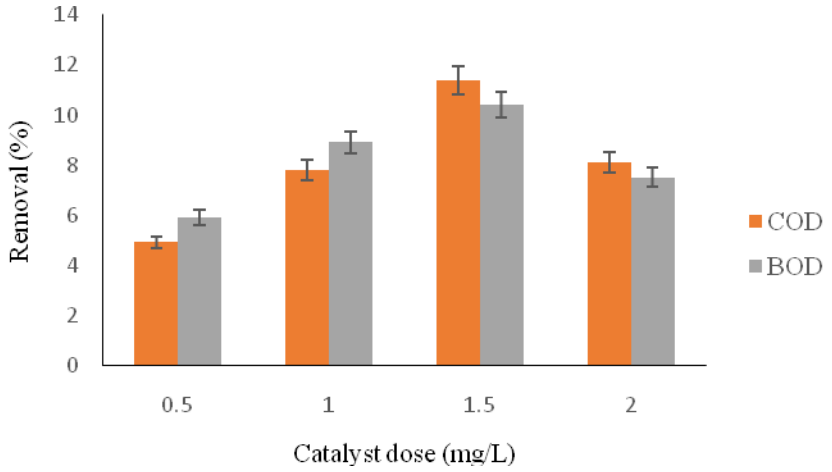

Fig 4.41 Effect of catalyst dose for degradation of simulated effluent in AOP treatment [Time =1 h]

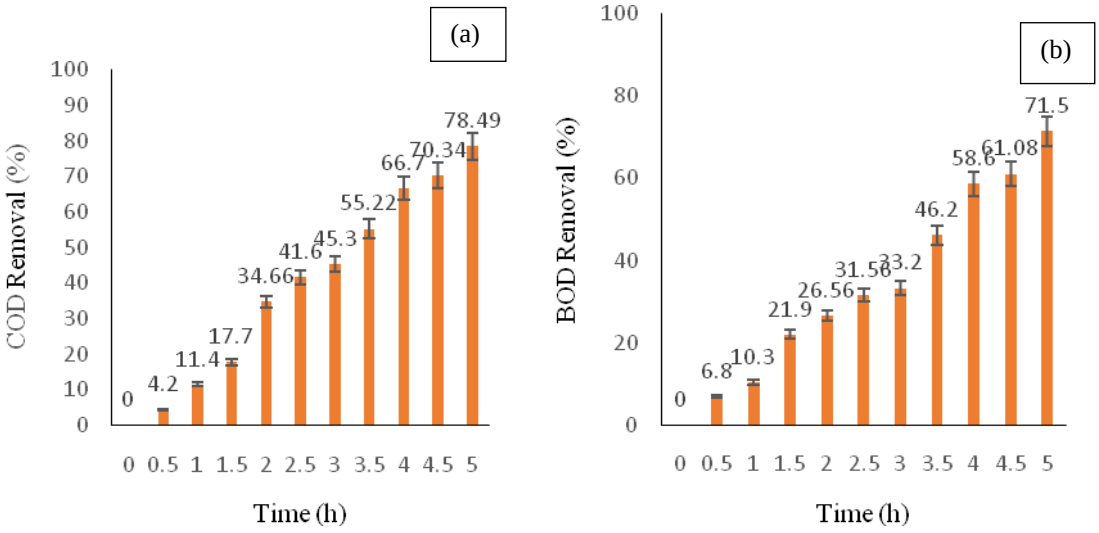

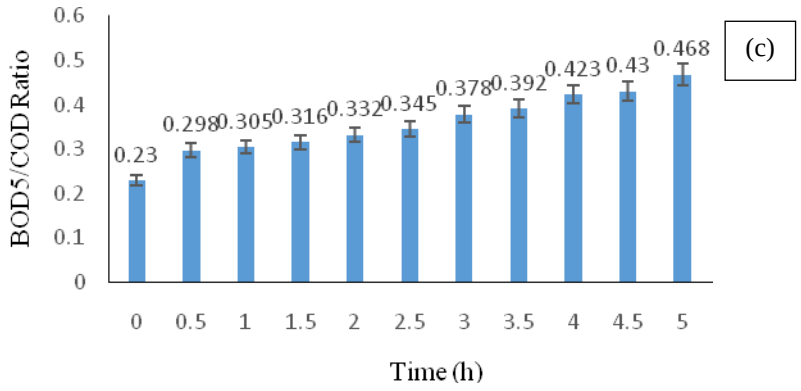

Fig 4.42 (a) COD removal (b) BOD removal (c) BOD_5/COD ratio in independent AOP treatment

4.7.2 Independent biological treatment

Simulated effluent was subjected to independent biological treatment with activated sludge from waste water treatment plant, Kipps lane, London, Ontario, so as to assess its degradation efficacy. As, microbial activity is strongly dependent on the sludge concentration as well as temperature of the reaction medium, so experiments were performed to adjudge the optimal sludge concentration and temperature. Sample was treated at natural pH of 6.9 with a sludge concentration of 2, 5, 10 & 15% in an incubator maintained at a temperature of 27ºC with continuous aeration and stirring for a period of 48 h.

Results indicate that 2% of sludge concentration resulted in 29.0 and 24.0% reduction of BOD and COD, respectively after 48 hof treatment (Fig 4.43). The low degradation efficacy may be attributed to comparatively high organic loading in simulated effluent with insufficient quantity of microbial biota. Using 5% activated sludge, BOD removal of 32.0& 37.0%, while COD removal of 32.0& 38.0%,was attained after 24 and 48h of treatment, respectively. Further increase in sludge concentration to 15% results in reduced degradation efficacy which may be because of the increase in MLSS that perturbs the biomass to food ratio as well as reduced transfer of oxygen, due to which survival of microbial community gets hampered and hence, leads to reduction in degradation efficiency.

In order to analyse the effect of temperature on biological activity of microorganisms, simulated effluent with optimal sludge concentration of 5% was subjected to biological treatment at two other temperatures of 20 and 37ºC. Results indicate that as the temperature was increased from 20 to 37ºC, there was gradual increase in the degradation efficiency which may be attributed to the increase in metabolic activity at elevated temperatures. BOD and COD removal of 46.3 and 46.2% was found at 37ºC, whereas removal of 37.0 and 32.0%

was observed at 20ºC, respectively after time period of 48h as shown in Fig 4.44. Hence, 5% of sludge concentration and 37^{o}C was considered as an optimal sludge concentration and temperature, respectively for biological treatment.

Table 4.18 Variation of COD removal in Biological treatment

	2% Sludge			**5% Sludge**			**10% sludge**			**15% sludge**		
Time(h)	**20ºC**	**27º C**	**37º C**	**20º C**	**27º C**	**37ºC**	**20ºC**	**27ºC**	**37ºC**	**20ºC**	**27º C**	**37º C**
0	0%	0%	0%	0%	0%	0%	0%	0%	0%	0%	0%	0%
3	3%	6%	11%	6%	9%	19%	4%	8%	12%	5%	10%	7%
6	6%	9%	21%	12%	15%	25%	11%	14%	18%	9%	12%	13%
12	12%	14%	29%	18%	26%	31.8%	16%	22%	26%	21%	21%	24%
24	15%	20%	31%	24%	32%	34.6%	20%	29%	32%	24%	29%	31%
48	19%	24%	39%	32%	38%	46.2%	31%	34%	39%	31%	36%	36%

Table 4.19 Variation of BOD removal in alone Biological treatment

	2% Sludge			**5% Sludge**			**10% sludge**			**15% sludge**		
Time (h)	**20ºC**	**27º C**	**37º C**	**20º C**	**27º C**	**37ºC**	**20ºC**	**27ºC**	**37ºC**	**20ºC**	**27º C**	**37º C**
0	0%	0%	0%	0%	0%	0%	0%	0%	0%	0%	0%	0%
3	7%	10%	14%	10%	11%	18%	8%	8%	14%	6%	9%	10%
6	9%	14%	19%	21%	21%	25%	9%	16%	19%	7%	12%	14%
12	11%	18%	26%	25%	25%	31.8%	12%	21%	26%	11%	19%	21%
24	16%	21%	32%	32%	32%	34.6%	17%	24%	27%	14%	22%	24%
48	21%	29%	37%	37%	37%	46.3%	24%	31%	39%	21%	27%	32%

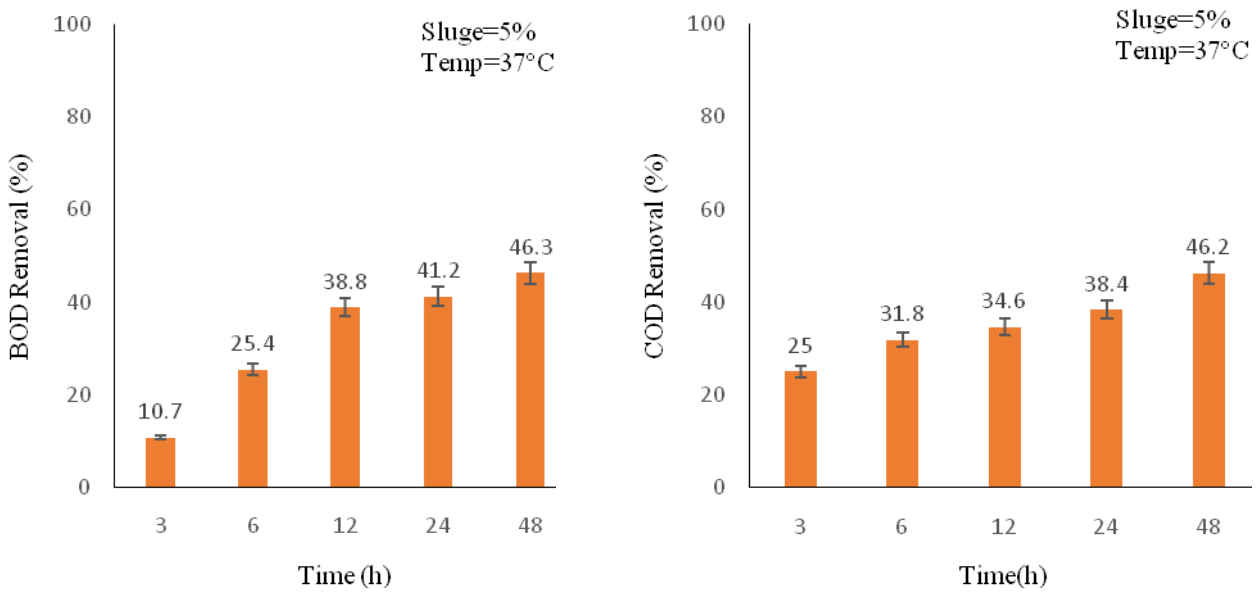

Fig 4.43 BOD and COD removal for Individual Biological Treatment

4.7.3Sequential photocatalytic-biological treatment

The phototreatment stage of the sequential system was intended to obtain a phototreated solution which is biologically compatible, after elimination of the initial bio-recalcitrant compound and the inhibitory intermediates. Determination of biodegradability of the phototreated effluent, allow us to determine an optimal phototreatment time required in the illuminated reactor of the sequential system. This time corresponds to the best compromise between the efficiency of the phototreatment and its cost. The shortest phototreatment time is desired to avoid long irradiation periods and the consequent high electrical consumption. In order to economize the treatment process, photocatalytic process needs to be employed in combination with existing biological treatment. Keeping in view of the low biodegradability of simulated effluent, photocatalytic treatment under solar simulator was employed prior to biological treatment.

Simulated effluent (1000ml) was subjected to prior photocatalytic treatment in 10 different sets with a time period varying from 0.5 to 5.0h with a gap of 0.5h under optimized conditions (1.5g/L of P25 TiO_2 at natural pH of 6.9 in solar simulator with intensity of 1000 W/m^2). Degradation efficacy was assessed in terms of BOD and COD removal. Every photo-treated set was further subjected to biological treatment under optimized conditions (37ºC, 5% sludge concentration) for a period of 48h. Fig 4.44 shows that 0.5h of photocatalytic treatment, followed by 48h of biological treatment results in 55.9 and 43.6% of COD & BOD removal, respectively. Whereas, 4.2 and 46.2% of COD removal was achieved in independent photocatalytic (0.5 h) and biological treatment (48h), respectively.

After 4h of photocatalytic treatment, BOD and COD removal of 58.6 and 66.7%, respectively was achieved under optimized conditions, whereas, the sequential treatment (4h of photo + 48h of Bio treatment) attained BOD and COD removal of 90.5 and 80.8%, respectively. The final TOC of this sequential treatment reduced to 40.11mg/L from 1301mg/L. The results indicate that the biodegradability was enhanced from 0.23 to 0.42 by the prior photocatalytic oxidation, which may be due to the conversion of the non-biodegradable organic substrates into more biodegradable compounds and the subsequent biological treatment becomes more effective. Further, increasing the time period beyond 4h, did not show any significant reduction in BOD and COD. Similarly, increasing the time period from 48 to 72 h in biological step of a sequential treatment yielded inappreciable change in the degradation efficacy. For instance, 93.7 and 95.0% COD reductions were achieved with 5h of Photo followed by 48 and 72 h of bio treatment, respectively. So, sequential treatment (4 h of solar induced Photocatalytic treatmentfollowed by 48 h of Biological treatment) was found to be more appropriate in the degradation of simulated effluents when compared to either of the independent photocatalytic or biological treatments.

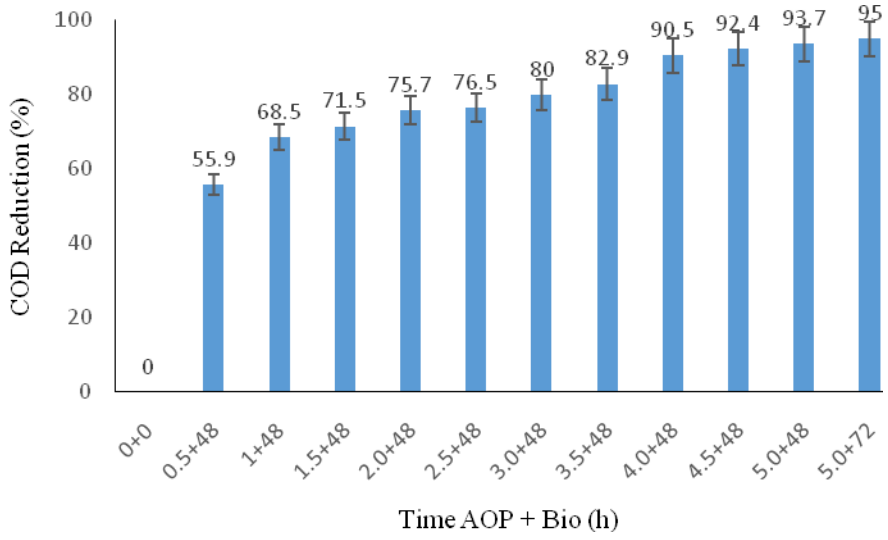

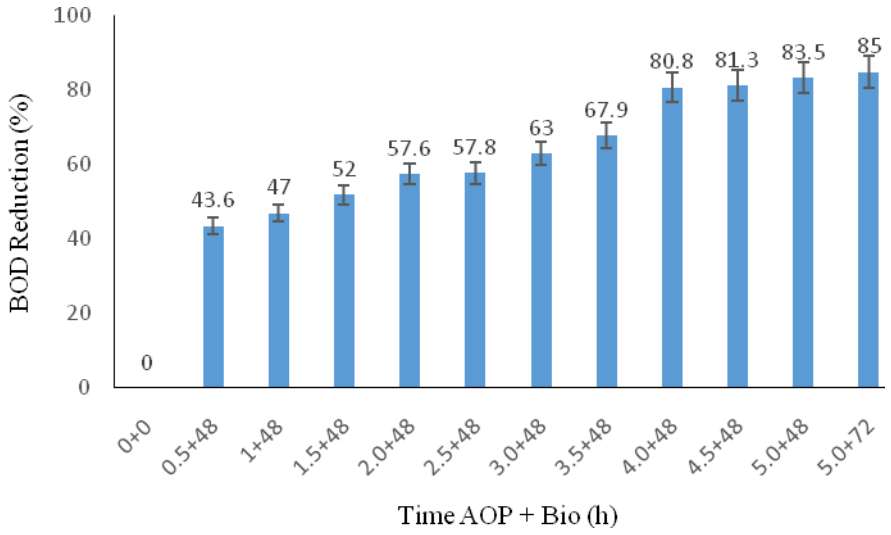

Fig 4.44 Photocatalytic + biological treatment for (a) COD and (b) BOD reduction

5.0 CONCLUSION

The present study is focussed on the degradation of pharmaceutical model compounds such as Aspirin, Ibuprofen, Ofloxacin and Atenolol through photocatalytic treatment under UV/solar irradiations. The degradation of model compounds were examined using commercial photocatalyst and lab synthesized doped photocatalyst. Graphene based composites were synthesized and their efficacy was evaluated under slurry/ immobilized mode for the degradation of Atenolol. Optimization of process parameters was conducted using BBD technique.Simulated pharmaceutical effluent was subjected to independent photocatalytic, biological and integrated treatment systems. An attempt was made to introduce photocatalytic treatment as a pre-treatment stepprior to existing biological treatment so as to maximize the degradation efficiency with little modifications and minimum input cost. The outcomes of the present study are summarized as follows:

1. Heterogeneous photocatalytic degradation is an effective method for the degradation persistent organic contaminants such as pharmaceuticals.
2. Photocatalytic degradation of all model compounds (Aspirin, Ibuprofen, Ofloxacin and Atenolol) was facilitated in the presence of catalyst. Experimental results indicate that initial rate of photodegradation of each compound increased with increase in catalyst dose upto an optimum loading. The rate of photocatalytic degradation was also strongly influenced by the pH of the solution.
3. Fe-TiO_2catalyst was synthesized using solgel method and was characterized for surface area, particle size and morphology. The BET surface area of Fe–TiO_2 was found to be 72 m^2/g. Doped catalyst showed better solar photocatalytic performance when compared to P25 TiO_2 in the degradation of Aspirin which may be due to shifting of absorbance spectrum into visible region. The degradation process with Fe-TiO_2followed the first order kinetics with rate constant of 1.0095min^{-1}.
4. Among various Bi-doped TiO_2 materials, the one doped with 0.25 wt% Bi showed the highest photocatalytic activity for degradation of Ibuprofen (IBP) under solar light.
5. Similarly, among various dopant concentration of Ni doped TiO_2 photocatalyst, 0.5wt% was found to be more effective in the degradation of IBP.
6. The orders of photocatalytic degradation of IBP using various catalyst was observed to be in the order of: Bi–TiO_2 (0.25wt %)> P25 TiO_2> Ni–TiO_2 (0.5wt %) with rate constants of 0.0064, 0.0046 & 0.0043 min^{-1}, respectively.

7. Comparison of the photocatalytic activity of Bi-Ni codoped TiO_2 with P25 TiO_2 under solar light indicate former to be better degrading catalyst than the latter in the degradation of the OFL.
8. TiO_2-G composite was prepared by hydrothermal method and the synthesized composites showed improved performance in photocatalytic degradation of Atenolol under simulated solar illumination. Complete TOC removal was obtained in 7h for Atenolol degradation.
9. ZnO-G was observed to be a better photocatalytic player when compared to TiO_2-Gas well as commercial ZnO under similar experimental conditions. It can be concluded that there is great potential for graphene-based composites for photocatalytic applications.
10. The Box–Behnken design was employed to optimize process parameters of photocatalytic degradation of atenolol using graphene based composites under slurry/ immobilized mode. The desired removal of Atenolol has been achieved by choosing the predicted conditions of the developed models.
11. Photocatalytic experiments under immobilized mode showed that TiO_2-G was a better photocatalyst when compared to P25 TiO_2in UV irradiations. It was found that at optimum conditions, the observed rate of degradation was 35% more in slurry system when compared to immobilized system. Although the slurry mode achieved higher degradation than immobilized mode, but the latter is practically more feasible at industrial scale.
12. Treatment of simulated effluent by independent photocatalytic and biological treatment did not resulted in their complete degradation, so sequential treatment was necessary for their effective degradation.
13. Due to the low biodegradability of simulated effluent, the prior photocatalytic pretreatment was necessary and the minimum pretreatment time required to increase biodegradability was identified, so that the effluent may subsequently be subjected to aerobic biological treatment.
14. Sequential 4h of solar/TiO_2 followed by 48h of biological treatment resulted in the reduction of Total Organic Carbon (TOC) of the simulated effluent to 96.9%, so integration of existing biological processes with solar induced photocatalytic treatment was observed to be more effective in the treatment of simulated effluent.

REFERENCES

- Abellan M.N, Bayarri B, Gimenez B.J, Costa J. (2007). Photocatalytic degradation of sulfamethoxazole in aqueous suspension of TiO_2. App. Catal. B 74, 233-241.
- Adameka E, Barana W, Sobczak A. (2016). Photocatalytic degradation of veterinary antibiotics: Biodegradability and antimicrobial activity of intermediates. Process Safety & Environ. Protect., 103, 1-9.
- Alder A.C, Schaffner C, Majewsky M, Klasmeier J, Fenner K. (2010). Fate of β-blocker human pharmaceuticals in surface water:Comparison of measured and simulated concentrations in the Glatt Valley Watershed, Switzerland. Water Res, 936-948.
- Albini A, Fagnoni M. (2010). Handbook of Synthetic Photochemistry, Wiley Publications; 1st Edn, 2010, 1-9.
- Alexy R, Kumpel T, Kummerer K. (2004). Assesment of degradation of eighteen antibiotics in the closed bottle test. Chemosphere. 57, 505-512.
- Annadurai G, Sivakumar T, Babu R.S. (2000). Photocatalytic decolorization of congo red over ZnO powder using Box–Behnken design of experiments, Bioprocess Engg., 23, 167-173.
- Andreozzi R, Caprio V, Insola A, Marotta R. (1999). Advanced oxidation processes (AOP) for water purification and recovery. Catalysis Today. 53, 51-59.
- APHA, standard methods for the examination of water and wastewater- 20th edition, method 5220 C
- APHA, standard methods for the examination of water and wastewater- 20th edition, method 5201B
- Asahi R, Morikawa T, Ohwaki T, Aoki K, Taga Y. (2001). Visible-light photocatalysis in nitrogen-doped titanium oxides. Science, 293, 269–271.
- Asiltürk M, Sayilkan F, Arpaç E. (2009).Effect of Fe^{3+} ion doping to TiO_2 on the photocatalytic degradation of Malachite Green dye under UV and vis-irradiation. J. Photochem. Photobio. A: Chem. 203, 64-71.
- Ashkarran A.A, Bahareh M. (2015). ZnO nanoparticles decorated on graphene sheets through liquid arc discharge approach with enhanced photocatalytic performance under visible-light. App. Surface. Sci. 342, 112-119.
- Atashfaraz M, Niassar M.S, Ohara S. (2007). Effect of titanium dioxide solubility on the formation of $BaTiO_3$ nanoparticles in supercritical water. Fluid Phase Equilibria. 257, 233–237.
- Auzay D.L.R, S, Brosillon S, Fourcade F, Amrane A. (2007). Integrated process for degradation of amitrole in wastewaters: photocatalysis/ biodegradation. Int. J Chem. Reactor Engg. 5, 1-9.
- Ay F, Catalkaya E.C, Kargi F. (2009). A statistical experiment design approach for advanced oxidation of Direct Red azo-dye by photo-Fenton treatment, J. Hazard. Mater., 162, 230–236.
- Aye T, Mehrvar M, Anderson W.A. (2004). Effects of photocatalysis on the biodegradability of Cibacron Brilliant Yellow 3G-P (Reactive Yellow 2)". J. Environ. Sci. Heal. A, 39, 113-126.
- Bahnemann W, Muneer M, Haque M.M. (2007).Titanium dioxide-mediated photocatalysed degradation of few selected organic pollutants in aqueous suspensions. Catal. Today.124, 133-148.
- Balcioglu I.A, Otker M. (2003). Treatment of pharmaceutical wastewater containing antibiotics by O_3 and O_3/ H_2O_2 processes. Chemosphere. 50, 85-95.

- Bandara J, Pulgarin C, Peringer P, Kiwi J. (1997). Chemical(photo-activated) coupled biological homogeneous degradation of p-nitro-o-toluene-sulfonic acid in a flow reactor. J. Photochem. Photobiol.Chem. A, 111, 253-263.Bansal P, Bhullar N, Sud D. (2009).Studies on photodegradation of malachite green using TiO_2/ZnO photocatalyst, Desal. & Water Treat.,12, 108-113
- Barakat M.A, Schaeffer H, Hayes G, Ismat-Shah S. (2004). Photocatalytic degradation of 2-chlorophenol by Co-doped TiO_2 nanoparticles. Catal. B Environ. 57, 23–30.
- Beausse J. (2004). Selected drugs in solid matrices: a review of environmental determination, occurrence and properties of principal substances, TrAC, Trends Anal. Chem. 23, 753–761.
- Bedford N.M, Pelaez M, Han C, Dionysiou D.D, Steckl A.J. (2012). Photocatalytic cellulosic electrospun fibers for the degradation of potent cyanobacteria toxin microcystin-LR. J. Mater. Chem. 22, 12666–12674.
- Begum N.S, Ahmed H.M.F, Gunashekar K.R. (2008). Effects of Ni doping on photocatalytic activity of TiO_2 thin films prepared by liquid phase deposition technique, Bull. Mater. Sci. 31, 747–751.
- Belgiorno V, Rizzo L, Fatta D, Della Rocca C, Lofrano G. (2007). Review on endocrine disrupting-emerging compounds in urban wastewater: occurrence and removal by photocatalysis and ultrasonic irradiation for wastewater reuse. Desalination 215, 166-176.
- Bideau M, Claudel B, Dubien C, Faure L, Kazouan H. (1995). On the "immobilization" of titanium dioxide in the photocatalytic oxidation of spent waters. J. Photochem. & Photobio., A: Chemistry, 91, 137-144.
- Bhattacharyya , Kawi S, Ray M.B. (2004). Photocatalytic Degradation of Orange II by TiO_2 Catalysts Supported on Adsorbents. Cata.Today., 98, 431-439.
- Blanch G.L, Badia-Fabregat M, Lucas D, Rodriguez-Mozaz S, Barcelo D, Pennanen T, Caminal G, Blanquez B. (2015). Degradation of pharmaceuticals from membrane biological reactor sludge with *Trametes versicolor*. Environ. Sci.: Processes Impacts**,**17, 429-440
- Braz F.S, Silva M.R.A, Silva F.S, Andrade S.J, Fonseca A.L, Kondo M.M. (2014). Photocatalytic degradation of ibuprofen using TiO_2 and ecotoxicological assessment of degradation intermediates against Daphnia similis, J. Environ Prot. 5, 620–626.
- Byrne J.A, Eggins B.R, Brown N.M.D, McKinley B, Rouse M. (1998b). Immobilisation of TiO_2 powder for the treatment of polluted water. Appl. Catal. B: Environ. 17, 25-36.
- Carballa M, Omil F, Ternes T, Lema J.M. (2007). Fate of pharmaceutical and personal care products (PPCPs) during anaerobic digestion of sewage sludge," Water Research. 41, 2139–2150.
- Carp O, Huisman C.L, Reller A. (2004). Photoinduced reactivity of titanium dioxide, Progress in Solid State Chemistry Prog. Solid State Chem. 32 (2004) 33–177.
- Casas M.E, Chhetri R.K, Ooi G, Hansen K.M, Litty K, Christensson M, Kragelund C, Andersen H.R, Bester K. (2015). Biodegradation of pharmaceuticals in hospital wastewater by staged Moving Bed Biofilm Reactors (MBBR).Water Res., 83,293-302.
- Castiglioni S, Bagnati R, Fanelli R, Pomati F, Calamari D, Zuccato E. (2006). Removal of pharmaceuticals in sewage treatment plants in Italy. Environ. Sci. Technol. 40, 357–363.
- Central pollution control board, (2010).Pollution control law series, PCLS/02/2010, 6^{th} edition, 1-1331.
- Chaibakhsh N, Ahmadi N, Zanjanchi Z.M. (2016). Optimization of photocatalytic degradation of neutral red dye using TiO_2 nanocatalyst via Box-Behnken design, Desalination and Water Treatment. 57, 9296-9306
- Cham B.E, Dykman J.H, Bochner F. (1982). Urinary excretion of aspirin. J. Clin. Pharmacol. 14, 562-564.

- Chatzitakis A, Berberidou C, Paspaltsis I, Kyriakou G, Sklaviadis T, Poulios I. (2008). Photocatalytic degradation and drug activity reduction of chloramphenicol. Water Research, 42, 386–394.
- Chen, D.W., Li, F.M., Ray, A.K., 2000b. Effect of mass transfer and catalyst layer thickness on photocatalytic reaction. AIChE J. 46, 1034–1045.
- Chen X, Mao S.S. (2007). Titanium dioxide nanomaterials: synthesis, properties, modifications and applications. Chemical Reviews, 7, 2891–2959.
- Chen Y.J, Stathatos E, Dionysiou D.D. (2008). Microstructure characterization and photocatalytic activity of mesoporous TiO_2 films with ultrafine anatase nanocrystallites. Surf. Coat. Technol.202, 1944–1950.
- Chen H, Nanayakkara C.E, Grassian V.H. (2012). Titanium dioxide photocatalysis in atmospheric chemistry, Chem. Rev., 112, 5919–5948
- Cherepy N.J, Liston D.B, Lovejoy J.A, Deng H, Zhang J.Z. (1998). Ultrafast studies of photoexcited electron dynamics in γ- and α-Fe_2O_3 semiconductor nanoparticles. J. Phys. Chem. B, 102, 770–776.
- Choi H.J, Kang M. (2007). Hydrogen production from methanol/water decomposition in a liquid photosystem using the anatase structure of Cu loaded TiO_2. Int. J. Hydrogen Energy 32, 3841– 3848.
- Choina J, Kosslick H, Fischer C, Flechsig G.U, Frunza L, Schulz A. (2013). Photocatalytic decomposition of pharmaceutical ibuprofen pollutions in water over titania catalyst, Appl. Catal. B: Environ. 129, 589–598.
- Chong M.N, Vimonses V, Lei S, Jin B, Chow C, Saint C. (2009). Synthesis and characterisation of novel titania impregnated kaolinite nano-photocatalyst. Microporus Mesoporus Mater. 117, 233-242.
- Chong M.N, Jin B, Laera G, Saint C.P. (2011). Evaluating the photodegradation of Carbamazepine in a sequential batch photoreactor system: Impacts of effluent organic matter and inorganic ions. Chem. Eng. J. 174, 595-602.
- Chowdhury, P., Elkamel, A. and Ray, A. K. (2015) Photocatalytic Processes for the Removal of Dye, in Green Chemistry for Dyes Removal from Wastewater: Research Trends and Applications (ed S. K. Sharma), John Wiley & Sons, Inc., Hoboken, NJ, USA.
- Coleman H.M, Chiang K, Amal R. (2005). Effects of Ag and Pt on photocatalytic degradation of endocrine disrupting chemicals in water. Chem. Engg. Journal 113, 65-72.
- Dahlan K.Z.M. (2001). Radiation Sciences. Advances in Tissue Banking. World Scientific Publishing Co. Pte. Ltd, Vol 5.
- Damodar R.A, You S.J, Chou H.H. (2009). Study the self cleaning, antibacterial and photocatalytic properties of TiO_2entrapped PVDF membranes. J. Hazard. Mater, 172, 1321–1328
- Della-Greca M, Iesce M.R, Pistillo P, Previtera L, Temussi F. (2009). Unusual products of the aqueous chlorination of atenolol, Chemosphere 74, 730–734.
- Deng L, Wang S, Liu D. (2009). Synthesis, characterization of Fe-doped TiO_2 nanotubes with high photocatalytic activity. Catalysis Letters, 129, 3-4, 513–518.
- Dhir A,Prakasha N.T, Sud D. (2011.) Studies on coupled biological and photochemical treatment of soda pulp bleaching effluents from agro residue based pulp and paper mill. J. Chem Technol Biotechnol. 86, 1508–1513.
- Djafer L, Ayral A, Ouagued, A. (2010). Robust synthesis and performance of a titania-based ultrafiltration membrane with photocatalytic properties. Sep. Purif. Technol. 75, 198–203

- Doll T.E, Frimmel F.H. (2005). Cross-flow microfiltration with periodical back-washing for photocatalytic degradation of pharmaceutical and diagnostic residues-evaluation of the long-term stability of the photocatalytic activity of TiO_2. Water Res. 39,847-854.
- Fan W, Lai Q, Zhang Q, Wang Y. (2011). Nanocomposites of TiO_2 and reduced graphene oxide as efficient photocatalysts for hydrogen evolution. J. Phys. Chem. C, 115, 10694.
- Fang X, Wu J. (1999). Some remark on applying radiation technology combined with other methods to the treatment of industrial wastes. Radiat. Phys. Chem. 55, 465-468.
- Feng F, Xu Z, Li X, You W, Zhen Y. (2010). Advanced treatment of dyeing wastewater towards reuse by the combined Fenton oxidation and membrane bioreactor process. J Environ Sci (China) 22: 1657-1665.
- FernandezIbanez P, Blanco J, Malato S, de las Nieves F.J. (2003). Application of the colloidal stability of TiO_2 particles for recovery and reuse in solar photocatalysis. Water Res. 37, 3180-3188.
- Fujishima A, Rao T.N, Tryk D.A. (2000). Titanium dioxide photocatalysis. J. Photochem. Photobiol. C Photochem. Rev., 1, 1–21.
- Geim A.K, Novoselov K.S. (2007). The rise of graphene. Nat. Mater. 2007, 6, 183-191.
- Ghajar S and Sohrabi M.R. (2012). Taguchi experimental design used for Nano photo catalytic degradation of the pharmaceutical agent Aspirin. J. Chem. Pharma. Res. 4, 814-821.
- Ginnivan M.J, Wools J.L, Callaghan J.R. (1981). Thermopile aerobic treatment of pig slurry. J. Agric. Eng. Res. 26, 455–466.
- Global good practices in industrial wastewater treatment and disposal/reuse, with special reference to common effluent treatment plants. 2007. Published by CPCB, New Delhi, http://cpcb.nic.in/Report_CETP_GGP.pdf
- Gobel A, McArdell C.S, Joss A, Siegrist H, Giger W. (2007). Fate of sulfonamides, macrolides, and trimethoprim in different wastewater treatment technologies. Sci Total Environ. 372, 361–371.
- Gogate P.R, and Pandit A.B. (2004). A review of imperative technologies for wastewater treatment I: Oxidation technologies at ambient conditions. Adv. Environ. Res., 8, 501–551.
- Gohary E.F, Abou-Elea S. (1995). Evaluation of biological technologies for wastewater treatment in the pharmaceutical industry. Water Sci. Tech., 11, 13-20.
- Gonzalez-Juarez J.C, Becerril J.J. (2006). Gamma radiation induces catalytic degradation of 4-chlorophenol using SiO_2, TiO_2 and Al2O3, Radiat. Phys. Chem. 75, 768-772.
- Grabowska E, Zaleska A, Sorgues A, Kunst M, Etcheberry A, Colbeau-Justin C, Remita H. (2013).Modification of Titanium(IV) Dioxide with Small Silver Nanoparticles: Application in Photocatalysis. J. Phys. Chem. *C*,117, 1955–196.
- Gros M, Petrovic M, Barcelo D. (2007). Wastewater treatment plants as a pathway for aquatic contamination by pharmaceuticals in the Ebro river basin (northeast Spain). Environ. Toxicol. Chem. 26, 1553–1562.
- Grzybows B, Słoczynski J, Grabowski R, Samson K, Gressel R, Wcisło K, Gengembre L, Barbaux Y. (2002). Effect of doping of TiO_2 support with altervalent ions on physicochemical and catalytic properties in oxidative dehydrogenation of propane of vanadia–titania catalysts. Applied Catalysis A: General. 230, 1-10.
- Gurkan Y.Y, Turkten N, Hatipoglu A, Cinar Z. (2012). Photocatalytic degradation of cefazolin over N-doped TiO_2 under UV and sunlight irradiation: Prediction of the reaction paths via conceptual DFT, Chem. Engg. J. 184. 113– 124

- Hahn D, Chang W.S, Yorm T.I. (1999). Dyestuff wastewater treatment used chemical oxidation, physical adsorption and fixed bed biofilm process. Process Biochem. 34, 429-439.
- Han W.Y, Zhu W.P, Zhang P.Y, Zhang Y, Li L.S. (2004). Photocatalytic degradation of phenols in aqueous solution under irradiation of 254 and 185 nm UV light. Catal. Today 90, 319-324.
- Hapeshi E, Achilleos A, Vasquez M.I, (2010).Drugs degrading photocatalytically: kinetics and mechanisms of ofloxacin and atenolol removal on titania suspensions. Water Res, 44, 1737-1746.
- Hayder I, Awan I.A, Khan M.A, Turabi T. (2012). Degradation and inactivation of ciprofloxacin by, Photocatalysis using TiO_2 nanoparticles, j app pharm., 01, 487-497.
- Heberer T.H, Stan H.J. (1997). Determination of clofibric acid and N- (Phenylsulfonyl)-Sarcosine in sewage, river and drinking water. Int J Environ Anal Chem, 67, 113-124.
- Hench L.L, West J.K. (1990). The sol-gel process. Chem. Rev., 90, 33–72
- Herrmann J.M, Guillard C, Arguello M, Aguera, A., Tejedor, A., Piedra, L., and Fernandez Alba, A. (1999). Photocatalytic degradation of pesticide pirimiphosmethyl. Determination of the reaction pathway and identification of intermediate products by various analytical methods. Catal. Today., 54, 353–367.
- Hoffmann M.R, Martin S.T, Choi W.Y, Bahnemann D.W. (1995). Environmental Applications of Semiconductor Photocatalysis. Chem. Rev., 95, 69-96.
- Horsch P, Speck A, Frimmel F.H. (2003). Combined advanced oxidation and biodegradation of industrial effluents from the production of stilbene-based fluorescent whitening agents. Water Res., 37, 2748-2756.
- Hossaini H, Moussavi G, Farrokhi M. (2014). The investigation of the LED-activated FeFNS-TiO_2 nanocatalyst for photocatalytic degradation and mineralization of organophosphate pesticides in water. Water Res., 59, 130-144.
- Hsieh C.T, Fan W.S, Chen W.Y, Lin J.Y. (2009). Adsorption and visible-light-derived photocatalytic kinetics of organic dye on Co-doped titania nanotubes prepared by hydrothermal synthesis," Sep & Purifi.Techn., 67, 312–318.
- Hu L, Flanders P.M, Miller P.L, Strathmann T.J. (2007). Oxidation of sulfamethoxazole and related antimicrobial agent by TiO_2 photocatalysis. Water Res. 41, 2612-2626.
- Huber M.M, Canonica S, Park G.Y, Gunten U.V. (2003).Environ. Sci. Technol. 37, 1016.
- Huggett D.B, Khan I.A, Foran C.M. (2003). Determination of beta-adrenergic receptor blocking pharmaceuticals in United States wastewater effluent Environ. Pollut, 121, 199-205.
- Hussain S, Shaikh S, Farooqui M. (2013). COD reduction of waste water streams of active pharmaceutical ingredient, Atenolol manufacturing unit by advanced oxidation-Fenton process. J. Saudi Chemi. Soc. 17, 199-202.
- Jaiswal R, Patel N, Kothari D.C, Miotello A. (2012). Improved visible light photocatalytic activity of TiO_2 co-doped with vanadium and nitrogen, Appl. Catal., B 126, 47–54.
- Jallouli N, Elghniji K, HentatiO, Ribeiro A.R, Mohamed Ksibi A.M.T.S. (2016). UV and solar photo-degradation of naproxen: TiO_2 catalyst effect, reaction kinetics, products identification and toxicity assessment, Journal of Hazardous Materials, 304,329–336
- Jelic A, Gros M, Petrovic M, Ginebreda A,and Barcelo D. (2012) Occurrence and Elimination of Pharmaceuticals During Conventional Wastewater Treatment. In Emerging and Priority Pollutants in Rivers. The Handbook of Environmental Chemistry. 1-23

- Janes R, Knightley L.J, Harding C.J. (2004). Structural and spectroscopic studies of iron (III) doped titania powders prepared by sol-gel synthesis and hydrothermal processing," Dyes and Pigments. 62, 3, 199–212.
- James T.C, Indian API Industry and Imports: An Industry Perspective, RIS Colloquium on India's Growing Dependence on Imports in the Area of Bulk Drugs, 23 Dec. 2014, New Delhi
- Jones O.A, Lester J.N, Voulvoulis N. (2005). Pharamceuticals: a threat to drinking water. Trends in Biology. 23, 163–167.
- Joss A, Keller E, Alder A, Gobel A, McArdell C, Ternes T, Siegrist H. (2005). Removal of pharmaceuticals and fragrances in biological wastewater treatment. Water Res. 39, 3139-3152.
- Kamat P.V. (2010). Graphene-based nanoarchitectures. Anchoring semiconductor and metal nanoparticles on a two-dimensional carbon support. J. Phys. Chem. Lett. 1, 520–527.
- Kansal S.K, Singh M, Sud D. (2007). Optimization of Photocatalytic Process Parameters for the Degradation of 2,4,6-Trichlorophenol in Aqueous Solutions. Chem. Eng. Comm.194,787-802.
- Kansal S.K, Singh M, Sud D. (2007a). Studies on photodegradation of two commercial dyes in aqueous phase using different photocatalysts. Hazard Mater. 141, 581–590.
- Kansal S.K, Singh M, Sud D. (2007b). Optimization of Photocatalytic Process Parameters for the Degradation of 2,4,6-Trichlorophenol in Aqueous Solutions. Chem. Eng. Comm. 4, 416-420.
- Kansal S.K, Singh M, Sud D. (2009). Optimization of process parameters for photocatalytic degradation of 2,4 dichlorophenol in aqueous solution . Journal of chemical reactor engineering, 7, 1542- 6580.
- Kimura K, Hara H, Watanabe Y. (2007). Elimination of selected acidic pharmaceuticals from municipal wastewater by an activated sludge system and membrane bioreactors. Environ Sci Technol. 15, 3708-14.
- Kim D.H, Choi D.K, Kim S.J, Lee K.S. (2008). The effect of phase type on photocatalytic activity in transition metal doped TiO_2 Nanoparticles, Catal. Commun. 9, 654-657.
- Kim H, Moon G, Monllor-Satoca D, Park Y, Choi W.J. (2012). Solar photoconversion using graphene/TiO_2 composites: Nanographene shell on TiO_2 core versus TiO_2 nanoparticles ongraphene sheet. Phys. Chem. C, 116, 1535-1543.
- Klavarioti M, Mantzavinos D, Kassinos, D. (2009). Removal of residual pharmaceuticals from aqueous systems by advanced oxidation processes. Environ. Int. 35, 402–417.
- Kleiman-Shwarsctein, A, Hu Y.S, Forman A.J, Stucky G.D. McFarland E. (2008). Electrodeposition of α-Fe2O3 doped with Mo or Cr as photoanodes for photocatalytic water splitting. J. Phys. Chem. C, 112, 15900–15907.
- Kobayakawa K, Sato C, Sato Y, Fujishima A. (1998). Continuous-flow photoreactor packed with titanium dioxide immobilized on large silica gel beads to decompose oxalic acid in excess water. Journal of Photochemistry & Photobiology, A: Chemistry, 118, 65-69.
- Kolpin D.W, Furlong E.T, Meyer M.T, Thurman E.M, Zaugg S.D, Barber L.B, Buxton H.T. (2002). Pharmaceuticals, hormones, and other organic wastewater contaminants in US streams, 1999–2000: a national reconnaissance. Environ Sci Technol. 36,1202-1211.
- Konstantinou K.I, and Albanis A.T. (2003). Photocatalytic transformation of pesticides in aqueous titanium dioxide suspensions using artificial and solar light: Intermediates and degradation pathways. Appl. Catal. B Environ., 42, 319–335.

- Konstantinou I.K, Albanis T.A. (2004). TiO_2-assisted photocatalytic degradation of azo dyes in aqueous solution: kinetic and mechanistic investigations: a review, Appl. Catal., B 49, 1–14.
- Kornaros M, Liberates G. (2006). Biological treatment of wastewater from a dye manufacturing company using a trickling filter. J. Hazard. Mater. 136, 95–102.
- Krishnakumar B, Swaminathan M. (2011). Influence of operational parameters on photocatalytic degradation of a genotoxic azo dye Acid Violet 7 in aqueous ZnO suspensions. Spectrochimica Acta Part A: Molecular and Biomolecular Spectroscopy, 81, 739-744.
- Koutantoua V, Kostadimaa M, Frontistis E.C.Z, Binas V, Venieri D, Mantzavinos D. (2013). Solar photocatalytic decomposition of estrogens over immobilized zinc oxide, Catalysis Today 209, 66–73
- Kudo A, Miseki Y. (2010). Heterogeneous photocatalyst materials for water splitting. Chem. Soc. Rev. 2009, 38, 253–278.
- Kouame N.A, Alaoui O.T, Herissan A, Larios E, Yacaman M.J, Colbeau-Justina A.C.C, Remita H. (2015). Visible light-induced photocatalytic activity of modified titanium(IV) oxide with zero-valent bismuth clusters. New J. Chem., 39, 2316-2322.
- Kumar A.S, Sivajothi S, Banu R.J. (2012). Coupled solar photo-Fenton process with aerobic sequential batch reactor for treatment of pharmaceutical wastewater. Desalination and water treatment. 48, 89-95.
- Kumar P, Kumar S, Bhardwaj N.K. (2012). Advanced Oxidation of ECF Bleaching Wastewater Using TiO_2 Photocatalysis. Intern. J. Environ. Sci. & Develop., 3, 501-506.
- Kummerer K and Al-Ahmad A. (1997). Biodegradability of the Anti-tumour Agents 5-Fluorouracil, Cytarabine, and Gemcitabine: Impact of the Chemical Structure and Synergistic Toxicity with Hospital Effluent. Acta Hydrochim. Hydrobiol. 25, 166–172.
- Kummererr K. (2001). Pharmaceuticals in the Environment: Sources, Fate, Effects and Risks, springer-verlang Berlin Heidelberg, Germany. 1, 1415-1420.
- Laera G, Chong M.N, Jin B, Lopez A.A. (2011). An integrated MBR–TiO_2 photocatalysis process for the removal of Carbamazepine from simulated pharmaceutical industrial effluent. Biores. Techno. 102, 7012–7015
- Lam S.W, Chiang K, Lim T.M, Amal R, Low G.K.C. (2007). The effect of platinum and silver deposits in the photocatalytic oxidation of resorcinol. Appl. Catal. B, 72, 363–372.
- Lambropoulou D.A, Hernando M.D, Ikonstantinou I.K, Thurmanb E.M, Ferrer I, Albanis T.A. (2008). J. Chromatography 1183, 38-48.
- Langdon K.A, Warne M.S.T.J, Kookanaz R.S. (2010). Aquatic hazard assessment for pharmaceuticals, personal care products, and endocrine-disrupting compounds from biosolids-amended land, Integr. Environ. Assess. Manage. 6, 663–676.
- Lapertot M, Ebrahimi S, Dazio S, Rubinelli A, Pulgarin C. (2007). Photo-Fenton and biological integrated process fordegradation of a mixture of pesticides. J. Photochem. Photobio. A: Chemistry 186, 34–40.
- Laoufi N.A, Hout S, Tassalit D, Ounnar A, Djouadi A, Chekir N, Bentahar F. (2013). Removal of a Persistent Pharmaceutical Micropollutant by UV/TiO_2 Process Using an Immobilized Titanium Dioxide Catalyst: Parametric Study. Chem. Engg. Transactions, 32, 1951-1956.

- Lee S.A, Choo K.H, Lee C.H, Lee H.I, Hyeon T, Choi W, Kwon H.H. (2001). Use of ultrafiltration membranes for the separation of TiO_2 photocatalysts in drinking water treatment. Ind. Eng. Chem. Res. 40, 1712-1719.
- Leitner N.K.V, Boukari S.O.B, Pellizzari F. (2011). Influence of persulfate ions on the removal of phenol in aqueous solution using electron beam irradiation, J Hazard Mater, 185, 844-851.
- Li Y, Li X, Li J, Yin J. (2006). Photocatalytic degradation of methyl orange by TiO_2-coated activated carbon and kinetic study. Water Res. 40, 1119–1126.
- Li J.H, Shen D.Z, Zhang J.Y, Zhao D.X, Li B.S, Liu Y.C, Fan X.W. (2007). The effect of Mn2+ doping on strcuture and photoluminescence of ZnO nanofilms synthesized by sol–gel method. J Luminescence, 122, 352-354.
- Li T.G, Liu J.X, Bai Renbi, Ohandja D. G, Wong F.S. (2007b) Biodegradation of organonitriles by adapted activated sludge consortium with acetonitrile-degrading microorganisms", Water Research.,41, 3465-3473.
- Li T, Liu J, Bai R, Ohandja D.G, Wong F.S. (2007c). Biodegradation of organonitriles by adapted activated sludge consortium with acetonitrile-degrading microorganisms.Water Res.,41, 3465-3473
- Liang Y, Wang H, Casalongue H. S, Chen Z, Dai H. (2010). TiO_2 nanocrystals grown on graphene as advanced photocatalytic hybrid materials. Nano Res, 3, 701-705.
- Lin Y.J, Chang Y.H, Yang W.D, Tsai B.S. (2006). Synthesis and characterization of ilmenite NiTiO3 and CoTiO3 prepared by a modified Pechini method, J. Non- Cryst. Solids 352, 789–794.
- Liu C.C, Hsieh Y.H, Lai P.F, Li C.H, Kao C.L. (2006).Photodegradation Treatment of Azo Dye Wastewater by UV/TiO_2 Process. Dye Pigment. 68, 191-195.
- Lutterbeck C.A, Baginskaa E, Machadob E.L, Kümmerer K. (2015). Removal of the anti-cancer drug methotrexate from water by advanced oxidation processes: Aerobic biodegradation and toxicity studies after treatment. Chemospehe, 141, 290-296.
- Loeffler D, Rombke J, Meller M, Ternes T. (2005). Environmental fate of pharmaceuticals in water/sediment systems. Environ. Sci. Technol. 39, 5209-5219.
- Malato S, FernandezIbanez P, Maldonado M.I, Blanco J, Gernjak W. (2009). Decontamination and disinfection of water by solar photocatalysis: recent overview and trends. Catal. Today 147, 1-59.
- Manu A.B, Mahamood S, Vittal H, Shrihari S. (2011). Novel catalytic route to degrade paracetamol by Fenton process. Int. J. Res. Chem. Environ. 1, 157-164.
- Martinez C, Canle L.M, Fernández M.I, Santaballa J.A, Faria J. (2011). Kinetics and mechanism of aqueous degradation of carbamazepine by heterogeneous photocatalysis using nanocrystalline TiO_2, ZnO and multi-walled carbon nanotubes-anatase composites, Appl. Catal. B: Environ. 102, 563–571.
- Murase T, Irie H, Hashimoto K. (2004). Visible light sensitive photocatalysts, nitrogen-doped Ta2O5 powders. J. Phys. Chem. B, 108, 15803–15807.
- Maurer M, Escher B.I, Richle P, Schaffner C, Alder A.C. (2007).Elimination of β-blockers in sewage treatment plants. Water Res, 41, 1614-1622.
- Mehrotra K, Yablonsky G. S, Ray A. K. (2003). Kinetic studies of photocatalytic degradation in a TiO_2 slurry system: Distinguishing working regimes and determining rate dependences. Ind. Eng. Chem. Res, 42, 2273-2281.

- Mehrvar M, Anderson W.A, Moo-Young M. (2001). Photocatalytic degradation of aqueous organic solvents in the presence of hydroxyl radical scavengers. Int. J. Photoenergy., 3, 187-191
- Milenova K, Stambolova I, Blaskov V, Eliyas A, Vassilev S, Shipochka M. (2013). The effect of introducing copper dopant on the photocatalytic activity of ZnO Nanoparticles. J. chem. Techno. metallurgy. 48, 259-264.
- Mogal S.I, Mishra1 M, Gandhi V.G, Tayade R.J. (2013). Metal Doped Titanium Dioxide: Synthesis and Effect of Metal ions on Physico-chemical and Photocatalytic properties. Mater. Sci. Forum., 734, 364-378.
- Mills A, and Hunte, S.L (1997). An overview of semiconductor photocatalysis. J Photochem. Photobiol. A Chem., 108, 1–35.
- Molinari R, Palmisano L, Drioli E, Schiavello M. (2002). Studies on various reactor configurations for coupling photocatalysis and membrane processes in water purification. J. Memb. Sci. 206,399-415.
- Mohammadi A.S, Marandi R, Olya M.E, Mehrdad S.A.A. (2014). Kinetic modeling of BB41 photocatalytic treatment in a semi batch flow photoreactor using a nanocomposite film. J. Saudi Chem. Soc. 18, 317-326.
- Monteiro S and Boxall A.A. (2010). Occurrence and fate of human pharmaceuticals in the environment," in Reviews of Environmental Contamination and Toxicology, D. M. Whitacre, Ed., 202,53–154
- Mudgal S, Toni A.D, Lockwood S, Sales K, Backhaus T, Sorensen B.H. (2013). Study on the environmental risks of medicinal products. Bio intelligence services. Pp310.
- http://ec.europa.eu/health/files/environment/study_environment.pdf
- Myer R.H, Montogomery D.C. (2002). Response Surface Methodology: Process and Product Optimization using Designed Experiment, second ed., John Wiley and Sons, 343.
- Naddeo V, Belgiorno V, Kassinos D, Mantzavinos D, Meric S. (2010). Ultrasonic degradation, mineralization and detoxification of diclofenac in water: optimization of operating parameters. Ultrason Sonochem 17, 179-185.
- Nagaveni K, Sivalingam G, Hegde M.S, Madras G. (2004a). Solar photocatalytic degradation of dyes. High activity of combustion synthesized nano TiO_2. Appl. Catal. B: Environ. 48, 83-93.
- Nagaveni K, Sivalingam, G, Hegde, M.S, Madras G. (2004b). Photocatalytic degradation of organic compounds over combustion synthesized nano-TiO_2. Environ. Sci. Technol. 38, 1600-1604.
- Nakada N, Tanishima T, Shinohara H, Kiri K, Takada H. (2006). Pharmaceutical chemicals and endocrine disrupters in municipal wastewater in Tokyo and their removal during activated sludge treatment. Water Res. 40, 3297–3303.
- Natarajan T.S, Natarajan K, Bajaj H.C, Tayade R.J. (2011). Energy efficient Uv-LED source and TiO_2 nanotube array-based reactor for photocatalytic application. Ind. Eng. Chem. Res. 50, 7753–7762.
- Ng Y.H, Iwase A, Bell N.J, Kudo A, Amal R. (2011). Semiconductor/reduced graphene oxide nanocomposites derived from photocatalytic reactions. Catal. Today. 164, 353-357.
- Noble J. (2006). GE ZeeWeed MBR technology for pharmaceutical wastewater treatment. Membrane Technology. 9,7-9.
- Neppolian B, Choi H.C, Sakthivel S., Arabindoo B., Murugesan V. (2002).Solar/UV-induced photocatalytic degradation of three commercial textile dyes, J. Hazard. Mater. 89, 303–317.

- Nickels P, Zhou H, Basahel S.N, Obaid A.Y, Ali T.T, Al-Ghamdi A.A, El-Mossalamy E.S.H, Ayoubi, A.O.; Lynch, S.A. (2012). Laboratory scale water circuit including a photocatalytic reactor and a portable in-stream sensor to monitor pollutant degradation. Ind. Eng. Chem. Res. 51, 3301–3308.
- Nikolai L. N, McClure E. L, MacLeod S. L, Wong C. S. (2006). Stereoisomer quantification of the β-blocker drugs atenolol, metoprolol, and propranolol in wastewaters by chiral highperformance liquid chromatography-tandem mass spectrometry. J. Chromatogr. A 1131, 103–109
- Ohtani B. (2008). Preparing articles on photocatalysis — Beyond the illusions, misconceptions and speculation. Chemistry Letters, 37, 217-229.
- Oller I, Malato S, Perez J.A.S, Gernjak W, Maldonado M.I, Estrada L.A.P, C. Pulgarın. (2007). A combined solar photocatalytic-biological field system for the mineralization of an industrial pollutant at pilot scale. Catal. Today. 122, 150–159.
- Oppenheimer J, Stephenson R, Burbano A, Liu Li. (2007). Characterizing the Passage of Personal Care Products Through Wastewater Treatment Processes. Water Environ. Res. 79, 2564-2577.
- Ortiz R, Wert F.L, Snyder E.C. (2010). Evaluation of UV/H_2O_2 treatment for the oxidation of pharmaceuticals in wastewater. Water Res. 44, 1440-1448.
- Palmisano G, Loddo V, Augugliaro V, Bellardita M, Roda G. C, Parrino F. (2015). Validation of a two-dimensional modeling of an externally irradiated slurry photoreactor. Chem. Eng. J. 262, 490-498
- Palominos R.A, Mora A, Mondaca M.A, Perez-Moya M, Mansilla H.D. (2008). Oxolinic acid photo-oxidation using immobilized TiO_2. J. Hazard. Mater. 158, 460-464.
- Paola A.D, Marcia L.E.G , Ikeda S, Marci G, Ohtani B, Palmisano L. (2002). Photocatalytic degradation of organic compounds in aqueous systems by transition metal doped polycrystalline TiO2, Catalysis Today, 75, 87-93.
- Paola A, Addamo M, Augugliaro V. (2006). Photodegradation of lincomycin in aqueous solution. Intern. J. Photoenerg.2006, 141-146.
- Park S, Lee K.S, Bozoklu G, Cai E, Nguyen S.T, Ruoff R.S. (2008). Graphene oxide papers modified by divalent ions-enhancing mechanical properties via chemical cross-linking. ACS Nano, 2, 572-578.
- Parsons S.A. (2004). Advanced oxidation processes for water and wastewater treatment. London: IWA Publishing, Alliance House.
- Patel N, Patel K, Shah H. (2010). Box-Behnken experimental design in the development of pectin-compritol ATO 888 compression coated colon targeted drug delivery of mesalamine Acta Pharm., 60, 39-54
- Patneedi C.B and Prasadu K.D. (2015). Impact of pharmaceutical wastes on human life and environment. Rasayan j. chem , 8, 67-70.
- Paul M.S.S, Aravind U.K, Pramod G, Saha A, Kuamr C.T.A. (2014). Hydroxyl radical induced oxidation of theophylline in water: a kinetic and mechanistic study Org. Biomol. Chem.,12, 5611-5620.
- Pelaez M, Nolan N.T, Pillai S C, Seery M.K, Falaras P, Kontos A.G, Dunlop P.S.M, Hamilton J.W.J, Byme J. A, Oshea K, Entezar M.H, Dionisiou D.D. (2012). A review on the visible light active titanium dioxide photocatalysts for environmental applications. Appl. Catal. B Environ., 125, 331–349.
- Pelentridou K, Stathatos E, Karasali H, Lianos P. (2009). Photodegradation of the herbicide azimsulfuron using nanocrystalline titania films as photocatalyst and low intensity black light radiation or simulated solar radiation as excitation source. J. Hazard. Mater, 163, 756–760.

- Penner S. (2006). Steps toward the hydrogen economy. Energy 31, 33–43.
- Pereira J.H, Reis A.C, Nunes O.C, Borges M.T, Vilar V.J, Boaventura R.A. Assessment of solar driven TiO_2-assisted photocatalysis efficiency on amoxicillin degradation. (2013). Environ. Sci. Pollu. Res. Intern. 139, 1292-1303.
- Pouretedal H, Norozi A, Keshavarz M.H, Semnani A. (2009). Nanoparticles of zinc sulfide doped with manganese, nickel and copper as nanophotocatalyst in the degradation of organic dyes, J. Hazard. Mater. 162, 674–681.
- Pouretedal H.R, Hasanali M.A. (2013). Photocatalytic degradation of some β-lactam antibiotics in aqueous suspension of ZnS nanoparticles, Desalination and Water Treatment. 51, 13-15.
- Pozzo R.L, Baltanas, M.A, Cassano, A.E. (1997). Supported titanium oxide as 56 A. Hänel, P. Moreń, A. Zaleska, J. Hupka photocatalyst in water decontamination: state of the art. Catalysis Today, 39, 219-231
- Qamar M, Munner M, Bahnemann D. (2006). Heterogeneous photocatalysed degradation of two selected pesticide derivatives, triclopyr and daminozid in aqueous suspensions of titanium dioxide.J. Environ. Manage. 80, 99-106.
- Raj D.S, Anjaneyulu Y. (2005). Evaluation of bio kinetic parameters for pharmaceutical wastewaters using aerobic oxidation integrated with chemical treatment. Process Biochem.40, 165-175.
- Radjenovic J, Petrovic M, Barcelo D. (2007). Analysis of pharmaceuticals in wastewater and removal using a membrane bioreactor. Anal. Bioanal. Chem. 387, 1365–1377.
- Radjenovic J, Petrovi M, Barcel D. (2009). Fate and distribution of pharmaceuticals in wastewater and sewage sludge of the conventional activated sludge (CAS) and advanced membrane bioreactor (MBR) treatment. Water Research. 43, 831–841.
- Ramesh .T, Saravanamuthu V, Shik Mo. (2008). A review on UV/TiO_2 photocatalytic oxidation process. Korean J. Chem. Eng. 25, 64-72.
- Ray S. 2006. RSM: a statistical tool for process optimization. Ind Tex J. 117, 24–30.
- Ray, A.K., Beenackers, A.A.C.M., 1997. Novel swirl-flow reactor for kinetic studies of semiconductor photocatalysis. AIChE J. 43, 2571–2578.
- Ray A.K, Beenackers A.A.C.M. (1998). Development of a new photocatalytic reactor for purification. Catalysis Today. 40, 73-83.
- Ray S, Lalman J.A, Biswas N. (2009). Using the Box-Benkhen technique to statistically model phenol photocatalytic degradation by titanium dioxide nanoparticles. Chem. Eng. J., 150, 15–24.
- Rengraj S,Li X.Z, Tanner P.A, Pan Z.F, Pang G.K.H. (2006). Photocatalytic degradation of methylparathion—an endocrine disruptor by Bi3+ doped TiO_2, J. Mol. Chem. A: Chem. 247, 36–43.
- Romanos G.E, Athanasekou C.P, Katsaros F.K, Kanellopoulos N.K, Dionysiou D.D, Likodimos V, Falaras P. (2012). Double-side active TiO_2-modified nanofiltration membranes in continuous flow photocatalytic reactors for effective water purification. J. Hazard. Mater, 211, 304–316
- Rosenfeldt E. J, Linden K.G, Canonica S, Von-Gunten U. (2006). Comparison of the efficiency of OH radical formation during ozonation and the advanced oxidation processes O3/H2O and UV/H2O2. Water Res., 40, 3695–3704.

- Sakkas V.A, Calza P, Medana C, Villioti A.E, Baiocchi C, Pelizzetti E, Albanis T. (2007). Heterogeneous photocatalytic degradation of the pharmaceutical agent salbutamol in aqueous titanium dioxide suspensions. Appl. Catal. B Environ. 77, 135–144.
- Sangave P.C, Gogate P.R, Pandit A.B. (2007). Ultrasound and ozone assisted biological degradation of thermally pretreated and anaerobically pretreated distillery wastewater. Chemosphere 68, 42-50.
- Saien J, Khezrianjoo S. (2008). Degradation of the fungicide carbendazim in aqueous solutions with UV/TiO_2 process; optimization, kinetics and toxicity studies. J Hazard. Mater. 157, 269-276.
- Schroder H.F. (1999). Substance-specific detection and pursuit of non-eliminable compounds during biological treatment of waste water from thepharmaceutical industry, Waste Manage. 19. 111–123.
- Sarkar S, Chakraborty S,Bhattacharjee C. (2015). Photocatalytic degradation of pharmaceutical wastes by alginate supported TiO_2 nanoparticles in packed bed photo reactor (PBPR) Ecotoxic. & Environ. Safety. 121, 263–270.
- Sahoo C, Gupta A.K. (2013). Application of statistical experimental design to optimize the photocatalytic degradation of a thiazin dye using silver ion-doped titanium dioxide, J Environ Sci Health A Tox Hazard Subst Environ Eng. 48, 694-705.
- Sakthivel S, Shankar M.V, Palanichamy M., Arabindoo B, Murugesan V. (2002). Photocatalytic decomposition of leather dye Comparative study of TiO_2 supported on alumina and glass beads. Journal of Photochemistry & Photobiology, A: Chemistry. 148, 153-159
- Santos J. L, Aparicio I, Alonso E. (2007). Occurrence and risk assessment of pharmaceutically active compounds in wastewater treatment plants. A case study: Seville city (Spain). Environ. Int. 33, 596–601.
- Serpone, N. (2006). Is the band gap of pristine TiO_2 narrowed by anion- and cation-doping of titanium dioxide in second-generation photocatalysts? J. Phys. Chem. B, 110, 24287–24293.
- Shah M. (2014). Effective treatment systems for azo dye degradation: A joint venture between physicochemical & microbiological process. Int. J. Environ. Bioremed. Biodegrad. 2, 231-242.
- Sharma P, Singh L, Dilaghi N. (2009).Optimization of process variables for decolorization of Disperse Yellow 211 by Bacillus subtilis using Box-Behnken design. J. Hazar., Mater. 164, 1024-1029
- Shi L.Y, Li C.Z, Gu H.C, Fang D.Y. (2000). TiO_2 Coupled Semiconductor Particles Mater. Chem., Phys. 62, 62-67.
- Shi J.W, Liu C, Ao H.Y, Chen J.W, Xie C, Li G, Yang S, Li S. (2015). One step to synthesize the nanocomposites of graphene nanosheets and N-doped titania nanoplates with exposed (001) facets for enhanced visible light photocatalytic activity. J. Nanopart Res.17, 1-10.
- Shokri M, Jodat A, Modirshahla N, Behnajady M.A. (2013). Photocatalytic degradation of chloramphenicol in an aqueous suspension of silver-doped TiO_2 nanoparticles, Environment. Techno. 34, 1161–1166.
- Singh P, Dhir A, Sangal V.K. (2015). Optimization of photocatalytic process parameters for the degradation of acrylonitrile using Box Behnken Design, Desalination and Water Treatment. 55, 1501-1508.
- Sirtori C, Aguera A, Gernjak W. (2010). Effect of water-matrix composition on trimethoprim solar photodegradation kinetics and pathways. Water Res. 44, 2735-2744.
- Sivalingam G.K, Hegde N.M.S, Madras G. (2003).Photocatalytic degradation of various dyes by combustion synthesized nano anatase TiO_2. Appl. Catal. 45, 23-38.

- Sohrabi M.R, Ghavami M. (2008). Photocatalytic degradation of Direct Red 23 dye using UV/TiO_2: effect of operational parameters, J. Hazard. Mater. 153, 1235–1239.
- Sreethawong T, Suzuki Y, Yoshikawa S. (2005). Photocatalytic evolution of hydrogen over mesoporous TiO_2 supported NiO_2 photocatalyst prepared by single-step sol–gel process with surfactant template. Int. J. Hydrogen Energy. 30, 1053–1062.
- Stumpf M, Ternes T.A, Wilken R.D, Rodrigues S.V, Baumann W. (1999). Polar drugs in sewage and natural waters in the State of Rio de Janeiro, Brazil.Sci Total Environ, 225, 135-141.
- Sud D, Sharotri N, (2015). A greener approach to synthesize visible light responsive nanoporous S-doped TiO_2 with enhanced photocatalytic activity. New J. Chem.,39**,** 2217-2223
- Sun H, Liu S, Liu S, Wang S. (2014). A comparative study of reduced graphene oxide modified TiO_2, ZnO and Ta_2O_5 in visible light photocatalytic/photochemical oxidation of methylene blue. Appl. Catal., 146, 162-171.
- Suriye K, Praserthdam P, Jongsomjit B. (2005). Impact of Ti3+ present in titania on characteristics and catalytic properties of the Co/TiO_2 catalyst. Industrial and Engg. Chem. Res. 44, 6599–6604.
- Tabrizi G.B, Mehrvar M. (2004). Integration of advanced oxidation technologies and biological processes: Recent developments, trends, and advances. J. Environ. Sci. Heal. A, 39, 3029-3081.
- Tang W.Z H. (1995). UV/TiO_2 photocatalytic oxidation of commercial dyes in aqueous solutions. Chemosphere 31, 4157-4170.
- Tang J, Zou Z, Ye J. (2004). Efficient photocatalytic decomposition of organic contaminants over CaBi2O4 under visible-light irradiation. Angew. Chem. Int. Ed. 43, 4463–4466.
- Tang Y, Liu X, Ma C, Zhou M, Huo P, Yu L, Pan J, Shia W, Yan Y. (2015). Enhanced photocatalytic degradation of tetracycline antibiotics by reduced graphene oxide–CdS/ZnS heterostructure photocatalysts. New J. Chem., 39, 5150.
- Tantriratna P, Wirojanagud W, Neramittagapong S ,Wantala K, Grisdanurak N. (2011). Optimization for UV-photocatalytic degradation of paraquat over titanium dioxide supported on rice husk silica using Box-Behnken design, IJCT.18 , 363-371.
- Tao H, Liang X, Zhang Q, Chang C.T. (2015). Enhanced photoactivity of graphene/titanium dioxide nanotubes for removal of Acetaminophen. App. Surface Sci. 324, 258-264.
- Tarr M.A. (2003). Chemical degradation methods for wastes and pollutants: Environmental and industrial applications. New York, NY: Marcel Dekker.
- Ternes T.A. (1998). Occurrence of drugs in German sewage treatment and rivers. Water Res. 32, 3245-3260.
- Theurich J, Lindner M, Bahnemann D.W. (1996). Photocatalytic degradation of 4-chlorophenol in aerated aqueous titanium dioxide suspensions: A kinetic and mechanistic study. Langmuir 12, 6368-6376.
- Thomas P.M, Foster G.D. (2005). Tracking acidic pharmaceuticals, caffeine, and triclosan through THE wastewater treatment process. Environ. Toxicol. Chem. 24, 25–30.
- Trovo A.G, Nogueira R.F.P, Aguera A, Alba A.R.F, Malato S. 2011. Degradation of the antibiotic amoxicillin by photo-Fenton process Chemical and toxicological assessment. Water Res. 45, 1394 -1402.
- Vaez M, Moghaddam A.Z, Alijani S. (2012). Optimization and Modeling of Photocatalytic Degradation of Azo Dye Using a Response Surface Methodology (RSM) Based on the Central Composite Design with Immobilized Titania Nanoparticles, *Ind. Eng. Chem. Res*, 51 (11), pp 4199–4207

- Varatharajan B, Kanmani S. (2007). Treatability study of pharmaceutical waste water by combined solar photo fenton and activated sludge process. Jr. of Industrial Pollution Control 23 (1)157-164.
- Vasanth K.K, Porkodi K, Selvaganapathi A. (2007). Constrain in solving Langmuir-Hinshelwood kinetic expression for the photocatalytic degradation of Auramine O aqueous solutions by ZnO catalyst. Dyes and Pigments, 75: 246-249.
- Wang Y, Hao Y, Cheng H. (1999). Photoelectrochemistry of transition metal-ion-doped TiO_2 nanocrystalline electrodes and higher solar cell conversion efficiency based on Zn2+-doped TiO_2 electrode, J. Mater. Sci. 34, 2773–2779.
- Wang Y. (2000). Solar photocatalytic degradation of eight commercial dyes in TiO_2 suspension. Water Res. 34, 990.
- Wang J, Sun W, Zhang Z, Jiang Z, Wang X, Xu R, Li R, Zhang X. (2008). Preparation of Fe-Doped Mixed Crystal TiO_2 Catalyst and Investigation of Its Sonocatalytic Activity during Degradation of Azo Fuchsine under Ultrasonic Irradiation. J. Colloid Interface Sci. 320, 202–209
- Wang W, Song G, Li J, Miao L, Zhang B. (2008). Direct hydrothermal synthesis and magnetic property of titanate nanotubes doped magnetic metal ions. J. Univ. of Sci. & Techn. 15, 644–648.
- Wang D, Duan Y, Luo Q, Li X, An J, Baoa L, Shi L. (2012). Novel preparation method for a new visible light photocatalyst: mesoporous TiO_2 supportedAg/AgBr, J. Mater. Chem. 22, 4847–4854.
- Wei Y, Chu H.Q, Dong B.Z, Li X. (2011). Evaluation of humic acid removal by a flat submerged membrane photoreactor, Chin. Sci. Bull. 56(32), 3437-3444.
- WHO Model List of Essential Medicines. 2015. 19th.edition
- Xekoukoulotakis N.P, Xinidis N, Chroni. M. (2010). UV-A/TiO_2 photocatalytic decomposition of erythromycin in water: Factors affecting mineralization and antibiotic activity. Catal. Today 151, 29-33.
- Xu X.H, Wang M, Hou Y, Yao W.F, Wang D, Wang H. (2002). Preparation and characterization of Bi-doped TiO_2 photocatalyst, J. Mater. Sci. Lett. 21 1655–1656.
- Wu M, Atchley D, Greer L, Janssen S, Rosenberg D, Sass J. (2009). Dosed without prescription: preventing pharmaceutical contamination of our nation's drinking water. NRDC. 1-64
- Yahiat S, Fourcade F, Brosillon S, Amrane A. (2011). Removal of antibiotics by an integrated process coupling photocatalysis and biological treatment e Case of tetracycline and tylosin , International Biodeterioration & Biodegradation 65. 997-1003
- Yamakata A, Ishibashi T, Kato H, Kudo A, Onishi H. (2003). Photodynamics of NaTaO3 catalysts for efficient water splitting. J. Phys. Chem. B 2003, 107, 14383–14387.
- Yang L, Yu L.E, Ray M.B. (2008). Degradation of paracetamol in aqueous solutions by TiO_2 photocatalysis. Water Res. 42, 3480-3488.
- Yang L, liyae Y.U, Ray M. (2009). Photocatalytic oxidation ofparacetamol: dominant reactants,intermediates, and reactionmechanisms. Environ. Sci. Technol.43, 460–465.
- Yang L, Yu L, Ray M.B. (2008). Degradation of Paracetamol in Aqueous Solutions by TiO2 photocatalysis. Water Research, 42, 3480-3488.
- Yoong L.S, Chong F.K, Dutta B.K. (2009). Development of copper-doped TiO_2 photocatalyst for hydrogen production under visible light. Energy 34 (10)1652–1661

- Yu J.C, Yu J, Zhao J. (2002). Enhanced photocatalytic activity of mesoporous and ordinary TiO_2 thin films by sulphuric acid treatment. Appl. Catal. B: Environ. 36, 31-43.
- Yu H, Zheng X, Yin Z, Tao F, Fang B, Hou K.C. (2007). Preparation of nitrogen-doped TiO_2 nanoparticle catalyst and its catalytic activity under visible light. J Chem. Eng. 15, 802-807.
- Yu J.G, Wang W.G, Cheng B, Su B.L. (2009). Enhancement of photocatalytic activity of Mesporous TiO_2 powders by hydrothermal surface fluorination treatment," Journal of Physical Chemistry C. 113, 6743–6750.
- Yu Y, Liu Y, Wu X, Weng Z, Hou Y, Wu L. (2015). Enhanced visible light photocatalytic degradation of metoprolol by Ag-Bi2WO6-graphene composite. Sep. & Purif. Techno. 142, 1-7.
- Zhang K.J, Xu W, Li X.J, Zheng S.J, Xu G, Wang J.H. (2006). Photocatalytic oxidation activity of titanium dioxide film enhanced by Mn non-uniform doping. Transactions of Nonferrous Metals Society of China.16, 1069–1075.
- Zhang X, Wu F, Wu X, Chen P, Deng N. (2008). Photodegradation of acetaminophen in TiO_2 suspended solution. J Hazard Mater.,157, 300-307
- Zhang X, Du A.J, Lee P, Sun D.D, Leckie J.O. (2008a). TiO_2 nanowire membrane for concurrent filtration and photocatalytic oxidation of humic acid in water. J. Memb. Sci. 313, 44-51.
- Zhang X, Du A.J, Lee P, Sun D.D, Leckie J.O. (2008b). Grafted multifunctional titanium dioxide nanotube membrane: separation and photodegradation of aquatic pollutant. Appl. Catal. B: Environ. 84, 262-267
- Zhang H, Lv X, Li Y, Wang Y, Li J. (2010).P25-graphene composite as a high performance photocatalyst. ACS Nano, 4, 380-386.
- Zhang J, Xiong Z, Zhao X.S. (2011). Graphene-metal-oxide composites for the degradation of dyes under visible light irradiation. J. Mater. Chem, 21, 3634-3640.
- Zhao Y, Zhong J, Li H, Xu N, Shi J. (2002). Fouling and regeneration of ceramic microfiltration membranes in processing acid wastewater containing fine TiO_2 particles. J. Memb. Sci. 208, 331-341.
- Zheng R.Y, Lin L, Xie J.L, Zhu Y.X, Me Y.C. (2008). State of doped phosphorus and its influence on the physicochemical and photocatalytic properties of P-doped Titania. J. Phys. Chem. 112, 15502–15509.
- Zhou M, Han D, Liu X, Ma C, Wang H,Tang Y, Huo P, Shi W, Yan Y, Yang J. (2015). Enhanced visible light photocatalytic activity of alkaline earth metal ions-doped CdSe/rGO photocatalytys synthesized by hydrothermal method. App. Catalysis B Environmental. 172-173, 174-184.
- Zhu J, Zheng W, He B, Zhang J, Anpo M. (2004). Characterization of Fe–TiO_2 photocatalysts synthesized by hydrothermal method and their photocatalytic reactivity for photodegradation of XRG dye diluted in water J. Mol. Catal. A: Chem. 216, 35-43.
- Zwiener C, Glauner T, Frimmel F.H. (2000). Biodegradation of pharmaceutical residues investigated by SPE-GC/ITD-MS and on-line derivatisation. J. High Res. Chromatography. 23, 474-478.
- Zhang Z, Anderson W.A, Moo-Young M. (2002).Photocatalytic pretreatment of contaminated groundwater for biological nitrification enhancement. J. Chem. Techn. & Biotech. 77 190–194.
- Zhuang J.D, Dai W.X, Tian Q.F, Li Z.H, Xie L.Y, Wang J.X, Liu P, Shi X.C, Wang D.H. (2010). Photocatalytic degradation of rhb over TiO_2 bilayer films: Effect of defects and their location. Langmuir. 26, 9686–9694

CONTRIBUTIONS

LIST OF PUBLICATIONS

1. Vibhu Bhatia, Ajay K. Ray, Amit Dhir, Enhanced photocatalytic degradation of ofloxacin by co-doped titanium dioxide under solar irradiation, Separation and Purification Technology, 161 (2016) 1–7.
2. Vibhu Bhatia, AmitDhir, Ajay K Ray, Enhanced photocatalytic degradation of Atenolol using Graphene TiO_2 Composite, Journal of Photochemistry and Photobiology A: Chemistry 332 (2017) 182–187.
3. Vibhu Bhatia, Amit Dhir, and Sushil Kumar Kansal, Solar Light Induced Photocatalytic Degradation of Aspirin Using Doped TiO_2 Nanoparticles, Journal of Nanoscience and Nanotechnology, 16(2015) 7444-7450.
4. Vibhu Bhatia and Amit Dhir, Transition metal doped TiO_2 mediated photocatalytic degradation of anti-inflammatory drug under solar irradiations, Journal of Environmental Chemical Engineering, 4 (2016) 1267–1273.

CONFERENCES

1. Vibhu Bhatia, Ghodsieh Malekshoar, Amit Dhir, Ajay K Ray, 2016, "Enhanced photocatalytic degradation of Atenolol using Graphene TiO_2 Composite", International conference on "Advanced materials for Health, Energy and Environment, IIT Roorkee.
2. Vibhu Bhatia and Amit Dhir, 2013, "ZnS medicated photocatalytic degradation of catechol", National conference on AOP-2013, Thapar University Patiala.

Article

Journal of
Nanoscience and Nanotechnology
Vol. 15, 1–7, 2015
www.aspbs.com/jnn

Solar Light Induced Photocatalytic Degradation of Aspirin Using Doped TiO_2 Nanoparticles

Vibhu Bhatia[1], Amit Dhir[1], and Sushil Kumar Kansal[2,*]

[1] School of Energy and Environment, Thapar University, Patiala
[2] Dr. S. S. Bhatnagar University Institute of Chemical Engineering and Technology, Panjab University, Chandigarh

The photocatalytic degradation of aspirin has been studied using TiO_2 and Fe^{3+} doped TiO_2 in both UV and solar light irradiations. Fe doped TiO_2 was prepared by sol–gel technique and characterized by X-ray diffraction, scanning electron microscope and Brunner Emmer Teller (BET) analysis. The crystallize size and BET surface area of Fe–TiO_2 was found to be 20.99 nm and 72 m^2/g respectively. It was observed that the absorption of Fe–TiO_2 shifted to longer wavelength and found to be higher in visible light which might be responsible for its improved activity under solar irradiations. The effect of experimental parameters such as pH, catalyst concentration, reaction kinetics and source of light were also investigated. The results indicated that degradation of aspirin was 72% with Degussa TiO_2 (D) in 6 hours whereas 96% degradation was achieved with Fe–TiO_2 under solar irradiations in the same duration which is likely because of higher surface area of Fe–TiO_2. These findings were confirmed with chromatographic analysis. Under UV irradiation, higher degradation efficiency was attained with TiO_2 (D) when compared to Fe–TiO_2 as the doping energy level of Fe ions in the band gap of TiO_2 act as the recombination centre of photo generated electrons and holes, leading to lower photocatalytic performance of Fe–TiO_2 than the corresponding undoped photocatalysts.

Keywords: Aspirin, Photocatalysis, Doped, Fe–TiO_2, Degradation.

1. INTRODUCTION

Pharmaceutical compounds are of major concern in today's era as their concentration is increasing day by day due to human consumption and their excretion in wastewater. These compounds generally enter the environment through different pathways, resulting in the contamination of surface/underground water. Diverse studies have revealed the presence of ibuprofen, acetaminophen, aspirin, and carbamazepine in different water bodies.[1–3] Now a days, the presence of non-steroidal anti-inflammatory drugs (NSAIDs) has been extensively observed in drinking water.[4] These are the most frequently prescribed medicines to treat fever, pain, arthritis etc. and aspirin belongs to this class of medications In addition to its effects on pain, fever, and inflammation, aspirin also has an important inhibitory effect on platelets in blood. This antiplatelet effect helps to prevent blood clot formation inside arteries, specifically in persons who have atherosclerosis (narrowing of the blood vessels), or are prone to expand blood clots in their arteries, thus preventing heart attack and strokes. It has been reported that rate of hydrolysis of aspirin to its metabolites is 4 μg per minutes in human urine at normal body temperature.[5] Aspirin is produced and consumed in large amount, thereby increasing its concentration in waste water and surface/groundwater which affects the aquatic ecosystem.

Conventional wastewater treatment processes cannot completely eliminate drug residues and their metabolites. Generally their treatment involves bioremediation which is inefficient in the removal of pharmaceutical compounds. Previous studies have demonstrated that pharmaceutical compounds are only moderately removed by biological treatment.[1,2,6] The concern of regarding accumulation of such substances and their consequent human contact has stimulated the development of advanced methods for their removal to avoid the contamination of aquatic environment. Advanced oxidation processes (AOPs) including heterogeneous photocatalysis have proved to be one of the most efficient methods for water treatment.[7–9] These processes are based on the generation of hydroxyl radicals (·OH) which oxidize a broad series of organic pollutants

*Author to whom correspondence should be addressed.

that could be present in water.[10, 11] Titanium dioxide (TiO_2) has been reported to be one the most popular and efficient phototocatalysts in the degradation of some antibiotics such as Lincomycin, tetracycline, oxolinic acid, and fluoroquinolone.[12, 13] Generally TiO_2 shows higher efficiency in UV light when compared to solar light.[14] References [15] reported the use of UV/TiO_2 to achieve 90% TOC reduction of erythromycin (ERM) after 90 minutes of reaction with 250 mg L^{-1} TiO_2. Similarly 82% of sulfamethoxazole degradation and 23% TOC removal by UV/TiO_2 in 6 hours has been reported by Ref. [16]. Reference [17] studied photocatalytic degradation of aspirin in aqueous solution using TiO_2 as photocatalyst under UV irradiation and obtained 73% degradation of the model compound. Another group of researchers[18, 19] investigated the photocatalytic degradation of Diclofenac and paracetamol in batch reactor using TiO_2 and observed that the residual concentration of these drugs decreased with increase in catalyst dose. Reference [20] reported that photocatalysis was more efficient than photolysis for the degradation of Bezofibrate in the presence of TiO_2/solar system. Reference [21] analyzed that the initial concentration of diclofenac (200 mg/L) decreased to 75% within 120 minutes under simulated solar irradiations using TiO_2 as photocatalyst. Photocatalytic degradation of amoxicillin using TiO_2 under solar radiation has been reported to be 71%.[22]

Different doping methods such as sol gel, co-precipitation, hydrothermal and impregnation have been used to impregnate the uniform distribution of dopant into the crystal lattice so as to increase its activity. Anionic impurities such as N, C, S, B and P have been utilized as dopants for extending the optical absorption of TiO_2 to the visible region of the spectrum.[23] Recent research findings have revealed that sol gel method is the most commonly used method for preparation of TiO_2 or doped TiO_2 since nanocrystals synthesized are of high purity at low temperatures.[24–27]

Reference [28] synthesized TiO_2 using co-precipitation method at different calcination temperatures (400–650 °C) and studied its photocatalytic degradation efficiency of the degradation of methylene blue. It was reported that maximum degradation of 92% was attained with catalyst calcined at 450 °C. Similarly,[29] analyzed degradation of methylene blue with nitrogen doped TiO_2 prepared by sol gel method at the calcinations temperature ranging from 300–700 °C and found that maximum degradation of 98% was attained with catalyst calcined at 500 °C.

Reference [30] studied the degradation of diclofenac drug was studied by photocatalytic process using Zr–TiO_2 and bare TiO_2 and found that Zr–TiO_2 exhibited better photocatalytic activity when compared to bare TiO_2. Reference [31] studied photocatalytic degradation of dizinon with FeFNS-doped TiO_2 in presence of UV LED and achieved 96.3% degradation in 100 minutes of irradiation exposure. It was stated that prepared Fe^{3+} doped TiO_2 extends its absorption wavelength, near to 500 nm. Moreover, XRD, EPR, AAS and XPS analyses showed that Fe exist in trivalent ionic state substituting Ti^{4+} in TiO_2 lattice and its concentration decreased from surface to the center of doped TiO_2.[32] Reference [33] reported that the crystallite size and the particle size of the Fe^{3+} doped TiO_2 were smaller than those of U-TiO_2 (without doping), which could signify that the presence of Fe^{3+} in the reaction media might be used to control the particle and crystallite sizes of the oxides. Moreover, increasing the Fe^{3+} ion concentration decreased the particle size, which resulted in larger surface area of catalyst that would further promote its photocatalytic performance. The optimized doping concentration of Fe^{3+} content in Fe doped TiO_2 was reported to be 0.5%.[34]

The literature studies on the photocatalytic degradation of pharmaceutical in aqueous solution did not address its photocatalytic oxidation using doped photocatalyst in solar light. Keeping this in view, the current study is focused on the degradation efficacy of aspirin using Fe^{3+} doped TiO_2 and its comparison with commercially available TiO_2 (Degussa P25) under natural and artificial light sources.

2. EXPERIMENTAL DETAILS

2.1. Materials

Aspirin was purchased from Aldrich, USA. Titanium dioxide (Degussa P25) was procured from Degussa Corporation, Germany. Ethanol, Titanium Isopropoxide (TIP), Iron nitrate (analytical grade) and Acetonitrile was purchased from Merck. 1 M NaOH and 1 M HCl were used to adjust the pH in alkaline and acidic range. All chemicals were used as received without further purification. The structure of aspirin is shown in Figure 1.

2.2. Preparation of Fe–TiO_2 Nanoparticles

Fe doped TiO_2 (0.5 wt%) was prepared using sol gel method with Titanium isopropoxide (TIP) as precursor. 2.5 mL of TIP was added drop by drop to a solution of 10 mL ethanol and 2.5 mL acetylacetone at room temperature and stirred for 30 minutes. Then 2 mL distilled water was added to above solution and pH was adjusted to 1.8 with 1 N HCl. Required quantity of $FeNO_3$ was added into prepared solution and a stable sol was finally obtained after stirring for 2 h. Then concentrated solution was placed at 90 °C for drying and dried powder was calcined at 400 °C for 2 h.

2.3. Characterizations of the Prepared Nanoparticles

The powder X-ray diffraction (XRD) analysis was performed at room temperature using Philips X-Ray diffractometer (Cuk$\alpha\lambda = 0.154$ nm) to study the crystal phase of the products. SEM images were obtained with Philips scanning electron microscope. The band gap was analyzed using UV spectrophotometer. The BET surface area of samples was analyzed by N_2 adsorption analyzer (NOVA2000e) USA.

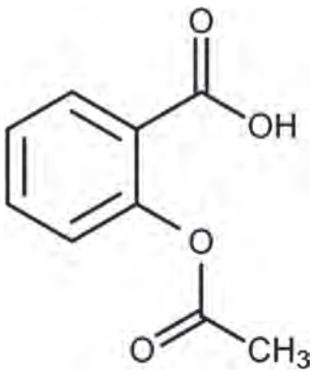

Figure 1. Chemical structure of aspirin.

2.4. Photocatalytic Performance of the Prepared Nanoparticles

Photocatalytic degradation experiments were carried out in indigenously designed UV light chamber having dimensions $45 \times 28 \times 28$ inch. The chamber consisted of seven lone wave 36 W UV tubes ($\lambda_{max} = 365$ nm) each having intensity of 1.6 W/m^2 serving four Pyrex glass reactor units. The power consumption per glass reactor was found to be 63 W. In each set of experiments, 150 mL of aspirin solution (25 mg/L) was kept in the glass reactor and mixed with pre determined quantity of TiO_2. This slurry was agitated with a magnetic stirrer and aerated with sparger. 5 mL of aliquot was pipetted out every hour from the reactor and was centrifuged to take apart the catalyst. The UV absorbance spectrum of the sample was taken. To determine the degradation of aspirin solution, HPLC was performed using shimadzu UV/VIS Diode array detector SPD-M20A and shimadzu LC-20AD pumps with 20 μL sample loop. The flow rate was set as 1 mL/min using C18 column with solvent system water/Acetonitrile (85/15) taking absorbance at 254 nm.

2.5. UV LED Reactor

The reactor having UV-LED as an irradiation source was made up of wood with dimensions of $45'' \times 28'' \times 28''$ and inner lining of cast iron which absorbs excessive heat. The reactor was divided into three chambers using sliding cast iron sheets. The whole chamber was painted black from inner side. The first chamber which was used in this study consists of 10 watts UV LED (wavelength of 365 nm).

3. RESULTS AND DISCUSSION

The photocatalytic degradation of aspirin was analyzed using Fe doped TiO_2 and commercially available TiO_2 (Degussa) under both UV and solar irradiations. The degradation efficiency was assessed at 290 nm. The effect of operational parameters like pH, catalyst dose, type of catalyst and effect of light source were assessed to attain maximum degradation of model compound.

3.1. Characterization of Fe Doped TiO_2 Nanoparticles

Fe doped TiO_2 was prepared using solgel method as described in Section 2.2 and its characterization was done to analyze various parameters such as particle size, surface morphology and surface area using XRD, SEM and BET, respectively.

Figures 2(a) and (b) depicts the XRD patterns of 0.5% Fe doped TiO_2 and TiO_2 (D). It can be seen that the XRD of Fe doped TiO_2 sample almost coincides with that of TiO_2 (D) and there is no diffraction peak due to metal ions species, thus depicting that the metal particles are well dispersed on TiO_2 surface. It can also be observed that doping with metal ions does not disturb the crystal structure of anatase TiO_2 indicating the metal dopants are placed on surface of crystal. Diffractions that are attributable to anatase TiO_2 are clearly present in the calcined materials.

SEM image of Fe–TiO_2 (Fig. 3(a)) indicates that the particles have spherical morphology and the presence of ferric ions on the surface of TiO_2 is not uniform. The image also shows that Fe–TiO_2 catalyst contains irregular particles which are the aggregation of tiny crystals. However, it cannot be ignored that some Fe particles are too small to be identified at the resolution of used microscope. EDS analysis performed for Fe doped TiO_2 presented in Figure 3(b) shows that 0.5% (by wt.) Fe–TiO_2 contains 0.41% of Fe content. The SEM image of pure TiO_2 shows that size of Titanium dioxide particles is even.

In general, the surface area of a catalyst is the most important factor influencing its catalytic activity. The surface area of Fe–TiO_2 was determined using nitrogen gas adsorption method and was found to be 72 m^2/g, which is higher than that of TiO_2 (D). Fe doping has an effect on the crystallization of TiO_2 and may prevent particle agglomeration, forming well-defined nanocrystalline particles with high surface area. With the integration of Fe dopants during the sol–gel preparation technique, there was crystal growth suppression, favoring the formation of smaller TiO_2 crystallite. This effect may be due to the

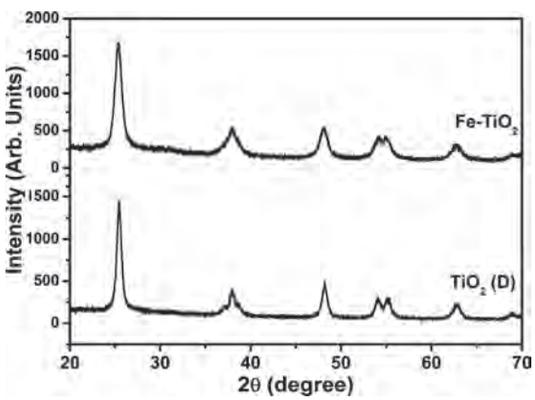

Figure 2. Typical XRD pattern of TiO_2 (Degussa) and Fe-doped TiO_2 nanoparticles.

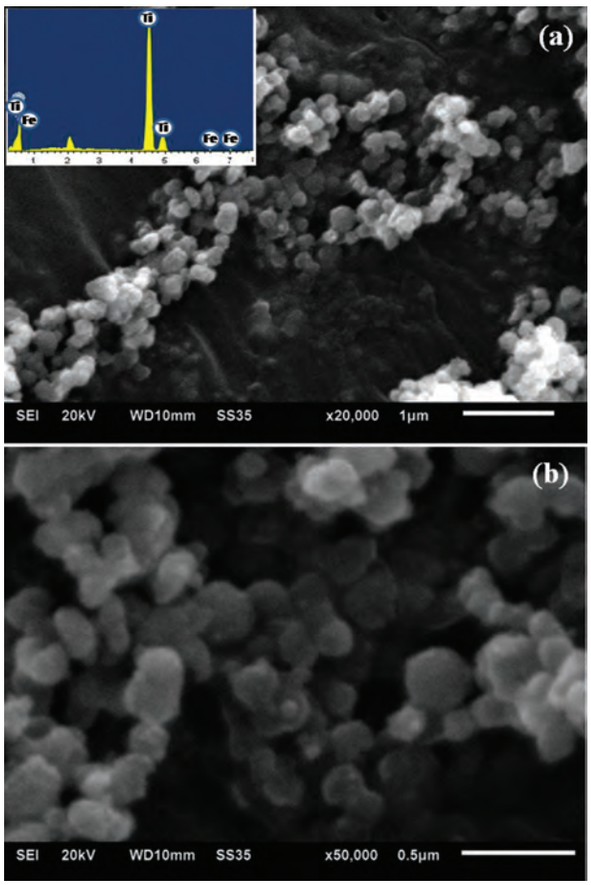

Figure 3. Typical SEM images of synthesized Fe-doped TiO_2 nanoparticles; inset shows the EDS spectrum of as-synthesized Fe-doped TiO_2 nanoparticles.

enhanced lattice strain in the doped TiO_2 network. Furthermore, this higher surface area values may also be because of the removal of nitrate from the crystal during calcinations at temperature of 400 °C. It increases the porosity of surface which ultimately increases the surface area of the doped TiO_2 than undoped one. Similar observations have also been reported for the degradation of rhodamine B dye and methylene blue dye with doped TiO_2 catalyst prepared by solgel method.[35, 36]

3.2. Photocatalytic Degradation of Aspirin Using Fe-Doped TiO_2 Nanoparticles

The photocatalytic degradation of aspirin was analyzed using Fe doped TiO_2 and TiO_2 (D) under UV irradiations and the degradation efficacy of doped catalyst were compared with that of TiO_2 (D). Thereafter, the effect of various operational parameters like pH and catalyst dose was assessed.

3.2.1. Effect of pH

The initial pH of the simulated aspirin solution was 4.6. It was varied from 3 to 10 (Fig. 4) in order to assess its

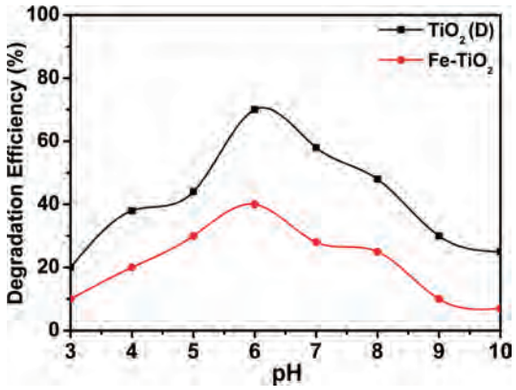

Figure 4. Effect of pH on the degradation of aspirin under UV light irradiation

impact on the degradation efficiency. The maximum degradation of 48% and 72% was obtained at pH 6 after 6 h of UV exposure with Fe–TiO_2 and TiO_2 (D), respectively. pH of the treated solution was also analyzed every hour and it was observed that there was decrease in pH of treated solution every time. Decrease in solution pH was considered as an indication for the degradation of model compound. This behavior may be attributed to the fact that variation in pH leads to alteration in properties of catalyst and aqueous solution, due to acid base equilibrium of hydroxyl radical. References [37, 38] also documented that there is a considerable dependence of the photocatalytic degradation efficiency on pH value, as the overall surface charge and hence the adsorptive properties of TiO_2 particles depend robustly on solution pH.

3.2.2. Effect of Catalyst Loading

The effect of catalyst dose on the degradation was assessed by varying catalyst concentration from 0.5–2.0 g/L under UV irradiation for 6 h. Figures 5(a) and (b) shows the aspirin degradation curves with different doses of catalyst for both Fe–TiO_2 and TiO_2 (D) photocatalysts, respectively. Degradation of aspirin increased with increasing catalyst loading up to 1 g/L with both photocatalysts, which may be attributed to the fact that the number of photons and the number of model molecules adsorbed increase with increase in the number of catalyst molecules. Beyond 1g/L of catalyst dose, the degradation efficacy decreased, it may be due to increase in the turbidity of the solution, which hinder with penetration of light transmission.

3.2.3. Comparison of UV-LED/UV-TUBE as Light Source

The degradation efficiency of aspirin solution (25 mg/L) was analyzed using Fe–TiO_2 and TiO_2 (D) under optimized conditions using two different light sources viz UV Tube and UV LED. The degradation efficiency with UV LED (10 W) was found to be 81% and with UV tubes (63 W) 70% using TiO_2 (D) as shown in (Fig. 6). However

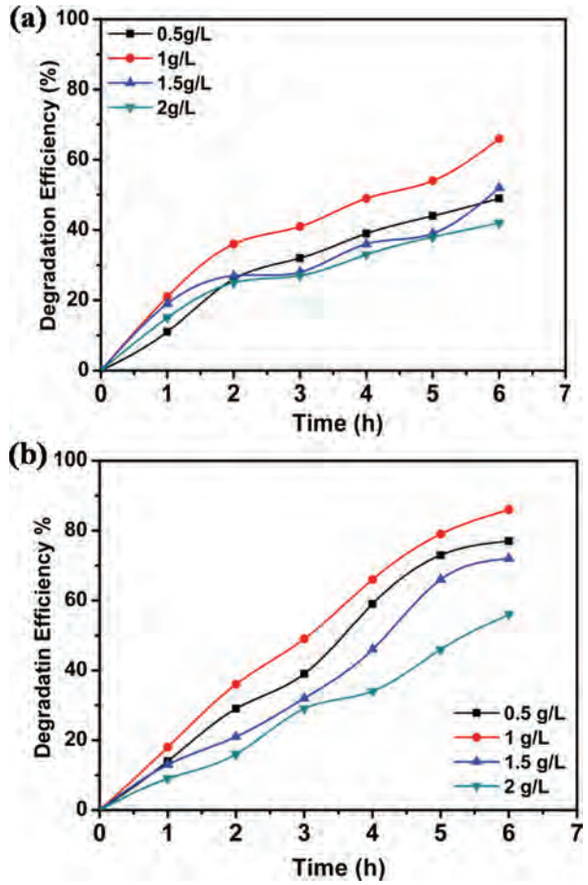

Figure 5. Effect of catalyst loading on degradation of aspirin (a) TiO_2 (D) and (b) Fe-doped TiO_2 nanoparticles.

with Fe–TiO_2, 58% degradation efficiency was achieved with UV LED, and 48% degradation was observed with UV tube as an irradiation source respectively. Thus, higher degradation efficiency was observed with UV LED as light source at much lower power consumption, which would subsequently reduce the operational cost of photocatalytic processes.

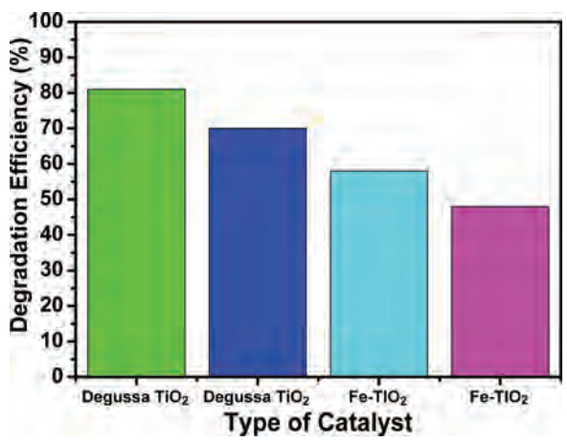

Figure 6. Comparison of degradation efficiency in presence of various types of catalysts

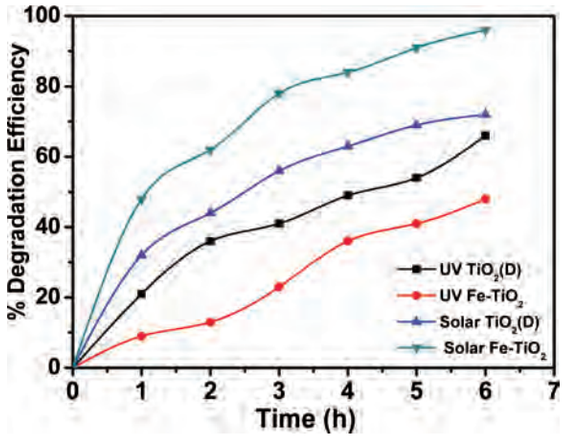

Figure 7. Effect of light source on degradation efficiency of aspirin

3.2.4. Solar Light Induced Photocatalytic Degradation

Aspirin solution (25 mg/L) was also treated with Fe–TiO_2 and TiO_2 (D) under solar irradiations at optimized conditions of pH and catalyst dose for 6 h. Under solar

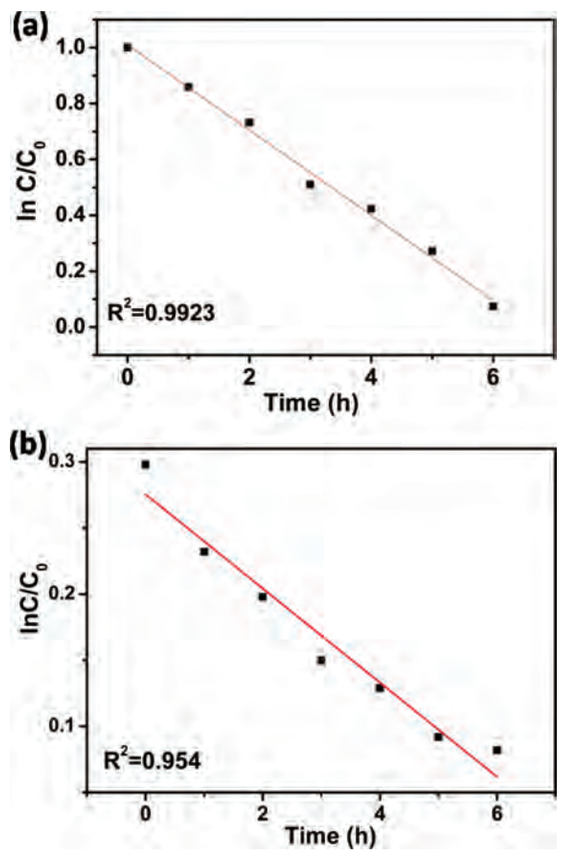

Figure 8. Kinetic analysis (a) TiO_2 (D), and (b) Fe-doped TiO_2 nanoparticles.

irradiations, Fe–TiO_2 and TiO_2 (D) showed 96% and 72% degradation of aspirin solution (25 mg/L) respectively under optimized conditions of pH and catalyst dose (Fig. 7). The better photocatalytic activity shown by Fe–TiO_2 can be explained on the basis of higher absorption of light in visible region and secondly iron being an acceptor impurity in doping of TiO_2, acts as an electron trap and prevents the electron hole recombination. Zhu et al.[32] also reported that Fe^{3+} doped TiO_2 prepared using sol–gel method, extends its absorption to visible region, which leads to an enhanced photocatalytic activity under solar irradiations.

3.2.5. Kinetic Studies

Kinetic studies for degradation of aspirin (25 mg/L) with catalyst dose of 1 g/L at pH 6 were carried out to find the reaction rate constant and order of reaction with Fe–TiO_2 and TiO_2 (D) as photocatalysts under solar irradiations. The plot of $\ln C/C_0$ v/s time gave straight line as shown in (Fig. 8) and the correlation constant was found to be 0.9618 and 0.9936 for TiO_2 (D) and Fe–TiO_2 respectively. Rate constant was calculated as 0.275 and 1.0094 for TiO_2 (D) and Fe–TiO_2 respectively. The results revealed that photocatalytic degradation of model compound followed first order kinetics by using $\ln(C/C_0) = kt$, where C_0 denotes initial concentration and C denotes the concentration at any time t.

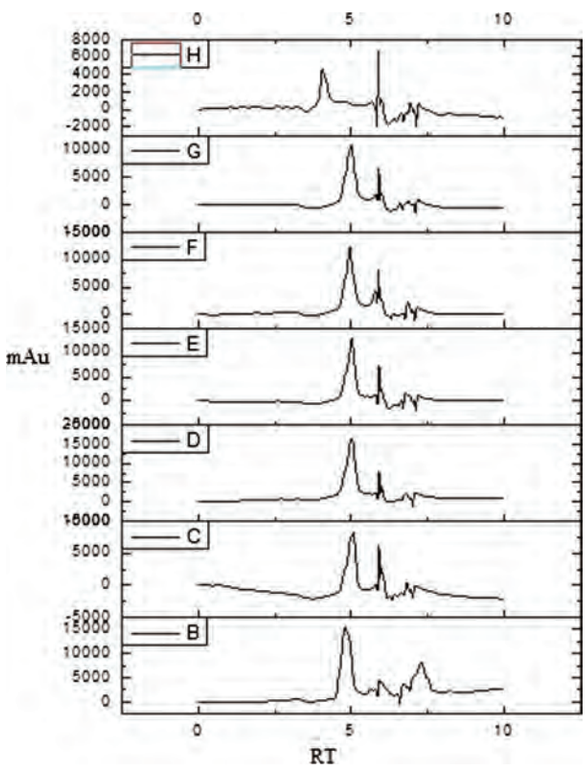

Figure 9. HPLC of initially and photocatalytically treated samples after different UV irradiation time.

3.2.6. Degradation Studies

HPLC technique was used to determine the photocatalytic intermediates of aspirin compound. Figure 9 shows the HPLC profiles recorded at 254 nm corresponding to the original aspirin solution (25 mg/L) and after treatment upto 6 h with a gap of every 1 h. Initially, strong peak was observed at retention time (t_R) of 4.8 minutes which corresponds to that of aspirin and it was observed that as the time of photocatalytic treatment increased, the peak area was decreasing which confirms that the model compound was degrading with time.

4. CONCLUSIONS

The photocatalytic degradation of aspirin solutions was investigated with Fe doped and commercial available TiO_2 catalyst illuminated with UV Tube/UV LED and solar light. Doped catalyst was characterized using XRD, SEM, BET, UV-visible spectrophotometer. The BET surface area of Fe–TiO_2 was found to be 72 m^2/g. Doped catalyst showed better photocatalytic performance than TiO_2 (D). The enhanced activity of Fe–TiO_2 may be due to shifting of absorbance spectrum into visible region. The adsorption of aspirin solution over the catalyst surface was found to be maximum at pH 6 and the optimum dose of catalyst was found to be 1.0 g/L. The results indicated that the aspirin was degraded upto 96% by 0.5% Fe–TiO_2 under solar irradiations. The degradation process followed the first order rate kinetics which was represented by Langmuir-Hinshelwood equation. The degradation of the model compound was also confirmed with the reduction of peak in the chromatographic analysis.

References and Notes

1. O. A. H. Jones, N. Voulvoulis, and J. N. Lester, *Water Res.* 36, 5013 **(2002)**.
2. M. M. Huber, S. Canonica, G. Y. Park, and U. V. Gunten, *Environ. Sci. Technol.* 37, 1016 **(2003)**.
3. D. Löeffler, J. Römbke, M. Meller, and T. Ternes, *Environ. Sci. Technol.* 39, 5209 **(2005)**.
4. C. C. Liu, Y. H. Hsieh, P. F. Lai, C. H. Li, and C. L. Kao, *Dye Pigment.* 68, 191 **(2006)**.
5. B. E. Cham, J. H. Dykman, and F. Bochner, *J. Clin. Pharmacol.* 14, 562 **(1982)**.
6. K. Kummererr, Springer-Verlang, Berlin, Heidelberg, Germany **(2001)**, Vol. 1, pp. 1415–1420.
7. H. Y. He, *Int. J. Environ. Res.* 2, 23 **(2008)**.
8. O. M. Alfano, D. Bahnemann, A. E. Cassano, R. Dilert, and R. Goslich, *Catal. Today* 58, 199 **(2000)**.
9. A. Fujishima, T. N. Rao, and D. A. Tryk, *J. Photoch. Photobio. C* 1, 1 **(2000)**.
10. W. Y. Han, W. P. Zhu, P. Y. Zhang, Y. Zhang, and L. S. Li, *Catal. Today* 90, 319 **(2004)**.
11. M. Qamar, M. Munner, and D. Bahnemann, *J. Environ. Manage.* 80, 99 **(2006)**.
12. A. Paola, M. Addamo, and V. Augugliaro, *Intern. J. Photoenerg.* 2006, 1 **(2006)**.
13. R. A. Palominos, A. Mora, M. A. Mondaca, M. Perez-Moya, and H. D. Mansilla, *J. Hazard. Mater.* 158, 460 **(2008)**.

14. G. Sivalingam, K. Nagaveni, M. S. Hegde, and G. Madras, *Appl. Catal.* 45, 23 (**2003**).
15. N. P. Xekoukoulotakis, N. Xinidis, and M. Chroni, *Catal. Today* 151, 29 (**2010**).
16. M. N. Abellan, B. Bayarri, B. J. Gimenez, and J. Costa, *App. Catal. B* 74, 233 (**2007**).
17. S. Ghajar and M. R. Sohrabi, *J. Chem. Pharma. Res.* 4, 814 (**2012**).
18. D. Vognaa, R. Marottab, A. Napolitanoa, R. Andreozzib, and M. Dischia, *Water Res.* 38, 414 (**2004**).
19. A. Desale, S. P. Kamble, and M. P. Deosarkar, *Intern. J. Chem. Phys. Sci.* 2, 140 (**2013**).
20. D. A. Lambropoulou, M. D. Hernando, I. K. Ikonstantinou, E. M. Thurmanb, I. Ferrer, and T. A. Albanis, *J. Chromatography* 1183, 38 (**2008**).
21. E. M. Arriaga, S. Esplugas, and J. Gimenez, *Water Res.* 42, 585 (**2008**).
22. J. H. Pereira, A. C. Reis, O. C. Nunes, M. T. Borges, V. J. Vilar, and R. A. Boaventura, *Environ. Sci. Pollu. Res. Intern.* 7, 139 (**2013**).
23. M. R. Hoffmann, S. T. Martin, W. Y. Choi, and D. W. Bahnemann, *Chem. Rev.* 95, 69 (**1995**).
24. C. H. Wei, X. H. Tang, J. R. Liang, and S. Tan, *J. Environ. Sci.* 19, 90 (**2007**).
25. S. Rengaraj, X. Z. Li, P. A. Tanner, Z. F. Pan, and G. K. H. Pang, *J. Mol. Catal. A: Chem.* 247, 36 (**2006**).
26. C. Su, B. Y. Hong, and C. M. Tseng, *Catal. Today* 96, 119 (**2004**).
27. J. Sun, X. Wang, J. Sun, R. Sun, S. Sun, and L. Qiao, *J. Mol. Catal. A: Chem.* 260, 241 (**2006**).
28. J. Moon, *J. Mater. Sci.* 36, 949 (**2001**).
29. H. Yu, X. Zheng, Z. Yin, F. Tao, B. Fang, and K. C. Hou, *J Chem. Eng.* 15, 802 (**2007**).
30. L. Das, S. K. Barodia, S. Sengupta, and J. K. Basu, *Int. J. Environ. Sci.* 10, 1 (**2014**).
31. H. Hossaini, G. Moussavi, and M. Farrokhi, *Water Res.* 59, 130 (**2014**).
32. J. Zhu, W. Zheng, B. He, J. Zhang, and M. Anpo, *J. Mol. Catal. A: Chem.* 216, 35 (**2004**).
33. M. Asiltürk, F. Sayilkan, and E. Arpaç *J. Photochem. Photobio. A: Chem.* 203, 64 (**2009**).
34. R. Nainani, P. Thakur, and M. Chaskar, *J. Mater. Sci. Engg.* 2, 52 (**2011**).
35. X. Yang, C. Cao, L. Erickson, K. Hohn, R. Maghirang, and K. Klabunde, *Appl. Catal. B: Environmental.* 91, 657 (**2009**).
36. G. Colon, M. Maicu, M. C. Hidalgo, and J. A. Navio, *Appl. Catal. B Environ.* 67, 41 (**2006**).
37. W. Z. Tang and H. An, *Chemosphere* 31, 4157 (**1995**).
38. Y. Wang, *Water Res.* 34, 990 (**2000**).

Received: 11 August 2014. Accepted: 12 February 2015.

Journal of Environmental Chemical Engineering 4 (2016) 1267–1273

Contents lists available at ScienceDirect

Journal of Environmental Chemical Engineering

journal homepage: www.elsevier.com/locate/jece

Transition metal doped TiO_2 mediated photocatalytic degradation of anti-inflammatory drug under solar irradiations

Vibhu Bhatia, Amit Dhir*

School of Energy and Environment, Thapar University, Patiala 147004, India

ARTICLE INFO

Article history:
Received 7 November 2015
Received in revised form 21 January 2016
Accepted 22 January 2016
Available online 24 January 2016

Keywords:
Photocatalysis
Doped
Ibuprofen
Bi–TiO_2
Ni–TiO_2
Solar irradiation

ABSTRACT

Bismuth (Bi) and Nickel (Ni) Doped Titanium Dioxide (TiO_2) nanoparticles were synthesized by sol–gel method and the prepared nanoparticles were characterized by X-Ray Diffraction, Scanning Electron Microscope, UV–vis reflectance spectroscopy and Brunauer–Emmett–Teller (BET) analysis. The concentration of dopant in synthesized catalysts was varied from 0.25 to 1.0 wt%. Maximum BET surface area of 47.8 and 45.7 m^2/g was observed with 0.25 wt% Bi–TiO_2 and 0.5 wt% Ni–TiO_2, respectively. EDX analysis has established the presence of 0.21% Bi ions and 0.36% Ni ions in 0.25 wt% Bi doped TiO_2 and 0.5 wt% Ni doped TiO_2, respectively. Band gap of Bi–TiO_2 (0.25 wt%) and Ni–TiO_2 (0.5 wt%) was obtained to be 2.99 eV, which is found to be minimum among the various synthesized catalysts. The photocatalytic activity of synthesized catalysts were tested and compared with Degussa TiO_2 for degradation of Ibuprofen (IBP) as a model compound. Bi–TiO_2 nanoparticles revealed higher photocatalytic activity when compared to Ni–TiO_2 or Degussa TiO_2 under solar irradiation, which may be attributed to increase in specific surface area, and decrease in the crystallite size. Maximum of 89% degradation was achieved with 0.25% Bi–TiO_2 photocatalyst under 6 h of illuminations with a solar light, whereas, 78% degradation has been achieved under similar experimental condition with Ni doped TiO_2. The kinetics of the degradation of IBP has been explained in terms of the Langmuir–Hinshelwood model and was found to follow first order kinetics with k value of 0.0064 and 0.0046 min^{-1} with Bi and Ni doped TiO_2, respectively.

1. Introduction

The existence of pharmaceuticals compounds and its residues has been reported frequently in literature [11,6] thus, receiving increasing attention as an emerging environmental issue. Numerous pharmaceutical compounds have been noticed in household wastewater, natural water bodies and groundwater in many countries all over the world. The presence of pharmaceutical compounds can cause severe environmental issues due to the chemical toxicity of the lively constituents in the formulations and sometimes, of their disintegration products. Ibuprofen [IBP] is one of the most commonly consumed medicines worldwide, mainly due to its use as a pain reliever. Concentration of IBP in the environment has been stated between 10 ng/L to 169 μg/L [16]. Sources of these contaminants are primarily the domestic waste water due to excretion of non-metabolized drugs by animal or human urine and faeces. Conventional treatment processes functional at sewage treatment plants are not efficient in removing such pharmaceutical substances by various physical or biological treatment steps. Therefore, alternative and effective treatment methods need to be explored for the degradation of such pharmaceutical compounds.

Several research outcomes have shown favorable results in the exclusion of pharmaceutical pollutants using the application of Advanced Oxidation Processes (AOPs). The AOPs are oxidative processes that have been shown to be efficient for the degradation of several organic compounds based on attack by the hydroxyl radicals ($^{\bullet}OH$), superoxide radical ($^{\bullet}O_2^-$), and hydrogen peroxide (H_2O_2) generated by UV-irritated [12]. The derivatives after AOPs have been reported to be degraded by biological oxidation [19].

Although, TiO_2 catalysts are capable of degrading a wide range of organic/inorganic pollutants and toxic materials in all phases such as liquid and gas systems, but the rapid recombination rate of electron–hole pairs generated by photons reduces the commercialization of this technology. For this reason, recent research laid prominence on catalyst doping with transition and noble metals [19]. Achilleos et al. investigated the degradation of IBP and carbamazepine using Degussa TiO_2 and it was documented that

* Corresponding author.
E-mail address: amit.dhir@thapar.edu (A. Dhir).

http://dx.doi.org/10.1016/j.jece.2016.01.032
2213-3437/

60% of compound was degraded within 120 min of irradiation time [1]. The presence of metals as dopant, such as Pt, Pd, Au and Ag has been reported to boost the photocatalytic activity of catalyst. Various studies have reported that bismuth oxide families such as $BiVO_4$, Bi_2O_3, and bismuth-doped TiO_2 are remarkable visible light lively photocatalysts for degradation of organic pollutants, hydrogen generation and dye-sensitized solar cell applications [18,8,23,21,7].

The literature studies on the photocatalytic degradation of pharmaceuticals in aqueous streams did not address its photocatalytic oxidation using doped photocatalyst under solar irradiations. Moreover, the suitable concentration of dopant in the photocatalyst needs to be explored for the effective degradation of pharmaceutical drug in aqueous stream. Keeping this in view, the present study focused on the degradation efficiency of IBP using lab synthesized Bi and Ni ions doped TiO_2 with different concentrations of dopants under UV/Solar irradiations and the degradation efficiency was compared with commercially available TiO_2.

2. Experimental

2.1. Materials

All the chemicals used in this study were of analytical grade and were used as such without further purification. Titanium dioxide (TiO_2 (D)) was procured from Degussa Corporation, Germany. Ibuprofen (>99% pure) was obtained from Sigma–Aldrich. Bi (NO_3) $5H_2O$ and Ni (NO_3) $5H_2O$ were purchased from Loba Chem., India. Titanium isopropoxide, as source of titanium dioxide, was purchased from Sigma–Aldrich. Ethanol, used as solvent, was procured from Merck. All the solutions were prepared with deionized water. Fig. 1 showing structure of ibuprofen.

2.2. Preparation of Bi–TiO_2 and Ni–TiO_2

Doped TiO_2 was prepared using solgel method with Titanium isopropoxide (TIP) as precursor. 2.5 ml of TIP was added drop by drop to a solution of 10 mL ethanol and 2.5 mL acetylacetone at room temperature and stirred for 30 min. Then 2 mL distilled water was added to above solution. Calculated amount of Bi (NO_3) $5H_2O$ and Ni (NO_3) $5H_2O$ were added respectively into prepared solution so as to prepare appropriate concentration of dopant and a stable sol was finally obtained after stirring for 2 h. Afterwards, concentrated solution was placed at 90 °C for drying and dried powder was calcined at 400 °C for 2 h.

2.3. Characterization of synthesized catalyst

The powder X-ray diffraction (XRD) was done at room temperature using X-ray diffractometer (Cukα $\lambda = 0.154$ nm) to study the crystal phase of the products. X-ray diffraction (XRD) patterns were collected using a Philips X-ray diffractometer with monochromatic high-intensity in a 2θ range of 20–70°. The crystallite size of the particles was calculated using Scherrer's equation (Eq. (1)).

$$D = \frac{K\lambda}{\beta \mathrm{Cos}\theta} \quad (1)$$

Scanning electron microscope (SEM) images were obtained with Philips SEM analyzer. The Brunauer–Emmett–Teller surface area was measured using N_2 adsorption/desorption (NOVA2000e) USA at liquid-nitrogen temperature (77 K). Band gap has been evaluated using UV–vis diffuse reflectance spectrophotophotometer of Hitachi U3900H at wavelength range of 190–800 nm.

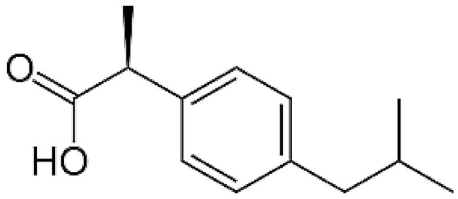

Fig. 1. Structure of ibuprofen.

2.4. Photocatalytic reactor and degradation methodology

Ibuprofen (IBP) was subjected to photocatalytic treatment in the presence of synthesized photo catalysts and TiO_2 (D). Photocatalytic activity was assessed in a batch glass reactor under slurry mode. Irradiation was provided by seven UV tubes of 36W (Philips) emitting radiation at around 254 nm placed at top of the reactor. Initially photodegradation of IBP (25 ppm) was assessed using TiO_2 by varying the catalyst dose from 0.5 to 2.5 g/L and pH from 3 to 10 under UV/solar irradiations. Afterwards IBP was subjected to photodegradation using various lab synthesized catalyst with varying dopant concentration (0.25–1.0 wt%) at 2 g/L of catalyst dose at pH 6.0 under UV/solar irradiations. Aliquots of the mixture were taken at different time intervals during the reaction and then analyzed for their absorbance in UV–vis spectrophotometer at 260 nm. Finally kinetics of the IBP degradation was also studied so as to evaluate rate constant using different photocatalysts. For the solar induced photocatalytic reactions, experiments were carried out in the same reactor placed at terrace in the presence of solar irradiations from 10.00 AM to 4.00 PM in the month of May–June. At regular intervals of 1 h, samples were injected out and were analyzed using spectrophotometer. The average intensity of sunlight was found to be in the range of 30–35 W/m^2 during the study period.

The surface adsorption of Ibuprofen on catalyst surface was carried out by dispersing the nanoparticles in solution of model compound with both catalysts in the dark. At regular intervals of 15 min, sample was pipetted out from the broth for centrifugation to separate nanoparticles and subsequently, the drug concentration in the solution was measured through spectrophotometer analysis. During the adsorption process, turbulence was created in the slurry with the help of a magnetic stirrer with an objective to enhance the mass transfer.

3. Results and discussion

3.1. Characterization

3.1.1. XRD

X-ray diffraction (XRD) patterns were collected monochromatic high-intensity in a 2θ range of 20–70° as shown in Fig. 2. No noteworthy shift in XRD peaks of Bi–TiO_2 and Ni–TiO_2 compared with Degussa TiO_2 has been observed indicating that Bi^{3+} did not move in the lattice to substitute Ti^{4+} particles. It may be due to higher radius of Bi^{3+} (1.03 Å) than that of Ti^{4+} (0.68 Å). The bismuth in the TiO_2 surface may increase the charge separation. Similar observation has been reported by Rengraj et al. [15] and Xu et al. [22] where doping of TiO_2 with Bi did not show any substantial variation in peaks of XRD. The reason for stabilizing Ni doped TiO_2 at lower levels has been credited to the almost similar ionic radius of Ni^{+2} (0.72 Å) to that of Ti^{+4} (0.68 Å), which was found to replace some portion of Ti^{+4} ions in TiO_2 lattice [25,24,20,4,9].

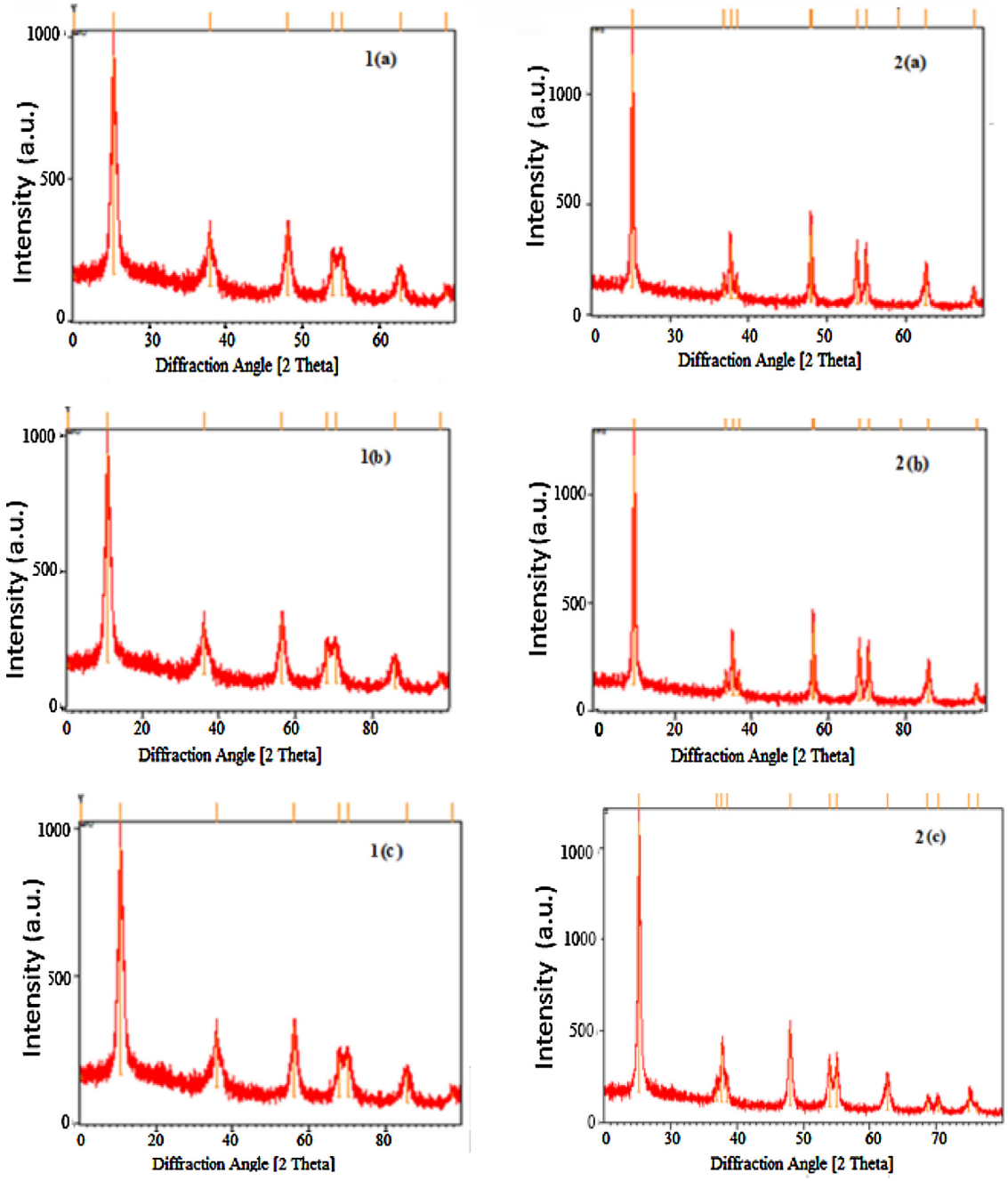

Fig. 2. XRD pattern of synthesized (1a) 0.25 wt% Ni–TiO_2 (1b) 0.5 wt% Ni–TiO_2 (1c) 1.0 wt% Ni–TiO_2, (2a) 0.25 wt% Bi–TiO_2 (2b) 0.5 wt% Bi–TiO_2 (2c) 1.0 wt% Bi–TiO_2.

The morphology of doped photocatalysts was analyzed by SEM. Fig. 3 depicted that particles have spherical shape and agglomeration had taken place. The EDS analysis of doped TiO_2 showed significant presence of Ni and Bi in synthesized samples. The analytical results from EDS are in realistic arrangement with 0.25–1.0 wt% of Bi^{3+} and Ni ions doped into TiO_2. The elemental records of samples for Ti, O and Bi showed homogeneous distribution of elements and no gathering of Bi ions was detected in the 0.25–1.0 wt% range of doped Bi–TiO_2 and Ni–TiO_2. From EDS analysis (Table 1), it has been observed that in 0.25 wt% of Bi–TiO_2 and Ni–TiO_2, 0.21 and 0.19% of Bi and Ni ions were present, respectively. Subsequently variations have been found in 0.25–1.0 wt% of Bi–TiO_2 and Ni–TiO_2.

3.1.1. BET surface area

The increase in surface area increases the number of active sites, which further promotes the separation efficiency of the electron–hole pair and subsequently, results in enhanced photocatalytic activity. Upon doping with 0.25 wt% Ni, the crystallite size was observed to be 13.84 nm and the surface area value was 41.71 m^2/g as shown in Table 2. As the dopant concentration was increased to 0.5 wt%, the crystallite size value decreased to 10.3 nm and the surface area value increased to 45.70 m^2/g. These results suggest that TiO_2 doped with Ni (<0.5 wt%) dopant concentration effectively inhibits TiO_2 grain growth possibly by remaining at boundaries of the grain thereby, increasing the crystallite size and decreasing the surface area [8,2,20,9]. The decrease in growth of

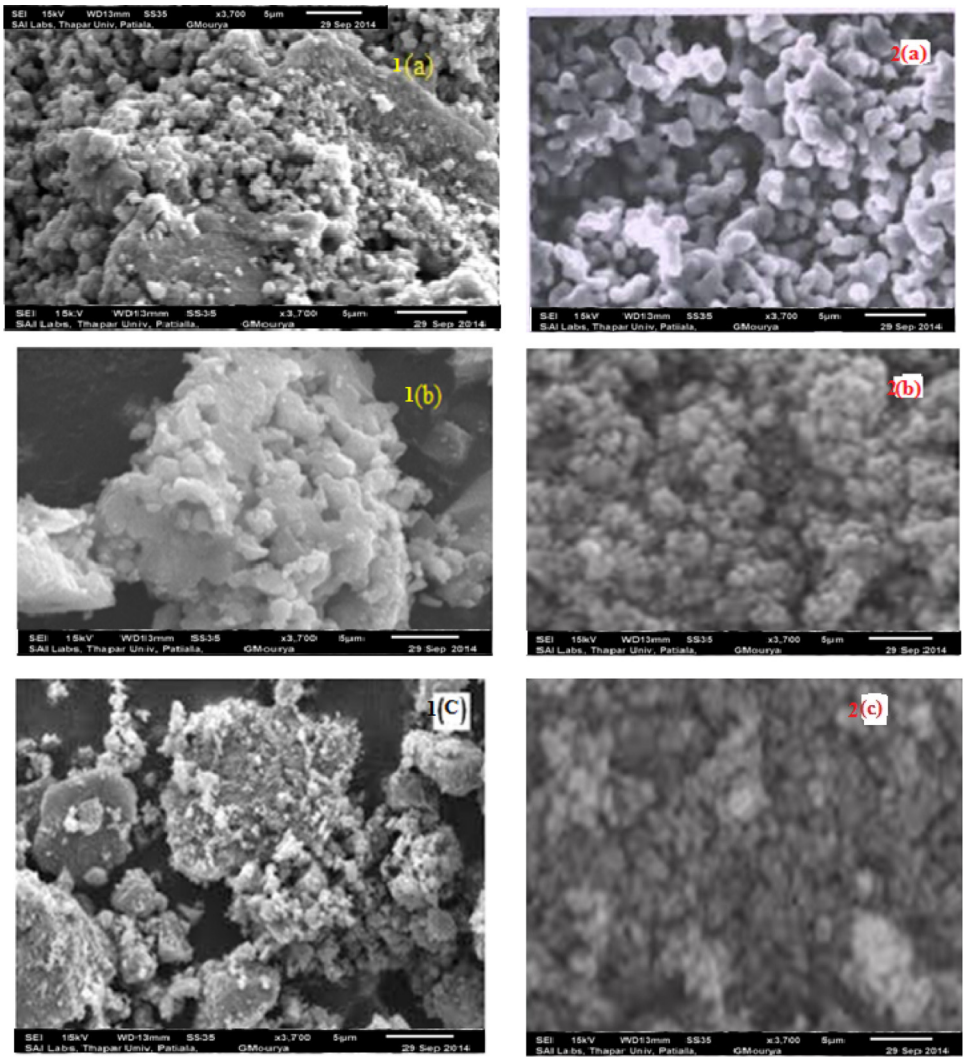

Fig. 3. SEM images of synthesized (1a) 0.25 wt% Ni–TiO_2 (1b) 0.5 wt% Ni–TiO_2 (1c) 1.0 wt% Ni–TiO_2, (2a) 0.25 wt% Bi–TiO_2 (2b) 0.5 wt% Bi–TiO_2 (2c) 1.0 wt% Bi–TiO_2.

Table 1
EDS of various dopant concentration.

Bi–TiO_2	Elements			Ni–TiO_2	Elements		
Dopant concentration	Bi	O	Ti	Dopant concentration	Ni	O	Ti
0.25 wt%	0.21	0.02	0.02	0.25 wt%	0.18	0.02	0.05
0.50 wt%	0.43	0.03	0.04	0.50 wt%	0.36	0.5	0.9
1.0 wt%	0.88	0.20	0.10	1.0 wt%	0.74	0.08	0.18

grain can also be due to the formation of Ni—O—Ti bonds in the doped powders, which inhibits the growth of the crystals. However, decrease in the dopant concentration to 0.25 wt%, leads to increase in crystalline size and decrease in surface area of synthesized catalyst.

However in case of Bi–TiO_2, it was observed that the surface area and crystal size was found to be as 47.8 m^2/g and 12.4 nm, respectively for dopant concentration of 0.25 wt%. Further, by increasing the dopant concentration from 0.25 wt% to 1.0 wt%, the decrease in surface area and increase in crystalline size was observed which may likely decrease the photocatalytic activity as shown in Table 3.

Table 2
Crystalline size and surface area of Ni doped TiO_2.

Ni (wt%)	Crystalline size	Surface area
0.25	13.84 nm	41.71 m^2/g
0.50	10.3 nm	45.7 m^2/g
1.0	16.92 nm	40.8 m^2/g

Table 3
Crystalline size and surface area of Bi doped TiO_2.

Bi (wt%)	Crystalline size	Surface area
0.25	12.4 nm	47.8 m^2/g
0.50	13.67 nm	43.4 m^2/g
1.0	15.6 nm	42.1 m^2/g

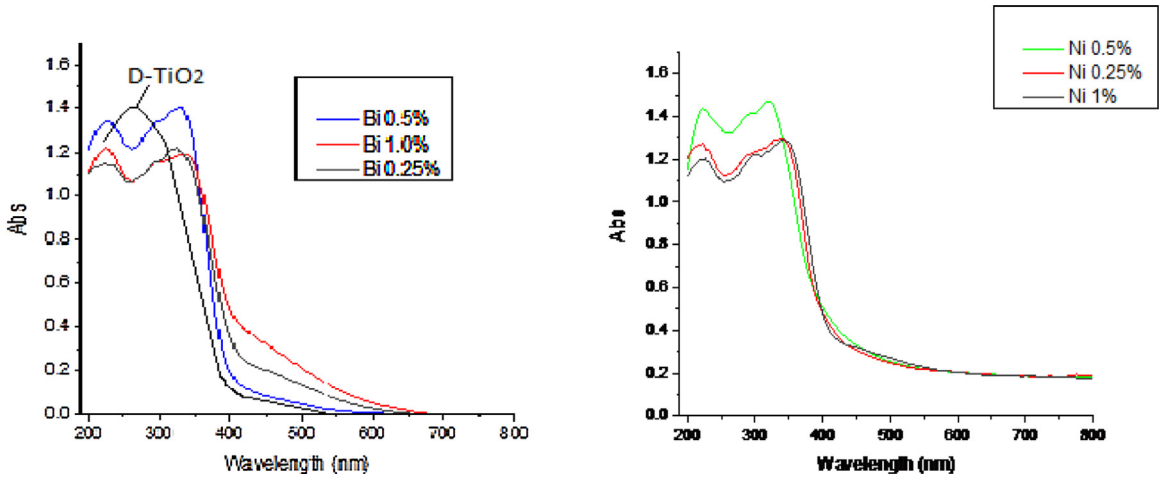

Fig. 4. UV–vis diffuse reflectance spectrum of (a) Bi–TiO_2 (b) Ni–TiO_2.

3.1.2. Band gap energy

The UV–vis diffuse reflectance spectrum of all the compositions are shown in Fig. 4. It is evident from the results that the UV–vis diffuse reflectance spectrum of Bi doped TiO_2 and Ni doped TiO_2, gave distinct band gap absorption edges at 422 nm, 415 nm, 405 nm for doped Bi(0.25 wt%), Bi(0.50 wt%), Bi(1.0 wt%), and 413 nm, 418 nm, 412 nm for doped Ni(0.25 wt%), Ni(0.50 wt%), Ni (1.0 wt%), respectively. The corresponding band gap energies were found to be 2.99, 3.05 and 3.08 eV for 0.25 wt%, 0.50 wt%, and 1.0 wt % Bi–TiO_2, respectively and 3.02, 2.99 and 3.03 eV for 0.25 wt%, 0.50 wt% and 1.0 wt% Ni doped TiO_2, respectively. At lowest concentration of Bi dopant, the absorption edge shift is maximum and hence, the corresponding calculated band gap energy is minimum. This may be attributed to the fact that when the amount of dopants is small, the metals ions are well incorporated into the lattice withstanding the evolvement of local strains. On the other hand, when the dopants are in excess, Bi ions cannot enter the TiO_2 lattice but cover on the surface of TiO_2 and leads to the formation of heterogeneity junction. So, Bi (0.25 wt%) photocatalysts has lower band gap energy (2.9 eV) within the temperature range in which the photocatalytic experiments were carried out when compared to other dopant concentrations. For Ni–TiO_2 the minimum band gap energy of 2.9 eV was obtained with dopant concentration of 0.5 wt%. As the concentration of dopant is either increased or decreased from 0.5 wt%, increase in the value of band gap energy was noticed, which may be due to formation of layer of dopant over TiO_2, hence, ions might not get inserted into lattice of TiO_2.

3.2. TiO_2 mediated photocatalytic degradation

In order to obtain baseline data with standard TiO_2 (Degussa), photocatalytic degradation of IBP was carried out in slurry mode under UV irradiation. pH of the initial IBP aqueous solution (25 ppm) was varied from 3 to 10 and TiO_2 (Degussa) was used as photocatalyst. It is observed (Fig. 5(a)) that the degradation efficiency increased with increase in value of pH up to 6.0 and thereafter, decrease in the degradation was observed. The maximum degradation of IBP was found to be 76% using 2 g/l TiO_2 (D) at pH 6.0. This behavior is attributed to the fact that the p*K*a value of IBP is 4.4 and it is reported as weak acid. The point of zero charge (pzc) of the TiO_2 (Degussa P25) is at pH 6.8 and TiO_2 surface is positively charged in acidic media (pH < 6.8), whereas it is negatively charged under alkaline conditions (pH > 6.8). Therefore, at acidic pH range, the surface of TiO_2 will be positively charged as well as the carboxyl group of IBP, hence, charge repulsion exists. Moreover, at acidic pH, the higher $^{\bullet}OH$ radicals generated are considered to be in equilibrium with the holes trapped at the TiO_2 surface. At alkaline pH range, IBP and TiO_2 both are negatively charged. Moreover, hydroxyl radicals are rapidly scavenged and they do not have the opportunity to react with

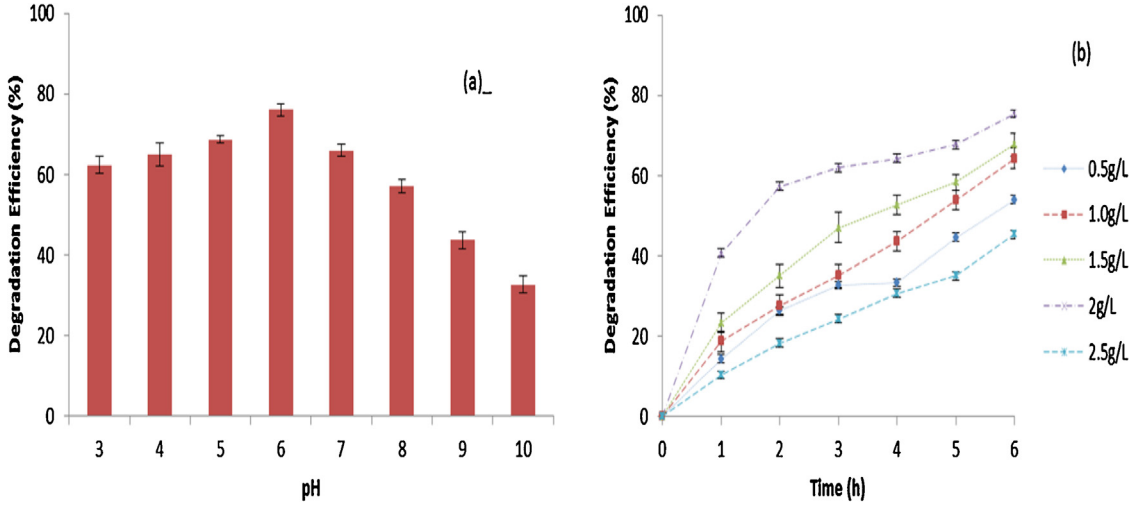

Fig. 5. Effect of photocatalytic parameters (a) variation of pH (b) variation of catalyst dose.

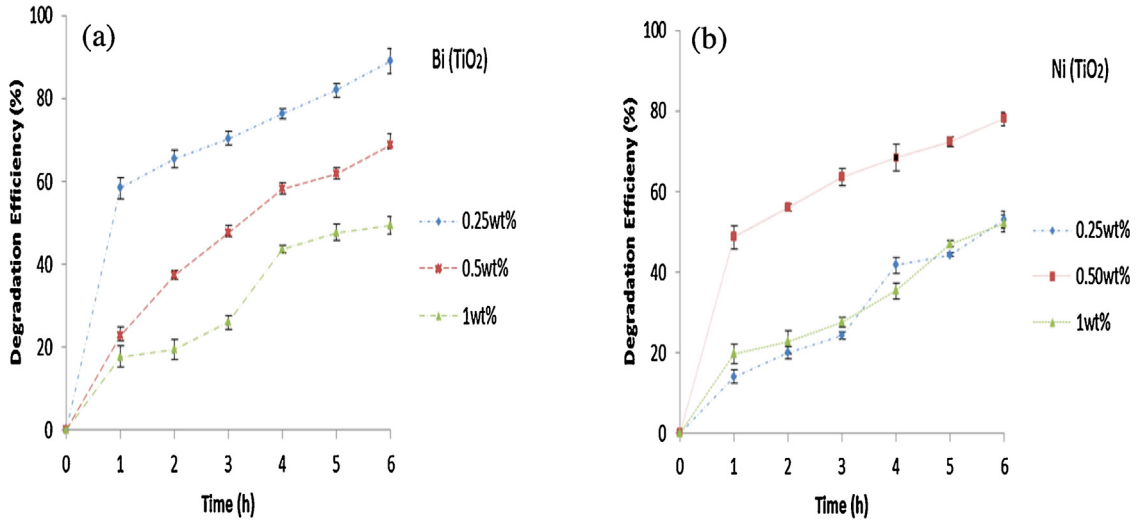

Fig. 6. Variation of dopant concentration (a) Bi (TiO_2) (b) Ni (TiO_2).

model compound so enhanced activity is expected at pH 6–7 [5]; Zhang et al., 2013.

Catalyst dose of TiO_2 was varied from 0.5 to 2.5 g/L as shown in Fig. 5(b). It was observed that increasing the concentration of catalyst from 0.5 g/L to 2.5 g/L, the degradation efficiency kept on increasing upto 2 g/L indicating the significance of available catalyst surface for degradation on its surface under UV illumination and maximum degradation of 76% was achieved with 2 g/L of TiO_2 (D) catalyst. Further, increasing the catalyst concentration beyond 2 g/L, the photocatalytic efficiency decreased directing that the optimal photons have been adsorbed. The amount of catalyst more than the certain limit may not be useful because of chances of aggregation, as well as reduction in irradiation field onto the surface due to increase in the turbidity of the solution. Moreover, at high concentration, there is a decrease in surface area availability for light-harvesting for the generation of h+/e− pairs, induced by accumulation as also explained in previous findings [13,10].

3.3. Variation in dopant concentration

Insertion of transition metal can serve as electron/hole separator and can eradicate the hasty recombination of excited e^-/hole pair all through photoreaction, resulting in enhancing the efficiency of the TiO_2 photocatalyst. But, this effect is subtle to dopant concentration also. The photocatalytic degradation of IBP (25 ppm) was assessed using lab synthesized Bi and Ni doped TiO_2 (2 g/L) at pH 6.0 under solar irradiations with varying concentrations of dopant. Dopant concentration was varied from 0.25 to 1.0 wt% for both Bi–TiO_2 and Ni–TiO_2. With (0.25 wt%) Bi–TiO_2 concentration, 89% of IBP degradation was observed in 6 h of solar irradiation as shown in Fig. 6(a) and as concentration of dopant was raised from 0.25 to 1.0 wt%, there was decrease in the degradation efficiency. The deferral effect of increase in Bi content on degradation rate may be credited to destruction of hydroxyl radicals due to entrapment of conduction band e^- by the adsorbed metal ions. However, with Ni–TiO_2, the maximum degradation of 78% was observed with 0.50 wt% dopant concentration and it was observed that on either increasing or decreasing the concentration of dopant from 0.50 wt%, there was decrease in degradation efficiency of IBP, which may be because of the increased impact of ions with increased dopant concentration up to certain limit (up to 0.50 wt%) and thereafter, the photocatalytic activity reduced due to surface charge separation.

3.4. Variation of type of catalyst

The effect of dopants might not be similar on trapping e^-/holes on the surface or during interface charge transfer because of the different locations of the dopant in the lattice. So, the photocatalytic competence would be different for various types of dopants [3,14]. In order to compare the efficiency of TiO_2 (D) with lab synthesized Bi and Ni doped TiO_2, IBP was subjected to photocatalytic degradation at pH 6 with photocatalyst dose of 2 g/L under solar irradiations. Degradation of 89% was achieved with Bi–TiO_2, whereas only 50 and 74% degradation was achieved with Ni–TiO_2 and TiO_2 (D), respectively, under similar experimental conditions as shown in Fig. 7. The bismuth in the TiO_2 surface may enhance the charge separation and improves its photocatalytic activity. In order to adjudge the extent of adsorption, experiments were conducted in the dark with Bi and Ni doped catalyst which showed negligible degradation efficiency (<5%). Thus, the orders of photocatalytic degradation of IBP followed by different catalyst has been observed as Bi–TiO_2 > TiO_2 > Ni–TiO_2.The cause for this enhancement has been timidly credited to the overpowering of recombination of electron–hole pairs on the surface of the TiO_2 catalyst by low valence Bi ions. Literature also revealed that among numerous transition metal ion dopants, Bi appears to be efficient dopant as the radius of Bi ions is almost similar to that of titanium ions, so this metal ion gets fused into titanium crystal lattice structure, which helps to shift absorbance

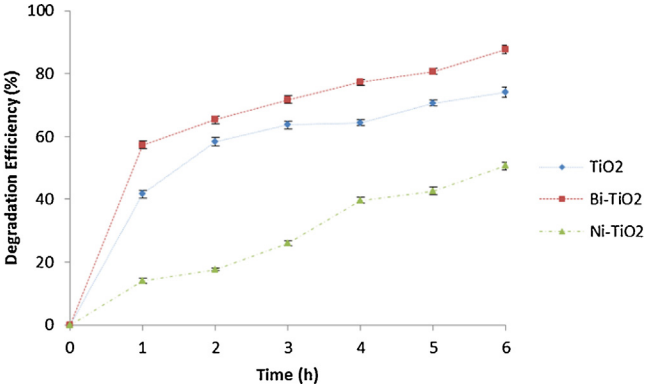

Fig. 7. Variation of type of catalyst.

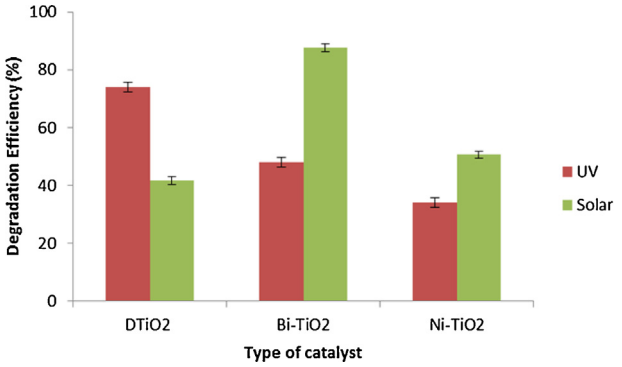

Fig. 8. Variation of light source.

in visible spectra, and hence, results in increasing the photocatalytic activity [2,17].

Kinetic studies of degradation of IBP (25 ppm) with catalyst dose of 2 g/L at pH 6 were carried out to find the reaction rate constant and order of reaction with Bi–TiO_2, Ni–TiO_2 and TiO_2 (D) as photocatalyst under solar irradiations. The rates constant were found to be 0.0064, 0.0046 and 0.0043 min^{-1} for Bi–TiO_2, Ni–TiO_2 and TiO_2 (D), respectively with first order kinetics.

3.5. Comparison of solar/UV as light source

Fig. 8 shows the comparison of degradation studies of IBP in aqueous solution under two different types of irradiation viz UV/solar irradiations. It was observed that under UV light the degradation was found to be 76% using TiO_2 (D) (2 g/L) at pH 6 after 6 h of luminescence. The maximum degradation of 89% was achieved with Bi–TiO_2 as photocatalyst in 6 h with dose of 2 g/L at pH 6. With the same catalyst under UV light, only 48% degradation was observed. Therefore, the photogenerated electrons in the excited IBP molecules have sufficient energy to produce the superoxide ion and hydroxyl radicals under solar irradiation. Hence it can be said that doping of catalyst with metal ions can reduce the power consumption as the absorbance spectra get shifted in visible region, therefore sunlight can be used as a cost effective source of irradiation.

4. Conclusion

The photocatalytic degradation of IBP has been studied in presence of doped catalyst under solar irradiations. Bi–TiO_2 nanoparticles exhibited higher photocatalytic activity when compared to Ni–TiO_2 and Degussa TiO_2 during the degradation of IBP. The highest BET surface area of Bi–TiO_2 (0.25 wt%) was found to be 47.8 m^2/g with crystalline size of 12.4 nm. A maximum of 89% IBP degradation was achieved with 0.25 wt% Bi–TiO_2 photocatalyst under 6 h illuminations with a solar light when compared to Ni–TiO_2 wherein, only 78% degradation was achieved under same experimental condition. Among various Ni-doped TiO_2 materials, the one doped with 0.5 wt% Ni showed the highest photocatalytic activity for Ibuprofen (IBP) degradation under solar light. The orders of photocatalytic degradation of IBP with different catalyst was observed to be in the order as Bi–TiO_2 > TiO_2 > Ni–TiO_2 with rate constants as 0.0064 min^{-1}, 0.0046 min^{-1}, 0.0043 min^{-1}, respectively.

References

[1] A. Achilleos, E. Hapeshi, N.P. Xekoukoulotakis, D. Mantzavinos, D. Fatta-Kassinos, UV-A and solar photodegradation of ibuprofen and carbamazepine catalyzed by TiO_2, Sep. Sci. Technol. 45 (2010) 1564–1570.
[2] N.S. Begum, H.M.F. Ahmed, K.R. Gunashekar, Effects of Ni doping on photocatalytic activity of TiO_2 thin films prepared by liquid phase deposition technique, Bull. Mater. Sci. 31 (2008) 747–751.
[3] M.A. Barakat, H. Schaeffer, G. Hayes, S. Ismat-Shah, Photocatalytic . . . metal ions in photocatalytic systems, Appl. Catal. B Environ. 57 (2004) 23–30.
[4] S.H. Chuang, M.L. Hsieh, S.C. Wu, H.C. Lin, T.S. Chao, T.H. Hou, Fabrication and characterization of high-k dielectric nickel titanate thin films using a modified sol–gel method, J. Am. Ceram. Soc. 94 (2011) 250–254.
[5] J. Choina, H. Kosslick, C. Fischer, G.U. Flechsig, L. Frunza, A. Schulz, Photocatalytic decomposition of pharmaceutical ibuprofen pollutions in water over titania catalyst, Appl. Catal. B: Environ. 129 (2013) 589–598.
[6] J.B. Halling-Sorensen, S. Nors Nielsen, P.F. Lanzky, F. Ingerslev, H.C. HoltenLiitzhofl, S.E. Jorgensen, occurrence, fate and effects of pharmaceutical substances in the environment—a review, Chemosphere 36 (1998) 357–393.
[7] T. Ji, F. Yang, Y. Lv, J. Zhou, J. Sun, Synthesis and visible light photocatalytic activity of Bi-doped TiO_2 nanobelts, Mater. Lett. 63 (2009) 2044–2046.
[8] Y.J. Lin, Y.H. Chang, W.D. Yang, B.S. Tsai, Synthesis and characterization of ilmenite $NiTiO_3$ and $CoTiO_3$ prepared by a modified Pechini method, J. Non-Cryst. Solids 352 (2006) 789–794.
[9] K.P. Lopes, L.S. Cavalcante, A.Z. Simoes, J.A. Varela, E. Longo, E.T. Leite, NiTiO3 powders obtained by polymeric precursor method: synthesis and characterization, J. Alloys Compd. 468 (2009) 327–332.
[10] C. Martínez, L.M. Canle, M.I. Fernández, J.A. Santaballa, J. Faria, Kinetics and mechanism of aqueous degradation of carbamazepine by heterogeneous photocatalysis using nanocrystalline TiO_2, ZnO and multi-walled carbon nanotubes-anatase composites, Appl. Catal. B: Environ. 102 (2011) 563–571.
[11] S.A.S. Melo, A.G. Trovo, I.R. Bautitz, R.F.P. Nogueira, Degradation of residual pharmaceuticals by advanced oxidation processes, Quím. Nova 32 (2009) 188–197.
[12] F. Mendez-Arriagad, R.A. Torres-Palma, C. Petriera, S. Esplugasd, J. Gimenezd, C. Pulgarin, Mineralization enhancement of a recalcitrant pharmaceutical pollutant in water by advanced oxidation hybrid processes, Water Res. 43 (2009) 3984–3991.
[13] B. Neppolian, H.C. Choi, S. Sakthivel, B. Arabindoo, V. Murugesan, Solar/UV-induced photocatalytic degradation of three commercial textile dyes, J. Hazard. Mater. 89 (2002) 303–317.
[14] H. Pouretedal, A. Norozi, M.H. Keshavarz, A. Semnani, Nanoparticles of zinc sulfide doped with manganese, nickel and copper as nanophotocatalyst in the degradation of organic dyes, J. Hazard. Mater. 162 (2009) 674–681.
[15] S. Rengraj, X.Z. Li, P.A. Tanner, Z.F. Pan, G.K.H. Pang, Photocatalytic degradation of methylparathion—an endocrine disruptor by Bi_3^+ doped TiO_2, J. Mol. Chem. A: Chem. 247 (2006) 36–43.
[16] J.L. Santos, L. Aparicio, E. Alonoso, Occurrence and risk assessment of pharmaceutically active compounds in waste water treatment plants a case study: seville city(Spain), Environ. Int. 33 (2007) 596–601.
[17] T. Sreethawong, Y. Suzuki, S. Yoshikawa, Photocatalytic evolution of hydrogen over mesoporous TiO_2 supported NiO_2 photocatalyst prepared by single-step sol–gel process with surfactant template, Int. J. Hydrogen Energy 30 (2005) 1053–1062.
[18] J.W. Tang, Z.G. Zou, J.H. Ye, Efficient photocatalytic decomposition of organic contaminants over $CaBi_2O_4$ under visible-light irradiation, Angew. Chem. Int. 43 (2004) 4463–4466.
[19] R. Torres, V. Sarria, W. Torres, P. Peringer, C. Pulgarin, Electrochemical treatment of industrial wastewater containing 5-amino-6-methyl-2-benzimidazolone: toward and electrochemical–biological coupling, Water Res. 37 (2003) 7–13.
[20] Y. Wang, Y. Hao, H. Cheng, Photoelectrochemistry of transition metal-ion-doped TiO_2 nanocrystalline electrodes and higher solar cell conversion efficiency based on Zn_2^+-doped TiO_2 electrode, J. Mater. Sci. 34 (1999) 2773–2779.
[21] J. Wang, L. Jing, L. Xue, Y. Qu, H. Fu, Enhanced activity of bismuth-compounded TiO_2 nanoparticles for photocatalytically degrading rhodamine B solution, J. Hazard. Mater. 160 (2008) 208–212.
[22] X.H. Xu, M. Wang, Y. Hou, W.F. Yao, D. Wang, H. Wang, Preparation and characterization of Bi-doped TiO_2 photocatalyst, J. Mater. Sci. Lett. 21 (2002) 1655–1656.
[23] J. Yu, S. Liu, Z. Xiu, W. Yu, G. Feng, Combustion synthesis and photocatalytic activities of Bi_3^+-doped TiO_2 nanocrystals, J. Alloys Compd. 461 (2008) 17–19.
[24] D. Wang, Y. Duan, Q. Luo, X. Li, J. An, L. Baoa, L. Shi, Novel preparation method for a new visible light photocatalyst: mesoporous TiO2 supportedAg/AgBr, J. Mater. Chem. 22 (2012) 4847–4854.
[25] F.S. Braz, M.R.A. Silva, F.S. Silva, S.J. Andrade, A.L. Fonseca, M.M. Kondo, Photocatalytic degradation of ibuprofen using TiO2 and ecotoxicological assessment of degradation intermediates against *Daphnia similis*, J. Environ Prot. 5 (2014) 620–626.

Journal of Photochemistry and Photobiology A: Chemistry 332 (2017) 182–187

Contents lists available at ScienceDirect

Journal of Photochemistry and Photobiology A: Chemistry

journal homepage: www.elsevier.com/locate/jphotochem

Enhanced photocatalytic degradation of atenolol using graphene TiO_2 composite

Vibhu Bhatia[a], Ghodsieh Malekshoar[b], Amit Dhir[a], Ajay K Ray[b,*]

[a] School of Energy & Environment, Thapar University, Patiala, 147004, India
[b] Department of Chemical & Biochemical Engineering, University of Western Ontario, London, ON N6A 3K7, Ontario, Canada

ARTICLE INFO

Article history:
Received 23 December 2015
Received in revised form 13 July 2016
Accepted 28 August 2016
Available online 29 August 2016

Keywords:
Photocatalysis
Graphene
Hydrothermal method
Atenolol
Pharmaceuticals

ABSTRACT

Graphene oxide-TiO_2 (TiO_2-G) composite synthesized by a facile route is able to exhibit significantly higher photocatalytic activity under visible light irradiation. The prepared composite was characterized by means of powder X-ray diffraction (XRD), Scanning electron microscopy (SEM), energy-dispersive X-ray spectrometry (EDS), UV–vis diffuse reflectance spectroscopy (DRS), and Brunauer Emmett Teller (BET). The photocatalytic activity was evaluated by photo-degradation of the Atenolol (ATL) as model pharmaceutical pollutant under UV–vis light and "simulated Sun" irradiation conditions. The results showed that TiO_2-G exhibited much higher photocatalytic performance than that of bare TiO_2. The enhanced activity can be ascribed to the incorporation of graphene. The effect of various factors such as variation of pH, catalyst concentration, initial substrate concentration, light intensity, and source of light as well as reaction kinetics were investigated. The results showed that 72% degradation of ATL (25 ppm) can be achieved with 1.5 g/L TiO_2-G in 1 h under solar irradiation. Complete TOC removal for atenolol degradation was obtained in 7 h. The work is expected to shed new light on the development of graphene composite nanostructures for gathering visible light energy and on the improvement of new photocatalytic materials for the exclusion of environmental pollutants.

1. Introduction

In the early 1980s the active pharmaceutical ingredients (APIs) are identified in the water stream [1]. An emerging environmental issue includes the presence of pharmaceutical compounds in surface water and offers a challenge to water treatment systems [2]. Pharmaceuticals are basically designed so that they can physiologically effect humans and animals even at low concentrations. These compounds remain in the environment for a long time and are not degraded biologically or by natural reduction [3]. The APIs consumed by the patients are excreted either as metabolites or as the unchanged main compounds. Beta blockers are involved in treatment of various of cardiovascular diseases such as hypertension, artery disease etc., by blocking the action of hormones such as epinephrine and norepinephrine in the body [4]. Due to its limited human metabolism and extensive usage, ATL was widely detected in sewage effluents and surface water, usually with a concentration ranging from ng/L to μm/L [5,6]. The studies also concluded that 2.2–50.8 g/d is the daily output loads of the ATL compound in the treated wastewater.

For the treatment of these pharmaceutical compounds, Conventional wastewater treatment methods such as use of activated sludge [7] is not effective. Furthermore, many studies have reported that the growth of human embryonic cells could been inhibited by ATL and was also found to be ecotoxic to freshwater species [8]. It has also been found that ATL possesses phytotoxic activity during its chlorination after the process of wastewater disinfection [9]. Therefore, it is need of an hour to develop the advanced treatment technologies for ensuring complete removal of ATL from wastewater before release into water stream. Recently, it has been reported in several studies that advanced oxidation processes (AOPs) are used for the degradation of beta-blockers [10–14]. Oxidation of organic and inorganic species can achieved by heterogeneous photocatalysis [15,16].

Composites consisting of carbonaceous materials have been studied, in order to further improve the photocatalytic efficiency. In particular, to take advantage of graphene's superior properties, many efforts have been devoted through coupling it with semiconductors. Graphene has a two-dimensional sp^2 hybridized carbon network [17,18]. Its unique properties include large specific surface area (2600 m^2/g), high thermal conductivity (3000 W/m/K), and high

* Corresponding author.
E-mail address: aray@eng.uwo.ca (A.K. Ray).

http://dx.doi.org/10.1016/j.jphotochem.2016.08.029
1010-6030/

intrinsic electron mobility (15,000 m^2/V/s) [20]. Therefore, to form a hybrid structure with different nanomaterials for photocatalytic applications it is highly advantageous and desirable to explore its potential. Several graphene-semiconductor composites have been reported in literature using either growing on surfactants or by physical mixing of pre-synthesized nanoparticles and graphene [19–22]. Recently, it has been studied that methylene blue in an aqueous solution has been degraded by photocatalysis using TiO_2-graphene based photocatalyst [19].

As a novel material, many extraordinary properties has been observed for graphene, such as it is chemically stable, having high specific surface area (~2600 m^2/g), tremendous motion of charge carriers (20,000 cm^2/V/s) and worthy optical transparency [23–25]. On the basis of above described properties, the graphene can leads to charge separation and function when used as an electron carrier in composite materials, thus composites of graphene and TiO_2 have shown enhancement of photocatalytic activity in different studies [26–28].

Several reports are published for the photocatalytic degradation of organic molecules by enhancements in photocatalytic activity of TiO_2 nanoparticle-reduced graphene composites. Zhang et al. and co-workers [29–31] have reported increased photocatalytic degradation of methylene blue by preparing a Graphene-TiO_2 nanoparticle composite. Xiaoyan et al. [32] studied the production of H_2 by splitting of water using TiO_2 nanoparticles on graphene and observed enhanced photocatalytic activity than that of only TiO_2.

The present work includes the degradation of atenolol via synthesized Graphene Oxide-TiO_2 (GO-TiO_2) and DegussaTiO_2 photocatalyst and different parameters has been studied, including catalyst loading, initial substrate concentration, variation of light intensity, pH of the solution, and introduction of UV filter in solar simulator on the atenolol degradation. The new features of this study include the interpretation of the kinetics of the atenolol removal with GO-TiO_2 and Degussa TiO_2 during photocatalysis. Adding to this, to the authors' knowledge, this is the first study that comprises a well-organized exploration of the various parameters that can affect the oxidation process of the model compound including the catalyst concentration, initial substrate concentration, variation of light intensity and pH using GO-TiO_2 and its comparison with commercial available Degussa TiO_2.

2. Experimental section

2.1. Materials

Atenolol (its chemical structure is shown in Fig. 1) was procured from Sigma-Aldrich and was used as such without further purification. Solutions of the ATL was prepared in deionized water at concentrations up to 25 mg/L and stirred for one 1 h to ensure complete mixing. Such concentrations, more than those usually found in water, were taken so as to (a) assess the efficiency of process within a measurable time period, and (b) accurately determining the remaining concentration of ATL with the analytical techniques employed in this work. Commercially available TiO_2 was employed by Aeroxide P25.

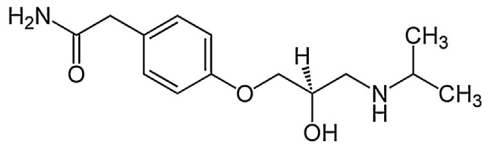

Fig. 1. Structure of Atenolol.

2.2. Synthesis of graphene – TiO_2 composite

To obtain graphite oxide (GO) from graphite powder, modified Hummers method was applied as described previously [33]. To obtain graphene-TiO_2 composite, 2 mg of GO was poured to a solution of water and ethanol (2:1) followed by ultrasonic treatment of 1 h. Then weighed amount of TiO_2 (200 mg) was added and further stirring was done for 2 h. The mixture was then transferred to a Teflon-lined autoclave, for the hydrothermal treatment process for 3 h at 120 °C. During this process, GO could be reduced to graphene and simultaneously the deposition of TiO_2 achieved. The obtained composites were centrifuged, rinsed with deionized water, and vacuum-dried at 60 °C. The prepared samples are denoted as GO-TiO_2.

2.3. Characterization

X-ray diffraction (XRD) patterns were obtained on a Rigaku-Ultima IV Advance X-ray diffraction meter using Cu Kα radiation (λ = 0.15 Å). The microstructures of the samples were analyzed by a Hitachi S-4500 scanning electron microscope (SEM) and transmission electron microscopy (TEM; JEOL 2010F). UV–vis diffuse reflectance spectra (DRS) were measured using a UV–vis spectrophotometer (UV-3600, Shimadzu). Raman spectroscopy was performed on a Renishaw Raman spectrometer Model 2000 using a 632.8 nm laser at 100% power. The X-ray photoelectron spectroscopic (XPS) analyses was done with a Kratos Axis Ultra spectrometer with a monochromatic Al Kα source (15 mA, 14 kV).

2.4. Photocatalytic measurement

Experiments of Photocatalysis were carried out as follows: Appropriate amount of photocatalyst in the range 0.5–2.0 g/L was added to 150 mL of an aqueous solution and was allowed to mix and poured into the reactor. Further, continuous mixing was done with magnetic stirrer at 800 rpm for 45 min in the dark to ensure complete adsorption of the ATL molecule on the surface of catalyst. Simulated Air Mass (AM) 1.5 solar light was produced by means of a solar simulator (model SS1KW, Sciencetech, Ontario, Canada, with a 1000 W Xe arc lamp and an AM 1.5G filter). During the photocatalytic experiments, the reaction mixture was continuously aerated. Samples were withdrawn after fixed interval of time and filtered through a 0.45 μm filter to separate catalyst particles. pH of the ATL solution were varied from 4, 6, 8 and 9.

2.5. Analytical technique

The absorbance of the sample was measured with a UV–vis spectrophotometer. Absorbance was measured at 224 nm for photocatalytic experiments, as this wavelength agrees to the characteristic peak of the ATL in the UV spectrum. The straight line curve has been obtained between absorbance and concentration with ATL concentration ranging from 5 to 25 mg/L.

3. Results and discussion

3.1. Characterization of graphene oxide – TiO_2 composite

The characterization of synthesized catalyst includes XRD, SEM, TEM, XPS and UV-DRS, which has been described and explained in details elsewhere [33]. The BET specific surface area (54–70 m^2/g) and pore volume (0.25–0.38 mL/g) of the Graphene-TiO_2 composite were controlled by graphene compared with those of TiO_2. The pore diameter (~3 nm) was quite uniform. The BET surface area of the Graphene-TiO_2 composite increased from 54 to 73 m^2/g with increasing graphene content. This result can be ascribed to the

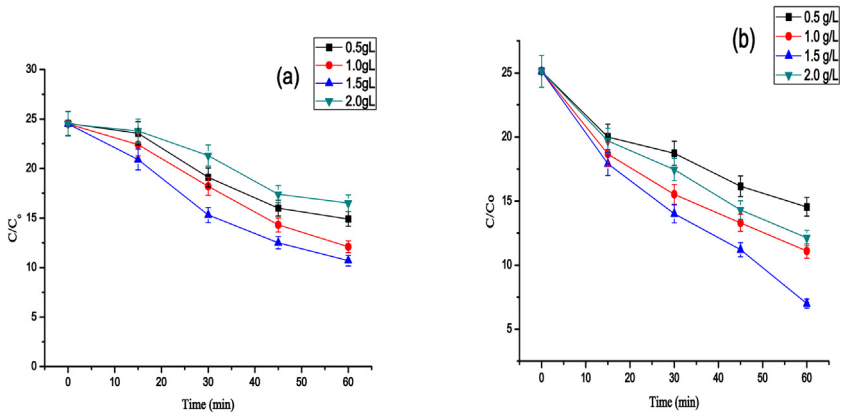

Fig. 2. Effect of catalyst loading on photocatalytic degradation of Atenolol. (a) Degussa P25 TiO_2. (b) TiO_2-Graphene (TiO_2-G). Experimental conditions: $[ATL]_0 = 25$ ppm, pH = 6, I = 750 mW/cm^2).

fraction of bare graphene in the composites. However, the BET surface area of the Graphene-TiO_2 composite was still quite low compared with that of pure graphene (2600 m^2/g). This is due to the minimal doping level of graphene and thus, surface area and porosity are primarily dominated by the TiO_2 component.

3.2. Effect of catalyst concentration

The concentration of catalyst has been varied from 0.5 to 2.0 g/L, to study effect on oxidation with initial substrate concentration of 25 mg/L and the results are depicted in Fig. 2(a) and (b). The figure clearly shows that with increase in catalyst concentration up to a certain value, the initial reaction rate increases. However, further increase results in reduced rates. It has been analyzed that the availability of active sites on catalyst surface for photocatalytic reactions rises with increase in catalyst loading and this take place up to a point where all catalyst particles are wholly lightened [34]. At higher concentrations, penetration of light get hindered and even reflected (scattered) due to a screening (light shielding) of surplus particles, thus covering portion of the photosensitive (active) area. Subsequently, these reductions of photons lead the rate of transformation to a plateau or even to decrease. It has been observed that 72% degradation has been achieved using TiO_2-G with concentration of 1.5 g/L whereas 56% degradation has been achieved using Degussa P25 as catalyst with 1.5 g/L catalyst dose in 1 h.

3.3. Effect of initial substrate concentration

The concentration of ATL has been varied from 5 to 25 mg/L in the experiment at catalyst loading of 1.5 gm/L and the results are depicted in Fig. 3(a) and (b). As can be seen, atenolol conversion is 85%, 79%, 71%, 63% and 57% using Degussa TiO_2 while 92%, 86%, 81%, 77% and 72% for TiO_2-G after 60 min at initial concentration of 5 mg/L, 10 mg/L, 15 mg/L, 20 mg/L and 25 mg/L respectively. From figures it can be analyzed that as there is increase in the ATL concentration, the photocatalytic rate decreases. With increase in the concentration of ATL, more and more molecules of model compound are adsorbed on the catalyst surface. In compare, because of same reaction conditions, the presence of $OH^\bullet$ and $O_2^{\bullet-}$ radicals attacking the atenolol molecules declines, due to this the photocatalytic degradation decreases. As found in several studies, that huge amount of reactive species are required for the degradation of pollutant if the concentration of target pollutant is high because many molecules of the model compound adsorbed on the photocatalyst surface. So as the formation of $OH^\bullet$ and $O_2^{\bullet-}$ remains constant on the catalyst surface at a constant reaction conditions. Therefore, the $OH^\bullet$ radicals are not sufficient for the

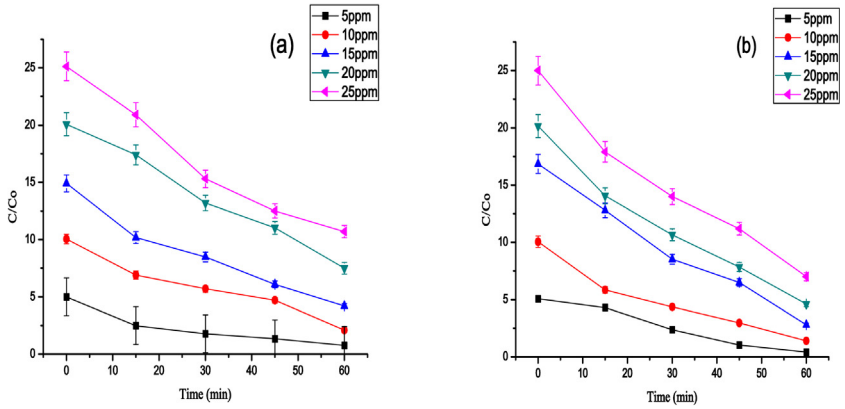

Fig. 3. Effect of Initial concentration on photocatalytic degradation of Atenolol. (a) Degussa P25 TiO_2. (b) TiO_2-Graphene (TiO_2-G). Experimental conditions: pH = 6, I = 750 mW/cm^2, [Catalyst] = 1.5 g/L.

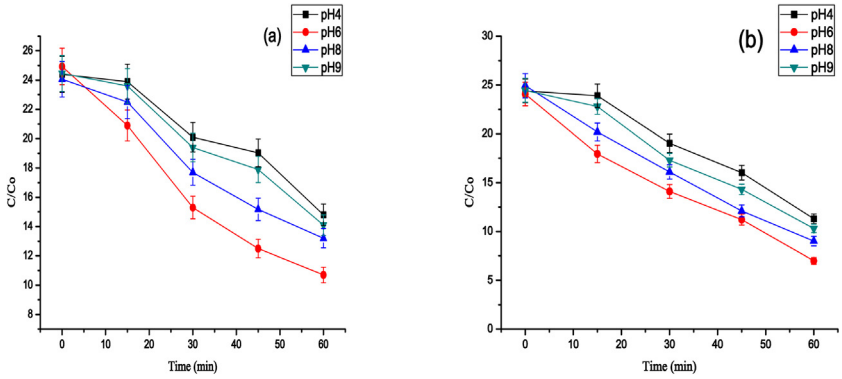

Fig. 4. Effect of pH on photocatalytic degradation of Atenolol. (a) Degussa P25 TiO_2. (b) TiO_2-Graphene (TiO_2-G). Experimental conditions: $[ATL]_0 = 25$ mg/L, I = 750 mW/cm^{2,} [Catalyst] = 1.5 g/L.

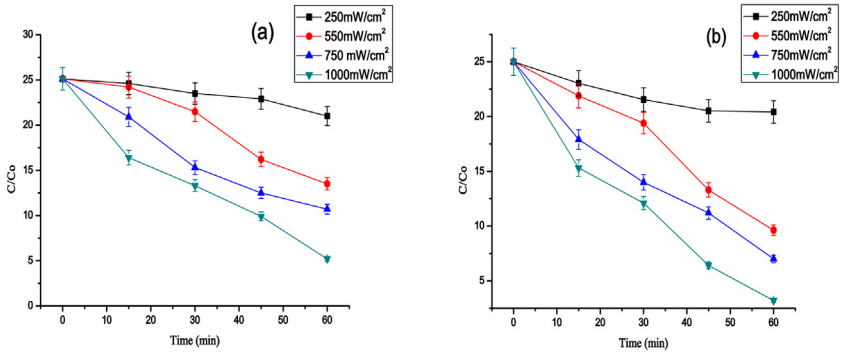

Fig. 5. Effect of Light Intensity on photocatalytic degradation of Atenolol. (a) Degussa P25 TiO_2. (b) TiO_2-Graphene (TiO_2-G). Experimental conditions: [ATL]0 = 25 mg/L, [Catalyst] = 1.5 g/L, pH = 6.

degradation of pollutant at greater concentrations, which ultimately results in decrease in the degradation rate of pollutant as the concentration increases [35].

3.4. Effect of pH

pH of the solution was varied to study its effect for degradation of atenolol. The natural pH of atenolol solutions (25 ppm) was 9 and it was varied from 4 to 9 using the required amount of NaOH or HCl solutions, respectively. Fig. 4(a) and (b) shows the photocatalytic conversion of atenolol at different pH values. pH of the ATL solution was varied in range, showing that degradation was observed maximum at pH 6 but decreased both in acidic and alkaline conditions. For illustration, the degradation of atenolol after 1 h of reaction was 60%, 72%, 63% and 57% at pH 4, 6, 8 and 9 using TiO_2-G respectively. For Degussa TiO_2, the observed conversions are 39%, 56%, 45% and 42% at pH 4, 6, 8 and 9, respectively. Atenolol has two reactive sites, (a) an aromatic ring and (b) an amine-moiety. The pH of the solution affects the reaction of amine-moiety, while it does not affect the reaction of the aromatic ring. Therefore, the degradation reaction of atenolol depends on the pH of the solution and also on the pK_a of the amines (which is 9.6). Due to protonation of amino group at 9.6 > pH > 6 the

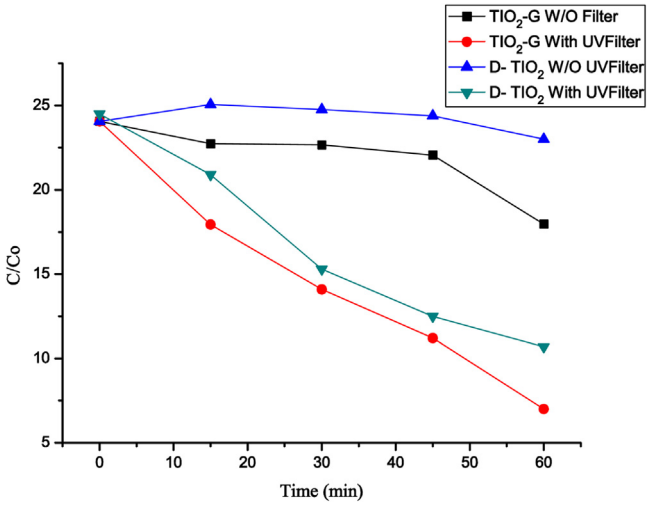

Fig. 6. Effect of Light source on photocatalytic degradation of Atenolol. Experimental conditions: $[ATL]_0 = 25$ mg/L, [catalyst] = 1.5 g/L, pH = 6, I = 750 mW/cm^2.

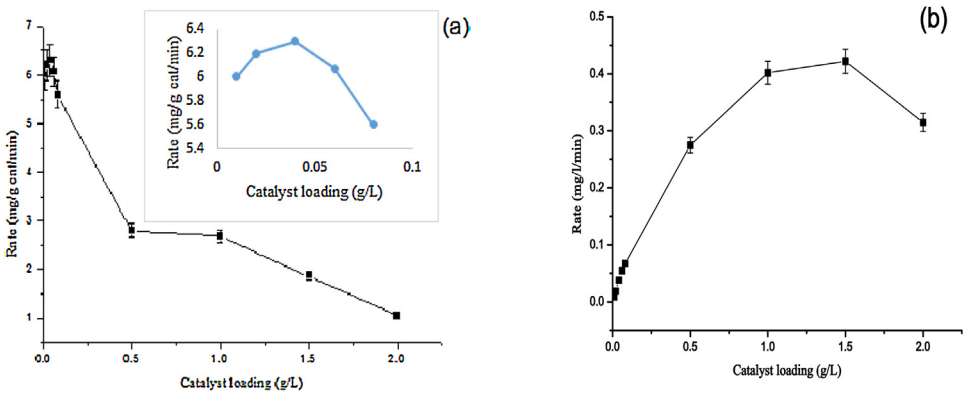

Fig. 7. Distinguishing Kinetic regimes for degradation of Atenolol. Experimental conditions: $[ATL]_0 = 25$ ppm, pH = 6, I = 750 mW/cm^2) (a) Rate plotted as mg/gcat/min. (b) Rate plotted as mg/l/min.

surface of catalyst get negatively charged. Thus, the electrostatic attraction of TiO_2 surface with atenolol seems to be increased.

3.5. Variation of light intensity

The effect of light intensity on the photocatalytic degradation rate of Atenolol was analyzed by keeping all other variables constant. The light intensity has been varied from 250 to 1000 W. The observed results are shown graphically in Fig. 5(a) and (b). The observation shows that degradation rate increases for ATL with increase in light intensity. The cause for the above observation is the number of photons covering per unit area of the semiconductor increases, with increase in intensity of light. It has been observed that degradation rate of ATL molecules increases with increase in light intensity. This change in rate of degradation of ATL molecules by variation in light intensity is because of increase in the number of hydroxyl radicals and super oxide ions ($O_2^{\bullet -}$) with increase in light intensity that resulted in increase in number of photons that can reach the active site of catalyst so number of exited catalyst molecules increases and hence rate of degradation of ATL molecules also increase.

3.6. Effect of variation of light source

The light source has been varied using solar simulator with UV filter and without UV filter. It has been observed from Fig. 6 that without using UV filter better rate of degradation was observed for atenolol at pH 6 within 1 h with 1.5 g/L catalyst dose. However, with incorporation of UV filter, the rate of degradation has been reduced much both in case of TiO_2-G and Degussa TiO_2.

3.7. Distinguishing kinetic regime from mass transfer limited regime by varying catalyst loading

Fig. 7 represents data of the experiments for the photocatalytic degradation rate of atenolol with different catalyst concentrations. The study have been done with catalyst concentration ranging from 0.01 to 2.0 g/L. The figure depicts that the degradation rate plotted as mol/gcat/min is almost constant (independent of catalyst loading) for catalyst concentration between 0.01 and 0.08 g/L. Thereafter, degradation rate decreases as the amount of catalyst is increased from 0.08 to 2.0 g/L. In the range of 0.01–0.08 g/L, reaction kinetics control the overall rate as with the increase in concentration of catalyst (in g of catalyst), the conversion (in mol/min) is increased in equal proportion resulting in rate (expressed as mol/gcat/min) to remain constant. All available surface area with increase of catalyst amount is available for reaction. The overall rate starts decreasing, when the catalyst loading is increased beyond 0.08 g/L, In this region, all theoretical surface area that should be available for reaction with increased catalyst amount is in fact is not available due to particle agglomeration. Hence, in this part, the observed rate is not completely due to kinetics but is limited due to transport of pollutant to the active sites. In this transport-limited region, the transformation enhances proportionately at a slower rate than the increase of the amount of catalyst, thereby, the overall rate decreases instead of remaining constant. In other words, different factors influence the conversion in this region, such as (a) complete catalyst surface area might not come in contact with a pollutant because of external mass-transfer resistance, (b) because of shielding effect of light, it cannot extent to some of the catalyst surface area and (c) light cannot activate the inner surfaces and penetrate in the agglomerates. Thus, Fig. 7 show two regimes: (1) the kinetic regime at the low catalyst range (<0.08 g/L) and (2) the transport (mass or light) limitation regime at the high catalyst concentration (0.08–2.0 g/L).

3.8. Kinetics of TOC disappearance

The complete mineralisation is confirmed from total organic carbon (TOC) content as given in Fig. 8. For atenolol concentration of 25 ppm, it has been observed that TOC has fully disappeared in 7 h. TOC value decrease with increase in irradiation time. The initial

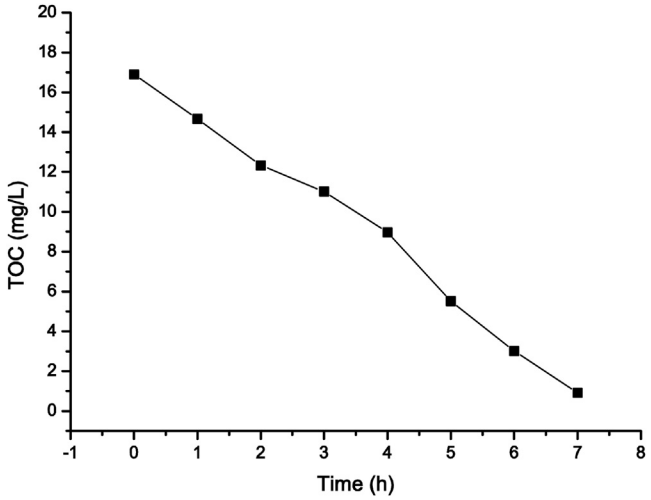

Fig. 8. TOC for Atenolol degradation.
Experimental conditions: $[ATL]_0 = 25$ ppm, pH = 6, $[TiO_2\text{-G}] = 1.5$ g/L, I = 750 mW/cm^2.

TOC of atenolol solution is obtained as 16.9 mg/L and it has been disappeared totally within 7 h of irradiation time. As all the residual carbon-containing metabolites is taken into account in TOC so it seems to be right technique for valuing the decontamination of polluted water.

4. Conclusions

TiO_2-G composite was prepared by simple hydrothermal method. The improved performance of synthesized composite has been observed in photocatalytic degradation of Atenolol under simulated solar illumination. More adsorption sites are facilitated by incorporation of graphene in photocatalyst and electron-hole pairs separation also enhances, and extension of the light absorption wavelength range has been obtained. In addition, the parametric study was carried out to optimize the reaction conditions. Experimental results showed that 1 h of 750 W/cm^2 solar irradiation was required to degrade 72% of 25 ppm Atenolol solution at pH 6, when 1.50 g/L of TiO_2-G composites was used. Complete TOC removal has been obtained in 7 h for Atenolol degradation. When the results found in this study are further compared with published results for photocatalytic atenolol degradation, it can be concluded that there is great potential for graphene-based composites for higher photocatalytic activity.

References

[1] M.L. Richardson, J.M. Bowron, J. Pharm. Pharmacol. 37 (1985) 1.
[2] K. Ikehata, N.J. Naghashkar, M.G. Ei-Din, Ozone Sci. Eng. 28 (2006) 353.
[3] M. Klavarioti, D. Mantzavinos, D. Kassinos, Environ. Int. 35 (2009) 102.
[4] M. Maurer, B.I. Escher, P. Richle, C. Schaffner, A.C. Alder, Water Res. 41 (2007) 1614.
[5] A.C. Alder, C. Schaffner, M. Majewsky, J. Klasmeier, K. Fenner, Water Res. (2010) 936.
[6] D.B. Huggett, I.A. Khan, C.M. Foran, Environ. Pollut. 121 (2003) 199.
[7] N. Paxeus, Water Sci. Technol. 50 (2004) 253.
[8] M. Della-Greca, M.R. Iesce, P. Pistillo, L. Previtera, F. Temussi, Chemosphere 74 (2009) 730.
[9] E. Hapeshi, A. Achilleos, M.I. Vasquez, Water Res. 44 (2010) 1737.
[10] W.H. Song, W.J. Cooper, S.P. Mezyk, J. Greaves, B.M. Peake, Environ. Sci. Technol. 42 (2008) 1256.
[11] R. Andreozzi, L. Campanella, B. Fraysse, J. Garric, A. Gonnella, R. Lo Giudice, R. Marotta, G. Pinto, A. Pollio, Water Sci. Technol. 50 (2004) 23.
[12] T.A. Ternes, M. Meisenheimer, D. McDowell, F. Sacher, H.J. Brauch, B.H. Gulde, G. Preuss, U. Wilme, N.Z. Seibert, Environ. Sci. Technol. 36 (2002) 3855.
[13] T.A. Ternes, J. Stuber, N. Herrmann, D. McDowell, A. Ried, M. Kampmann, B. Teiser, Water Res. 37 (2003) 1976.
[14] C. Medana, P. Calza, F. Carbone, E. Pelizzetti, H. Hidaka, C. Baiocchi, Rapid Commun. Mass Spectrom. 22 (2008) 301.
[15] T.E. Doll, F.H. Frimmel, Catal. Today 101 (2005) 195.
[16] P. Calza, V.A. Sakkas, C. Medana, C. Baiocchi, A. Dimou, E. Pelizzetti, T. Albanis, Appl. Catal. B—Environ. 67 (2006) 197.
[17] X. Zhang, Y. Tang, Y. Li, Y. Wang, X. Liu, C. Liu, S. Luo, Appl. Catal. A 457 (2013) 78.
[18] Y. Liu, Y. Hu, M. Zhou, H. Qian, H. Xiao, Appl. Catal. B 125 (2012) 425.
[19] H. Zhang, X. Lv, Y. Li, Y. Wang, J. Li, ACS Nano 4 (2010) 380.
[20] Y. Liang, H. Wang, H.S. Casalongue, Z. Chen, H. Dai, Nano Res. 3 (2010) 701.
[21] W. Fan, Q. Lai, Q. Zhang, Y.J. Wang, Phys. Chem. C 115 (2011) 10694.
[22] J. Zhang, Z. Xiong, X.S. Zhao, J. Mater. Chem. 21 (2011) 3634.
[23] A.K. Geim, K.S. Novoselov, Nat. Mater. 6 (2007) 183.
[24] S. Park, K.S. Lee, G. Bozoklu, W. Cai, S.T. Nguyen, R.S. Ruoff, ACS Nano 2 (2008) 572.
[25] O. Akhavan, E.J. Ghaderi, Chem. C 113 (2009) 20214.
[26] H. Zhang, X.J. Lv, Y.M. Li, Y. Wang, J.H. Li, ACS Nano 4 (2010) 380.
[27] H. Kim, G. Moon, D. Monllor-Satoca, Y. Park, W.J. Choi, Phys. Chem. C 116 (2012) 1535.
[28] Y.H. Ng, A. Iwase, N.J. Bell, A. Kudo, R. Amal, Catal. Today 164 (2011) 353.
[29] Y. Zhang, Z.R. Tang, X. Fu, Y.J. Xu, ACS Nano 4 (2010) 7303.
[30] X. Lin, F. Rong, X. Ji, D.J. Fu, Sol-Gel Sci. Technol. 59 (2011) 283.
[31] G. Williams, B. Seger, P. Kamt, ACS Nano 2 (2008) 1487.
[32] X. Zhang, Y. Sun, X. Cui, Z. Jiang, Int. J. Hydrog. Energy 37 (2012) 811.
[33] G. Malekshoar, K. Pal, Q. He, A. Yu, A.K. Ray, Ind. Eng. Chem. Res. 53 (2014) 18824.
[34] L. Yang, L.E. Yu, M.B. Ray, Water Res. 42 (2008) 3480.
[35] W. Bahnemann, M. Muneer, M.M. Haque, Catal. Today 124 (2007) 133.

Separation and Purification Technology 161 (2016) 1–7

Contents lists available at ScienceDirect

Separation and Purification Technology

journal homepage: www.elsevier.com/locate/seppur

Enhanced photocatalytic degradation of ofloxacin by co-doped titanium dioxide under solar irradiation

Vibhu Bhatia [a], Ajay K. Ray [b,*], Amit Dhir [a]

[a] School of Energy and Environment, Thapar University, Patiala, India
[b] Department of Chemical & Biochemical Engineering, University of Western Ontario, London, ON N6A 3K7, Canada

ARTICLE INFO

Article history:
Received 9 September 2015
Received in revised form 20 January 2016
Accepted 21 January 2016
Available online 22 January 2016

Keywords:
Ofloxacin
Photocatalytic degradation
Nanoparticles
Co-doping

ABSTRACT

The photocatalytic degradation of Ofloxacin (OFL) was studied in aqueous solution using co-doped TiO_2 nanoparticles. The catalyst samples were synthesized by sol–gel method from Titanium isopropoxide using different concentration of Bi and Ni metal as dopant. The co-doped catalysts were characterized by (X-ray Diffraction) XRD, (Brunauer–Emmett–Teller) BET, (Scanning electron microscope) SEM and (Energy Dispersive Spectroscopy) EDS. The results revealed that the catalyst possessed spherical morphology and excellent crystalline properties. The surface area of the catalyst was found to be 74, 55 and 18.66 m^2/g for 0.25 wt%, 0.5 wt% and 1.0 wt% dopant concentration, respectively. Photocatalytic capability of Bi/Ni co-doped TiO_2 nanoparticles were estimated by means of OFL degradation under different light sources. Parameters affecting the photocatalytic process such as type of catalyst, dopant concentration, catalyst concentration, different light sources and solution pH have been explored. The photo-degradation kinetics follows a pseudo first-order reaction. Bi–Ni co-doped TiO_2 showed higher activity for photocatalytic degradation of OFL under solar light compared to Degussa TiO_2. The photo-degradation process was optimized using 25 mg/L Ofloxacin with dopant concentration of 0.25 wt% and catalyst dose of 1.5 g/L. Degradation efficiency of 86% was attained at pH 3 after 6 h of solar irradiations.

1. Introduction

The occurrence of antibiotics in the environment is an emerging environmental issue causing the selection of antibiotic-resistant microbes in wastewater treatment plants and other hot-spots with genes capable of spreading by the lateral gene transfer mechanism [1,2]. The decrease of biodegradation of leaf and other plant materials, the primary food source for freshwater biota, due to the release of antibiotics to the environment is a new relevant concern as well [3]. The investigation of the processes that may enhance their removal from water and wastewater and detoxification are in the core of scientific interest. Biotic (e.g., biodegradation) and abiotic processes (e.g., photocatalytic treatment and hydrolysis) are evaluated in order to understand the fate of antibiotics and the inherent risks they may pose to the environment. Aerobic biotransformation in the environment and during aerobic secondary treatment of wastewater has been identified as a removal mechanism for some antibiotics [4–6]. However, abiotic processes are considered to be the most important processes for their mineralization or for their transformation to more biodegradable products less persistent in the environment [7].

Among antibiotics, Ofloxacin (OFL) represents a synthetic fluoroquinolone antibiotic [8] of great environmental significance due to its widespread occurrence, its genotoxic properties [9] and persistence in the environment due to its limited microbial degradation potential [8]. The chemical structure and active sites of fluoroquinolones are presented in Fig. 1. They have been found in sewage treatment plants' influents and effluents, pharmaceuticals' production and hospital effluents, ground-, river-, sea and drinking water [10]. They are sorbed onto activated sludge, inhibiting the nitrite-oxidizing bacteria activity and making activated sludge a significant reservoir of fluoroquinolones due to their long-term cycling and persistence [11,12].

In particular, OFL is known to persist in sludge-treated soils in concentrations as high as few milligrams per kilogram [13] and has recently been characterized as a high hazard to the aquatic ecosystem due to the use of the sludge on agricultural land [14]. Some fluoroquinolones are subjected to biotransformation by fungi and bacteria to a lesser extent. The degradation of OFX induced by various AOPs at a bench scale has been investigated under different experimental conditions: photocatalysis in the presence of TiO_2 [15–17] solar Fenton [16], sono photocatalysis [18], photolysis

* Corresponding author.
E-mail address: aray@eng.uwo.ca (A.K. Ray).

http://dx.doi.org/10.1016/j.seppur.2016.01.028
1383-5866/

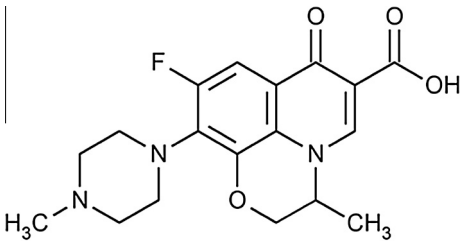

Fig. 1. Structure of Ofloxacin (pK_{a1} = 5.45, pK_{a2} = 6.2).

[19] and γ-radiolysis [20]. TiO_2 photocatalysis was also used by Michael et al. [16] to degrade 10 mg/L ofloxacin with catalyst concentration of 3 g/L. 60% degradation was obtained after 120 min of irradiation. Various methods available for the synthesis of TiO_2 photocatalyst include precipitation [21], hydrothermal, solvothermal [22], chemical vapor deposition [23] and electrospinning [24]. Among several methods available for synthesis of nanopowders, sol–gel method is advantageous because powders of high purity and of homogenous concentrations can be synthesized at very low temperature under stoichiometry control [25]. Kundu et al. [26] studied the photocatalytic activity of Ni-doped TiO_2 prepared by hydrothermal method for the degradation of ofloxacin (25 ppm) for which almost 70% degradation has been achieved with 1 g/L catalyst dose. It has been shown by earlier studies that degradation of compound is always better by co-doped catalyst compared to Degussa P25. The result of photocatalytic degradation of methylene blue indicated that photocatalytic activity of N- and S-codoped TiO_2 (98%) was better than P25 (82%) photocatalyst due to the band-gap of N-, S-codoped TiO_2 is lower than that of P25 photocatalyst [27]. Similarly I and F has been co-doped and appeared to be better photocatalyst for methylene blue degradation in comparison to Degussa P25 [28]. Hence, sol–gel method has been followed for the synthesis of Bismuth and Nickel co-doped TiO_2 (Bi/Ni–TiO_2) photocatalysts.

The photocatalytic transformation mechanisms of OFX through solar light oxidation using co-doped catalyst have not been studied earlier, even if studies involving to its environmental risks are described in the literature [29,30].

2. Materials and methods

2.1. Chemicals

Ofloxacin was purchased from Sigma Aldrich and were at least of analytical grade (⩾98%). Aeroxide P25 TiO_2 powder was used for the PC experiments. All the chemicals used in this study were of analytical grade and were used as such without further purification. Bi (NO_3), $5H_2O$ and Ni (NO_3), $5H_2O$ was purchased from Loba Chem, India. Titanium isopropoxide, as source of titanium dioxide, was purchased from Sigma Aldrich. Ethanol, used as solvent, was procured from Merck. All the solutions were prepared with deionized water. Fig 1 depicts structure of Ofloxacin.

2.2. Preparation of co-doped Bi/Ni–TiO_2 nano-catalyst

Co-doped TiO_2 with varying percentage of dopant (0.25–1.0 wt %) was prepared using sol–gel method with Titanium isopropoxide (TIP) as precursor. 2.5 mL of TIP was added drop by drop to a solution of 10 mL ethanol and 2.5 mL acetylacetone at room temperature and stirred for 30 min. Then 2 mL distilled water was added to above solution. Calculated amount of Bi (NO_3), $5H_2O$ and Ni (NO_3), $5H_2O$ was added according to percentage variation of dopant from 0.25 to 1.0 wt% respectively, into prepared solution and a stable sol was finally obtained after stirring 2 h. Then concentrated solution was placed at 90 °C for drying and dried powder was calcined at 400 °C for 2 h.

2.3. Characterization of synthesized catalyst

The above-prepared TiO_2 samples were characterized for microstructural properties by Scanning electron microscopy (Philips, SEM Analyzer). The Brunauer, Emmett and Teller (BET) surface area was obtained from nitrogen adsorption–desorption data (NOVA 2000e, USA). The chemical composition was confirmed using the electron spectroscopy for chemical analysis. The powder X-ray Diffraction (XRD) was done at room temperature using X-ray diffractometer (Cu Kα λ = 0.154 nm) to study the crystal phase of the products. X-ray Diffraction (XRD) patterns were obtained using a Philips X-ray diffractometer with monochromatic high-intensity in a 2θ range of 20–70°. All peaks measured by XRD analysis were allocated by comparing with those of JCPDS data. Band gap has been evaluated using UV–vis diffuse reflectance spectrophotophotometer of Hitachi U3900H at wavelength range of 190–800 nm. The average size of the TiO_2 particles was attained by Scherrer's equation (Eq. (1)).

$$D = K\lambda/\beta \mathrm{Cos}\,\theta \quad (1)$$

2.4. Experimental set-up

The degradation experiment of OFL was conducted on a self-designed, cubic, stainless steel reactor. An electric fan was installed on the side wall of the reactor for proper circulation of air. The seven UV Tubes, 36 W each with wavelength of 365 nm provided the light source. Weighed amount (0.5–2.0 g/L) of co-doped photocatalyst with dopant concentration ranging from (0.25–1.0 wt%) was well dispersed on a Pyrex glass dish (diameter 15 cm), which was placed into the reactor and was positioned at 15 cm above the bottom. A known quantity of OFL (25 ppm) was injected into vessel. The degradation experiment was allowed to run for 6 h. The concentration of OFL was periodically measured by taking samples after every 1 h and measured its absorbance.

3. Results and discussion

3.1. Characterization

Bi/Ni co-doped TiO_2 nanoparticles were prepared using sol–gel method as described in Section 2.2 and its characterization was done to analyze various parameters such as particle size, surface morphology, band-gap and surface area using XRD, SEM, UV-DRS and BET, respectively. All XRD spectra presented in Fig. 2 shows the peaks confirming anatase structure and it was observed that the prepared Bi–Ni co-doped photocatalyst consisted only of anatase and the doping would enhance the photocatalytic activity. Since Bismuth might get fused into the crystal structure of TiO_2, reduces the band gap of TiO_2, the co-doped photocatalyst displayed enhanced photocatalytic activity in the visible region. Nickel existing and dispersed on the surface of TiO_2, reduces the recombination of photogenerated electron–hole pairs, increasing photo quantum efficiency, and increasing the photoactivity.

The SEM images were used to evaluate primary structure of doped TiO_2. The morphology of the samples has been presented in Fig. 3. The photocatalysts are in the form of small agglomerates of crystals. The nanometer size of the particles resulted in an increase in surface area and a subsequent increase in the amount of photocatalytic reaction sites, which increases the photocatalytic activity. The EDS analysis of codoped TiO_2 showed significant

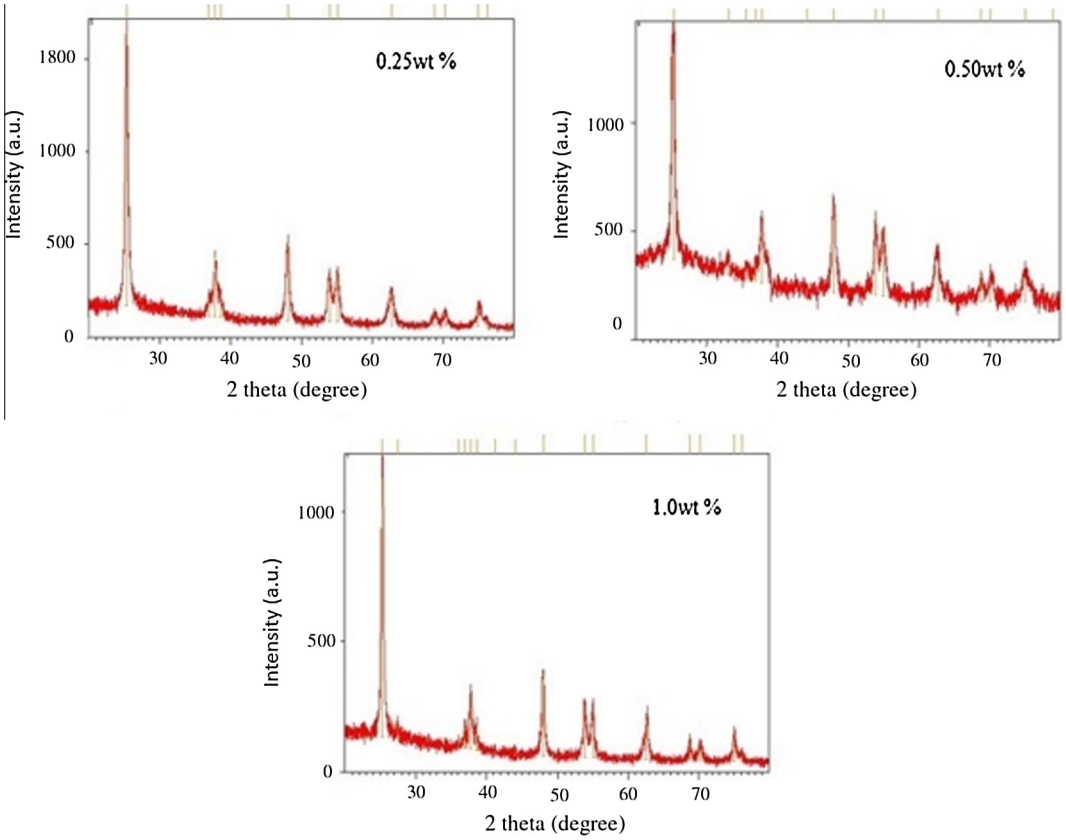

Fig. 2. XRD Pattern of Bi + Ni doped TiO_2 with different dopant concentration.

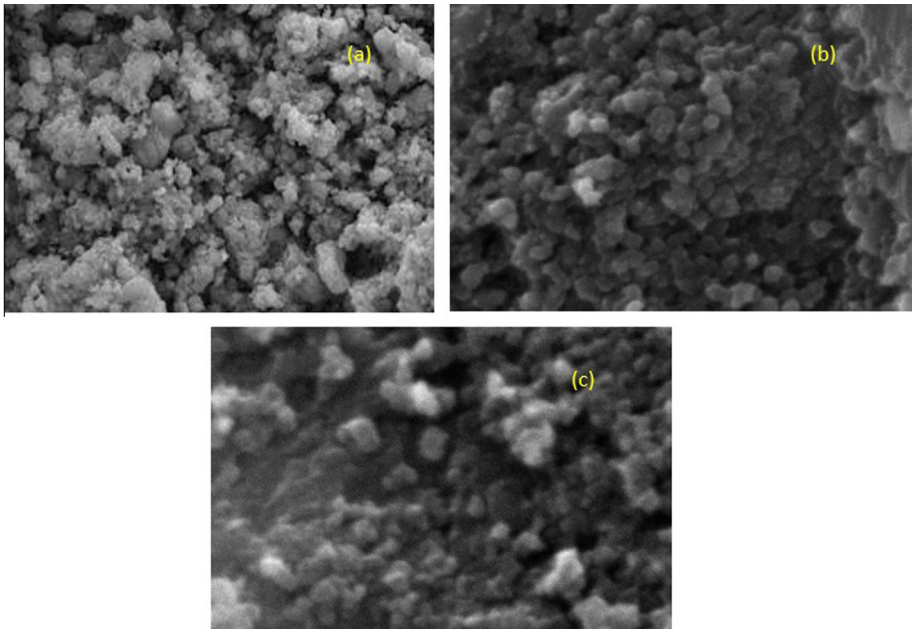

Fig. 3. SEM Images of Bi + Ni co-doped TiO_2 (a) 0.25 wt%, (b) 0.5 wt% and (c) 1.0 wt%.

presence of Ni and Bi ions in synthesized samples. The analytical results from EDS are in realistic arrangement with 0.25–1.0 wt% of Bi and Ni ions doped into TiO_2. The elemental records of samples for Ti, O, Ni and Bi showed homogeneous distribution of elements in the 0.25–1.0 wt% range of co-doped Bi/Ni–TiO_2. From EDS analysis (Table 1), it has been observed that in 0.25 wt% of Bi + Ni–TiO_2, 0.26, 3.04, 16.36 and 80.33% of Bi, Ni, O and Ti ions were present. Subsequently variations have been found in 0.25–1.0 wt% of Bi + Ni–TiO_2.

The BET surface area of Bi + Ni co-doped TiO_2 was found to be 74, 55 and 18.66 m^2/g for 0.25, 0.5 and 1.0 wt% of dopant concentration respectively. It has been analyzed that increase in dopant

Table 1
EDS of various dopant concentration.

Bi + Ni–TiO_2	Elements			
Dopant concentration (wt%)	Bi (%)	Ni (%)	O (%)	Ti (%)
0.25	0.26	3.04	16.36	80.33
0.50	1.37	1.88	43.53	53.4
1.0	2.48	0.72	70.70	26.10

concentration resulted in reduction of surface area of catalyst. This decrease of surface area with increase in dopant concentration may be due to increase in grain size, which is consistent with results of SEM.

3.1.1. Band gap energy

The UV–vis diffuse reflectance spectrum of all the compositions are shown in Fig. 4. It is evident from the results that the UV–vis diffuse reflectance spectrum of Bi/Ni codoped TiO_2, gave distinct band-gap absorption edges at 422 nm, 415 nm, 405 nm for doped Bi/Ni (0.25 wt%), Bi/Ni (0.50 wt%), Bi/Ni (1.0 wt%), respectively. The corresponding band-gap energies were found to be 2.89, 3.09 and 3.11 eV for 0.25 wt%, 0.50 wt%, and 1.0 wt% Bi/Ni co-doped TiO_2, respectively. At lowest concentration of dopant, the absorption edge shift is maximum, and hence, the corresponding calculated band-gap energy is minimum. This may be attributed to the fact that when the amount of dopants is small, the metals ions are well incorporated into the lattice withstanding the evolvement of local strains. On the other hand, when the dopants are in excess, ions cannot enter the TiO_2 lattice, but cover on the surface of TiO_2 and leads to the formation of heterogeneity junction. So, Bi/Ni (0.25 wt%) photocatalysts has lower band gap energy (2.9 eV) within the temperature range in which the photocatalytic experiments were carried out when compared to other dopant concentrations.

3.2. TiO_2 mediated photocatalytic activity

Photocatalytic activity of OFL was assessed with TiO_2 Degussa P25 and its concentration was varied from 0.5 to 2.0 g/L at natural pH of 6. Fig. 5(a) depicts that maximum photocatalytic degradation of OFL was found to be 72% after 6 h of irradiation at catalyst dose of 1.5 g/L. It has been observed that as catalyst concentration was allowed to rise from 0.5 g/L to 1.5 g/L; there is continuous increase in extent of degradation, further on increasing the concentration to 2 g/L, results in reduction of degradation efficiency, which might be due to decline in penetration of light (shielding effect). High concentration of catalyst leads to more turbid solution, thus obstruct the penetration of incident UV radiation and impart the effectiveness of the photocatalytic process. The correlation between degradation rate and the catalyst concentration is due to large number of active TiO_2 sites accessible for the photocatalytic reaction.

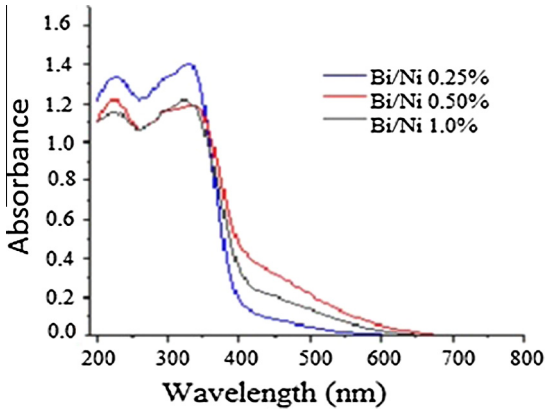

Fig. 4. UV–vis diffuse reflectance spectrum of Bi/Ni co-doped TiO_2.

pH is an important factor that effect photocatalytic reactions. In this study the degradation of ofloxacin was investigated by varying pH from 3 to 10 using Degussa TiO_2 as catalyst with dose of 1.5 g/L. It has been observed that photocatalytic activity is related to surface ionization state of catalyst. Change in the pH can change the adsorption of ofloxacin on catalyst surface, which is determinant factor for the existence of photocatalytic oxidation reactions. At pH 3, 72% degradation of OFL (initial concentration 25 mg/L) has been achieved within 6 h (Fig. 5(b)). Similar result has been reported by [31]. The effect of solution pH on conversion is a complex issue related to the ionization states of the catalyst surface and the substrate, as well as the rate of formation of radicals and other reactive species in the reaction mixture. The point of zero charge (pzc) of Degussa P25 is reported to be 6 [32]. At pH < 6 the catalyst surface is charged positively, while at pH > 6 the surface becomes negatively charged.

Ofloxacin is cationic below pK_{a1} (due to the presence of nitrogen in position 4 of the piperazinyl group), anionic above pK_{a2} (due to 6-carboxyl group), and zwitterionic i.e., neutral between pK_{a1} and pK_{a2}. Due to this, in photocatalytic degradation, the effect of the pH of the ofloxacin solution cannot be explained in terms of the ionization state of the catalyst and the substrate as both carry either negative or positive charges at alkaline or acidic conditions, respectively; i.e. neither environment should particularly favor substrate adsorption on the surface. At low pH values, positive holes are the main oxidation species, while at neutral or high pH, hydroxyl radicals are reflected the major species [33–35] it appears that ofloxacin oxidative transformation is primarily by valence band holes rather than radicals.

3.3. Doped TiO_2 induced photocatalytic activity

The concentration of dopant-metal ions plays a very significant role in Photocatalytic activity. The concentration of dopant was varied from 0.25 wt% to 1.0 wt% as shown in Fig. 6(a). The maximum degradation efficiency of doped catalyst has been obtained with dopant concentration of 0.25 wt%, further increasing the concentration of dopant above 0.25 wt% leads to decrease in degradation efficiency. It may be attributed to the fact that, metal ions, at low concentration, act as trapping centers for photo-generated electron (e^-) and/or hole (h^+) within the titania band-gap thus increasing the recombination time of e^-/h^+ pairs. These primarily trapped charges may then migrate, toward the surface of the semiconductor where further redox reaction occurs, thus enhances the photocatalytic activity. However, a high concentration of metal ions results in the recombination of the photo-generated e^- and h^+. There persists a finest concentration amount of dopant-metal ions at which the concentrated amount of e^- and/or h^+ are confined without recombination; on increasing the amount above this optimum value the photocatalytic activity decreases because of the increase in recombination rate [36].

The degradation of OFL has been studied with co-doped TiO_2 and Degussa P25 TiO_2 of OFL. The OFL (initial concentration 25 g/L) was allowed to undergo photocatalytic treatment for 6 h using optimum catalyst concentration of 1.5 g/L at pH 3. It has been observed (Fig. 6(b)) that 86% of OFL has been degraded using Bi–Ni co-doped TiO_2 under solar irradiations and only 42% OFL has been degraded using Degussa TiO_2 which shows that introduction of metal ions leads to increase in the efficiency of TiO_2 catalyst. The introduction of metal ions leads to decrease in band-gap of TiO_2.

A lesser amount of rutile phase was formed with Bi doping in TiO_2. For Bi-doped anatase, the energy levels of the impurity Bi 6s states lie below the bottom of the conduction band while the

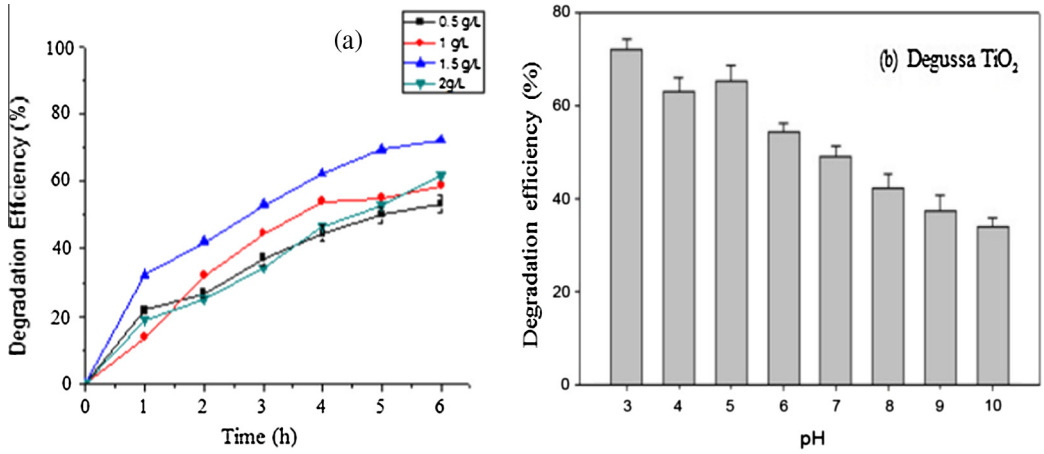

Fig. 5. (a) Effect of variation of catalyst concentration and (b) variation of pH.

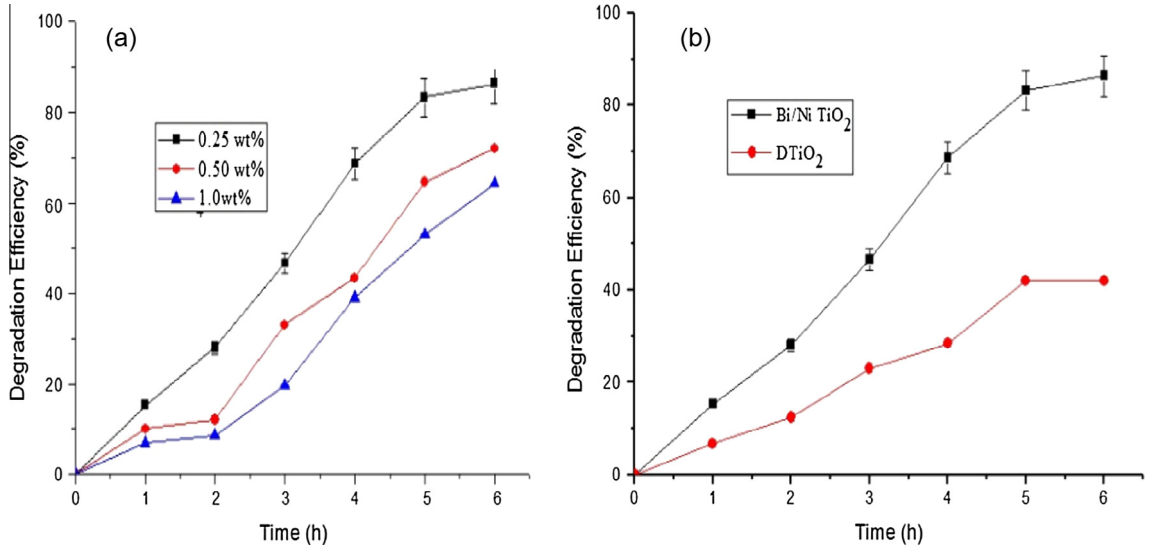

Fig. 6. (a) Effect of variation in dopant concentration and (b) variation of type of catalyst.

Fermi level EF lies above the gap states, indicating the gap states are fully occupied. The transition from Bi 6s to Ti 3d states is responsible for a red-shift of the visible light absorption edge. This observation suggests that photocatalytic efficiency would be improved significantly due to greater separation of electron–hole pairs. These findings present a reasonable explanation of recent experimental results. While on the other hand, Ni^{2+} could expand the optical absorption range by changing bandgaps. The another reason for using Ni metal ions is that insertion of Ni ions leads to enhancement of photocatalytic activity that has been tentatively attributed to the suppression of recombination of electron–hole pairs on the surface of the TiO_2 catalyst by low valence Ni^{2+} ions. Various studies reported synergetic effect of metal–metal co-doping as a result of charge equilibrium. These facts indicate that introducing two or more appropriate metals onto nano-crystalline TiO_2 particles will improve the photocatalytic effect of TiO_2. Hence, the advantages of incorporation of both the ions (Bi/Ni)-codoped TiO_2.

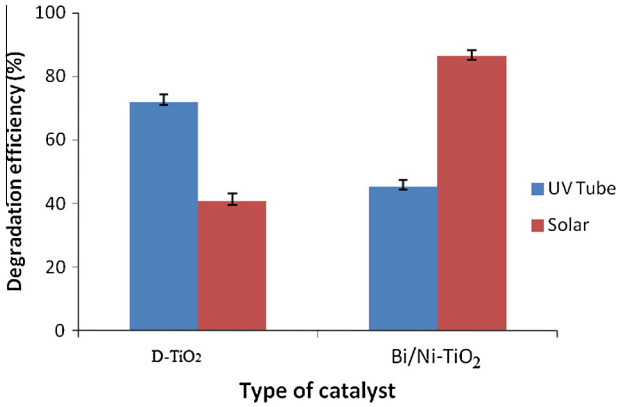

Fig. 7. Effect of variation of light source.

3.4. Comparison of solar light/UV light

Plot of photocatalytic degradation of OFL under UV and solar irradiation as a function of time using 1.5 g/L photocatalyst, OFL initial concentration 25 ppm and pH 3 is presented in Fig. 7. The photocatalytic degradation efficiency of OFL was higher under solar light than under UV light. At 6 h of reaction time using Bi/Ni co-doped TiO_2, maximum degradation of OFL under solar and UV irradiation were found to be 86% and 42.2%, respectively. However, with Degussa TiO_2 76% and 40% degradation was obtained under UV and solar light respectively in 6 h at pH 3.

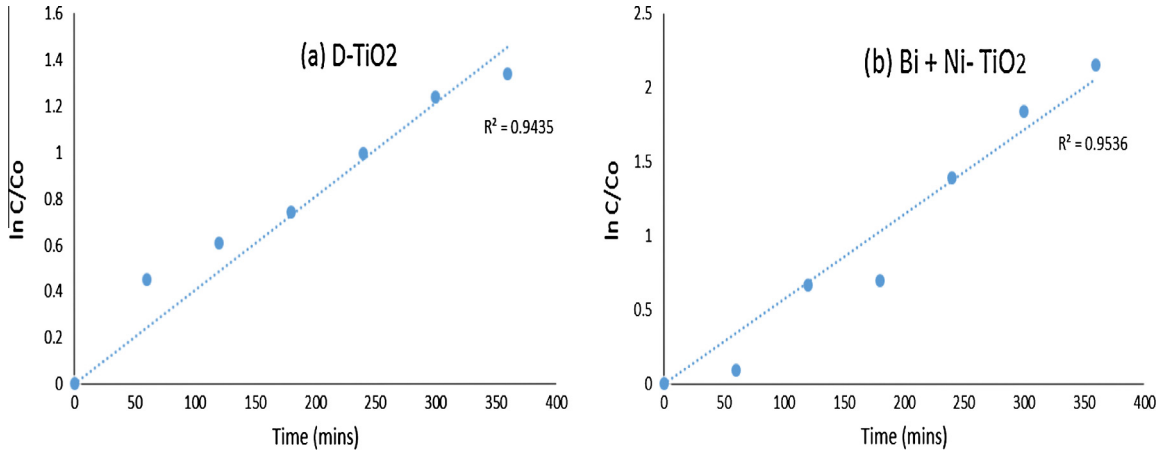

Fig. 8. Kinetic study of degradation of OFL using (a) Degussa TiO_2 and (b) Bi–Ni codoped TiO_2.

3.5. Kinetic study

Kinetic studies for degradation of OFL with catalyst dose of 1.5 g/L at pH 3 were carried out to find the reaction rate constant and order of reaction with Bi/Ni co-doped TiO_2 as photocatalysts under solar irradiations. The plot of $\ln C/C_o$ v/s time gave straight line as shown in (Fig. 8). Rate constant was calculated as 0.0062 min^{-1} for Bi–Ni co-doped TiO_2 with while for Degussa P25 TiO_2 rate constant obtained was 0.0036 min^{-1}, which is less as compared to co-doped catalyst. The results revealed that photocatalytic degradation of model compound followed first order kinetics by using $\ln (C/C_o) = kt$, where C_o denotes initial concentration and C denotes the concentration at any time t.

4. Conclusions

The photocatalyst co-doped with Bismuth and nickel was prepared by using sol–gel method. The effect of pH, catalyst dose, light source and the doping quantity of Bismuth and nickel on the photocatalytic activity of the Bi–Ni co-doped photocatalyst were reported. Compared with Degussa TiO_2, an increase in photoactivity for the degradation of OFL under visible light for the Bi–Ni (0.25 wt%) co-doped photocatalyst calcined was observed. It was found that 86% of ofloxacin was degraded in aqueous solution within 6 h at pH 3. The kinetic study for degradation for Ofloxacin has shown that rate of reaction was higher with co-doped TiO_2 catalyst compared to Degussa P25 TiO_2. This study confirms the effectiveness of heterogeneous photocatalysis to decontaminate the water containing organic micro-pollutants.

References

[1] G. Bonemann, M. Stiens, A. Pühler, A. Schlüter, Mobilizable IncQ-related plasmid carrying a new quinolone resistance gene, qnrS2, isolated from the bacterial community of a wastewater treatment plant, Antimicrob. Agents Chemother. 50 (2006) 3075–3080, http://dx.doi.org/10.1128/AAC.00378-06.
[2] A. Schluter, R. Szczepanowski, A. Puhler, E.M. Top, Genomics of IncP-1 antibiotic resistance plasmids isolated from wastewater treatment plants provides evidence for a widely accessible drug resistance gene pool, FEMS Microbiol. Rev. 31 (2007) 449–477, http://dx.doi.org/10.1111/j.1574-6976.2007.00074.x.
[3] S.D. Richardson, T.A. Ternes, Water analysis: emerging contaminants and current issues, Anal. Chem. 83 (2011) 4614–4648, http://dx.doi.org/10.1021/ac200915.
[4] M. Lahti, A. Oikari, Microbial transformation of pharmaceuticals naproxen, bisoprolol, and diclofenac in aerobic and anaerobic environments, Arch. Environ. Contam. Toxicol. 61 (2011) 202–210, http://dx.doi.org/10.1007/s00244-010-9622-2.
[5] K.M. Onesios, J.T. Yu, E.J. Bouwer, Biodegradation and removal of pharmaceuticals and personal care products in treatment systems: a review, Biodegradation 20 (2009) 441–466, http://dx.doi.org/10.1007/s10532-008-9237-8.
[6] T. Urase, T. Kikuta, Separate estimation of adsorption and degradation of pharmaceutical substances and estrogens in the activated sludge process, Water Res. 20 (2005) 441–466, http://dx.doi.org/10.1016/j.watres.2005.01.015.
[7] D. Fatta-Kassinos, M.I. Vasquez, K. Kümmerer, Transformation products of pharmaceuticals in surface waters and wastewater formed during photolysis and advanced oxidation processes—degradation, elucidation of byproducts and assessment of their biological potency, Chemosphere 85 (2011) 693–709, http://dx.doi.org/10.1016/j.chemosphere.2011.06.082.
[8] C.M. Jung, T.M. Heinze, R. Strakosha, C.A. Elkins, J.B. Sutherland, Acetylation of fluoroquinolone antimicrobial agents by an *Escherichia coli* strain isolated from a municipal wastewater treatment plant, J. Appl. Microbiol. 106 (2009) 564–571, http://dx.doi.org/10.1111/j.1365-2672.2008.04026x.
[9] K. Kümmerer, A. Al-Ahmad, V. Mersch-Sundermann, Biodegradability of some antibiotics, elimination of the genotoxicity and affection of wastewater bacteria in a simple test, Chemosphere 40 (2000) 701–710, http://dx.doi.org/10.1016/S0045-6535(99)00439-7.
[10] L.H. Santos, A.N. Araujo, A. Fachini, A. Pena, C. Delerue-Matos, M.C. Montenegro, Ecotoxicological aspects related to the presence of pharmaceuticals in the aquatic environment, J. Hazard. Mater. 175 (2010) 45–95, http://dx.doi.org/10.1016/j.jhazmat.2009.10.100.
[11] S.N. Dokianakis, M.E. Kornaros, G. Lyberatos, On the effect of pharmaceuticals on bacterial nitrite oxidation, Water Sci. Technol. 50 (2004) 341–346.
[12] A. Jia, Y. Wan, Y. Xiao, J. Hu, Occurrence and fate of quinolone and fluoroquinolone antibiotics in a municipal sewage treatment plant, Water Res. 46 (2012) 387–394, http://dx.doi.org/10.1016/j.watres.2011.10.055.
[13] J. Beausse, Selected drugs in solid matrices: a review of environmental determination, occurrence and properties of principal substances, TrAC, Trends Anal. Chem. 23 (2004) 753–761, http://dx.doi.org/10.1016/j.trac.2004.08.005.
[14] K.A. Langdon, M.S.T.J. Warne, R.S. Kookanaz, Aquatic hazard assessment for pharmaceuticals, personal care products, and endocrine-disrupting compounds from biosolids-amended land, Integr. Environ. Assess. Manage. 6 (2010) 663–676, http://dx.doi.org/10.1002/ieam.74.
[15] P. Calza, C. Medana, F. Carbone, V. Giancotti, C. Baiocchi, Characterization of intermediate compounds formed upon photoinduced degradation of quinolones by high-performance liquid chromatography/high-resolution multiple-stage mass spectrometry, Rapid Commun. Mass Spectrom. 22 (2008) 1533–1552, http://dx.doi.org/10.1002/rcm.3537.
[16] I. Michael, E. Hapeshi, C. Michael, D. Fatta-Kassinos, Solar Fenton and solar TiO_2 catalytic treatment of ofloxacin in secondary treated effluents: evaluation of operational and kinetic parameters, Water Res. 44 (2010) 5450–5462, http://dx.doi.org/10.1016/j.watres.2010.06.053.
[17] M.I. Vasquez, M. Garcia-Käufer, E. Hapeshi, J. Menz, K. Kostarelos, D. Fatta-Kassinos, K. Kümmerer, Chronic ecotoxic effects to *Pseudomonas putida* and *Vibrio fischeri*, and cytostatic and genotoxic effects to the hepatoma cell line (HepG2) of ofloxacin photocatalytically treated solutions, Sci. Total Environ. 450–451 (2013) 356–365, http://dx.doi.org/10.1016/j.scitotenv.2012.05.096.
[18] E. Hapeshi, I. Fotiou, D. Fatta-Kassinos, Sonophotocatalytic treatment of ofloxacin in secondary treated effluent and elucidation of its transformation products, Chem. Eng. J. 461–462 (2013) 39–48, http://dx.doi.org/10.1016/j.cej.2012.11.048 (in press).
[19] K.H. Wammer, A.R. Korte, R.A. Lundeen, J.E. Sundberg, K. McNeill, W.A. Arnold, Direct photochemistry of three fluoroquinolone 1 antibacterials: norfloxacin, ofloxacin, and enrofloxacin, Water Res. 47 (2003) 439–448, http://dx.doi.org/10.1016/j.watres.2012.10.025.
[20] H. Santoke, W. Song, W.J. Cooper, J. Greaves, G.E. Mille, Free-radical-induced oxidative and reductive degradation of fluoroquinolone pharmaceuticals:

kinetic studies and degradation mechanism, J. Phys. Chem. A 113 (2009) 7846–7851, http://dx.doi.org/10.1021/jp9029453.
[21] D. Dvoranova, V. Brezova, M. Mazur, M.A. Malathi, Investigations of metal-doped titanium dioxide photocatalysts, Appl. Catal., B 37 (2002) 91–105, http://dx.doi.org/10.1016/S0926-3373(01)00335-6.
[22] J. Zhu, Z. Deng, F. Chen, et al., Hydrothermal doping method for preparation of Cr^{3+}–TiO_2 photocatalysts with concentration gradient distribution of Cr^{3+}, Appl. Catal., B 62 (2006) 329–335, http://dx.doi.org/10.1155/2014/962419.
[23] G. Wu, T. Nishikawa, B. Ohtani, A. Chen, Synthesis and characterization of carbon-doped TiO_2 nanostructures with enhanced visible light response, Chem. Mater. 19 (2007) 4530–4537, http://dx.doi.org/10.1021/cm071244m.
[24] K.R. Patil, S.D. Sathaye, Y.B. Khollam, S.B. Deshpande, N.R. Pawaskar, A.B. Mandale, Preparation of TiO_2 thin films by modified spin-coating method using an aqueous precursor, Mater. Lett. 57 (2003) 1775–1780.
[25] U.G. Akpan, B.H. Hameed, The advancements in sol–gel method of doped-TiO_2 photocatalysts, Appl. Catal., A 375 (2010) 1–11, http://dx.doi.org/10.1016/j.apcata.2009.12.023.
[26] P. Kundu, A. Kaur, S.K. Mehta, S.K. Kansal, Removal of ofloxacin from aqueous phase using Ni-doped TiO_2 nanoparticles under solar irradiation, J. Nanosci. Nanotechnol. 14 (2014) 6991–6995.
[27] R. Rahimi, R. Mahboubeh, S.S. Moghaddam, Application of N, S-codoped TiO_2 photocatalyst for degradation of methylene blue, in: 16th International Electronic Conference On Synthetic Organic Chemistry, 30 Nov 2012.
[28] C. Wen, Y.-J. Zhu, T. Kanbara, H.-Z. Zhu, C.-F. Xiao, Effects of I and F codoped TiO_2 on the photocatalytic degradation of methylene blue, Desalination 249 (2009) 621–625, http://dx.doi.org/10.1016/j.desal.2009.01.028.
[29] A. Albini, S. Monti, Photophysics and photochemistry of fluoroquinolones, Chem. Soc. Rev. 32 (2003) 238–250.
[30] H.R. Park, T.H. Kim, K.M. Bark, Physicochemical properties of quinolone antibiotics in various environments, Eur. J. Med. Chem. 37 (2002) 443–460, http://dx.doi.org/10.1016/S0223-5234(02)01361-2.
[31] E. Hapeshi, A. Achilleos, M.I. Vasquez, C. Michael, N.P. Xekoukoulotakis, D. Mantzavinos, D. Kassinos, Drugs degrading photocatalytically: kinetics and mechanisms of ofloxacin and atenolol removal on titania suspensions, Water Res. 44 (2010) 1737–1746;
E. Hapeshi, A. Achilleos, M.I. Vasquez, C. Michael, N.P. Xekoukoulotakis, D. Mantzavinos, D. Kassinos, Drugs degrading photocatalytically: kinetics and mechanisms of ofloxacin and atenolol removal on titania suspensions, Water Res. 44 (2010) 1737–1746, http://dx.doi.org/10.1016/j.watres.2009.11.044.
[32] C.G. Silva, J. Wang, W.L. Faria, Photocatalytic and photochemical degradation of mono-, di- and tri-azo dyes in aqueous solution under UV irradiation, J. Photochem. Photobiol., A 181 (2006) 314–324, http://dx.doi.org/10.1016/j.watres.2009.11.044.
[33] Z. Shourong, H. Qingguo, Z. Jun, W. Bingkun, A study on dye photoremoval in TiO_2 suspension solution, J. Photochem. Photobiol., A 108 (1997) 235–238.
[34] I.K. Konstantinou, T.A. Albanis, TiO_2-assisted photocatalytic degradation of azo dyes in aqueous solution: kinetic and mechanistic investigations: a review, Appl. Catal., B 49 (2004) 1–14, http://dx.doi.org/10.1016/j.apcatb.2003.11.010.
[35] M.R. Sohrabi, M. Ghavami, Photocatalytic degradation of Direct Red 23 dye using UV/TiO_2: effect of operational parameters, J. Hazard. Mater. 153 (2008) 1235–1239, http://dx.doi.org/10.1016/j.jhazmat.2007.09.114.
[36] R. Jaiswal, N. Patel, D.C. Kothari, A. Miotello, Improved visible light photocatalytic activity of TiO_2 co-doped with vanadium and nitrogen, Appl. Catal., B 126 (2012) 47–54, http://dx.doi.org/10.1016/j.apcatb.2012.06.030.